



# LUND UNIVERSITY

## Fire Engineering Design of Steel Structures

Pettersson, Ove; Magnusson, Sven Erik; Thor, Jörgen

1976

[Link to publication](#)

*Citation for published version (APA):*

Pettersson, O., Magnusson, S. E., & Thor, J. (1976). *Fire Engineering Design of Steel Structures*. (Bulletin of Division of Structural Mechanics and Concrete Construction, Bulletin 52; Vol. Bulletin 52). Lund Institute of Technology.

*Total number of authors:*

3

### General rights

Unless other specific re-use rights are stated the following general rights apply:

Copyright and moral rights for the publications made accessible in the public portal are retained by the authors and/or other copyright owners and it is a condition of accessing publications that users recognise and abide by the legal requirements associated with these rights.

- Users may download and print one copy of any publication from the public portal for the purpose of private study or research.
- You may not further distribute the material or use it for any profit-making activity or commercial gain
- You may freely distribute the URL identifying the publication in the public portal

Read more about Creative commons licenses: <https://creativecommons.org/licenses/>

### Take down policy

If you believe that this document breaches copyright please contact us providing details, and we will remove access to the work immediately and investigate your claim.

LUND UNIVERSITY

PO Box 117  
221 00 Lund  
+46 46-222 00 00

# Fire Engineering Design of Steel Structures

Ove Pettersson Sven-Erik Magnusson Jörgen Thor



STÅLBYGGNADSINSTITUTET  
Swedish Institute of Steel Construction

# **Fire Engineering Design of Steel Structures**

**Ove Pettersson Sven-Erik Magnusson Jörgen Thor**



**STÅLBYGGNADSINSTITUTET**  
**Swedish Institute of Steel Construction**

## **FIRE ENGINEERING DESIGN OF STEEL STRUCTURES**

Ove Pettersson, Prof, Dr. Techn  
Sven-Erik Magnusson, Dr. Techn

Division of Structural Mechanics  
and Concrete Construction,  
Lund Institute of Technology,  
Lund, Sweden

Jörgen Thor, Dr. Techn

Swedish Institute of Steel Construction  
Stockholm, Sweden

Translated by

L. J. Gruber, BSc(Eng), MICE, MStructE

Division of Structural Mechanics  
and Concrete Construction

Lund Institute of Technology

Lund Sweden

Bulletin 52, 1976

Swedish Institute of Steel Construction  
Stockholm, Sweden

Publication 50, 1976



## FOREWORD

This handbook describes a rational fire engineering design process for loadbearing structures and partitions of steel on the basis of performance requirements. The design methods presented are based on the regulations, advisory notes and recommendations given in the Swedish Building Regulations and in the separate publication on rational fire engineering design which has been compiled on the instructions of the National Swedish Board of Physical Planning and Building. The methods presented in this handbook have been given the general approval of the Board (General Approval Certificate No 2698/73).

The handbook is primarily intended for buildings for which, requirements are given in the regulations with respect to fire resistance of load bearing structures and partitions. For buildings such as single-storey industrial and warehouse buildings for which there is generally no requirement with regard to fire resistance the handbook is supplemented by the publication "Fire engineering design of single-storey industrial and warehouse buildings with a loadbearing frame of steel", issued by the Swedish Institute of Steel Construction.

The handbook discusses the principles which govern rational fire engineering design and also gives a detailed method for practical application. Owing to comprehensive information in the form of diagrams and tables, practical design can normally be carried out quickly and easily. A rational fire engineering design often permits a considerable reduction in the costs of providing the necessary protection for structural steelwork, in comparison with the more standardised type of design.

The handbook is primarily intended for application in practical design. It has however been drawn up in such a way that it can also be used in the course of instruction in technical schools.

The handbook has been drawn up in continuous collaboration between the Division of Structural Mechanics and Concrete Construction, Lund Institute of Technology, and the Swedish Institute of Steel Construction. In this connection, extensive use has been made of material previously produced at the Division of Structural Mechanics and Concrete Construction, which has been published in its most detailed form by Sven-Erik Magnusson and Ove Pettersson in the Chapter "Fire Engineering Design of Steel Constructions" in the NJA Structural Steel Handbook 1972, pp. 556-641. More recent work at both the Division of Structural Mechanics and the Swedish Institute of Steel Construction has been added to this. Considerable parts of the handbook are of international news value.

The rational fire engineering design method, as well as its assumptions and general characteristics, was first described by Ove Pettersson in a series of publications during the period 1962-1965. A partial summary of these publications is given in Chapter 2. The results of research and development work which form the basis of this handbook have also been largely produced by research carried out by Ove Pettersson himself or under his leadership.

The position regarding the origin of the various sections of the handbook is as fol-

lows. The assumptions and general characteristics in Chapter 2 were drawn up by Ove Pettersson. Statistical data in Chapter 3 concerning the magnitude of the fire load in different types of premises and buildings are based on surveys carried out by the Division of Structural Mechanics and Concrete Construction and the Swedish Institute of Steel Construction. Chapter 4 concerning the temperature-time curve in the fire compartment has been mainly based on previous original work by Sven-Erik Magnusson and Sven Thelandersson. Chapters 5-8, which deal with the calculation under fire exposure conditions of the temperature-time curves for different types of insulated and uninsulated steel constructions, may to a large extent be regarded as the result of previous original work by Sven-Erik Magnusson and Ove Pettersson and, with regard to rational consideration of the effect of radiation, new research results produced by Jörgen Thor. A new analytical model for determination of the temperature-time curve under fire exposure conditions for a steel construction with insulation in the form of a suspended ceiling, developed by Sven-Erik Magnusson and Jörgen Thor, is presented in Chapter 7. Determination of the loadbearing capacity under fire exposure conditions, in Chapter 9, of steel structures in flexure is based in all essentials on work carried out by Jörgen Thor, while treatment of structures acted upon by an axial load, in Chapter 10, mainly comprises new contributions by Torbjörn Larsson and Ove Pettersson. Chapter 11 concerning materials for protection of structural steelwork has been compiled by Jörgen Thor. A separate section dealing with an alternative design method which permits the conversion of standard fire test data into the action of an actual fire, has been drawn up by Ove Pettersson.

Research and development in the field of structural fire protection in the broad sense of the term has been characterised in recent years by a considerable increase in effort on an international scale. This is likely, in the relatively near future, to enable some improvements to be made to the design data presented in this handbook. A further development of urgent importance is more rational consideration of the type of fire process.

Work on the actual arrangement of the handbook and the preparation of data has been divided about equally between the three authors. In addition, Jörgen Thor has been responsible for co-ordination of the text and design aids, compilation of worked examples and editorial treatment and production, and Sven-Erik Magnusson for most of the numerical computer calculations necessary for production of the design data in the handbook.

The Swedish Institute of Steel Construction wish to take this opportunity of thanking all those who contributed to the production of this handbook, and hope that it will prove to be of great practical utility.

Stockholm, October 1974.

SWEDISH INSTITUTE OF STEEL CONSTRUCTION

This handbook was published in Swedish during 1974 and the present publication is a literal translation of the original handbook. Since 1974 a new edition of the Swedish Building Regulations, SBN 1975, has been issued. When references in detailed matters are made in the handbook to the Building Regulations these apply to the previous edition of the Regulations, SBN 1967. This circumstance does not affect the use of this handbook. In the new edition of the Building Regulations, SBN 1975, the alternative of the more rational fire engineering design, which this handbook deals with, is more strongly marked.

Stockholm, February 1976.

SWEDISH INSTITUTE OF STEEL CONSTRUCTION

## CONTENTS

MAIN SECTION	Page
1 THE ARRANGEMENT OF THE HANDBOOK	13
2 THE PRINCIPLES GOVERNING THE DESIGN AND SCOPE OF FIRE PROTECTION	16
2.1 The extent of damage due to fire and the principles of economic optimisation	16
2.2 Minimum conditions for structural fire protection	18
2.3 Factors which influence the extent of total fire protection measures	20
2.4 Performance requirements and loading and safety problems in fire engineering design of loadbearing structures and partitions	22
2.4.1 Loadbearing structures	23
2.4.2 Partitions	26
2.5 The principles governing fire engineering design of loadbearing structures and partitions by means of classification	27
2.6 The principles governing rational fire engineering design of loadbearing structures and partitions	30
3 FIRE LOAD	33
3.1 Definition of fire compartment and fire load	33
3.2 Statistical determination of the fire load in different types of buildings	35
3.2.1 Dwellings	36
3.2.2 Office buildings	36
3.2.3 Schools	38
3.2.4 Hospitals	38
3.2.5 Hotels	40
3.2.6 Other premises and buildings	40
3.3 The actual degree of combustion and uneven distribution of the fire load	40

4	THE TEMPERATURE-TIME PROCESS IN THE FIRE COMPARTMENT	42
4.1	General characterisation of the fire process	42
4.2	Calculation of the temperature-time curves of the combustion gases for an arbitrarily chosen type of fire load	45
4.2.1	Heat balance equations	45
4.2.2	Brief treatment of the terms comprised in the heat balance equation	46
4.2.2.1	The term $I_B$	46
4.2.2.2	The term $I_R$	46
4.2.2.3	The term $I_W$	47
4.2.2.4	The term $I_L$	49
4.2.2.5	The term $I_C$	51
4.2.3	Calculation procedure	52
4.3	Calculation of the temperature-time curve of the combustion gases for fire loads mainly of the wood fuel type	54
4.3.1	Assumptions	54
4.3.2	Calculation of the opening factor $A\sqrt{h}/A_t$	56
4.3.3	Calculated temperature-time curves for fire compartment Type A (standard fire compartment) for different fire loads $q$ and opening factors $A\sqrt{h}/A_t$	58
4.3.4	Conversion of the fire process in another type of fire compartment into a fire process in fire compartment Type A (standard fire compartment)	62
4.4	Transition from a ventilation controlled fire to a fire load controlled fire	64
5	TEMPERATURE-TIME CURVES FOR UNINSULATED STEEL STRUCTURES	68
5.1	The heat balance equation	68
5.2	The quantities included in the heat balance equation	69
5.2.1	The length of the time interval $\Delta t$	69
5.2.2	The density of steel $\gamma_s$	69
5.2.3	The specific heat capacity $c_{ps}$ of steel	69
5.2.4	The surface coefficient of heat transfer $\alpha$ of the boundary layer	70
5.2.5	The $F_s/V_s$ ratio of the steel section	73
5.3	Dependence of the maximum steel temperature on $F_s/V_s$ , $\epsilon_r$ and $\vartheta_t$	74
5.4	Worked example	75
5.5	Comparison of the calculated steel temperature-time curve with that measured in fire tests	77



6	TEMPERATURE-TIME CURVES FOR INSULATED STEEL STRUCTURES	78
6.1	The heat balance equation	78
6.2	The quantities included in the heat balance equation	80
6.2.1	Thermal conductivity $\lambda_i$ of the insulation	80
6.2.2	The specific heat capacity $c_{pi}$ of the insulation	81
6.2.3	The $A_i/V_s$ ratio of the steel section	81
6.3	Dependence of the maximum steel temperature on $A_i/V_s$ , $d_i/\lambda_i$ and $\dot{\vartheta}_t$	81
6.4	Worked example	82
6.5	Comparison of the calculated steel temperature-time curve with that measured in fire tests	84
7	TEMPERATURE-TIME CURVES FOR STEEL STRUCTURES WITH INSULATION IN THE FORM OF A SUSPENDED CEILING	86
7.1	The heat balance equation	86
7.1.1	Calculation of the surface temperature of the floor slab and the suspended ceiling	86
7.1.2	Calculation of the steel temperature	89
7.2	Comparison of the calculated steel temperature-time curve with that measured in fire tests	91
7.3	Influence of the material and thickness of the floor slab on the steel temperature	92
7.4	Practical design and the need for fire tests	94
8	TEMPERATURE-TIME CURVES FOR PARTITIONS	96
9	CRITICAL LOAD UNDER FIRE EXPOSURE CONDITIONS FOR A STEEL STRUCTURE SUBJECT TO A FLEXURAL, TENSILE OR COMPRESSIVE LOADING WITHOUT THE CONCOMITANT RISK OF INSTABILITY	100
9.1	Determination of the critical load on the basis of the yield stress at elevated temperatures or the 0.2% proof stress	100
9.2	Determination of the critical load for beams on the basis of the calculated deformation curve	103
9.2.1	Deformation curve and failure criterion	103
9.2.2	Evaluation of the critical load under certain given conditions	104
9.2.3	Evaluation of the critical load under conditions different from those in Subsection 9.2.2	106
9.2.3.1	Other types of loading	106
9.2.3.2	Continuous beams	106

	9.2.3.3 Other steel grades	107
	9.2.3.4 Other cross sections	108
	9.2.3.5 Uneven temperature distribution in the beam	110
	9.2.3.6 Restraint on longitudinal expansion	111
10	CRITICAL LOAD UNDER FIRE EXPOSURE CONDITIONS FOR A STEEL STRUCTURE SUBJECT TO AN AXIAL COMPRESSIVE FORCE	115
	10.1 Determination of the buckling load under in-plane instability conditions when there is no restraint on longitudinal expansion	115
	10.2 Determination of the buckling load under in-plane instability conditions when longitudinal expansion is partially prevented	118
	10.2.1 Determination of the degree of expansion $\gamma$	120
	10.3 Determination of the critical load in a structure subject to simultaneous flexure and axial compressive force	125
	10.4 Determination of the buckling load under out-of-plane instability conditions	126
11	PROTECTION OF STRUCTURAL STEELWORK	128
	11.1 Materials and methods	128
	11.1.1 Sprayed mineral wool	129
	11.1.2 Sprayed asbestos	130
	11.1.3 Fire retardant plasters	131
	11.1.4 Fire retardant paints	131
	11.1.5 Mineral wool slabs	132
	11.1.6 Vermiculite slabs	133
	11.1.7 Gypsum plaster slabs	134
	11.1.8 Prefabricated gypsum plaster sections	135
	11.1.9 Suspended ceilings and partitions	137
	11.1.10 Other methods	138
	11.2 Costs	138
	11.3 Classification of fire insulation materials	139

DESIGN SECTION - TABLES AND DIAGRAMS FOR FIRE ENGINEERING DESIGN	141
1 Flow chart which illustrates the design procedure	144
2 Determination of the design static load in the event of fire	145
3 Determination of the design fire load and opening factor	146
4 Conversion to equivalent fire load and opening factor	148
5 Determination of the maximum temperature in the event of fire in uninsulated steel structures	150
6 Determination of the maximum temperature in the event of fire in insulated steel structures	154
7 Determination of the maximum temperature in the event of fire in steel structures with insulation in the form of a suspended ceiling	162
8 Check on the function of partitions	164
9 Determination of the critical load for steel girders under fire exposure conditions	165
10 Determination of the critical load for steel columns under fire exposure conditions	169
WORKED EXAMPLES	177
ALTERNATIVE DESIGN METHOD BASED ON THE CONCEPT OF EQUIVALENT FIRE DURATION	217
LITERATURE	226





## MAIN SECTION



# 1 THE ARRANGEMENT OF THE HANDBOOK

This handbook consists of four, more or less independent, parts namely the Main Section, the Design Section, Worked Examples and Alternative Method of Design Based on the Concept of Equivalent Fire Duration. At the end of the handbook there is also a list of references which is common to all the sections.

Chapter 2 of the Main Section is introduced by a general description of the different principles which govern planning and design of structural fire protection measures and total fire protection measures. In the light of this overall problem, an account is given in Section 2.5 of the principles governing standardised fire engineering design of loadbearing structures and partitions according to a fire engineering classification based on a standard fire curve. Section 2.6 gives a description of the principles underlying a more rational design process governed by performance requirements, based on an actual fire process. The difference between the standardised and rational design method is illustrated in Figs. 1 a and 1 b. Chapters 3-10 of the Main Section deal with the various stages which make up this rational design process, in which connection there is a comparatively detailed discussion of the theories and calculation methods employed. In Chapter 11 of the Main Section, an account is given of the different materials and methods used in providing protection for structural steelwork.

There are several reasons for this comparatively detailed discussion of the principles, theories and calculation methods. In the normal case, practical design can be carried out very easily with the aid of only a few design diagrams and design tables, in spite of the great complexity of the underlying theories in many cases. In order, however, to ensure that the design process is applied in the correct way in different cases, it has been considered essential to give a comparatively detailed description of the background of the diagrams and tables. This is also necessary in order that cases which are not fully covered by the design diagrams and tables may be dealt with. Furthermore, it is important from the point of view of the authorities which scrutinise calculations and issue permits that the theories and calculation principles underlying the diagrams and tables should be clearly set out. By virtue of the detailed discussion in the Main Section, the Handbook can also be used as a textbook, and also provide the stimulus for further research and development work in the fields of fire protection and fire engineering design of buildings.

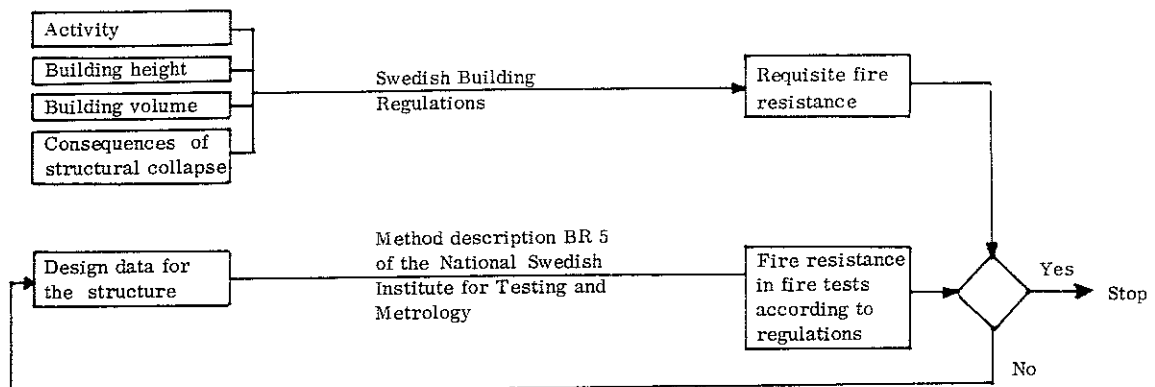


Fig. 1 a. Flow chart for standardised fire engineering design of a loadbearing structure

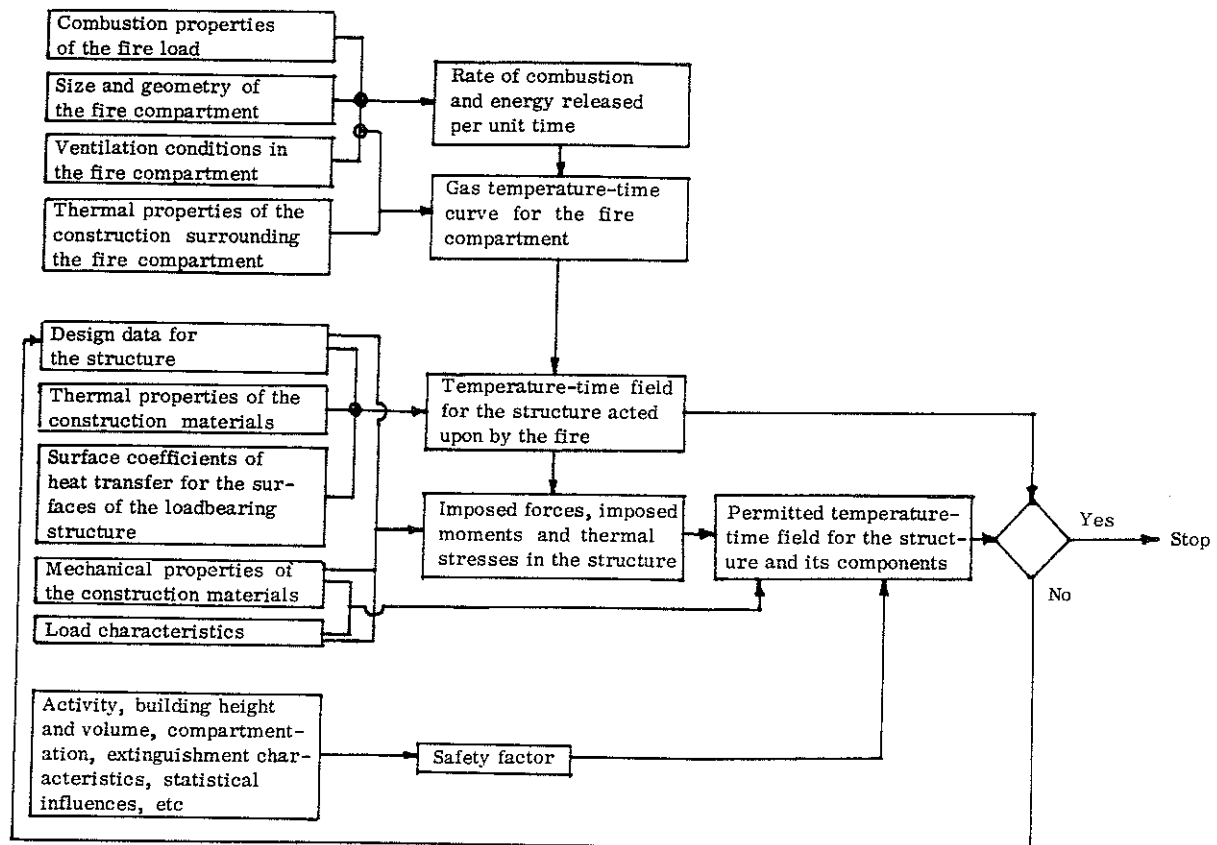


Fig. 1 b. Flow chart for rational fire engineering design of a loadbearing structure

The sections in the Main Section which give the background of the principles governing the planning and design of structural fire protection and total fire protection, Sections 2.1 - 2.3, deal with a very complex problem. It is therefore unavoidable that thorough understanding of these sections should demand that readers are reasonably familiar with fire engineering design, and it may be advisable for those who have had no previous experience in this field to defer study of these sections until they have read the remainder of the book.

The Design Section contains diagrams and tables and instructions for practical application of the rational design method. These diagrams and tables are normally sufficient for fire engineering design of loadbearing structures or partitions. The Design Section is introduced by a flow chart which illustrates the design procedure. This Section is subdivided in the same way as the Main Section. Specific references are also made in conjunction with each diagram and table to the Main Section.

The Worked Examples consist of 10 examples with detailed solutions which deal with different problems and different types of construction and building.

A description of an Alternative Method of Design Based on the Concept of Equivalent Fire Duration completes the handbook. This concept has recently been introduced into the international discussion as an aid in converting conditions applicable to standard fire tests to those in an actual fire, and vice versa. Certain principles of fire engineering design, based on this concept, have also been developed. This is the reason why there is a brief discussion in the handbook of the concept of equivalent fire duration, as well as a number of diagrams with the assistance of which the equivalent fire duration can be determined in a rational manner for different conditions. A design process based on the equivalent fire duration can in certain



cases prove to be a valuable complement to the fire engineering design method described in the Main Section and Design Section, which is based directly on the actual fire process. The diagrams for a quick determination of the equivalent fire duration in various applications also permit utilisation of a comprehensive body of data obtained from standard fire tests performed on insulated and uninsulated steel structures in designing for the effect of a realistic fire process. Practical application of the concept of equivalent fire duration is illustrated by two examples.

The system of technical units so far used in the Swedish building industry is used in the handbook. The corresponding SI units are given alongside in curly brackets { } in the body of the text, equations and figures. As a result, some duplication of equations and scales on the axes of diagrams has been necessary. However, it is considered that the inconvenience which this may cause in some cases is compensated for by the advantage of having both systems included until the SI units have gained general acceptance.

## 2 THE PRINCIPLES GOVERNING THE DESIGN AND SCOPE OF FIRE PROTECTION

### 2.1 The extent of damage due to fire and the principles of economic optimisation

Over the past 50 years, the annual cost of damage directly attributable to fire rose in Sweden from about Skr. 40m to 350m. The cost curve is shown in Fig. 2.1a. In terms of current prices, the cost of fire damage has more than doubled over the past 10-year period, and has approximately quadrupled over the past 20-year period. In real terms, the increases for the above periods amount to 12% and 70% respectively. To these direct fire damage costs must be added indirect costs due to breakdowns, stoppages in operation, defaults in deliveries and missed economic opportunities, as well as losses of human lives, work and dwellings. It is difficult to calculate these indirect costs, but they may be roughly estimated to be of the same order as the direct costs due to fire damage.

The annual costs of fire prevention measures amount to about 2% of the volume of investment in buildings, or about Skr. 250m. The State and municipal fire fighting services in Sweden cost Skr. 150-200m annually, to which must be added the costs of industrial fire services, sprinkler plants, etc. If the costs incurred in administering the fire insurance system are also added, then the total annual costs of fire protection and fire damage in Sweden are in the order of Skr. 1500m.

On the national level, the endeavour guiding investment in fire prevention and fire fighting services must be (1) - (5)

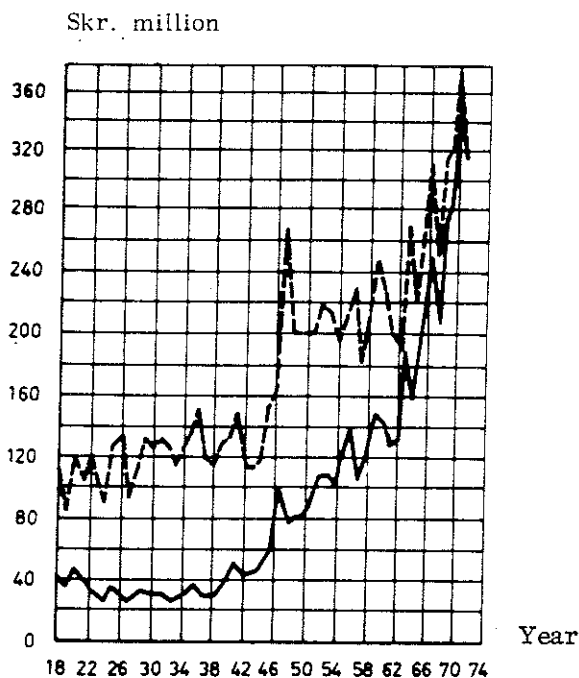


Fig. 2.1 a. Direct annual fire damage costs in Sweden over the period 1918 - 1971. ----- values with index correction, — values without index correction

- to design and allocate fire protection measures in such a way, within the framework of the total investment costs, that the effect is the optimum possible
- to make the level of this optimally allocated total investment cost such that the sum of fire damage costs and investment costs is a minimum

This principle is illustrated in Fig. 2.1b. In the figure,  $a$  designates the optimally allocated total investment in fire prevention and fire fighting, and  $b$  total cost due to fire damage including the cost of fire insurance administration. An increase in the investment  $a$  in fire prevention and fire fighting is accompanied by a reduction in direct and indirect fire damage and the total cost  $b$  of damage due to fire. For a certain level of investment  $a$ , the sum of fire protection and fire damage costs,  $a+b$ , will be a minimum as shown by point A in the figure. In relation to this level of investment, both an increase and a decrease in the investment in fire prevention and fire fighting will lead to a rise in the aggregate total fire protection and fire damage costs, as shown by points B and C in the figure.

This principle of optimising fire protection and fire damage costs at national levels also applies in an approximate manner to e.g. a municipality, a fire brigade district, an industrial area or a major industry with its own fire fighting resources, i.e. to units which are unambiguously delineated from the point of view of total costs. On the other hand, the principle must be modified when it is applied to individual buildings, since the investments made in fire prevention and fire fighting measures with respect to a single building are an integral part of the overall fire protection service, of which the municipal and State fire fighting and rescue resources are the most essential components.

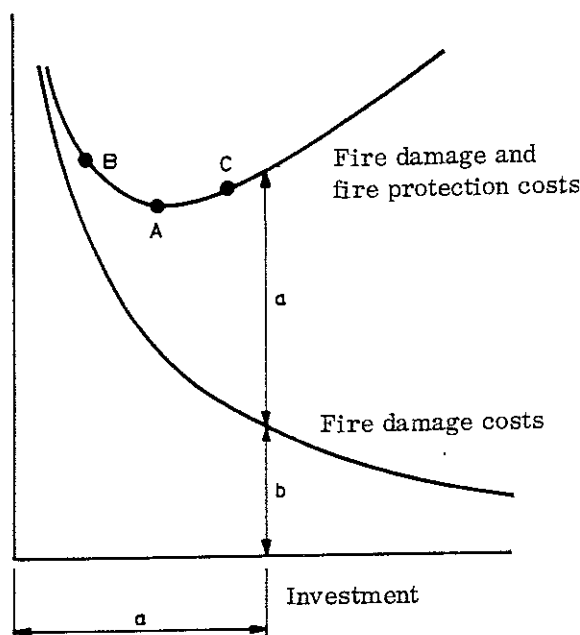


Fig. 2.1b. Relationship between total investment of fire prevention and fire fighting  $a$ , total cost due to fire damage  $b$ , and the aggregated total fire protection and fire damage costs  $a+b$  (1) - (5)

## 2.2 Minimum conditions for structural fire protection

In designing according to the guidelines outlined above concerning economic optimisation of the aggregate total fire protection and fire damage costs, the fire prevention measures and fire fighting services must normally meet a certain minimum standard. In the case of loadbearing structures or partitions, the conditions to be satisfied can be explained with reference to Fig. 2.2a. The figure contains three curves showing the relationship between the required fire resistance period  $T$  and the effective fire load  $q$  for a loadbearing structure or a partition. The curves depend on the ventilation conditions and thermal properties of the fire compartment concerned.

In Figure 2.2a curve 1 describes the fire resistance time for different fire load levels for the heating phase of an undisturbed fire development process. This is the least fire resistance period for which the structure must be designed if its loadbearing or separating function is to be ensured during the heating phase. If the requirement is raised to the effect that the function of the structure affected by the fire must be ensured during the complete fire process, comprising both the heating phase and the subsequent cooling phase, the relationship is expressed by the analogous curve 2. In this case, the required fire resistance time  $T$  for the given fire load  $q$  can be regarded as the equivalent length of a heating phase which produces the same maximum action as the complete fire process which comprises both the heating and cooling phases. In the case of a loadbearing structure, curves 1 and 2 are characterised by the requirement that the loadbearing function

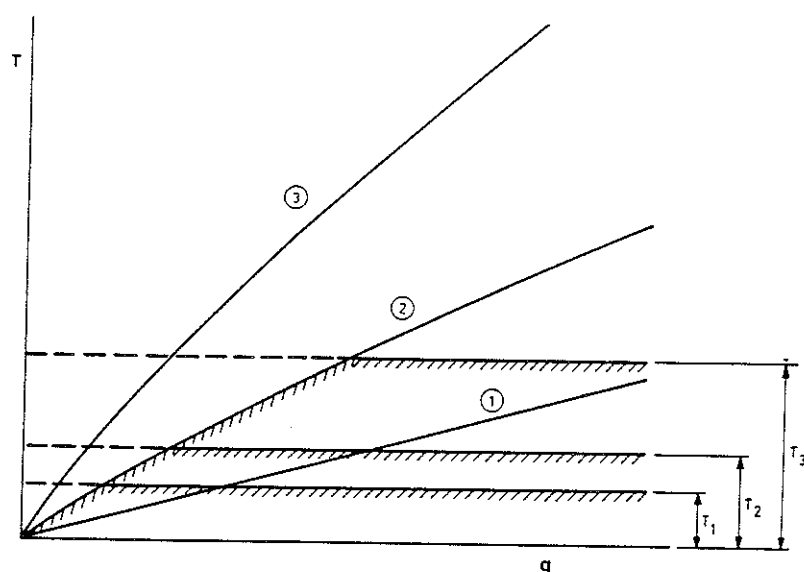


Fig. 2.2 a. Relationship between equivalent fire resistance time  $T$  and effective fire load  $q$  for given fire compartment characteristics and a given type of structure. Curve 1 takes into account only the heating phase of the fire, while Curve 2 also allows for the effect of the cooling phase. The relationship according to Curve 3 applies when stringent requirements are imposed regarding the serviceability of the structure immediately after a fire.  $T_1$  denotes the time required for complete evacuation of people, and  $T_2$  the time required for the evacuation of people combined with partial or complete evacuation of property.  $T_3$  denotes the fire resistance time which is required in view of the safety of e.g. the firemen against collapse of the structure



must be maintained in respect of the static load which may be considered as representative in the event of a fire.

In the case of buildings accommodating activities which are very significant from the economic point of view, it may be justified to raise the fire protection requirement further to a level that ensures that the building can be used again after a fire, either straight away or after repairs of only limited extent, for the intended activity on the same scale as before. An effective way of ensuring this is to endeavour to limit the spread of fire, for instance by installing an automatic sprinkler plant. Another possibility is to raise the fire resistance of the loadbearing structure to such an extent that its original loadbearing capacity is either relatively unchanged at the end of an undisturbed complete fire process, or has not been reduced to such an extent that it cannot be restored to its original state by a moderate amount of work. In Figure 2.2a, curve 3 is taken to correspond to a loadbearing framework whose fire engineering design satisfies this requirement. This requirement has been indicated in terms of an equivalent fire resistance time  $T_1$  defined as the length of a heating phase which produces the same action as the complete fire process comprising both the heating and cooling phases, at the static load which may be regarded representative in the event of a fire. The requirement that the building must be capable of use after a fire must be satisfied for the static load for which the building was originally designed. Fire engineering requirements at the level associated with curve 3 will, in the case of loadbearing structures and partitions impose re-serviceability criteria as a supplement to the more conventional fire resistance criteria.

It is normally a minimum condition which fire prevention and fire fighting measures must satisfy that evacuation of people must be guaranteed in the event of a fire. From the point of view of international regulations, this may imply either complete evacuation of people from the whole building or, as stipulated in the case of very tall buildings, removal of people situated in part of a building which is directly affected by the fire, to a safe place of refuge inside the building. The requirement stipulates that design with respect to separation of fire compartments, sectioning and evacuation routes must be such that the necessary evacuation or removal of people can take place in such a way that there is no risk due to smoke, toxic gases or heat. In the case of a loadbearing structure or partition which is exposed to fire, the requirement that the building must be completely evacuated is equivalent to stipulating that the loadbearing or separating function is to be ensured during the required evacuation time  $T_1$ . In Figure 2.2a, this gives a minimum fire resistance period  $T$  which, as the fire load  $q$  increases, is determined by the curve 2 up to the level  $T_1$  and thereafter by the horizontal line corresponding to the evacuation time  $T_1$ .

In the case of buildings which house vital and particularly expensive equipment and fittings, there may be reason to increase the minimum stipulation applicable to fire prevention and fire fighting measures to such an extent that combined evacuation of people and property is ensured. Such an increased requirement is associated with a requisite evacuation time  $T_2$  which is greater than the time  $T_1$  that relates only to evacuation of people. The requisite fire resistance time  $T$  according to Fig. 2.2a is determined by curve 2 up to the level  $T_2$ , after which it remains constant.

In the case where people must be moved from the part of the building which is exposed to fire to another part of the building, the requirement concerning the minimum fire resistance period  $T$  of the loadbearing structure and partition must be further

intensified. It must be possible for the intended function to be guaranteed with the prescribed factor of safety during the complete fire sequence or during the time  $T_3$  which is needed under the most unfavourable conditions in order that a fire with the actual fire characteristics should be brought completely under control. With reference to Fig. 2.2a, this gives a least fire resistance period  $T$  which, as the fire load  $q$  increases, follows either the curve 2 or curve 3 or some other specified curves between these to the level  $T_3$  and remains thereafter on the horizontal line corresponding to the level  $T_3$ . A requirement concerning the necessary fire resistance at this level can be based, apart from the requirement concerning the safety of people in the building, on a factor of safety against collapse of the loadbearing structure which is stipulated in view of the safety of firemen.

In cases where a structure has a higher residual loadbearing capacity at the end of a fire and the subsequent cooling period than the least loadbearing capacity during fire exposure, then the stipulated fire resistance requirement guarantees the safety of clearance personnel. In the case of structures in which cooling after fire exposure causes further reduction in loadbearing capacity, the requirement concerning the safety of clearance personnel may necessitate a further increase of the required least fire resistance period beyond the level  $T_3$ .

### 2.3 Factors which influence the extent of total fire protection measures

In order that fire prevention and fire fighting measures may in practical cases be designed according to the above principles of overall economic optimisation, knowledge of a large number of often very complicated statistical variables is necessary. Examples of such variables are

- the risk of occurrence of fire
- the risk that a fire will cause flashover in the fire compartment concerned
- the statistical variations in fire load and various types of static loading
- the statistical scatter in fire compartment and fire characteristics
- the statistical variation in material and product properties at different temperatures
- deviations in workmanship, unavoidable in practice, from the specifications and recommendations given in various documents
- the risk that safety regulations set out with regard to fire prevention measures are not complied with in all particulars
- uncertainties in the function of detectors, alarm and extinguisher systems, control systems for smoke and other products of combustion, and evacuation routes

Preliminary estimates of the economic consequences of different types of fire damage are further examples of factors which cause complications. Present know-

ledge of the exemplified variables and factors is very limited and is very far from the stage that it normally enables design of fire protection measures to be carried out in the form of overall economic optimisation. Even if there is very extensive research and development work in this field in the future, it is not realistic to expect that the conditions necessary for a more general application of overall economic design, according to the structure outlined above, will be satisfied over the next few decades.

In spite of this, it is essential that practical design of fire prevention and fire fighting measures according to simplified design procedures should, today and in the future, be carried out with the aim of attaining an overall economic optimum. Overall economic examinations and analyses of experience data obtained gradually, as well as functionally based rational design methods for part problems in the field of fire protection, constitute essential aids in this connection. The rational procedure described in this handbook for the fire engineering design of load-bearing structures and partitions is an example of such a design method for an essential part problem.

The point system introduced in several countries, which defines different levels of safety for fire prevention and fire fighting measures in a qualitative manner, is of great interest in this context. An example which may be mentioned is the Swiss system for classification of buildings into four danger classes (6). In this, by an aggregation of a number of points, each of which has been allocated marks, consideration can be given to

- . the magnitude of the fire load
- . the occurrence of components which burn explosively
- . storey height
- . building height
- . the size of the fire compartment
- . the design of the roof
- . the exposure to fire of parts of the building
- . the number of people in the building
- . the organisation of the fire fighting service and the time taken by this to become operational

Mention may also be made of a systems analysis approach proposed in the USA in 1971 for a qualitative description of the total fire protection system (7). This systems analysis approach, which bears a relationship to the Swiss point system, has the following components

- . detector system
- . warning system
- . the fire resistance of structural components

- sectioning
- evacuation system
- extinguisher system
- control of fire load
- control and inspection to ensure that functions inside the building which are essential in this context are not changed in an unfavourable direction

There is a direct relationship between several of the system components comprised in such an analysis. The fire resistance of structural components - the extent of the extinguisher system relationship is shown schematically in Fig. 2.3 a.

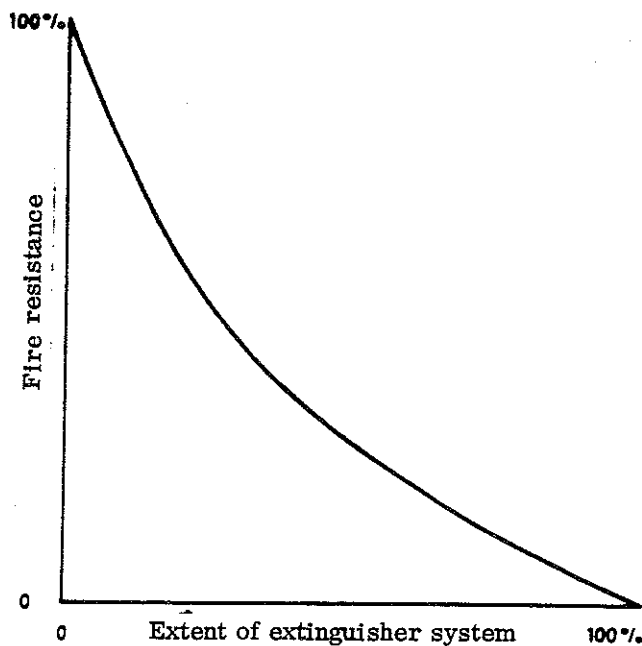


Fig. 2.3 a. Relationship between the system components fire resistance of the load-bearing structure and extent of the fire extinguisher system

This proposal has recently been developed further into a goal oriented system, designed for practical application, for determination of the probability of success in limiting the consequences of a fire, for fires of different sizes. The system, which is built up in the form of a design procedure containing both interchangeable components and components which are of necessity coupled together, can be applied for the fire engineering design of tall buildings (8).

#### 2.4 Performance requirements and loading and safety problems in fire engineering design of loadbearing structures and partitions

According to the current regulations governing fire engineering design of loadbearing structures and partitions, the Swedish Building Regulations SBN, it is to be proved, theoretically or experimentally, that a structure exposed to fire satisfies the stipulated performance requirements with regard to the fire load, fire process and fire duration which apply in the case under consideration.

### 2.4.1 Loadbearing structures

In the case of structures for which performance requirements are stipulated in the SBN, it is specified that the loadbearing capacity of the structure during the heating and cooling phases of the fire under consideration must be shown not to drop below a value which corresponds to a reasonable factor of safety against collapse due to the loads in the actual case. The principle of the relevant safety problem may be summarised in the following way.

The loadbearing structure is acted upon by a load which may be a combination of dead load and live load. This load is subject to a statistical variation. This can be described by means of a frequency function comprising all the values of load to which the building in consideration, or parts thereof, will be subjected during its whole life span. At ordinary room temperatures, the loadbearing capacity of the loadbearing structure is  $B$ , see Figure 2.4.1a. The loadbearing capacity is also subject to a statistical variation which is mainly determined by the scatter in material properties and manufacturing accuracy. This scatter can also be described by a frequency function. During fire exposure, the loadbearing capacity corresponding to ordinary room temperatures is reduced. For a given fire compartment design, this reduction is determined by the fire load  $q$ . The fire compartment is characterised by its geometry and ventilation properties, and by the thermal properties of the surrounding construction. The fire load is subject to a statistical variation with its associated frequency function. Taken together, the frequency functions relating to the loadbearing capacity at ordinary room temperatures and to the fire load form the basis whereby the frequency function relating to the minimum loadbearing capacity during fire exposure,  $B_f$ , is determined. In such a determination, the change to which the scatter in material properties may be subjected as a result of a rise in temperature, must be included. Consideration must also be given to the uncertainty which characterises the calculation of the fire process and the temperature-time field, as well as the loadbearing capacity of the loadbearing structure under fire exposure conditions.

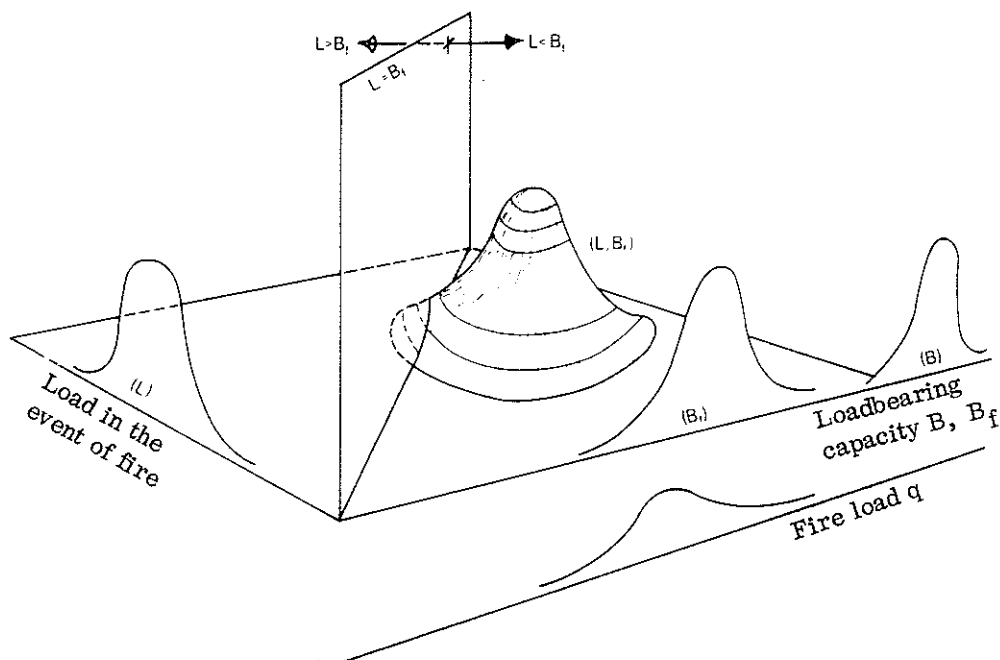


Fig. 2.4.1 a. Illustration of the safety problem in fire engineering design of a loadbearing structure

If the frequency functions relating to the load  $L$  during the fire and to the loadbearing capacity  $B_f$  for the structural design in question, which is reduced as a result of the action of fire, are known and are independent of one another, then the associated risk of failure can be calculated by using a frequency function  $(L, B_f)$ . This is obtained by direct multiplication of the two frequency functions relating to  $L$  and  $B_f$ . As illustrated in Fig. 2.4.1 a, the frequency function  $(L, B_f)$  describes a volume above the horizontal  $L - B_f$  base plane. By means of a vertical plane  $L = B_f$  through the origin, this volume is cut into two parts, and the size of the volume in the region  $L > B_f$  represents the risk of failure of the structure in the event of an undisturbed fire process.

A risk of failure calculated as above corresponds to a probability of 1 that fire will break out and cause flashover in the fire compartment under consideration. The risk of failure must therefore be corrected by multiplying it by the probability that fire will occur and that flashover will take place in the fire compartment. Values given in the literature for this probability are 0.3 for industrial buildings, 0.04 for office buildings and 0.02 for residential buildings with assumed lives of 50 years (9). The above values are applicable to complete buildings of representative average size and not to individual fire compartments in the building. Further essential reductions in the calculated risk of failure will be due, for instance to the arrival of the fire brigade within a certain time, subject to variations in the time of arrival and the extent of operations, and to the presence of detector, alarm and sprinkler systems, with statistical variations in their reliabilities.

A computerised procedure for failure risk analysis according to the principles outlined above is described in (10). This procedure, which is based on the Monte Carlo method, can at present be applied in practice in special cases. The method enables the risk of failure due to fire exposure to be compared with the risks of failure due to other types of action, for instance static loading. A more general application of failure risk analysis in practical fire engineering design is impossible at present due to insufficient knowledge concerning the statistical variables. In spite of this, however, this procedure can already be made use of for the production of information which may facilitate drawing up of code regulations concerning reasonable load and fire load levels to be applied in conjunction with a rational fire engineering design.

From the point of view of safety, the procedure at present applied internationally for fire engineering design of loadbearing structures which must have a stipulated resistance to fire is characterised by the fact that the structure, when exposed to fire of standardised behaviour, must not collapse under the action of the design load in the normal load combination case, the fire being of a duration which is determined by the magnitude of the fire load in question. Such a regulation is also included in the Swedish Building Regulations for the simplified fire engineering design alternative which is associated with classification of buildings and building components. One of the reasons for the acceptance of a formal factor of safety as low as 1 is the awareness of the low level of probability that a fully developed fire will occur, and that full design load will be operative at the time of this fire. Due to these favourable effects, the real factor of safety in the course of a standardised design procedure as outlined above will therefore be appreciably larger than 1. As a temporary solution, the load factors and safety factors set out below can be used for more rational fire engineering design according to the procedure described in this handbook, unless it is shown by means of detailed safety analysis in conformity with the method outlined above that other basic data are more representative statistically. The recommendations can be disregarded and replaced

by the design rules set out in the draft NKB (Nordic Committee on Building Regulations) regulations when these have been approved (11). The load factors and safety factors set out below presuppose that the level of fire load is in accordance with Section 3.2 of this handbook.

- a) Buildings in which complete evacuation of people in the event of fire cannot be assumed

Current Swedish regulations concerning the provision of evacuation routes stipulate that evacuation of people in the event of fire shall at all times be possible. This does not imply, however, that complete evacuation of people is always carried out in conjunction with a fire. In buildings such as larger hotels, blocks of flats, offices etc, it is possible for fire to be in progress in limited parts of the building without complete evacuation of people taking place. In the case of buildings in which complete evacuation of people in the event of fire cannot be assumed with absolute certainty, it must be shown that loadbearing structural components will not collapse due to the most dangerous combination of

dead load

live load, multiplied by the load factor 1.4

snow load, multiplied by the load factor 1.2.

The following values shall be applied for the live load:

Type of premises	Static load		Mobile load	
	kgf/m <sup>2</sup>	{ kN/m <sup>2</sup> }	kgf/m <sup>2</sup>	{ kN/m <sup>2</sup> }
Dwelling and hotel rooms, hospital wards, etc	35	0.35	70	0.70
Offices and schools (classrooms and group study rooms)	35	0.35	100	1.00
Shops, department stores, assembly halls (excl. records rooms and warehouses containing compact stacked loading)	35	0.35	250	2.50

In the case of snow load, the values to be applied for the static and mobile constituents are to be 80% of the values according to current loading regulations.

- b) Buildings in which complete evacuation of people in the event of fire can be assumed

For special types of buildings, complete evacuation of people in the event of fire can be assumed. Typical examples of such buildings are unsectioned single-storey buildings. Even in the case of buildings with two or three storeys, there may be reason in special cases to assume complete evacuation of people in the event of fire. To this end, it is stipulated that the design of the building and the type of activity in the building should be such that complete evacuation of the building in the event of fire is regarded as quite natural. For a building in which complete evacuation of people in the event of fire can be assumed with absolute certainty, the values chosen for fire engineering design are to be the same as in case a)

above, with the difference that the values of live load are to be as follows:

Type of premises	Static load		Mobile load	
	kgf/m <sup>2</sup> {	kN/m <sup>2</sup> }	kgf/m <sup>2</sup> {	kN/m <sup>2</sup> }
Dwelling and hotel rooms, hospital wards, etc	35	0.35	35	0.35
Offices and schools (classrooms and group study rooms)	35	0.35	55	0.55
Shops, department stores, assembly halls (excl. records rooms and warehouses containing compact stacked loading)	35	0.35	70	0.70

In appropriate cases, an estimate is to be made of the local increase in the live load which may occur as a result of people being moved from part of the building which is affected by fire to another part of the building, or in conjunction with the evacuation of the building, and this must be allowed for in design.

The values of loads and load factors set out in a) and b) above may be regarded as temporary values which are substantially on the safe side. On the whole, they provide a level of safety which is the same as that applied internationally and conventionally in conjunction with the more simplified fire engineering design.

#### 2.4.2 Partitions

The performance requirement imposed for partitions implies that these must be impervious to the penetration of flames and also, in the case of certain types of building components, that these must limit the rise in temperature on the unexposed side of the construction, during both the heating phase and the subsequent cooling phase. According to current regulations, the risk of fire spread to the adjacent fire compartment is considered negligible if the average rise in temperature is not greater than 140°C on the side of the construction which is not exposed to fire, and not greater than 180°C over limited areas on the same side. The values of maximum temperature rise of partitions have been taken from internationally valid requirements. These have a limited association with the heating phase of a standardised fire process, and are chosen in such a way that they also allow for a reasonable further rise in temperature which it is considered will occur during the cooling phase (12), (13). In a rational fire engineering design comprising a complete fire process, the temperature criteria must be modified in view of this. If there is a simultaneous change to permitted maximum temperatures instead of temperature rises, the result will be that the average temperature on the side of the partition which is not exposed to fire must not exceed 200°C, and the temperature over limited areas of this side must not exceed 240°C.

On the basis of American investigations, these values of maximum temperature may be regarded safe even when easily ignitable material is placed very near the unexposed side of the partition (13), (14). In special cases, a detailed analysis is recommended.



Such an analysis may comprise determination by means of conventional radiation calculations of the maximum temperature, on the unexposed side of the partition that is acceptable from the point of view of the risk of fire spread. As an auxiliary criterion for the determination of the risk of ignition in adjacent fire compartments, the results of certain British, American and Swedish investigations can be utilised (15) - (17). According to these investigations, spontaneous ignition of dry unpainted wood occurs at a radiation intensity of  $0.8 \text{ cal/cm}^2 \text{ s}$   $\{33 \text{ kW/m}^2\}$ . In the event of combined radiation and short-term exposure to flames, ignition occurs at the considerably lower radiation intensity of  $0.3 \text{ cal/cm}^2 \text{ s}$   $\{13 \text{ kW/m}^2\}$ .

## 2.5 The principles governing fire engineering design of loadbearing structures and partitions by means of classification

The current international procedure for fire engineering design of loadbearing structures and partitions is based on classification of the building components on the basis of fire engineering tests according to a standardised method. Such design is also included in the Swedish Building Regulations as a design alternative.

Fire engineering classification of building components is unambiguously related to a standardised fire which takes place according to a stipulated time curve for the gas temperature during the fire. In the Swedish Building Regulations, this standard fire curve is described by the relationship

$$\vartheta_t - \vartheta_0 = 1325 - 430e^{-0.2t} - 270e^{-1.7t} - 625e^{-19t} \quad (2.5 \text{ a})$$

where  $t$  = time (h)

$\vartheta_t$  = gas temperature at time  $t$  ( $^{\circ}\text{C}$ )  
 $\vartheta_0$  = gas temperature at time  $t = 0$  ( $^{\circ}\text{C}$ )

For the characterisation of the fire resistance of a building component, class designations of the type A15, B15, A30, B30, A60, B60, etc are used. The numeral in the class designation indicates the time in minutes over which the building component must be capable of withstanding a standardised fire test comprising a heating phase with a temperature-time curve according to Equation (2.5 a) and also a subsequent cooling phase, the stipulated requirements regarding the loadbearing, separating, or combined loadbearing and separating functions being satisfied. The numeral in the class designation is thus directly related to the length of the heating phase of the fire test. With regard to the loadbearing function, the requirement normally implies that the building component shall not collapse during the prescribed heating phase and subsequent cooling phase under the action of the design load in the normal load combination case. The letter A in the class designation indicates that the building component consists almost entirely of incombustible materials, and the letter B indicates that the building component contains combustible materials to an extent that is not negligible from the point of view of the fire engineering function. In a standardised fire test for classification purposes, the building component is subjected to a fire action, for instance with regard to the number of sides exposed to fire, that is to the greatest possible extent representative of its use in practice.

A list of products for which there is a fire engineering classification, comprising materials, claddings, surface linings and building components, is published with an annual revision by the National Swedish Board of Physical Planning and Building.

With regard to buildings, Swedish building regulations distinguish between fire resistant buildings, fire retardant buildings, and buildings other than fire resistant or fire retardant. There are detailed regulations regarding fire resistance time, cladding and surface linings, sectioning and provision for evacuation in the event of fire, for the different types.

Whether a building is to be constructed as fire resistant or fire retardant is determined by Section 44 Paragraphs 2 and 3 of the Building Ordinance, which state

Paragraph 2. "A building of two storeys shall, if its area is greater than 200 m<sup>2</sup> and it is not divided by means of fire resistant walls into units not exceeding this size, be constructed in such a way that it may be designated as fire retardant. The same applies to buildings of two storeys which contain more than two flats, if a dwelling room or workroom is provided in the attic".

Table 2.5 a. Stipulated lowest fire resistance time of building components for fire resistant buildings, fire retardant buildings, and buildings other than fire resistant or fire retardant, according to Swedish Building Regulations SBN 67. { The fire load in MJ/m<sup>2</sup> is obtained by multiplying the fire load in Mcal/m<sup>2</sup> by 4.2 }. A new edition of the Swedish Building Regulations will be published in 1975

Building component	In buildings other than fire resistant or fire retardant	In fire retardant buildings	In fire resistant buildings, where the fire load (expressed in Mcal per m <sup>2</sup> of total surface area) is			
			not more than 25	more than 25 but not more than 50	more than 50 but not more than 100	more than 100
	1	2	3	4	5	6
1. Vertical structural elements and structural elements provided for horizontal stability						
a) in buildings of not more than 2 storeys	—	B 30 <sup>a</sup>	B 30 <sup>a</sup>	B 60 <sup>a</sup>	B 120	B 240
b) in buildings of 3 or 4 storeys	—	—	A 30	A 60	A 120	A 240
c) in buildings of more than 4 storeys	—	—	A 60	A 90 <sup>b</sup>	A 180 <sup>c</sup>	A 240
d) in basements situated below the top basement level	A 60	A 60	A 60	A 90	A 180	A 240
2. Horizontal structural elements not provided for horizontal stability, with the exception of roof construction over an attic space not converted into living accommodation, which has a floor with a fire separating function <sup>d</sup>	—	B 30 <sup>a</sup>	B 30 <sup>a</sup>	B 60 <sup>a</sup>	B 120	B 240
3. Non-loadbearing building component with a fire separating function, with the exception of external walls and lintels to apartment doors	—	B 30	B 30	B 60	B 120	B 240
4. Enclosing ceiling and walls for that part of an attic which is used as living accommodation (adjacent to a space that cannot be used for storage or as living accommodation), unless a higher fire resistance is required according to 1 or 3	—	B 30 <sup>e</sup>	B 30 <sup>e</sup>	B 30 <sup>e</sup>	B 60 <sup>e</sup>	B 120 <sup>e</sup>
5. Stairs (flight and landing) with a fire separating function	—	B 30	A 30	A 60	A 120	A 240
6. Stairs with no fire separating function <sup>f</sup>	—	—	A 30	A 30	A 30	A 30
7. Window, door or trapdoor in a building component with a fire separation function, unless the opposite is specially stated	—	B 30	B 30	A 60	A 60	A 60
8. Wall enclosing a ventilation duct (or group of ducts) and refuse chute which passes through a building component with a fire separating function	A 30 <sup>g</sup>	A 30 <sup>h</sup>	A 30	A 30	A 60	A 120
9. Joint fire wall	A 120	A 120	A 120	A 240	A 240	A 240
10. A fire wall other than a joint one	A 120 <sup>e</sup>	A 120 <sup>e</sup>	A 120	A 120	A 180	A 240
11. Fire resistant wall with properties specified in the Building Ordinance, Section 44, Paragraphs 1 and 2	A 60	—	—	—	—	—

<sup>a</sup>In buildings without an attic, or with an attic that cannot be used as a storage space or converted into living accommodation, the stipulated requirements need not be satisfied by a roof construction that is incombustible or is protected against fire from below by means of an ignition resistant lining. It is stipulated in this context that the thermal insulation must consist of incombustible material.

<sup>b</sup>In buildings of not more than 8 storeys, a minimum class of A60 may however be used for floor constructions.

<sup>c</sup>In buildings of not more than 8 storeys, a minimum class of A90 may however be used for floor constructions.

<sup>d</sup>In fire resistant buildings, the floor construction immediately above the basement shall however be of Class A, the numerals applied being those quoted.

<sup>e</sup>Only against a fire from the inside.

<sup>f</sup>The stipulated requirements need not be satisfied by communication stairs inside a fire compartment other than the staircase.

<sup>g</sup>Applies only where it is stipulated that the building component with a fire separating function must be constructed in a class not lower than A60.

<sup>h</sup>A15 in the case where it is not stipulated that the building component with a fire separating function must be constructed in a class not lower than A60.

Paragraph 3. "A building of three or more storeys shall be constructed in such a way that it may be designated as fire resistant. The above also applies in the case of buildings of two storeys, if the following is to be accommodated in the building:

- a) an assembly hall for more than 150 people
- b) a teaching institution for more than 150 students
- c) a hotel or boarding house for more than 50 clients
- d) a hospital, student home or comparable establishment with more than 50 places, or
- e) an industrial firm which usually employs more than 50 people or which, in view of the type of activity, entails a particular fire hazard".

Table 2.5 a which is taken from Swedish Building Regulations SBN 67 gives the required lowest fire resistance time for building components which are comprised in one of the above types of building. For fire resistant buildings in the normal case, e.g. residential and office apartments, schools, hotels, garages for cars, premises containing store rooms for flats, etc, a construction according to column 4 can be chosen without special investigation. The same column can also be used in the case of fire loads higher than  $50 \text{ Mcal/m}^2$  ( $210 \text{ MJ/m}^2$ ) if the conditions are such that it is probable that a fire will have been brought completely under control not later than 60 minutes after the outbreak of fire. For a

Table 2.5 b. Stipulated lowest fire resistance time of building components for fire resistant industrial buildings in conformity with Swedish Building Regulations SBN 67. The tabulated values may be used instead of those given in Table 2.5 a under conditions specified in Swedish Building Regulations. { The fire load in  $\text{MJ/m}^2$  is obtained by multiplying the fire load in  $\text{Mcal/m}^2$  by 4.2 }. A new edition of the Swedish Building Regulations will be published in 1975

Building component	In fire resistant buildings, where the fire load (expressed in Mcal per $\text{m}^2$ of total surface area) is		
	In a building protected by a sprinkler installation		
	not greater than 10 1	not greater than 100 2	greater than 100 3
1. Vertical structural elements and structural elements provided for horizontal stability			
a) in buildings of not more than 2 storeys <sup>a</sup>	B 30	B 60 <sup>b</sup>	B 120
b) in buildings of 3 or 4 storeys	A 30	A 60	A 120
c) in buildings of more than 4 storeys	A 30	A 90	A 180
d) in basements situated below the top basement level	A 30	A 90	A 180
2. Horizontal structural elements not provided for horizontal stability, with the exception of roof construction over an attic space not converted into living accommodation, which has a floor with a fire separating function <sup>a, c</sup>	B 30	B 30 <sup>b</sup>	B 60
3. Non-loadbearing building component with a fire separating function, with the exception of external walls	B 30	B 30	B 60
4. Enclosing ceiling and walls for that part of an attic which is used as living accommodation (adjacent to a space that cannot be used for storage or as living accommodation), unless a higher fire resistance is required according to 1 or 3	B 30 <sup>d</sup>	B 30 <sup>d</sup>	A 30 <sup>d</sup> or B 60 <sup>d</sup>
5. Stairs (flight and landings) with a fire separating function	B 30	A 30	A 60
6. Stairs with no fire separating function <sup>e</sup>	B 15 <sup>b</sup>	B 15 <sup>b</sup>	B 15
7. Window, door or trapdoor in a building component with a fire separating function, unless the opposite is specially stated	B 30	B 30 <sup>b</sup>	B 30
8. Wall enclosing a ventilation duct (or group of ducts) and refuse chute which passes through a building component with a fire separating function	A 30 <sup>f</sup>	A 30 <sup>f</sup>	A 30

<sup>a</sup> In buildings without an attic, or with an attic that cannot be used as a storage space or converted into living accommodation, the stipulated requirements need not be satisfied by a roof construction that is incombustible or is protected against fire from below by means of an ignition resistant lining. It is stipulated in this context that the thermal insulation must be of incombustible material.

<sup>b</sup> At a fire load not greater than  $50 \text{ Mcal per m}^2$  of total surface area, a steel construction which is shown to have a fire resistance of at least 10 minutes at the prevailing fire load and material stresses, will also be approved.

<sup>c</sup> The floor construction immediately above the basement shall however be of Class A, the numerals applied being those quoted.

<sup>d</sup> Only against a fire from the inside.

<sup>e</sup> The stipulated requirements need not be satisfied by communication stairs inside a fire compartment other than the staircase.

<sup>f</sup> A15 in the case where it is not stipulated that the building component with a fire separating function must be constructed in a class not lower than B60.

fire resistant building, a construction according to column 3 can only be employed if it can be shown by statistics representative for this type of building or premises that the design fire load does not exceed  $25 \text{ Mcal/m}^2 \{ 105 \text{ MJ/m}^2 \}$  of surface area.

The fundamental regulations in the Swedish Building Regulations are supplemented by additional regulations for certain types of buildings and premises. As an example of this, Table 2.5 b gives a summary taken from SBN 67 concerning the least fire resistance time of different building components to be met in an industrial building constructed as a fire resistant building. These regulations may be applied instead of the more general regulations set out in Table 2.5 a if, with respect to column 1, it is shown by means of representative statistics or a special investigation that the design fire load does not exceed  $10 \text{ Mcal/m}^2 \{ 42 \text{ MJ/m}^2 \}$  of surface area. As regards columns 2 and 3, these may be applied if the building is protected in an appropriate manner by means of an automatic sprinkler plant. With regard to the fire engineering design of single-storey industrial and warehouse buildings with a loadbearing skeleton of steel, reference should also be made to (18).

## 2.6 The principles governing rational fire engineering design of loadbearing structures and partitions

As an alternative to the comparatively schematic fire engineering design by means of classification, as described in outline in the previous section, the Swedish Building Code permits a design procedure which is functionally better substantiated and more rational. This is based on the gas temperature - time curve relating to the complete fire process. This is determined in the individual case from heat or mass balance equations or in some other way, consideration being given to the combustion characteristics of the fire load, the ventilation characteristics of the fire compartment, and the thermal properties of the structures enclosing the fire compartment and contained in this.

In addition to such more general treatment, SBN 67 also permits a simplified rational procedure for fire compartments with a known opening factor and a fire load whose properties with regard to rate of combustion and radiation are approximately the same as those of wood. The procedure implies that fire engineering design may be carried out on the basis of a time curve for the gas temperature of the fire compartment which is determined according to Fig. 2.6 a on the basis of the opening factor  $A\sqrt{h}/A_t$ . The duration of fire  $T$  is obtained from the relationship

$$T = \frac{qA_t}{25A\sqrt{h}} = \left\{ \frac{qA_t}{105A\sqrt{h}} \right\} \quad (2.6 \text{ a})$$

where  $T$  = duration of fire (min)

$q$  = the fire load ( $\text{Mcal/m}^2 \{ \text{MJ/m}^2 \}$ ) of surface area

$A_t$  = the total internal surface area of the fire compartment ( $\text{m}^2$ )

$A$  = the total opening area ( $\text{m}^2$ )

$h$  = the mean value of the opening height of the openings in the fire compartment, weighted in relation to the opening area concerned (m)

The curves in Fig. 2.6 a are drawn on the assumption that the thermal properties of the constructions enclosing the fire compartment concerned are approximately representative for concrete and brick. In the case of fire compartments whose enclosing structures have different thermal properties, a conversion can be performed by calculating the equivalent values of the opening factor.

With regard to the cooling phase of the fire, Swedish Building Regulations SBN 67 specifies, as a rough approximation, a linear reduction in temperature of  $10^{\circ}\text{C}/\text{min}$ . A different temperature-time relationship may be employed for the cooling phase if this can be shown to be more accurate.

In conformity with development proceeding on an international basis towards rational fire engineering design, one of the consequences of which will be to cut the future need of fire engineering classification, the treatment in the following will concentrate on a design method of the greatest possible functional structure, based on a complete fire process determined by the opening factor  $\sqrt{A_f h}/A_t$  of the fire compartment and the fire load  $q$ . The fire process is characterised by a heating phase according to Fig. 2.6 a and a cooling phase with a temperature-time curve determined on the basis of recent research findings (19), (20). These detailed temperature-time curves for a complete fire process, as shown in Fig. 4.3.3 a and Table 4.3.3 a, will supersede the curves according to Fig. 2.6 a in the new edition of Swedish Building Regulations which will be published in 1975.

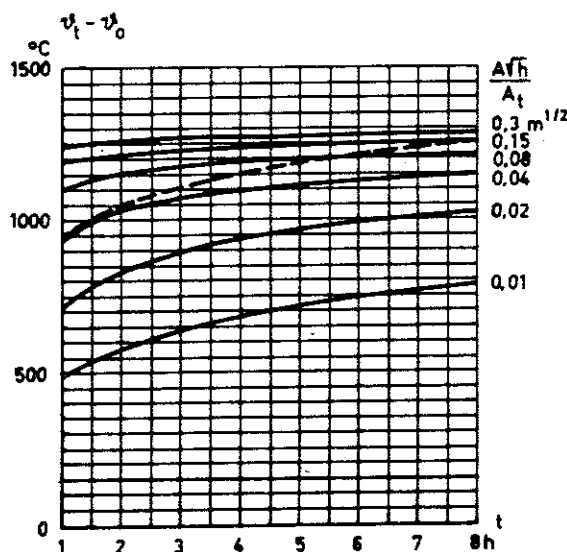
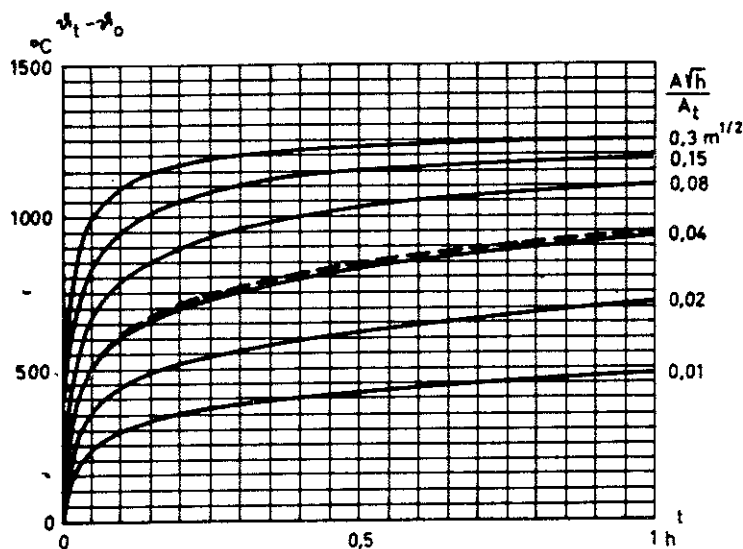


Fig. 2.6 a. Relationship between the fire compartment temperature  $\vartheta_t$  during the heating phase (flame phase) and the time  $t$  according to Swedish Building Regulations SBN 67 for some opening factors  $\sqrt{A_f h}/A_t$  for a fire load mainly of the wood fuel type.  $\vartheta_0$  = fire compartment temperature at time  $t = 0$ . The dashed curve is the standard fire curve according to Equation (2.5 a). A new edition of the Swedish Building Regulations will be published in 1975

For loadbearing structures, a functional rational design method comprises the following essential stages (2), (3), (21) - (32).

- . determination of the magnitude of fire load and the representative combustion characteristics of this
- . determination of the gas temperature-time curve of the fire compartment for the complete fire process on the basis of the actual combustion characteristics, due consideration being given to the volume of the fire compartment, the size and shape of door and window openings, and the thermal properties of the enclosing structures
- . determination of the temperature-time curve for the loadbearing structure affected by the fire, on the basis of the gas temperature-time curve for the fire compartment
- . determination of the minimum loadbearing capacity of the loadbearing structure in conjunction with the appropriate temperature-time curve, or, alternatively, determination of the time when failure occurs at the load in question

For a corresponding fire engineering design of structures which have only a separating function, the last stage is usually omitted.

The various stages of a rational fire engineering procedure according to the above will be dealt with in detail in the following, accompanied by presentation of tables and diagrams which facilitate practical design.

### 3 FIRE LOAD

#### 3.1 Definition of fire compartment and fire load

The fire load is a measure of the quantity of combustible material in a building or fire compartment. A fire compartment is defined as such a delineated part of a building that a fire can freely develop in this without spreading to another part of the building over a period of time specific to the type of premises. The enclosing structures of the fire compartment may contain portions necessary for its function which have a fire resistance lower than that corresponding to this time, e.g. windows and doors. It is stipulated in this context that spread of fire through these parts can be prevented by the action of the fire brigade which arrives on the scene within the normal time, or by some other method.

The maximum permitted size of a fire compartment is regulated by Swedish Building Regulations. It is specified, inter alia, that each dwelling and each office apartment shall be constructed as an independent fire compartment. For hotels it is specified that each room or suite of rooms shall be constructed as a fire compartment, and in the case of hospitals it is prescribed that each ward, operating theatre or similar functional unit shall be placed inside its own fire compartment. With regard to schools, it is stipulated that each teaching room with its ancillary premises, each assembly hall with its ancillary premises, the gymnasium with its ancillary premises, and a separate school dining room together with the kitchen, shall be constructed as a separate fire compartment. In the case of assembly rooms, each assembly room with its ancillary premises shall be placed inside its own fire compartment. Depending on the materials used and the method of construction, each individual room unit can act as a separate fire compartment in practice.

The fire load in a fire compartment is the total quantity of heat released upon complete combustion of all the combustible material contained inside the fire compartment, inclusive of building frame, furnishings, cladding and floor coverings. The fire load per unit area is given by the total internal surface area of the fire compartment, and is calculated from the relationship

$$q = \frac{\sum m_{\nu} H_{\nu}}{A_t} \quad (\text{Mcal/m}^2) \{ \text{MJ/m}^2 \} \quad (3.1 a)$$

where  $m_{\nu}$  = the total weight of each individual combustible material constituent  $\nu$  in the fire compartment (kg)

$H_{\nu}$  = the effective calorific value of each individual combustible material constituent  $\nu$  in the fire compartment (Mcal/kg) { MJ/kg }

$A_t$  = the total internal surface area of the fire compartment (walls, floor and ceiling) (m<sup>2</sup>)

The effective calorific value of some solid, liquid and gaseous materials is set out in Table 3.1 a (32).

The calculation of the fire load using Equation (3.1 a) for a hotel room which is statistically representative of Swedish conditions is illustrated in Fig. 3.1 a.

**Table 3.1 a.** The effective calorific value  $H$  in Mcal/kg of some solid, liquid and gaseous materials. { The effective calorific value in MJ/kg is obtained by multiplying the tabulated values by 4.2 }

### Solids

Anthracite	7.6-8.7	Leather	4.0-5.0	Rubber	
Asphalt	9.5	Linoleum	5.0	Foam rubber	7.6
Cellulose	3.6	Masonite	4.8	Gutta-percha	10.7
Charcoal	7.2	Paper and cardboard	3.8-4.2	Rubber waste	5.0
Clothes	4.0-5.0	Paraffin wax	11.2	Silk	4.0-5.0
Coal	7.0	Plastics		Straw	4.1
Coke	6.6-8.2	Acrylic resins	6.4	Wood	4.1-4.7
Cork(Grade SP)	8.3	Celluloid	4.5	Wool	5.5
Cork(Grade F)	7.3	Polyester	5.6-6.9		
Cotton	4.2	Polyethylene	11.0		
Dynamite(75%)	1.3	Polystyrene	8.6-9.8		
Grain	4.0	Expanded polyurethane	6.0-6.9		
Grease	9.5	Polyvinyl chloride(PVC)	4.4-5.2		
Kitchen refuse	2.0-5.0	Expanded urea-formaldehyde	2.9-3.6		

The above values apply for materials in the dry state. The following relationship applies for the calorific value  $H_F$  (Mcal/kg) of moist materials:

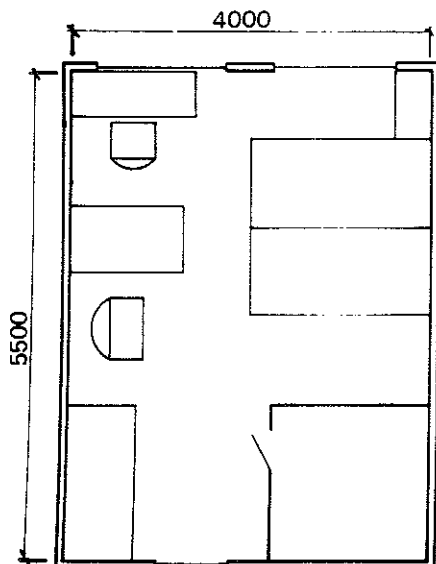
$$H_F = H(1 - 0.01 F) - 0.006 F \quad F = \text{moisture content of material in \% by weight}$$

### Liquids

Crude oil	10.3
Diesel oil	9.7-10.1
Linseed oil	9.4
Paraffin	9.8
Petrol	10.4
Spirits	7.6-8.2
Tar	9.0

### Gases ( $H$ in Mcal/m<sup>3</sup> n)

Acetylene	13.6
Carbon monoxide(CO)	3.0
Coal gas	4.0
Hydrogen	34.0



	$m_v$ (kg)	$H_v$ (Mcal/kg)	$m_v H_v$ (Mcal)
Beds (wood)	90	4.4	395
(textiles)	24	4.5	108
(plastics)	15	7.6	114
Headboards	32	4.4	141
Bedside tables	5	4.4	22
Table	9	4.4	40
Desk	18	4.4	79
Chairs	15	4.4	66
Wardrobe	46	4.4	202
Doors	15	4.4	66
Carpet	43	4.5	193
Soft furnishings	7	4.5	32
Paper	6	4.0	24
Others	10	4.5	45

$$\Sigma m_v H_v = 1527 \text{ Mcal}$$

$$A_t = 2 \cdot 4.00 \cdot 5.50 + 2.85 \cdot 2(4.00 + 5.50) = 98 \text{ m}^2$$

$$q = 15.6 \text{ Mcal/m}^2 \quad \{65.2 \text{ MJ/m}^2\}$$

**Fig. 3.1 a.** Example of fire load calculation for a hotel room



The design fire load for a certain building can be determined by direct calculation of the fire load according to the above. This necessitates however that the types and quantities of the furniture and fittings in the building should be relatively well known. In this context, the consequences of laying down the fire load far too rigidly must also be borne in mind. Far too rigid specification of the level of fire loading may result in certain drawbacks in the event of future alterations and rearrangements in the building. It is therefore often more convenient to determine the design fire load on the basis of statistical investigations concerning the magnitude of the fire load for the type of building or premises in question. This procedure also agrees with the procedure employed in determining the design live load.

### 3.2 Statistical determination of the fire load in different types of buildings

Statistical investigations have been carried out in order to determine the magnitude of the fire load, and results are at present available in respect to the following types of buildings

- dwellings
- office buildings
- schools
- hospitals
- hotels

One of the ways in which these results are given is the histogram. From these histograms, the fire load which represents a certain statistic level can be determined. This means that a certain percentage of the total statistical population has a fire load that is lower than this fire load.

The design fire load recommended is the value which applies in 80% of the cases for the type of building or premises concerned. This level of fire load in combination with the loads and load factors for static loads which are recommended in Subsection 2.4.1 provides, on the whole, a level of safety which is the same as that obtained in conjunction with the conventional standardised fire engineering design which is employed internationally.

Table 3 a in the Design Section gives a summary of the mean value and standard deviation of the fire load, and of the fire load which applies in 80% of the cases for the building types set out above. As a rule, only the fire load due to furniture and fittings is given. The increment in fire load due to the building frame and other fixed components such as floor coverings can be controlled by the designer, and calculated in each individual case by means of Equation (3.1 a).

### 3.2.1 Dwellings (33)

Histograms for the magnitude of the fire load in two and three-room flats are shown in Figs. 3.2.1 a and 3.2.1 b. Both a minimum fire load which includes only easily ignitable fire load components, and also a maximum fire load comprising the total fire load, are given in the Figure. In the histograms in Figs. 3.2.1 a and b the fire load due to the floor covering is not included (see Section 3.3).

An extensive theoretical and experimental investigation of the fire load in dwellings has shown that ignition and complete combustion of the fire load components which ignite less readily does not occur if the minimum fire load is less than about  $15 \text{ Mcal/m}^2$   $\{63 \text{ MJ/m}^2\}$  (33). If the minimum fire load is less than this value, the actual fire load is therefore represented by the curve for the minimum fire load. If, on the other hand, the minimum fire load is greater than about  $15 \text{ Mcal/m}^2$   $\{63 \text{ MJ/m}^2\}$ , the heavier and more compact fire load components will also be ignited. In such a case the actual effective fire load must be based on the curve for the maximum fire load, unless more detailed information is available regarding the actual degree of combustion of the more compact fire load components.

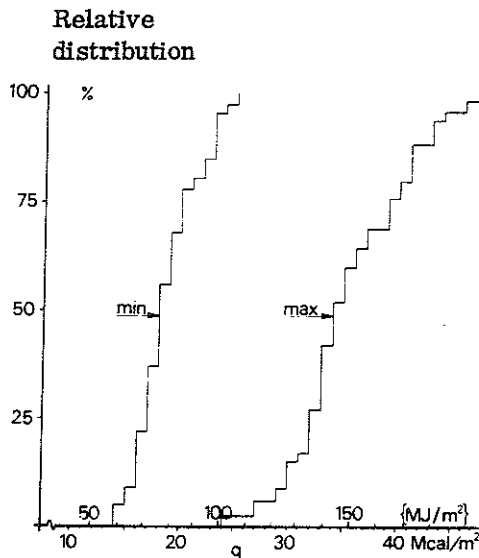


Fig. 3.2.1 a. Histograms for the magnitude of the fire load  $q$  in two-room flats. The fire load due to the floor covering is not included. The minimum histogram refers only to easily ignitable fire load components, while the maximum histogram refers to the total fire load

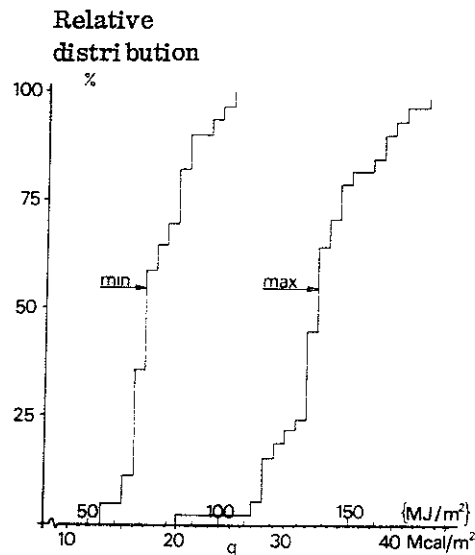


Fig. 3.2.1 b. Histograms for the magnitude of the fire load  $q$  in three-room flats. The fire load due to the floor covering is not included. The minimum histogram refers only to easily ignitable fire load components, while the maximum histogram refers to the total fire load

### 3.2.2 Office buildings (34)

Histograms relating to the magnitude of the fire load in office buildings are shown in Figs. 3.2.2 a - 3.2.2 f. Only the fire load due to furniture and fittings has been included.

A rough division has been made into two different categories of office premises namely office premises mainly engaged in technical work such as architects' offices, design offices, etc and office premises mainly engaged on economic activity, such as insurance offices, bank offices, etc. Histograms are given for both these categories and also for the whole of the statistical material, the fire load being referred to the total enclosing surface area of the office rooms and also to the floor area of the office premises. The reason why the fire load is referred both to the surface area and the floor area is as follows. Regulations stipulate

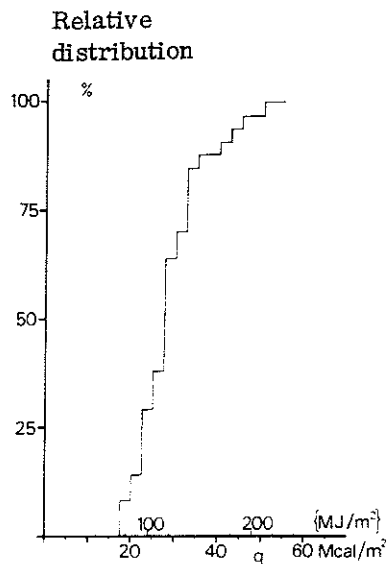


Fig. 3.2.2 a. Histogram for the magnitude of the fire load  $q$  in technical offices, referred to the total area of the enclosing surfaces. The fire load comprises only furniture and fittings

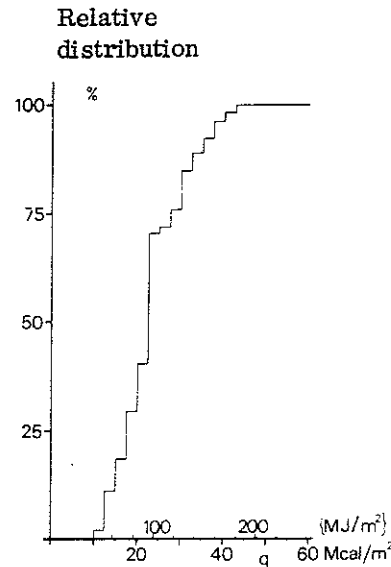


Fig. 3.2.2 b. Histogram for the magnitude of the fire load  $q$  for economic offices, referred to the total area of the enclosing surfaces. The fire load comprises only furniture and fittings

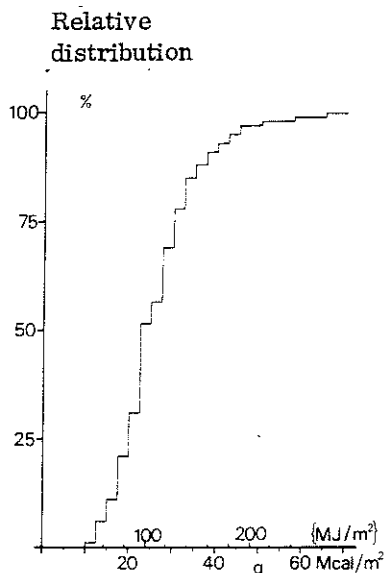


Fig. 3.2.2 c. Histogram for the magnitude of the fire load  $q$  for all the office premises in the statistical investigation, referred to the total area of the enclosing surfaces. The fire load comprises only furniture and fittings

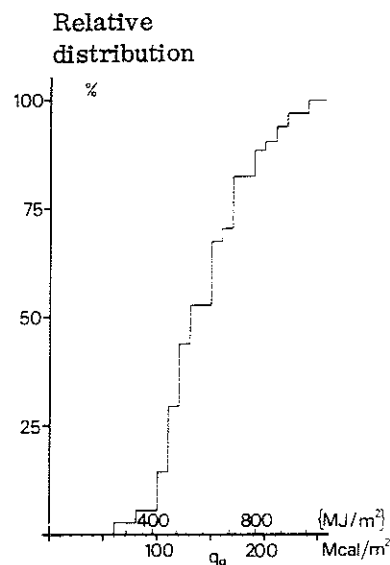


Fig 3.2.2 d. Histogram for the magnitude of the fire load  $q_g$  in technical offices, referred to the floor area of the office. The fire load comprises only furniture and fittings

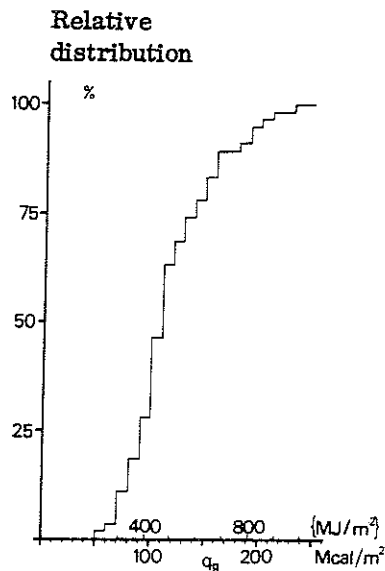


Fig. 3.2.2 e. Histogram for the magnitude of the fire load  $q_g$  in economic offices, referred to the floor area of the office. The fire load comprises only furniture and fittings

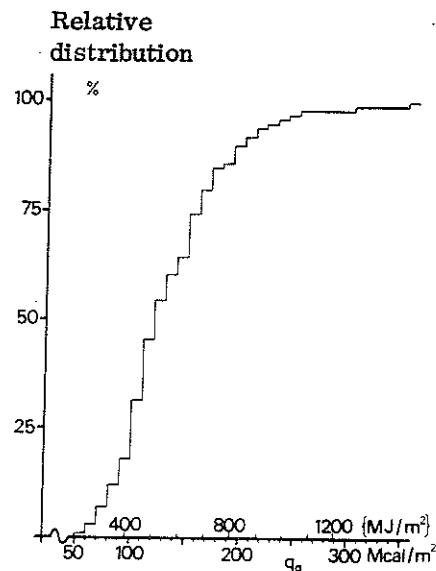


Fig 3.2.2 f. Histogram for the magnitude of the fire load  $q_g$  for all the office premises in the statistical investigation, referred to the floor area of the offices. The fire load comprises only furniture and fittings

that each office apartment should be constructed as a separate fire compartment. In the statistical investigation difficulties were however experienced in determining the surface area of the fire compartment according to regulations. Furthermore, the partition walls between individual office rooms are often constructed of such materials and in such a way in modern office buildings that they satisfy the fire resistance requirements for partitions in office premises. In such cases the fire load as referred to the surface area of the office room can be used in the design. When division into fire compartments is made arbitrarily the histograms with the fire load referred to the floor area can be used in converting the fire load into fire load per  $m^2$  of surface area.

### 3.2.3 Schools (35)

Histograms relating to the magnitude of the fire load in schools are shown in Figs. 3.2.3 a - 3.2.3 d. Separate histograms are given for the junior level, intermediate level and senior level of the compulsory 9-year comprehensive school, and also for the whole statistical material aggregated. Only the fire load due to furniture and fittings has been included.

### 3.2.4 Hospitals (26), (32)

A histogram relating to the magnitude of the fire load in hospitals is shown in Fig. 3.2.4 a. The values include combustible materials in wall coverings and floor coverings.

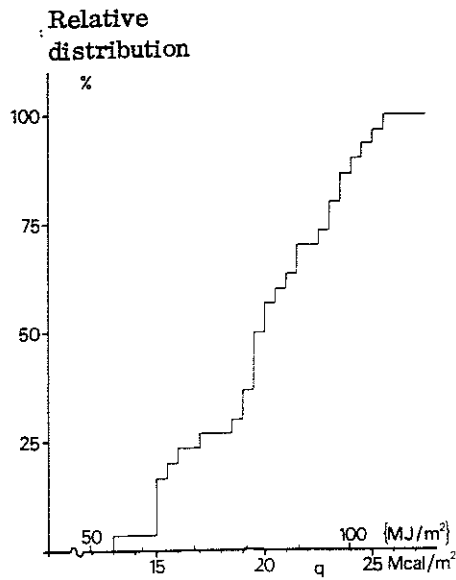


Fig 3.2.3 a. Histogram for the magnitude of the fire load  $q$  in junior level schools. The fire load comprises only furniture and fittings

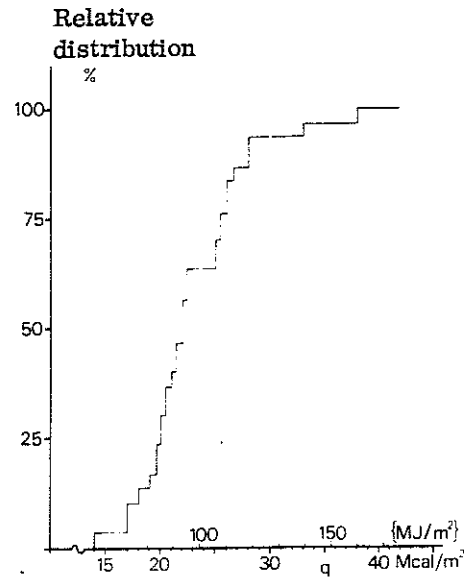


Fig. 3.2.3 b. Histogram for the magnitude of the fire load  $q$  in intermediate level schools. The fire load comprises only furniture and fittings

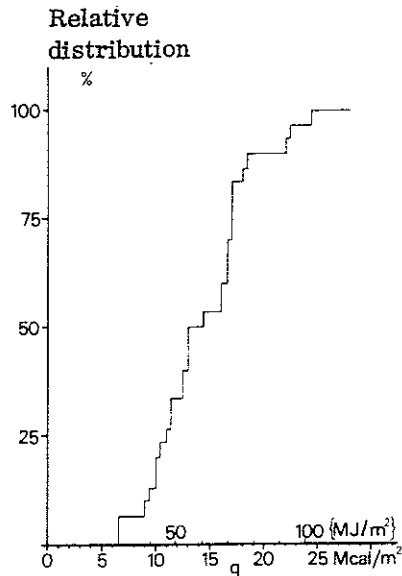


Fig. 3.2.3 c. Histogram for the magnitude of the fire load  $q$  in senior level schools. The fire load comprises only furniture and fittings

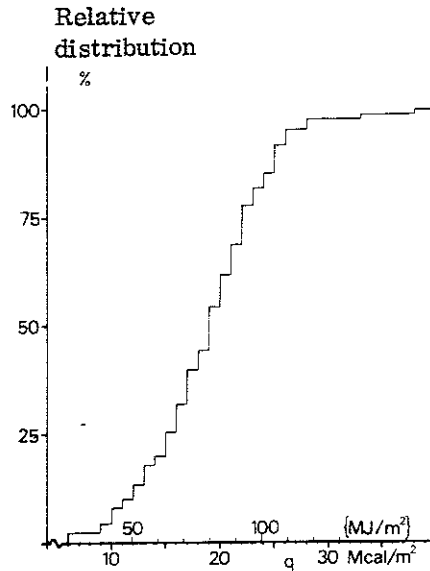


Fig. 3.2.3 d. Histogram for the magnitude of the fire load  $q$  in all the school premises in the statistical investigation. The fire load comprises only furniture and fittings

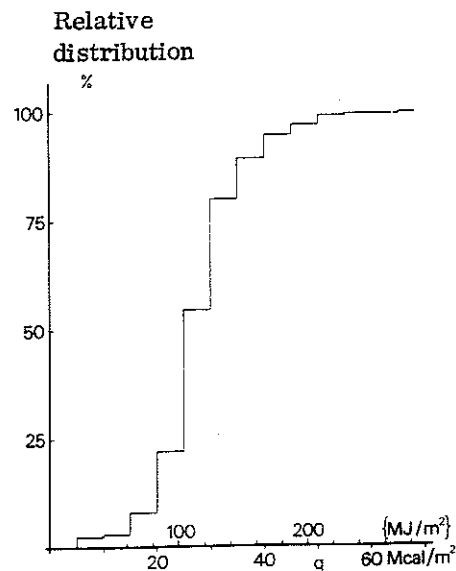


Fig. 3.2.4 a. Histogram for the magnitude of the fire load  $q$  in hospitals. The values include combustible materials in wall coverings and floor coverings

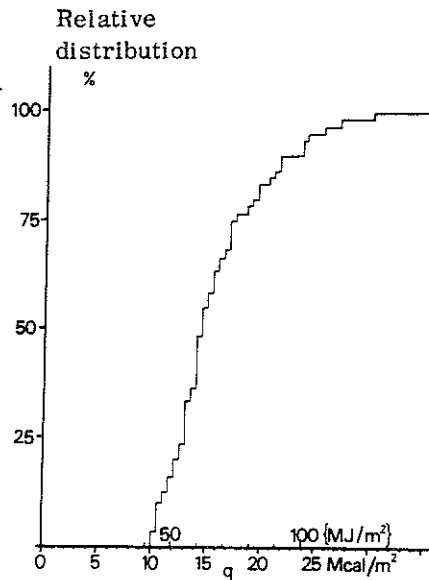


Fig. 3.2.5 a. Histogram for the magnitude of the fire load  $q$  in hotel buildings. The fire load comprises only furniture and fittings

### 3.2.5 Hotels (35)

A histogram relating to the magnitude of the fire load in hotel buildings is shown in Fig. 3.2.5 a. Only the fire load due to furniture and fittings has been included.

### 3.2.6 Other premises and buildings

In regard to other premises and buildings, there is at present insufficient statistical data for the preparation of histograms for the magnitude of the fire load. For these, calculation of the fire load must be carried out in each individual case according to Equation (3.1 a) on the basis of an assessment of the composition of furniture and fittings in the premises or building. Alternatively, the design fire load may be given a value that is probably the same as, or in excess of, the fire load which applies to 80% of the cases for the type of building or premises in question. Examples of premises and buildings which usually have a very low fire load are open multistorey car parks (36), swimming baths and ice rinks.

## 3.3 The actual degree of combustion and uneven distribution of the fire load

As a rule, complete combustion of all combustible material in a fire compartment does not take place during a fire. This can be taken into account in the course of calculation by using a factor which indicates the actual degree of combustion of each fire load component, and by characterising the fire load in a more detailed manner than in Equation (3.1 a). The relationship employed (28) is

$$q = \frac{\sum \mu_{\nu} m_{\nu} H_{\nu}}{A_t} \quad (3.3 a)$$

where  $\mu_{\nu}$  = a non-dimensional factor with a value between 0 and 1 which indicates the actual degree of combustion for each fire load component  $\nu$

Bookcases and floor coverings are examples of fire load components whose actual degree of combustion is low, and whose  $\mu$  values are probably appreciably below unity. At present, however, there is a lack of experimentally substantiated and verified  $\mu$  values to the desired extent, and it is therefore usually necessary in the course of practical design to employ a fire load characterisation according to the more schematic relationship in Equation (3.1 a). Calculation of the fire load according to Equation (3.1 a) will thus in many cases result in an not inconsiderable overestimation of the actual effective fire load.

As a rule, the fire load is not uniformly distributed inside the fire compartment. Owing to the violent turbulence which develops during a fire, however, a moderate lack of uniformity in distribution does not give rise to temperature differences of practical significance in different parts of the fire compartment. If, on the other hand, distribution of the fire load is very uneven, then certain structural components in the fire compartment will be subjected to higher temperatures than others. A fire load of extremely uneven distribution which may cause unforeseen temperature effects in certain structural components is regarded as a form of excessive action and is to be treated in conformity with the regulations of the National Swedish Board of Physical Planning and Building concerning excessive action and progressive collapse (37).

## 4 THE TEMPERATURE - TIME PROCESS IN THE FIRE COMPARTMENT

### 4.1 General characterisation of the fire process

A fire entails a complex interaction between several mechanical and heat transfer processes and a large number of chemical reactions. The nature of many of the physical and chemical phenomena which occur is far from clear, even in conditions where they are examined in isolation. Essential combustion characteristics for usual types of fire loads are not available. In the case of wood fuel, for instance, we have no knowledge of the principles governing conversion of the loss in weight of the wood in kg per unit time into the heat released during different phases of the fire process. In spite of these difficulties, various models have been constructed over the past decade for theoretical treatment of the fire process. One of the aims has been to facilitate such reliable calculation of the temperature-time curve of the fire process that the results can be used for rational fire engineering design. The principal criterion in this context has been that the analytical model should, in practical application, provide an acceptable description of the temperature-time field and mode of action of structural components when these are exposed to the action of fire. On the other hand, it has been found impossible so far to construct an analytical model for the fire process which will also provide an acceptable description of e. g. the gas temperature-time curve of the fire process for all types of fire. However, in relation to a complete design procedure for loadbearing structures or partitions under fire exposure conditions, this is not of critical significance.

Some of the essential factors which must be taken into consideration by an analytical model for the fire, which is to be capable of practical use in rational fire engineering design, are

- . the quantity and type of combustible material in the fire compartment
- . the form and method of storage of the combustible material
- . the distribution of the combustible material in the fire compartment
- . the quantity of air supplied per unit of time
- . the geometry of the fire compartment, i. e. the areas of the floor, walls, ceiling and the openings
- . the thermal properties of the structural components which enclose the fire compartment

Owing to the complexity of the fire process, certain approximations must be made. Of the factors enumerated above, it is chiefly the second and third which are at present difficult to describe in an analytical model. As regards the third factor, it is generally assumed that the entire fire compartment attains the same temperature, and this assumption is well satisfied in the case of fire compartments of normal room geometry. Fire tests namely show that, owing to the violent turbulence which occurs during a fire, the temperature differences in such fire compartments are fairly small. In the case of fire compartments of very large extent and very unevenly distributed fire load, and also in the case of fire compartments of great depth in which ventilation is concentrated to one of the short sides,



however, it is likely that the condition relating to uniformity of temperature in the whole fire compartment cannot at all times be considered satisfied (see also Section 3.3).

The problem of taking into account in an analytical model the second of the factors enumerated above is associated with the fact that a fully developed fire process consisting of ignition phase, flame phase and cooling phase (Fig. 4.1 a) can be roughly classified as one of two types (20), (38) - (40), (67), (68), (70) - (72). For one of these types, the rate of combustion during the flame phase is determined by the ventilation in the fire compartment, the mean rate of combustion of the flame phase,  $R_m$ , being proportional to the air flow factor  $A\sqrt{h}$

$$R_m = k A \sqrt{h} \quad (\text{kg/h}) \quad (4.1 a)$$

where  $k$  = a constant which depends on, and can be calculated from, the chemical composition of the fuel ( $\text{kg/h m}^{5/2}$ )

$A$  = the total opening area of the fire compartment ( $\text{m}^2$ )

$h$  = the mean height of the fire compartment openings (m)

Equation (4.1 a) holds if the surface area  $A_q$  of the fuel which is exposed to fire has a certain minimum size in relation to the magnitude of the air flow factor  $A\sqrt{h}$ , i.e. if the ratio  $A_q/A\sqrt{h}$  exceeds a certain value, the rate of combustion is controlled by the air supply. If this is satisfied, then  $R_m$  is not influenced to any significant extent by the magnitude of the fire load or its porosity. This type of fire is referred to as a ventilation controlled fire.

In the second type of fire process, all the inflowing air is not used up for combustion. As a result, ventilation of the fire compartment ceases to be the limiting factor for the mean rate of combustion  $R_m$ ; and this has a lower value than that obtained by means of Equation (4.1 a). It is then the properties of the combustible material, primarily its quantity but also its particle shape and method of storage, which determines the value of  $R_m$ . This type of fire is referred to as fire load controlled fire.

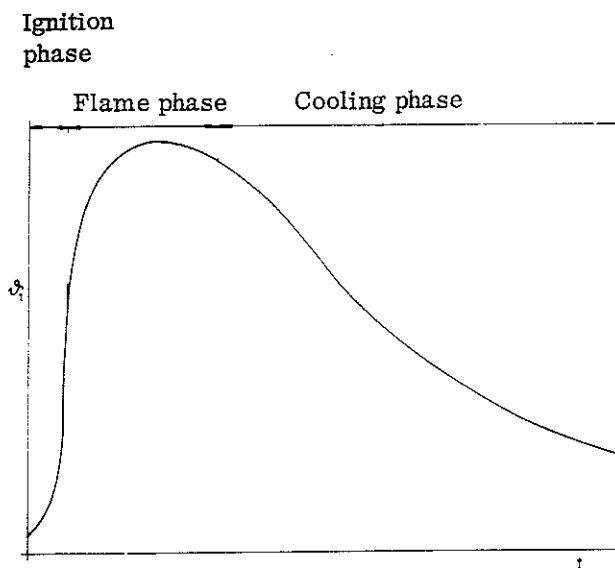


Fig. 4.1 a. The phases of the fire process.  $\theta_t$  = gas temperature,  $t$  = time

Fig. 4.1 b shows an experimentally determined relationship between the mean rate of combustion  $R_m$  during the flame phase and the air flow factor  $A\sqrt{h}$  or the opening factor  $A\sqrt{h}/A_t$ , for different values of the fire load  $q_g$  in  $\text{kg}/\text{m}^2$  of floor area (39). Here,  $A_t$  is the total internal surface area of the fire compartment, including the area of openings. The fire load consists of a wood crib. For wood, the value of the constant  $k$  in Equation (4.1 a) is in the range 300-360 ( $\text{kg}/\text{h m}^{5/2}$ ). It is seen from Fig. 4.1 b how  $R_m$  increases with  $q_g$  for a certain value of  $A\sqrt{h}$  within the fire load controlled region, until it ultimately attains a limiting value corresponding to a ventilation controlled fire.

For a fire load of a given size, particle shape and storage density, a fire becomes ventilation controlled when the opening factor is less than a certain limiting value. For opening factors below this limiting value, the rate of combustion is proportional to the size of the opening factor. On the other hand, for opening factors greater than this limiting value, the rate of combustion does not increase in proportion to the opening factor, the reason being that the maximum rate of growth of the carbon layer which applies in a given case, has been reached. The rate of combustion of the fire is now fire load controlled. The limiting value of the opening factor varies with the size, particle shape and storage density of the fire load. For a given particle shape and storage density, this limiting value increases as the magnitude of the fire load increases. Furthermore, for a given fire load, the less compact the fire load is, the greater the limiting value.

The present state of knowledge is far too limited for a reasonably reliable calculation of the rate of combustion, in the case of a fire load controlled fire based on a realistic fire load of furniture and other fittings, to be possible. This is due primarily to the difficulty of defining the method of storage and the particle shape for such a fire load. The gas temperature-time curves set out in the next

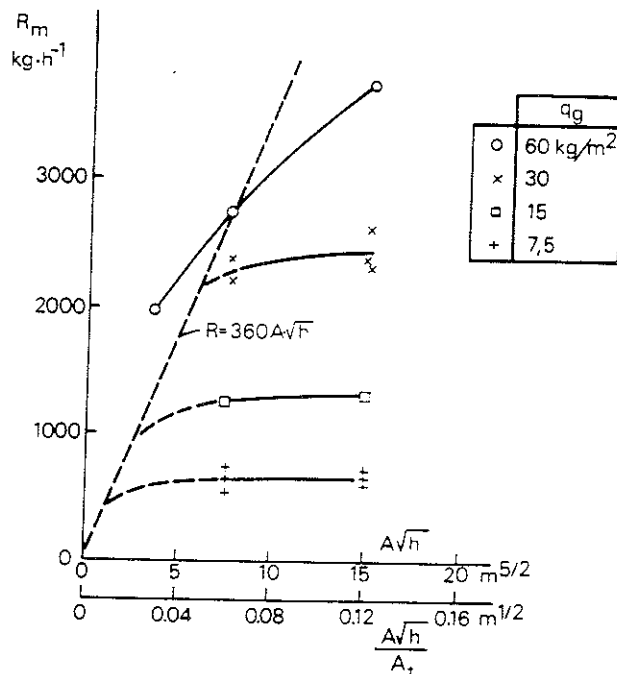


Fig. 4.1 b. Relationship between the mean rate of combustion  $R_m$  ( $\text{kg}/\text{h}$ ) during the flame phase of the fire and the air flow factor  $A\sqrt{h}$  ( $\text{m}^{5/2}$ ) or the opening factor  $A\sqrt{h}/A_t$  ( $\text{m}^{1/2}$ ). The results of full-scale experiments with a fire load consisting of a wood crib of 4.5 cm thick slats (39). The fire load  $q$  is given in  $\text{kg}$  of wood/ $\text{m}^2$  floor area

Section, on which the rational fire engineering design method presented in this handbook is based, have therefore generally been calculated on the assumption that the fire is controlled by ventilation during the flame phase. In consequence, the rate of combustion is independent of the size of fire load, its storage density and particle shape, being dependent only on the size of the opening factor. The calculated maximum temperature in a steel construction exposed to fire is higher if the calculation is based on a gas temperature-time curve determined on the assumption that the fire is ventilation controlled than if the calculation is based on a curve for a fire load controlled fire. If, therefore, a fire is really controlled by the fire load, rational fire engineering design of a steel construction on the basis of the simplified assumption that the fire is controlled by ventilation, gives rise to results on the safe side. Overdesign is however comparatively small in normal cases. Reference should also be made to the discussion set out in Section 4.4.

#### 4.2 Calculation of the temperature-time curves of the combustion gases for an arbitrarily chosen type of fire load

##### 4.2.1 Heat balance equations

It was not until the sixties that models for calculation of the gas temperature-time curve of a fire compartment were developed. In the first projects, a study was made of the energy balance during a fire based on wood as fuel, and the expressions constructed for the terms in the heat balance restricted treatment to the flame phase of the fire (41), (42). A procedure is presented in the following which makes it possible to calculate the gas temperature-time curve of the complete fire process, i.e. both the flame phase and cooling phase, for any fire load (19), (20). The theoretical treatment is based on the fact that it is possible to construct a relationship which, for each time  $t$ , describes the balance between the heat energy produced and consumed per unit time in the fire compartment in question. In its full form, this heat balance relationship reads

$$I_C = I_L + I_W + I_R + I_B \quad (4.2.1a)$$

where  $I_C$  = the heat released during combustion  
 $I_L$  = the heat removed due to the replacement of hot gases by cold air  
 $I_W$  = the heat dissipated to and through the wall, ceiling and floor structures  
 $I_R$  = the heat dissipated by radiation through openings in the fire compartment  
 $I_B$  = the quantity of heat stored in the gas volume in the fire compartment per unit time

This Equation is illustrated schematically in Fig. 4.2.1 a. The treatment is based on the following simplifying assumptions

- combustion is complete and takes place exclusively inside the fire compartment

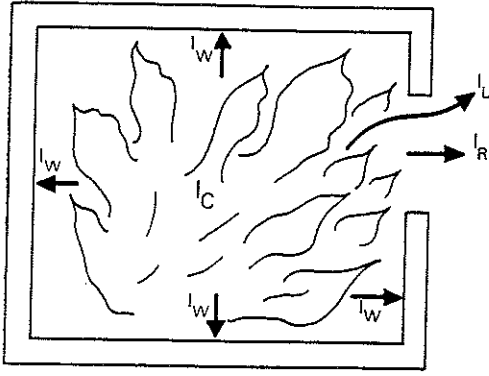


Fig. 4.2.1 a. Illustration of the heat balance in the fire compartment, Equation (4.2.1 a)

- at every instant, the temperature is uniformly distributed within the entire fire compartment
- at every instant, the surface coefficient of heat transfer for the internal enclosing surface of the fire compartment is uniformly distributed
- the heat flow to and through the enclosing structures is unidimensional and, with the exception of any door and window openings, is uniformly distributed for each type of enclosing structure

#### 4.2.2 Brief treatment of the terms comprised in the heat balance equation

##### 4.2.2.1 The term $I_B$

In comparison with the other heat quantities in conjunction with a fire, the quantity of heat that can be stored in the gas volume in the fire compartment is of subordinate significance. This quantity of heat,  $I_B$ , can therefore safely be ignored.

##### 4.2.2.2 The term $I_R$

The quantity of heat  $I_R$  which is dissipated by radiation through the openings in the fire compartment can be calculated using the Stefan-Boltzman law

$$I_R = A(E_g - E_0) \quad (\text{kcal/h}) \{ \text{W} \} \quad (4.2.2.2 \text{ a})$$

where  $A$  = the total area of the openings in the fire compartment ( $\text{m}^2$ )

$$E_g = 4.96 \left( \frac{\vartheta_t + 273}{100} \right)^4 \quad (\text{kcal/h m}^2) \quad (4.2.2.2 \text{ b})$$

$$E_g = 5.77 \left( \frac{\vartheta_t + 273}{100} \right)^4 \quad \{ \text{W/m}^2 \}$$

$$E_0 = 4.96 \left( \frac{\vartheta_0 + 273}{100} \right)^4 \quad (\text{kcal/h m}^2)$$

$$E_0 = 5.77 \left( \frac{\vartheta_0 + 273}{100} \right)^4 \quad \{ \text{W/m}^2 \} \quad (4.2.2.2 \text{ c})$$

$\vartheta_t$  = the gas temperature in the fire compartment ( $^{\circ}\text{C}$ )  
 $\vartheta_o$  = outside temperature ( $^{\circ}\text{C}$ )

#### 4.2.2.3 The term $L_W$

The quantity of heat  $L_W$  which dissipate per unit time to and through the structures enclosing the fire compartment can be determined by solving the general thermal conduction equation for unidimensional nonsteady thermal conduction, consideration being given to the temperature dependence of the thermal material properties, vaporisation of contained water, as well as any structural changes which may occur in the materials comprised in the enclosing structures.

The thermal conduction equation reads as follows

$$c\gamma \frac{\partial \vartheta}{\partial t} = \frac{\partial}{\partial x} \left( \lambda_x \frac{\partial \vartheta}{\partial x} \right) \quad (4.2.2.3a)$$

where  $c$  = specific heat capacity                       $\vartheta$  = temperature  
 $\gamma$  = density     $t$  = time  
 $\lambda_x$  = thermal conductivity                               $x$  = positional coordinate

The enclosing wall, ceiling and floor structures are divided into  $n$  layers, the term  $\Delta x_k$  indicating the thickness of a layer  $k$ . Over a time interval  $\Delta t$  of the fire, the thermal conduction equation gives the following expressions for the different layers (see Fig. 4.2.2.3 a)

$$\begin{aligned} \Delta x_1 c(x, \vartheta) \gamma \frac{\Delta \vartheta_1}{\Delta t} &= \frac{1}{\frac{1}{\alpha_i(\vartheta)} + \frac{\Delta x_1}{2\lambda(x, \vartheta)}} (\vartheta_t - \vartheta_1) - \frac{1}{\frac{\Delta x_1}{2\lambda(x, \vartheta)} + \frac{\Delta x_2}{2\lambda(x, \vartheta)}} (\vartheta_1 - \vartheta_2) \\ \Delta x_k c(x, \vartheta) \gamma \frac{\Delta \vartheta_k}{\Delta t} &= \frac{1}{\frac{\Delta x_{k-1}}{2\lambda(x, \vartheta)} + \frac{\Delta x_k}{2\lambda(x, \vartheta)}} (\vartheta_{k-1} - \vartheta_k) - \frac{1}{\frac{\Delta x_k}{2\lambda(x, \vartheta)} + \frac{\Delta x_{k+1}}{2\lambda(x, \vartheta)}} (\vartheta_k - \vartheta_{k+1}) \\ \Delta x_n c(x, \vartheta) \gamma \frac{\Delta \vartheta_n}{\Delta t} &= \frac{1}{\frac{\Delta x_{n-1}}{2\lambda(x, \vartheta)} + \frac{\Delta x_n}{2\lambda(x, \vartheta)}} (\vartheta_{n-1} - \vartheta_n) - \frac{1}{\frac{\Delta x_n}{2\lambda(x, \vartheta)} + \frac{1}{\alpha_u(\vartheta)}} (\vartheta_n - \vartheta_o) \end{aligned} \quad (4.2.2.3b)$$

where

$\alpha_i(\vartheta)$  = surface coefficient of heat transfer at the inner surface which is exposed to fire ( $\text{kcal/m}^2 \text{ } ^{\circ}\text{C h}$ )  $\{ \text{W/m}^2 \text{ } ^{\circ}\text{C} \}$   
 $\alpha_u(\vartheta)$  = surface coefficient of heat transfer at the outer surface ( $\text{kcal/m}^2 \text{ } ^{\circ}\text{C h}$ )  $\{ \text{W/m}^2 \text{ } ^{\circ}\text{C} \}$   
 $\lambda(x, \vartheta)$  = thermal conductivity at the section  $x$  at the temperature  $\vartheta$  ( $\text{kcal/m}^2 \text{ } ^{\circ}\text{C h}$ )  $\{ \text{W/m}^2 \text{ } ^{\circ}\text{C} \}$   
 $c(x, \vartheta)$  = specific heat capacity at the section  $x$  at the temperature  $\vartheta$  ( $\text{kcal/kg } ^{\circ}\text{C}$ )  $\{ \text{J/kg } ^{\circ}\text{C} \}$   
 $\gamma$  = density at the section  $x$  ( $\text{kg/m}^3$ )  
 $\vartheta$  = gas temperature in the fire compartment at time  $t$  ( $^{\circ}\text{C}$ )  
 $\vartheta^t$  = outside air temperature at time  $t$  ( $^{\circ}\text{C}$ )  
 $\vartheta_k^o$  = temperature in the centre of layer  $k$  ( $^{\circ}\text{C}$ )  
 $\Delta x_k$  = thickness of the layer  $k$  (m)

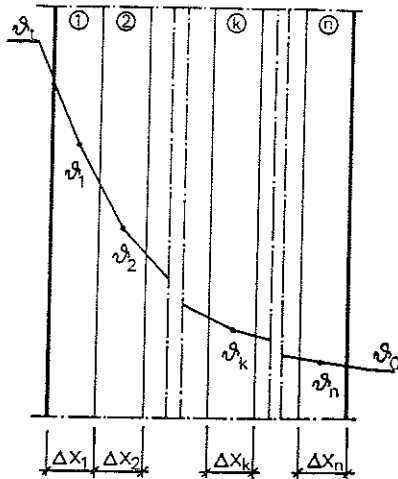


Fig. 4.2.2.3 a. Thermal conduction in enclosing construction divided into elements

The surface coefficient of heat transfer  $\alpha_i$  at the inner surface which is exposed to fire may be assumed to be made up of a radiation component which is dominant at the high temperatures which occur during a fire, and of a convection component which, with satisfactory accuracy, can be put constant and equal to  $20 \text{ kcal/m}^2 \text{ }^\circ\text{C h}$   $\{ 23 \text{ W/m}^2 \text{ }^\circ\text{C} \}$ . By applying the Stefan-Boltzman law, this gives for  $\alpha_i$

$$\alpha_i = \frac{4.96 \epsilon_r}{\vartheta_i - \vartheta_i} \left[ \left( \frac{\vartheta_i + 273}{100} \right)^4 - \left( \frac{\vartheta_i + 273}{100} \right)^4 \right] + 20 \quad (\text{kcal/m}^2 \text{ }^\circ\text{C h})$$

$$\alpha_i = \frac{5.77 \epsilon_r}{\vartheta_i - \vartheta_i} \left[ \left( \frac{\vartheta_i + 273}{100} \right)^4 - \left( \frac{\vartheta_i + 273}{100} \right)^4 \right] + 23 \quad \{ \text{W/m}^2 \text{ }^\circ\text{C} \}$$

(4.2.2.3 c)

where  $\vartheta_i$  = the temperature of the internal surface ( $^\circ\text{C}$ )  
 $\epsilon_r$  = the resultant emissivity for the radiation between flames, combustion gases and internal surface

$\epsilon_r$  is determined from the formula (19)

$$\epsilon_r = \frac{1}{1/\epsilon_t + 1/\epsilon_i - 1}$$

(4.2.2.3 d)

where  $\epsilon_t$  = the emissivity of flames and combustion gases  
 $\epsilon_i$  = the emissivity of the surfaces which are exposed to fire.

The approximate expression for the surface coefficient of heat transfer  $\alpha_u$  at the unexposed surface is (19)

$$\alpha_u = 7.5 + 0.028 \vartheta_u \quad (\text{kcal/m}^2 \text{ h } ^\circ\text{C})$$

$$\alpha_u = 8.7 + 0.033 \vartheta_u \quad \{ \text{W/m}^2 \text{ }^\circ\text{C} \}$$

(4.2.2.3 e)

where  $\vartheta_u$  = the temperature of the outside surface ( $^\circ\text{C}$ )

The system of first order difference equations (4.2.2.3 b) is solved numerically (see Subsection 4.2.3), after which  $I_w$  at the time  $t$  is obtained from the expression

$$I_w = (A_i - A) \frac{1}{\frac{1}{\alpha_i(\vartheta)} + \frac{\Delta x_1}{2\lambda(x, \vartheta)}} (\vartheta_i - \vartheta_1)$$

(kcal/h)  $\{ \text{W} \}$  (4.2.2.3 f)

where  $A_t$  = the size of the total internal surface area of the fire compartment inclusive of the opening area  $A$  ( $m^2$ )

The above relationship assumes that the enclosing structures are of uniform construction. If these enclosing structures consist of different materials or have different thicknesses, which is usually the case in practice, then the calculations are performed separately for each type of structure, the expression  $(A_t - A)$  in Eq. (4.2.2.3 f) being replaced by the area of the appropriate part structure  $A_{tj}$ .

For  $I_W$  at the time  $t$ , the expression is therefore

$$I_w = \sum_j I_{w_j} = \sum_j A_{t_j} \left[ \frac{1}{\frac{1}{\alpha_i(\vartheta)} + \frac{\Delta x_1}{2\lambda(x, \vartheta)}} \right] (\vartheta_t - \vartheta_{1j}) \quad (\text{kcal/h}) \quad \{ W \} \quad (4.2.2.3 g)$$

#### 4.2.2.4 The term $I_L$

The replacement of combustion gases by combustion air takes place due to the fact that the density of the hot gases is lower than that of the cold air outside the fire compartment. Theoretical treatment of this process is based on the fundamental assumption that there is a linear pressure distribution in the vertical direction over the area of the opening in the fire compartment. This means that there is a neutral layer where there is no difference in static pressure between the outside and inside (see Fig. 4.2.2.4 a). On the assumption that the whole fire compartment is at the same temperature and that there exists a neutral layer, the quantity of gas  $Q_{out}$  flowing outwards and the quantity of air  $Q_{in}$  flowing inwards can be calculated by means of Bernoulli's theorem. According to this (19),

$$Q_{out} = \frac{2}{3} \mu B (h'')^{3/2} \sqrt{2g \gamma_t (\gamma_0 - \gamma_t)} \quad (\text{kg/h}) \quad (4.2.2.4 a)$$

$$Q_{in} = \frac{2}{3} \mu B (h')^{3/2} \sqrt{2g \gamma_0 (\gamma_0 - \gamma_t)} \quad (\text{kg/h}) \quad (4.2.2.4 b)$$

where  $\mu$  = flow coefficient which is a function of the internal friction of the air and gas flow and its contraction in the opening

$B$  = width of opening (m)

$g$  = acceleration due to gravity ( $m/s^2$ )

$\gamma_0$  = density of air ( $kg/m^3$ )

$\gamma_t$  = density of combustion gases ( $kg/m^3$ )

$h$  = distance from the neutral layer to the bottom of the opening (m)

$h''$  = distance from the neutral layer to the top of the opening (m)

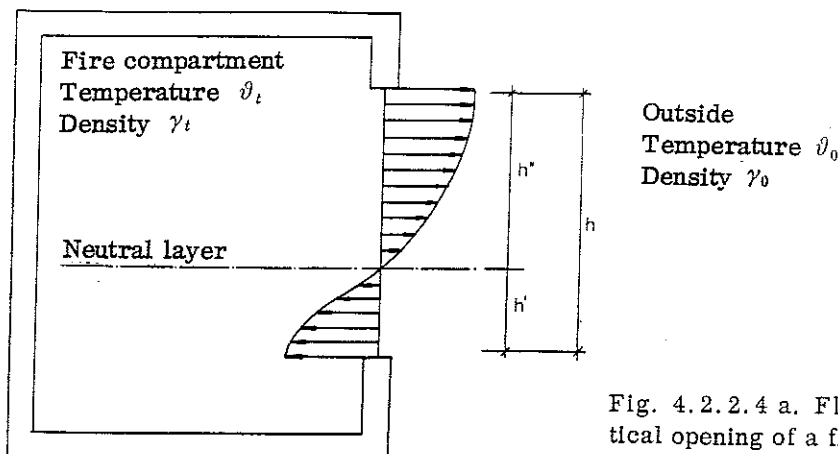


Fig. 4.2.2.4 a. Flow conditions for a vertical opening of a fire compartment

The position of the neutral layer ( $h'$  and  $h''$ ) is determined by the interchange of gases in the fire compartment. This implies that the net interchange of gases between the fire compartment and the outside must be balanced by the difference between the production and consumption of gases during combustion, i.e.

$$Q_{ut} - Q_{in} = G_0 R - L R \quad (\text{kg/h}) \quad (4.2.2.4 \text{ c})$$

where  $G_0$  = quantity of gases produced during combustion of 1 kg fuel (kg/kg)  
 $L$  = quantity of air consumed during combustion of 1 kg fuel (kg/kg)  
 $R$  = rate of combustion (kg/h)

$Q_{out}$  can be determined from Equations (4.2.2.4 a - 4.2.2.4 c) and used for the determination of the term  $I_L$ . For  $I_L$ ,

$$I_L = Q_{ut} c_p (\vartheta_t - \vartheta_0) \quad (\text{kcal/h})$$

$$I_L = Q_{ut} c_p (\vartheta_t - \vartheta_0) / 3600 \quad \{W\} \quad (4.2.2.4 \text{ d})$$

This relationship can also be written in the form

$$I_L = \kappa c_p (\vartheta_t - \vartheta_0) A \sqrt{h} \quad (\text{kcal/h})$$

$$I_L = \kappa c_p (\vartheta_t - \vartheta_0) A \sqrt{h} / 3600 \quad \{W\} \quad (4.2.2.4 \text{ e})$$

$$\kappa = \frac{Q_{ut}}{A \sqrt{h}} \quad (\text{kg/h m}^{5/2})$$

where  $\vartheta_t$  = gas temperature in the fire compartment ( $^{\circ}\text{C}$ )

$\vartheta_0$  = temperature of outside air ( $^{\circ}\text{C}$ )

$A$  = opening area of the fire compartment ( $\text{m}^2$ )

$h$  = height of opening (m)

$c_p$  = specific heat capacity of the combustion gases ( $\text{kcal/kg}^{\circ}\text{C}$ )  $\{ \text{J/kg}^{\circ}\text{C} \}$   
 (see Fig. 4.2.2.4 b)

An approximate relationship between the coefficient  $\kappa$  and the effective calorific value  $H$  of the fuel is given in Fig. 4.2.2.4 c. This relationship has been calculated on the assumption that the flow coefficient  $\mu$  is equal to 0.7 (see Equation 4.2.2.4 a). The coefficient  $\kappa$  is given for gas temperatures of 500 and  $1000^{\circ}\text{C}$ , the assumptions made being that all air supplied is used up during combustion ( $a = 1$ ) and that no air is consumed ( $a = 0$ ). As will be seen from the figure, the coefficient  $\kappa$  is dependent only to a relatively slight extent on the effective calo-

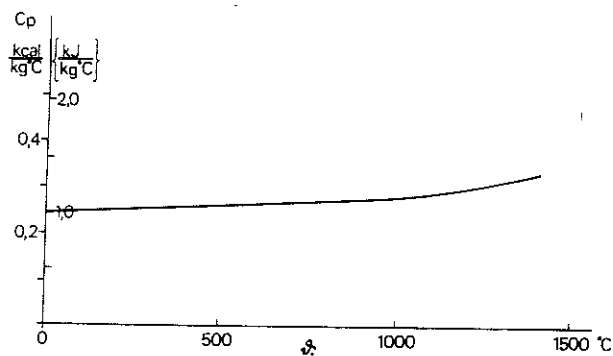


Fig. 4.2.2.4 b. Variation in the specific heat capacity  $c_p$  of the combustion gases with the temperature  $\vartheta_t$



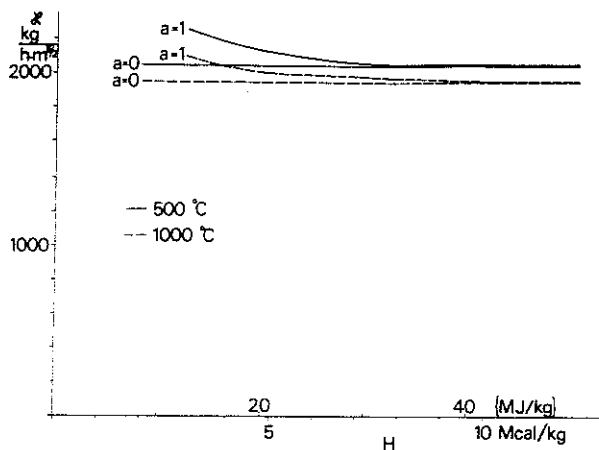


Fig. 4.2.2.4 c. The coefficient  $\kappa$  in Equation (4.2.2.4 e) as a function of the effective calorific value  $H$  of the fuel. The coefficient  $\kappa$  is given for gas temperatures of 500°C and 1000°C, the assumptions being that all air supplied is used up during combustion ( $a=1$ ) and that no air is consumed ( $a=0$ )

ric value of the fuel, the degree of combustion and the gas temperature. The value of  $\kappa$  can therefore be put at 2000 kg/h m<sup>5/2</sup> with an accuracy that is acceptable in this context when  $I_L$  is being calculated.

#### 4.2.2.5 The term $I_C$

The heat  $I_C$  released during combustion can be written as

$$I_C = R H \quad (\text{kcal/h}) \quad (4.2.2.5 \text{ a})$$

$$I_C = R H / 3600 \quad \{ \text{W} \}$$

where  $R$  = rate of combustion (kg/h)

$H$  = effective calorific value of the fuel (kcal/kg) { J/kg }

For a ventilation controlled fire (see Section 4.1), the mean rate of combustion during the flame phase is

$$R_m = k A \sqrt{h} \quad (\text{kg/h}) \quad (4.2.2.5 \text{ b})$$

The heat released is therefore

$$I_C = k A \sqrt{h} H \quad (\text{kcal/h}) \quad (4.2.2.5 \text{ c})$$

$$I_C = k A \sqrt{h} H / 3600 \quad \{ \text{W} \}$$

where  $k$  = coefficient which is a function of fuel characteristics (kg/h m<sup>5/2</sup>)

$A$  = total opening area of the fire compartment (m<sup>2</sup>)

$h$  = weighted mean value of the height of fire compartment openings (m)

$H$  = effective calorific value of the fuel (kcal/kg) { J/kg }

The coefficient  $k$  is dependent on the volume of air that is required for complete combustion of a definite quantity of the fuel in question. In turn, this volume of air depends on the effective calorific value of the fuel, and an approximate relationship between  $k$  and the effective calorific value  $H$  is given in Fig. 4.2.2.5 a. This relationship is based on the assumption that the flow coefficient  $\mu$  is equal to 0.7. (see Equation 4.2.2.4 a).

Equation (4.2.2.5 c) is valid for the whole fire process only on condition that

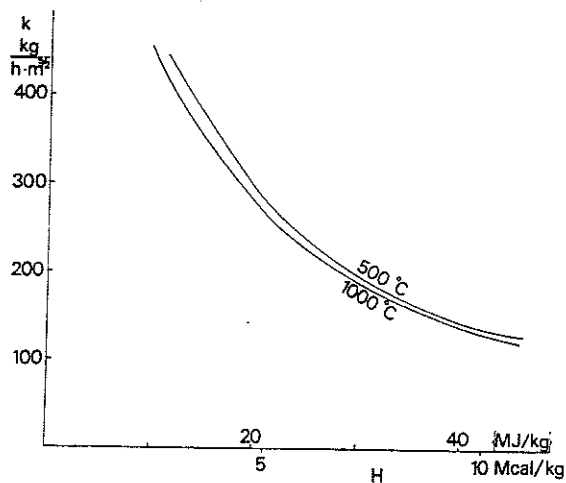


Fig. 4.2.2.5 a. Approximate relationship between the coefficient  $k$  in Equation (4.2.2.5 b) and the effective calorific value  $H$  of the fuel at temperatures of 500 and 1000°C

the fire is ventilation controlled and that the fire load is of such type that the combustion characteristics are constant during the whole fire. Strictly speaking, this holds only in exceptional cases, for instance in the case of liquid fuels which have no cooling phase or incandescent phase when burning. In other cases, a relationship between time and rate of heat released must be constructed in advance in order to form the basis for calculation of the temperature-time curve of the combustion gases. The following guidelines can be given

- the maximum value of the quantity of heat  $I_C$  released per unit time is calculated according to Equation (4.2.2.5 c), the coefficient  $k$  being according to Figure 4.2.2.5 a
- the total energy released during the complete fire process is equal to the quantity of heat which is initially stored in the fuel

$$\int I_C dt = MH \quad (4.2.2.5 d)$$

where  $M$  = quantity of combustible material (kg)  
 $H$  = effective calorific value (kcal/kg) { J/kg }

- for wood fires, comparative calculations have shown (see Section 4.3) that an assumption that the flame phase is ventilation controlled gives results that are on the safe side in most practical cases. In principle the results should be the same for other types of fire load. In doubtful cases, it is advisable to perform calculations using alternative relationships between time and rate of heat released, account being taken of Equation (4.2.2.5 d)

#### 4.2.3 Calculation procedure

According to Equation (4.2.1 a), the heat balance equation for compartment fires can be written as

$$I_C = I_L + I_W + I_R + I_B$$

It was stated in Subsection 4.2.2.1 that the term  $I_B$  can be ignored. According to Equations (4.2.2.2 a), (4.2.2.3 f) and (4.2.2.4 e), we also have that

$$I_R = A(E_g - E_0)$$

$$I_W = (A_t - A) \frac{1}{\frac{1}{\alpha_i(\vartheta)} + \frac{\Delta x_1}{2\lambda(x, \vartheta)}} (\vartheta_t - \vartheta_1)$$

$$I_L = \kappa c_p A \sqrt{h} (\vartheta_t - \vartheta_0)$$

The term  $I_C$  is to be calculated in view of the guidelines set out in Subsection 4.2.2.5.

Calculation of the fire process from the heat balance equation takes place in increments of time  $\Delta t$  from time  $t$  to time  $t + \Delta t$ . The time increment  $\Delta t$  must not be made so large that the calculation becomes unstable. Experience has indicated that, when the development of energy  $I_C$  is not too high and the surrounding structures have a normal thermal inertia,  $\Delta t$  should be in the range of 0.1 - 5 minutes. For  $\Delta t$  of this order, the surface coefficients of heat transfer may, with a satisfactory approximation, be regarded constant during each time increment. With the expressions for the various terms inserted into the heat balance equation, the sought combustion temperature  $\vartheta_t$  can be determined from the relationship

$$\vartheta_t = \frac{I_C + \kappa c_p A \sqrt{h} \vartheta_0 + (A_t - A) \frac{1}{\frac{1}{\alpha_i} + \frac{\Delta x_1}{2\lambda}} \vartheta_1 - I_R}{\kappa c_p A \sqrt{h} + (A_t - A) \frac{1}{\frac{1}{\alpha_i} + \frac{\Delta x_1}{2\lambda}}} \quad (4.2.3 a)$$

This expression is valid for fire compartments with uniform enclosing structures. For the more general case, the expression can be modified by application of Equation (4.2.2.3 g).

The temperature  $\vartheta_1$  in Equation (4.2.3 a) is a function of the sought combustion gas temperature  $\vartheta_t$ , since the system of equations (Equation 4.2.2.3 b) which must first be solved in order that  $\vartheta_1$  may be determined also contains the combustion gas temperature  $\vartheta_t$ . Solution is by numerical integration, for instance by the application of the Runge-Kutta procedure. This stipulates that the system of equations is solved a certain number of times during each increment of time  $\Delta t$ , in the Runge-Kutta procedure five times. For each solution, the value of the combustion gas temperature which is employed is that calculated in the immediately preceding step by means of Equation (4.2.3 a).  $I_R$  and  $c_p$  in the Equation (4.2.3 a) are also functions of the sought gas temperature  $\vartheta_t$ . In the same way as for  $\vartheta_1$ , the values of these quantities which are inserted are also those calculated in the immediately preceding solution on the basis of the combustion gas temperature.

### 4.3 Calculation of the temperature-time curve of the combustion gases for fire loads mainly of the wood fuel type

#### 4.3.1 Assumptions

In Section 4.2, the calculation of the gas temperature-time curve was described for the complete fire process in the case of a general fire load. The dominant fire load in residential buildings, office buildings, hotels and similar buildings has combustion characteristics that are mainly the same as those of wood fuel. For this reason, the design data in this handbook in the form of tables and diagrams from which the maximum steel temperature can be directly determined as a function of the fire load and opening factor of the fire compartment, etc., has been based on the temperature-time curves relating to wood fuel.

In Swedish Building Regulations of 1967, temperature-time curves calculated for the flame phase of the fire process are presented as a function of the opening factor  $A\sqrt{h}/A_t$  of the fire compartment. These curves assume that the fire load is mainly of the wood fuel type. The curves have been calculated for a standard fire compartment for which the thermal properties of the surrounding structures are the same as the average figures for concrete, brick and lightweight concrete. In the calculations, it was assumed that the surrounding construction has a thickness of 20 cm. Deviations from this thickness which occur in practice have no significance for the application of the presented temperature-time curves. Furthermore, the curves are based on the assumption that the fire is controlled by ventilation, i.e. the rate of combustion  $R$  during the flame phase must conform to Equation (4.2.2.5 b). At the time that these curves were constructed, it was not possible to allow for the variation in the rate of combustion during the cooling phase. The Regulations therefore specify that the drop in temperature during the cooling phase shall be assumed to have a standard value of  $10^\circ\text{C}/\text{min}$ , unless some other time curve can be shown to be more correct. It must however be regarded as very unsatisfactory that different parts of the same fire process should be described with entirely different degrees of accuracy. Also, the code specification of a drop in temperature of  $10^\circ\text{C}/\text{min}$  results, chiefly in uninsulated and lightly insulated steel structures, in calculated steel temperatures which are generally substantially in excess of the actual steel temperatures. Later work enables rational calculation of the gas temperature-time curve to be carried out also during the cooling phase (19), (20).

The basis of a rational calculation of the gas temperature-time curve has been an analysis of more than 30 well documented fire tests at full scale performed in different laboratories. Calculated and experimentally determined gas temperature-time curves are exemplified in Figs. 4.3.1 a and 4.3.1 b. The inset curves are the calculated time curves for the heat released  $I_C$ . The figures give examples of both a short-term and a long-term fire process. The fundamental assumption in the theoretical calculation has generally been that the energy which is liberated by combustion during the fire process, i.e. the area underneath the  $I_C$ -time curve, must be the same as the quantity of heat initially present in the fuel (see also Subsection 4.2.2.5). The close agreement between the calculated and measured temperature-time curve demonstrates that the heat balance relationships in Equations (4.2.1 a) and (4.2.3 a) are well suitable as the basis for the simulation of a fire process. Owing to the performed calculations for the gas temperature-time curve and the comparison of this with corresponding test results, it is possible to construct the time curve for the heat released  $I_C$  for the entire fire process, i.e. also for the cooling phase, for different val-

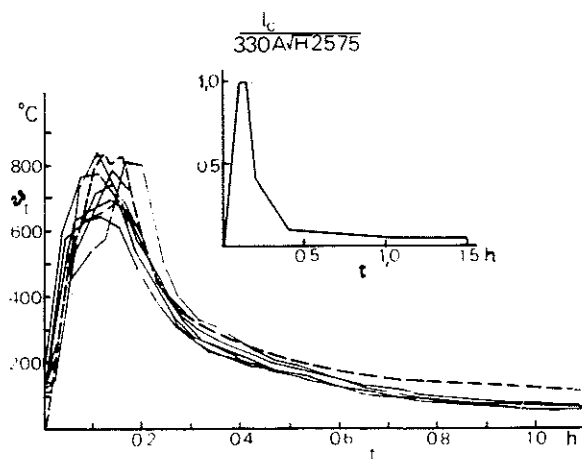


Fig. 4.3.1 a. Calculated (---) and experimentally measured (—) gas temperature-time curves in full-scale test using furniture as the fire load. Fire load  $q = 23 \text{ Mcal/m}^2 \{96 \text{ MJ/m}^2\}$  of total surface area, opening factor  $A\sqrt{h}/A_t = 0.068 \text{ m}^{1/2}$ . The inset curve shows the calculated variation with time of the rate of heat release  $I_c$  in Mcal/h (19)

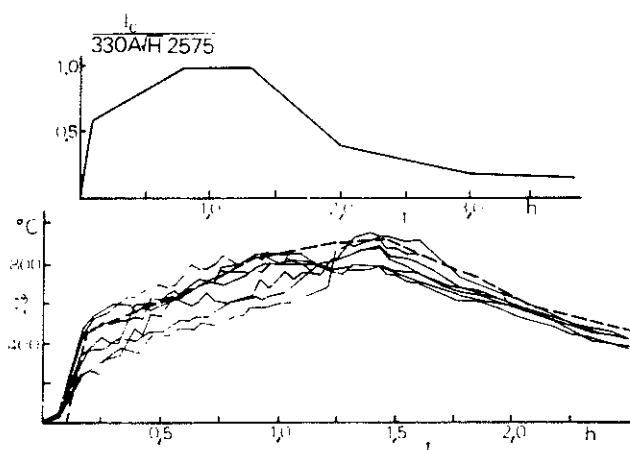


Fig. 4.3.1 b. Calculated (---) and experimentally measured (—) gas temperature-time curves in full-scale test using wood cribs as the fire load. Fire load  $q = 83.5 \text{ Mcal/m}^2 \{350 \text{ MJ/m}^2\}$  of total surface area, opening factor  $A\sqrt{h}/A_t = 0.0467 \text{ m}^{1/2}$ . The inset curve shows the calculated variation with time of the rate of heat release  $I_c$  in Mcal/h (19)

ues of the fire load and opening factor. Using these time-heat curves as input data in the heat balance equation, it has been possible to perform systematic calculations of the temperature-time curves of the combustion gases for different fire loads and opening factors, and also for different materials in the structure surrounding the fire compartment (19). Temperature-time curves for only one type of fire compartment, designated fire compartment type A or standard fire compartment, are reproduced in this handbook. This is the same fire compartment as that used for calculation of the gas temperature-time curves in the Swedish Building Regulations. For fire compartments with surrounding construction whose thermal properties are evidently different from those applicable in this standard fire compartment, the temperature-time curves can be converted into those in the standard fire compartment by means of equivalent fire loads and opening factors (see Subsection 4.3.4).

The following assumptions were made in calculating the gas temperature-time curves:

- $G_o$  = gas produced during combustion = 6.3 kg/kg wood
- $L$  = air supply necessary for combustion = 5.2 kg/kg wood
- $c_p$  = specific heat capacity of the combustion gases, see Fig. 4.2.2.4 b
- $R_m$  = mean rate of combustion during the flame phase =  $330 A\sqrt{h} \text{ kg/h}$
- $H$  = effective calorific value of wood fuel = 4500 kcal/kg wood {18,800 kJ/kg}
- $\mu$  = flow coefficient = 0.7

The temperature-time curves for fire compartment type A are given in Subsection 4.3.3, both in the form of diagrams and tables, for different fire loads  $q$  and opening factors  $A\sqrt{h}/A_t$ .

#### 4.3.2 Calculation of the opening factor $A\sqrt{h}/A_t$

The terms  $I_C$  and  $I_L$  in the heat balance equation are proportional to the air flow factor  $A\sqrt{h}$ . The quantity of heat which enters the surrounding structures per unit time, the term  $I_W$ , is proportional to the internal surface area  $A_t$  of the fire compartment. These two geometrical quantities can be combined in the concept of the opening factor, defined as  $A\sqrt{h}/A_t$ . In consequence, it is natural to define the fire load  $q$  of the fire compartment as the energy per unit area of the enclosing surface  $A_t$ . The opening factor of the fire compartment is thus made up of the following quantities

- $A_t$  = the total internal surface area of the fire compartment, i.e. the area of the walls, floor and ceiling, inclusive of openings ( $m^2$ )
- $A$  = the total area of the vertical openings in the fire compartment, i.e. the windows, ventilation openings and other vertical openings ( $m^2$ )
- $h$  = a mean value of the height of these openings, weighted in view of the sizes of the openings, calculated according to Equation (4.3.2 a) (m)

$$h = \frac{\sum A_v h_v}{\sum A_v} \quad (m) \quad (4.3.2 a)$$

where  $A_v$  = the area of each opening  $v$  in the fire compartment ( $m^2$ )  
 $h_v$  = the height of each opening  $v$  in the fire compartment (m)

For a fire compartment according to Fig. 4.3.2 a which also contains horizontal openings, the opening factor can be calculated from the expression

$$\frac{A\sqrt{h}}{A_t} = f_k \left( \frac{A\sqrt{h}}{A_t} \right)_v \quad (m^{\frac{1}{2}}) \quad (4.3.2 b)$$

where  $(A\sqrt{h}/A_t)_v$  = the opening factor for the vertical openings, calculated as above ( $m^{\frac{1}{2}}$ )  
 $f_k$  = correction coefficient determined from the nomogram in Fig. 4.3.2 b. The symbols used in the nomogram are set out in Figs. 4.3.2 a and 4.3.2 b

Calculation of the opening factor according to Equation (4.3.2 b) presupposes that the flow through the horizontal openings is not dominant. This can be determined with the assistance of the ratio  $A_h\sqrt{h_2}/A\sqrt{h}$  which has an upper bound above which the assumed model of the flow conditions ceases to be relevant. This upper bound is

$$\frac{A_h\sqrt{h_2}}{A\sqrt{h}} = \begin{cases} 1.76 & \text{vid } 1000^\circ\text{C} \\ 1.37 & \text{vid } 500^\circ\text{C} \end{cases} \quad (4.3.2 c)$$

$A_h$  = total area of all horizontal openings ( $m^2$ )  
 $h_2$  = distance between the neutral layers of the vertical openings and the horizontal openings (m) (see Fig. 4.3.2 a).

At this upper bound, the neutral layer is situated at the top of the vertical opening, and  $h_2$  is then identical with the vertical distance between the level of the horizontal opening and the top of the vertical opening. For values of  $A_h\sqrt{h_2}/(A\sqrt{h})$  greater than the upper bound according to Equation (4.3.2 c), all combustion gases will be ventilated through the horizontal opening. When the flow of air and gases takes place mainly through horizontal openings, the flow becomes unstable and difficult to describe by means of a simple theoretical model.

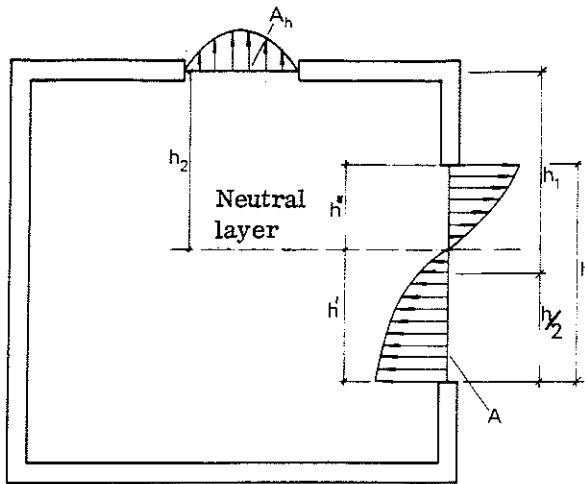


Fig. 4.3.2 a. Gas flow in fire compartment with vertical and horizontal openings.  $A$  = area of vertical opening,  $A_h$  = area of horizontal opening,  $h$  = height of vertical opening,  $h''$  and  $h'$  = height of vertical opening above and below the neutral layer,  $h_1$  = vertical distance between the midpoint of the vertical opening and the level of horizontal opening,  $h_2$  = vertical distance between the neutral layer and the level of horizontal opening

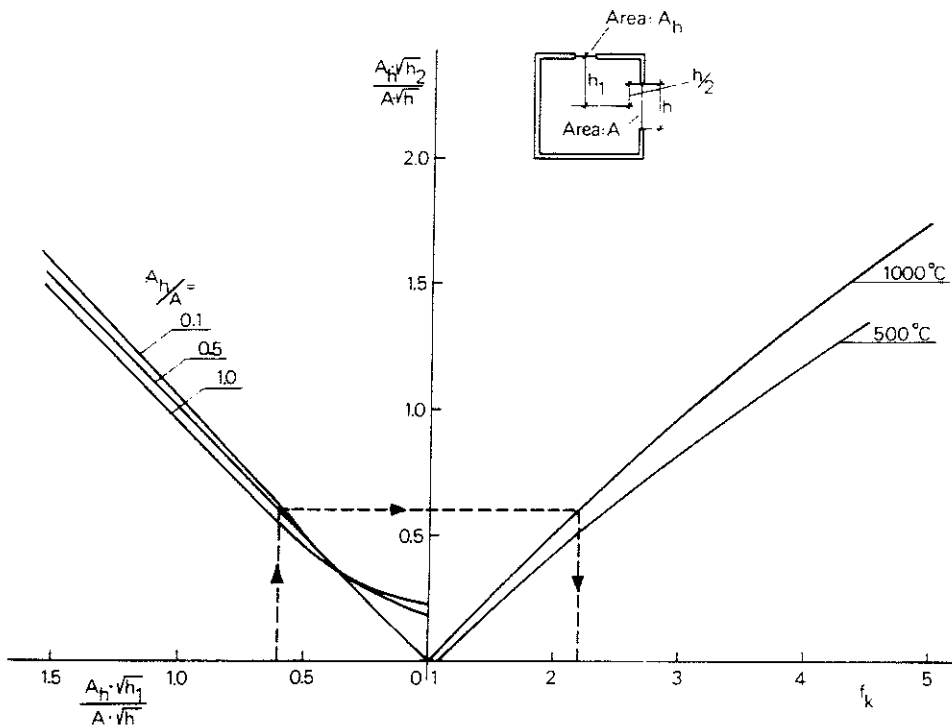


Fig. 4.3.2 b. Nomogram for calculation of the coefficient  $f_k$  in Equation (4.3.2 b). Symbols as in Fig. 4.3.2 a. Example: Calculate the opening factor for a fire compartment of the following characteristics.  $A = 2 \text{ m}^2$ ,  $h = 1 \text{ m}$ ,  $A_h = 1 \text{ m}^2$ ,  $h_1 = 1.5 \text{ m}$ ,  $A_t = 50 \text{ m}^2$ . The input data in the nomogram are  $(A_h \sqrt{h_1}) / (A \sqrt{h}) = 0.61$  and  $A_h/A = 0.5$ . This gives a value of  $f_k = 2.2$ . Equation (4.3.2 b) then gives the opening factor =  $2.2 [(2\sqrt{1})/50] = 2.2 \cdot 0.04 = 0.088 \text{ m}^{1/2}$

In calculating the opening factor, it is assumed that ordinary window glass is immediately destroyed when fire breaks out. In the case of fire compartments containing windows with reinforced glass or doors of a certain fire resistance time, it may be difficult to decide whether these windows and doors will remain

intact for the entire duration of the fire, or whether they will be open right from the beginning of the fire. In such cases, a calculation of the temperature-time curve of the fire compartment and of the maximum temperature of the steel structure should be carried out for both alternative opening factors. As a rule, the smaller the opening factor, the higher will be the maximum steel temperature for a given fire load. Design based on the lower value of the opening factor will therefore, as a rule, yield results on the safe side.

#### 4.3.3 Calculated gas temperature-time curves for fire compartment type A (standard fire compartment) for different fire loads $q$ and opening factors $A\sqrt{h}/A_t$

Calculated gas temperature-time curves for fire compartment type A (standard fire compartment) for different values of the fire load  $q$  and the opening factor  $A\sqrt{h}/A_t$  are given in Fig. 4.3.3.a and Table 4.3.3.a. The term fire compartment type A is taken to refer to a fire compartment with surrounding structures whose thermal properties are the same as the average values for concrete, brick and lightweight concrete. The thermal conductivity has been assumed to have a value of  $0.7 \text{ kcal/m h } ^\circ\text{C}$   $\{0.8 \text{ W/m } ^\circ\text{C}\}$ , and the product of the specific heat capacity and density  $c\gamma = 400 \text{ kcal/m}^3 ^\circ\text{C}$   $\{1700 \text{ kJ/m}^3 ^\circ\text{C}\}$ .

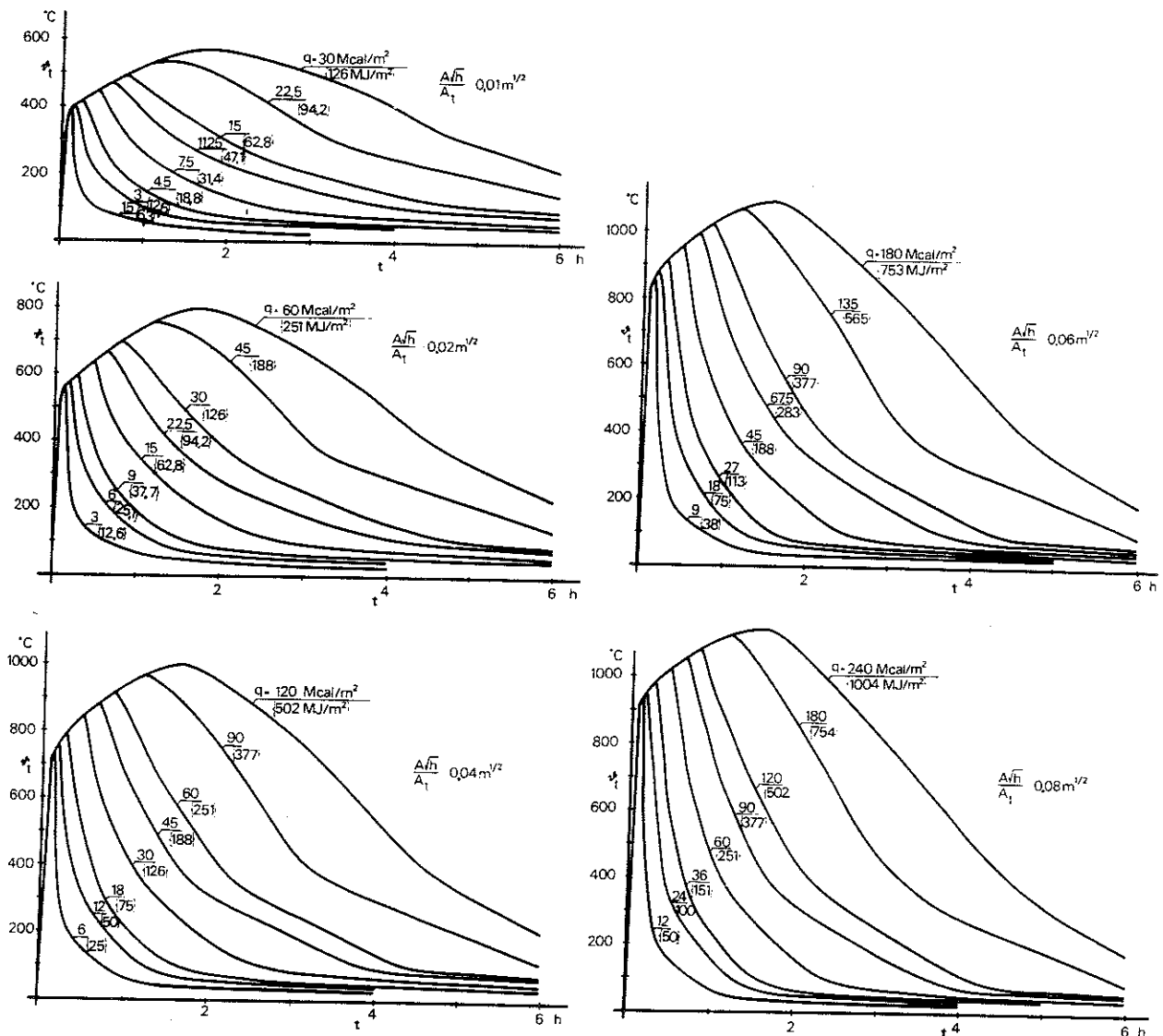
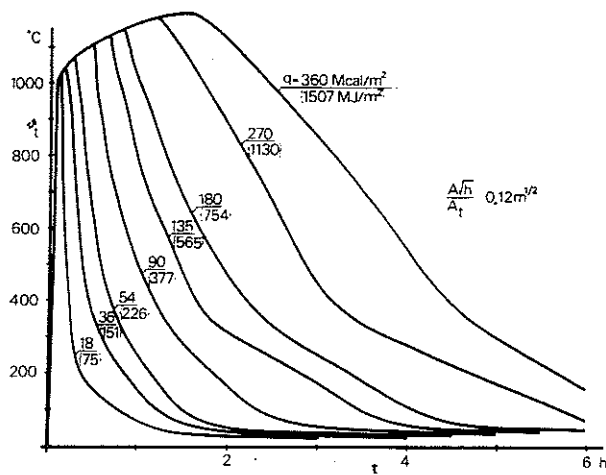


Fig. 4.3.3 a. Calculated gas temperature-time curves for complete fire processes for different fire loads  $q$  and opening factors  $A\sqrt{h}/A_t$  in fire compartment Type A (standard fire cell), the fuel being of wooden type (19)

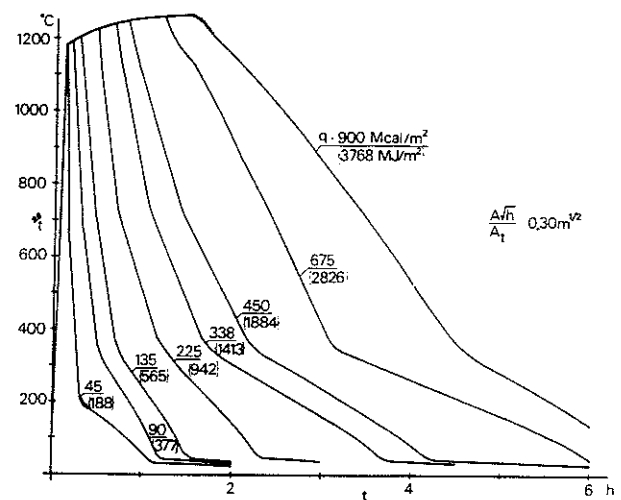




$$A\sqrt{h}/A_t = 0.01 \text{ m}^{1/2}$$

$q \text{ (Mcal/m}^2\text{)}$								
1.5	3.0	4.5	7.5	11.25	15.0	22.5	30.0	
$q \text{ (MJ/m}^2\text{)}$								
$t \text{ (h)}$	6.3	12.6	18.8	31.4	47.1	62.8	94.2	126

0.05	272	272	272	272	272	272	272	272
0.10	395	395	395	395	328	328	328	328
0.15	228	390	390	390	360	360	360	360
0.20	196	368	401	401	406	406	406	406
0.25	150	313	409	410	405	405	405	405
0.30	98	257	385	421	415	415	415	415
0.35	97	241	354	429	425	425	425	425
0.40	94	218	320	437	434	434	434	434
0.45	91	193	282	441	442	442	442	442
0.50	88	167	269	412	449	449	449	449
0.60	82	157	229	370	463	463	463	463
0.65	79	150	215	355	460	470	470	470
0.70	75	144	187	314	451	476	476	476
0.80	69	131	178	302	426	488	488	488
0.90	61	118	166	283	399	468	500	500
1.00	54	104	154	263	367	456	511	511
1.10	46	89	142	242	344	439	521	521
1.20	45	74	129	218	331	421	531	531
1.30	43	71	116	209	315	400	524	541
1.40	42	68	102	199	299	376	524	550
1.50	41	65	88	190	282	366	522	559
1.60	40	63	85	180	263	353	515	567
1.70	39	61	81	170	244	340	506	559
1.80	38	59	79	160	237	326	496	562
1.90	37	58	76	150	230	311	485	561
2.00	36	56	74	139	223	296	473	560
2.20	35	53	70	117	210	263	448	552
2.40	34	51	66	103	197	249	422	542
2.60	33	49	63	97	185	235	393	529
2.80	32	47	61	92	172	221	361	514
3.00	32	46	59	87	159	207	327	497
3.20		44	56	83	146	194	301	480
3.40		43	55	80	132	181	286	461
3.60		42	53	77	118	168	273	441
3.80		41	52	75	109	154	261	419
4.00		40	50	72	104	140	249	396
4.20		39	49	70	100	125	238	371
4.40		39	48	68	96	119	227	345
4.60		38	47	66	93	114	216	323
4.80		37	46	65	90	110	205	307
5.00		37	45	63	87	106	194	292
5.20		36	44	62	85	103	184	277
5.40		35	43	60	82	100	173	262
5.60		35	42	59	80	97	162	247
5.80		35	42	58	78	94	151	231
6.00		34	41	57	77	92	140	216



$$A\sqrt{h}/A_t = 0.02 \text{ m}^{1/2}$$

$q \text{ (Mcal/m}^2\text{)}$								
3.0	6.0	9.0	15.0	22.5	30.0	45.0	60.0	
$q \text{ (MJ/m}^2\text{)}$								
$t \text{ (h)}$	12.6	25.1	37.7	62.8	94.2	126	188	251

0.05	396	396	396	396	397	397	397	398
0.10	568	568	568	568	467	467	467	467
0.15	322	556	556	556	511	511	511	511
0.20	277	519	572	572	581	581	581	581
0.25	210	450	585	587	578	578	578	578
0.30	134	361	549	602	593	593	593	593
0.35	131	339	501	615	615	615	615	615
0.40	126	304	452	624	620	620	620	620
0.45	121	268	397	632	632	632	632	632
0.50	117	228	376	586	642	642	642	642
0.60	107	212	317	523	662	662	662	662
0.65	102	201	287	485	660	671	671	671
0.70	98	193	254	440	642	680	680	680
0.80	88	174	239	419	604	697	697	697
0.90	77	154	220	390	562	666	714	714
1.00	66	132	202	359	513	645	729	729
1.10	54	109	184	325	475	618	742	742
1.20	51	86	165	289	453	588	756	756
1.30	49	82	144	275	429	555	743	768
1.40	47	79	123	260	402	517	740	779
1.50	45	75	101	244	375	498	735	790
1.60	44	72	97	229	347	478	721	800
1.70	43	70	93	214	316	456	706	787
1.80	42	67	89	199	305	434	688	788
1.90	40	65	86	184	294	410	669	784
2.00	40	63	83	168	284	386	648	780
2.20	38	59	78	135	263	335	605	763
2.40	36	56	73	113	244	312	562	743
2.60	35	53	70	106	225	291	515	719
2.80	34	51	66	99	206	270	465	692
3.00	33	49	63	94	187	250	410	662
3.20	32	47	61	89	168	230	370	632
3.40	31	46	58	85	148	210	348	601
3.60	31	44	56	81	128	191	328	568
3.80	30	43	54	78	114	172	309	533
4.00	30	42	52	75	108	151	293	496
4.20		41	51	73	103	130	276	457
4.40		40	49	71	99	123	261	417
4.60		39	48	68	95	117	245	384
4.80		38	47	66	91	112	229	360
5.00		37	46	64	88	107	214	337
5.20		36	45	63	85	103	199	314
5.40		36	44	61	83	100	184	293
5.60		35	43	59	80	96	169	271
5.80		35	42	58	78	93	154	250
6.00		34	41	56	76	91	138	228

Table 4.3.3 a. Gas temperature  $\theta_t$  (°C) in fire compartment Type A for a complete fire process as a function of time  $t$  for different values of the opening factor  $A\sqrt{h}/A_t$  and the fire load  $q$ , this being of wooden type

$$A\sqrt{h}/A_t = 0,04 \text{ m}^{1/2}$$

$t$ (h)	$q$ (Mcal/m <sup>2</sup> )							
	6,0	12,0	18,0	30,0	45,0	60,0	90,0	120,0
	$q$ {MJ/m <sup>2</sup> }							
	25	50	75	126	188	251	377	502
0,05	504	504	504	504	504	504	504	504
0,10	745	745	745	745	621	621	621	621
0,15	422	747	747	747	681	681	681	681
0,20	360	696	767	767	777	777	777	777
0,25	268	587	784	784	776	776	776	776
0,30	164	472	734	799	793	793	793	793
0,35	162	437	665	814	808	808	808	808
0,40	155	389	593	828	822	822	822	822
0,45	148	337	513	841	836	836	836	836
0,50	142	281	481	779	848	848	848	848
0,60	128	259	397	682	874	874	874	874
0,65	120	246	352	626	882	882	882	882
0,70	114	232	307	565	839	894	894	894
0,80	100	204	285	527	785	912	912	912
0,90	86	178	260	483	720	862	928	928
1,00	71	149	235	437	645	827	942	942
1,10	54	118	208	388	589	787	955	955
1,20	51	85	183	337	555	740	967	967
1,30	49	82	156	316	518	688	942	977
1,40	46	77	128	296	480	632	931	987
1,50	45	74	98	276	441	602	919	996
1,60	43	70	94	255	400	571	895	1004
1,70	41	68	89	235	358	540	870	981
1,80	40	65	85	214	343	507	843	973
1,90	39	62	82	194	328	474	813	963
2,00	38	60	79	174	313	440	781	953
2,20	36	56	73	131	288	369	718	923
2,40	35	52	69	104	263	339	655	890
2,60	33	50	64	96	238	311	587	853
2,80	32	47	61	90	214	286	516	813
3,00	31	45	57	84	190	261	442	769
3,20		43	55	80	166	236	388	727
3,40		42	52	76	141	211	362	682
3,60		40	50	72	115	187	338	635
3,80		39	48	69	99	163	316	587
4,00		38	47	66	94	137	296	537
4,20		37	45	64	89	110	277	485
4,40		36	44	61	85	104	258	431
4,60		35	42	59	81	99	240	388
4,80		34	41	57	78	94	221	360
5,00		33	40	55	75	90	204	332
5,20			39	53	73	87	186	305
5,40			38	52	70	83	168	280
5,60			37	50	68	81	150	255
5,80			37	49	66	78	131	229
6,00			36	48	64	75	111	203

$$A\sqrt{h}/A_t = 0,06 \text{ m}^{1/2}$$

$t$ (h)	$q$ (Mcal/m <sup>2</sup> )							
	9,0	18,0	27,0	45,0	67,5	90,0	135,0	180,0
	$q$ {MJ/m <sup>2</sup> }							
	38	75	113	188	283	377	565	753
0,05	575	575	575	575	575	575	575	575
0,10	858	858	858	858	704	704	704	704
0,15	493	861	861	861	784	784	784	784
0,20	404	802	879	879	882	882	882	882
0,25	296	679	898	898	889	889	889	890
0,30	175	538	838	914	908	908	908	908
0,35	174	490	761	928	923	923	923	923
0,40	166	430	669	942	936	936	937	937
0,45	159	369	572	954	949	949	949	949
0,50	151	303	532	877	961	961	961	961
0,60	136	277	433	762	982	982	982	982
0,65	128	262	402	694	992	992	992	992
0,70	120	247	326	620	939	1 001	1 001	1 001
0,80	104	215	300	574	872	1 018	1 018	1 018
0,90	89	185	272	520	795	954	1 032	1 032
1,00	71	152	243	466	705	909	1 044	1 044
1,10	51	116	213	409	637	858	1 054	1 054
1,20	48	80	184	343	593	803	1 064	1 064
1,30	45	76	155	327	550	742	1 029	1 072
1,40	43	72	123	303	505	675	1 013	1 080
1,50	41	68	89	281	460	640	996	1 087
1,60	40	65	86	259	413	603	966	1 093
1,70	38	62	81	236	364	567	935	1 062
1,80	37	59	78	213	348	529	902	1 049
1,90	36	56	74	191	332	491	866	1 036
2,00	35	54	71	169	317	452	830	1 022
2,20	33	50	66	121	289	371	756	984
2,40	32	47	61	93	263	340	683	943
2,60	31	44	57	85	236	310	605	900
2,80	30	42	54	79	210	283	524	854
3,00	29	40	51	74	185	257	440	805
3,20		39	48	70	159	230	381	756
3,40		37	46	67	131	204	355	705
3,60		36	44	63	103	178	331	652
3,80		35	42	60	86	152	308	597
4,00		34	41	57	81	123	288	541
4,20		33	40	55	77	95	269	483
4,40		32	38	53	73	90	249	423
4,60		31	37	51	70	85	230	377
4,80		31	36	49	67	81	211	348
5,00		30	35	47	64	77	193	319
5,20			35	46	62	74	174	292
5,40			34	44	59	71	155	265
5,60			33	43	57	69	135	238
5,80			32	42	55	66	114	210
6,00			32	41	54	64	94	185

$$A\sqrt{h}/A_t = 0,08 \text{ m}^{1/2}$$

$t$ (h)	$q$ (Mcal/m <sup>2</sup> )							
	12,0	24,0	36,0	60,0	90,0	120,0	180,0	240,0
	$q$ {MJ/m <sup>2</sup> }							
	50	100	151	251	377	502	754	1 004
0,05	622	622	622	622	622	622	622	622
0,10	935	935	935	935	766	766	766	767
0,15	532	937	937	937	853	853	853	853
0,20	432	869	955	955	959	959	959	959
0,25	314	734	973	973	965	965	965	965
0,30	181	575	903	987	981	981	981	982
0,35	180	521	818	1 001	995	995	995	995
0,40	171	454	720	1 013	1 008	1 008	1 008	1 008
0,45	163	386	611	1 024	1 020	1 020	1 020	1 020
0,50	155	314	561	937	1 031	1 031	1 031	1 031
0,60	139	285	454	807	1 050	1 050	1 050	1 050
0,65	131	269	396	732	1 058	1 058	1 058	1 058
0,70	122	253	336	651	996	1 066	1 066	1 066
0,80	106	219	306	598	920	1 081	1 081	1 081
0,90	89	186	275	539	833	1 005	1 092	1 092
1,00	70	151	245	479	735	953	1 102	1 102
1,10	47	113	214	417	659	897	1 111	1 111
1,20	44	73	185	352	612	836	1 119	1 119
1,30	42	70	151	328	564	769	1 077	1 126
1,40	40	66	117	304	516	695	1 058	1 132
1,50	39	62	81	281	466	657	1 038	1 138
1,60	37	59	78	257	415	618	1 004	1 143
1,70	36	56	74	234	363	577	969	1 105
1,80	35	53	71	210	347	537	932	1 090
1,90	34	51	68	187	331	496	893	1 074
2,00	33	49	65	163	316	454	853	1 058
2,20	31	46	59	112	287	368	774	1 016
2,40	30	43	55	83	260	337	695	971
2,60	29	40	51	77	233	307	611	923
2,80	28	38	48	71	206	279	524	873
3,00	27	37	45	67	180	252	434	820
3,20		35	43	62	153	224	373	769
3,40		34	41	59	124	198	347	714
3,60		33	40	55	94	171	323	658
3,80		32	38	53	77	143	302	599
4,00		31	37	50	72	113	282	539
4,20			36	48	68	84	262	478
4,40			35	46	65	79	242	415
4,60			34	45	62	75	222	368
4,80			33	43	59	71	203	338
5,00			32	42	56	68	185	309
5,20				40	54	65	166	282
5,40				39	52	62	146	254
5,60					38	50	125	227
5,80					37	48	104	199
6,00					36	47	82	172

$$A\sqrt{h}/A_t = 0,12 \text{ m}^{1/2}$$

$t$ (h)	$q$ (Mcal/m <sup>2</sup> )							
	18,0	36,0	54,0	90,0	135,0	180,0	270,0	360,0
	$q$ {MJ/m <sup>2</sup> }							
	75	151	226	377	565	754	1 130	1 507
0,05	670	670	670	670	670	670	670	670
0,10	1 027	1 027	1 027	1 027	847	847	847	847
0,15	581	1 033	1 033	1 033	933	933	933	933
0,20	465	951	1 049	1 049	1 051	1 051	1 051	1 051
0,25	333	799	1 063	1 063	1 057	1 057	1 057	1 057
0,30	186	620	981	1 076	1 071	1 071	1 071	1 071
0,35	185	556	882	1 088	1 083	1 083	1 083	1 083
0,40	176	480	774	1 098	1 094	1 094	1 094	1 094
0,45	168	404	650	1 107	1 103	1 103	1 103	1 103
0,50	159	324	593	1 004	1 112	1 112	1 112	1 112
0,60	142	292	472	856	1 127	1 127	1 127	1 127
0,65	133	275	407	774	1 133	1 133	1 133	1 133
0,70	124	257	341	681	1 060	1 139	1 139	1 139
0,80	106	221	309	622	971	1 150	1 150	1 150
0,90	88	186	276	556	873	1 062	1 159	1 159
1,00	67	149	244	490	765	1 001	1 166	1 166
1,10	41	107	211	422	680	937	1 173	1 173
1,20	39	63	178	351	628	868	1 178	1 178
1,30	37	60	145	327	575	794	1 128	1 183
1,40	36	56	108	301	523	713	1 106	1 188
1,50	34	53	69	277	469	672	1 082	1 192
1,60	33	50	67	253	414	629	1 043	1 195
1,70	32	47	63	228	358	585	1 003	1 151
1,80	31	45	60	203	343	542	962	1 133
1,90	30	43	57	180	327	497	919	1 114
2,00	29	42	54	155	311	452	874	1 096
2,20		39	49	100	283	361	789	1 048
2,40		37	46	70	255	330	704	998
2,60		35	43	64	227	300	613	946
2,80		33	40	59	200	272	519	891
3,00		32	38	54	173	245	423	834
3,20			37	51	144	216	361	780
3,40			35	48	113	190	336	721
3,60			34	46	83	162	313	660
3,80			33	43	64	132	293	598
4,00			32	42	59	102	273	534
4,20				40	55	69	253	469
4,40				39	52	65	233	403
4,60				37	50	61	213	355
4,80				36	48	58	194	325
5,00				35	46	55	175	297
5,20				34	44	52	144	269
5,40				33	42	50	134	241
5,60				33	41	48	112	213
5,80				32	40	46	91	186
6,00				31	38	45	57	158

$$A\sqrt{h}/A_t = 0.30 \text{ m}^{1/2}$$

$t$ (h)	$q$ (Mcal/m <sup>2</sup> )							
	45	90	135	225	338	450	675	900
	$q$ {MJ/m <sup>2</sup> }							
	188	377	565	942	1 413	1 884	2 826	3 768
0,05	774	774	774	774	774	774	774	774
0,10	1 193	1 193	1 193	1 193	970	970	970	970
0,15	666	1 187	1 187	1 187	1 068	1 068	1 068	1 068
0,20	515	1 079	1 196	1 196	1 205	1 205	1 205	1 205
0,25	357	894	1 204	1 204	1 201	1 201	1 201	1 201
0,30	189	684	1 098	1 211	1 208	1 208	1 208	1 208
0,35	188	603	976	1 216	1 214	1 214	1 214	1 214
0,40	187	513	846	1 222	1 220	1 220	1 220	1 220
0,45	170	423	701	1 226	1 224	1 224	1 224	1 224
0,50	161	330	633	1 099	1 229	1 229	1 229	1 229
0,60	142	295	488	919	1 236	1 236	1 236	1 236
0,65	133	277	414	821	1 239	1 239	1 239	1 239
0,70	123	258	338	715	1 148	1 242	1 242	1 242
0,80	104	219	306	646	1 039	1 247	1 247	1 247
0,90	84	181	273	570	922	1 136	1 251	1 251
1,00	60	140	238	495	796	1 063	1 254	1 254
1,10	30	95	203	419	700	986	1 257	1 257
1,20		41	169	341	641	905	1 259	1 259
1,30		39	132	317	582	820	1 195	1 267
1,40		37	93	292	524	728	1 167	1 263
1,50		35	45	268	464	684	1 138	1 264
1,60		33	42	242	404	636	1 092	1 266
1,70		32	40	217	344	588	1 046	1 211
1,80		31	38	191	330	540	998	1 188
1,90		30	36	166	315	492	949	1 166
2,00			35	139	301	443	898	1 144
2,20				81	273	345	804	1 089
2,40				43	245	316	709	1 032
2,60				39	216	288	609	973
2,80				36	189	261	507	912
3,00				34	161	232	402	849
3,20					130	204	340	790
3,40					99	177	318	726
3,60					63	147	298	660
3,80					39	115	278	591
4,00					36	83	259	523
4,20					35	42	239	454
4,40						39	219	383
4,60						37	200	334
4,80						35	181	305
5,00						34	161	278
5,20						33	140	251
5,40						32	118	222
5,60						31	96	194
5,80							72	166
6,00							41	136

For fire loads and opening factors between those in the diagrams and the tables, the gas temperature-time curve can be determined by interpolation. It must be pointed out that the lowest and highest values of the opening factor have no significance in practice. They have been included merely to facilitate translation of fire processes in fire compartments with different surrounding structures into fire processes in fire compartment A (see Subsection 4.3.4).

#### 4.3.4 Conversion of fire process in another type of fire compartment into a fire process in fire compartment type A (standard fire compartment)

For practical reasons, the design data in this handbook in the form of tables and diagrams for direct determination of the maximum steel temperature have been based only on the temperature-time curves for fire compartment type A (standard fire compartment). However, these design data can also be used for other types of fire compartments, since the temperature-time curve in the fire compartment in question can be translated into a temperature-time curve in fire compartment type A by conversion of the actual fire load and opening factor into equivalent fire

load and equivalent opening factor. These equivalents are obtained by multiplying the actual fire load and opening factor by a factor  $k_f$ . When the transition is made from one fire compartment to another, Equations (4.2.2.5 c) and (4.2.2.5 d) must both be satisfied at all times, i.e. both the fire load and the opening factor must be multiplied by the same value of the factor  $k_f$ . For one and the same fire compartment, the value of  $k_f$  can vary as a function of the size of opening factor and sometimes also as a function of the magnitude of the fire load. In Table 4 a in the Design Section, values of the factor  $k_f$  are given for the following types of fire compartment, characterised by their surrounding construction.

- fire compartment type A  
Materials with thermal properties corresponding to the average values for concrete, brick and lightweight concrete
- fire compartment type B  
Concrete
- fire compartment type C  
Lightweight concrete (density  $\gamma \approx 500 \text{ kg/m}^3$ )
- fire compartment type D  
50% concrete  
50% lightweight concrete (density  $\gamma \approx 500 \text{ kg/m}^3$ )
- fire compartment type E  
50% lightweight concrete (density  $\gamma \approx 500 \text{ kg/m}^3$ )  
33% concrete  
17% composite construction comprising, from the inside outwards,  
13 mm gypsum (density  $\gamma = 790 \text{ kg/m}^3$ )  
100 mm mineral wool (density  $\gamma = 50 \text{ kg/m}^3$ )  
brickwork (density  $\gamma = 1800 \text{ kg/m}^3$ )
- fire compartment type F  
80% uninsulated steel sheeting  
20% concrete  
This fire compartment represents a warehouse or similar premises with uninsulated roof and walls of steel sheeting and a concrete floor
- fire compartment type G  
20% concrete  
80% composite construction comprising  
double gypsum plasterboard, 2x13 mm (density  $\gamma = 790 \text{ kg/m}^3$ )  
100 mm air gap  
double gypsum plasterboard, 2x13 mm (density  $\gamma = 790 \text{ kg/m}^3$ )
- fire compartment type H  
Composite construction comprising  
steel sheeting  
100 mm mineral wool  
steel sheeting

The influence of the thermal properties of the construction surrounding the fire compartment on the calculated gas temperature-time curve is illustrated in Fig. 4.3.4 a. Fig. 4.3.4 b shows that the calculated gas temperature-time curves for fire compartment type B, for different fire loads  $q$  and an opening factor of  $\sqrt{A_v h}/A_t = 0.06 \text{ m}^2$ , can with fully acceptable accuracy be replaced by gas temperature-time curves for fire compartment type A in which the opening factor and the fire loads are 85% of those for fire compartment type B. The conversion factor  $k_f$  in this case is thus 0.85.

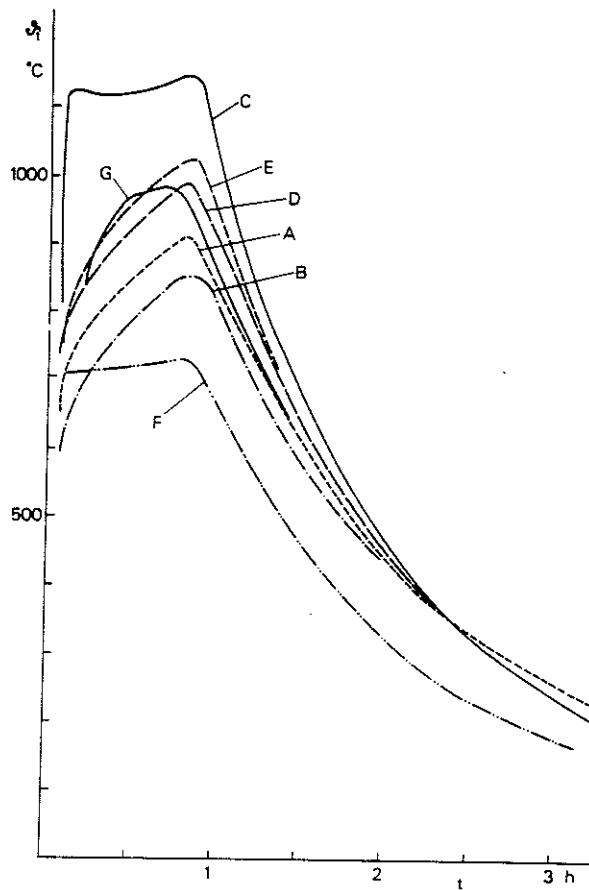


Fig. 4.3.4 a. Temperature-time curves for fire compartments Types A-G. In all cases, the opening factor  $A\sqrt{h}/A_t = 0.04 \text{ m}^{1/2}$  and the fire load  $q = 60 \text{ Mcal/m}^2$   $\{250 \text{ MJ/m}^2\}$  of surface area

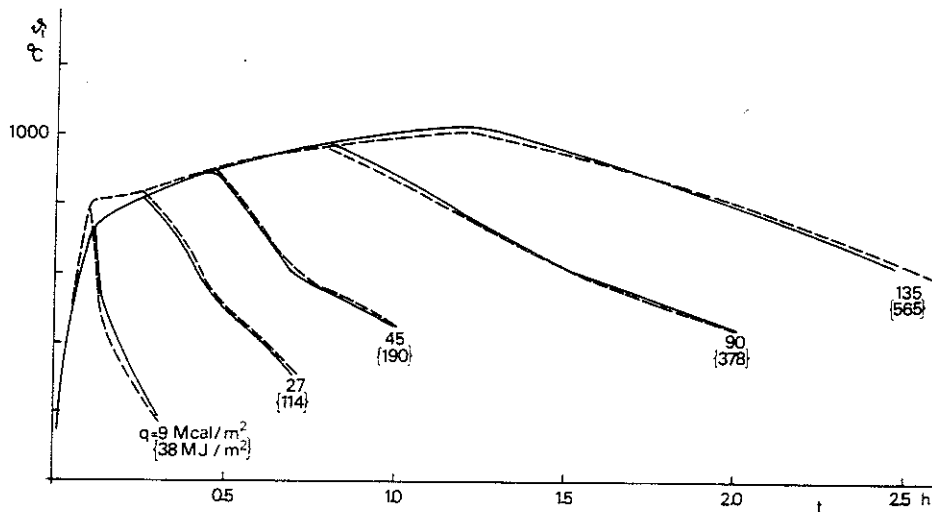


Fig. 4.3.4 b. Temperature-time curves for fire compartment Type B (—) with an opening factor  $A\sqrt{h}/A_t = 0.06 \text{ m}^{1/2}$  for different fire loads  $q$ , and temperature-time curves for fire compartment Type A, standard fire compartment, (---) with an opening factor and fire loads that are 85% of those in fire compartment Type B

#### 4.4 Transition from a ventilation controlled fire to a fire load controlled fire

The temperature-time curves presented in Subsection 4.3.3 are based on the

assumption that the combustion process is ventilation controlled and that the mean rate of combustion of wood during the flame phase, in kg per unit time, is thereby known and proportional to the air flow factor  $A\sqrt{h}$ . In practice, there are many cases where this condition is not satisfied. It is mainly a combination of low fire load and large opening surfaces which can result in rates of combustion that are clearly less than those in a ventilation controlled fire (see Section 4.1). Further determination of the rate of combustion in these fire load controlled fires is very difficult, since, apart from the size of the fire load, the combustion process is also governed to a decisive extent by the method of storage and degree of distribution of the fuel. This difficulty is greatly accentuated when the fire load consists of furniture, textiles and similar materials.

The fire load controlled combustion process is further complicated by the fact that it mainly occurs in fire compartments with large openings. The interchange of gases between the fire compartment and the outside, for the gas temperature-time curves presented in Subsection 4.3.3, has been calculated on the assumption that the flow configuration is in conformity with Fig. 4.2.2.4 a. This implies, inter alia, that the gas flow through the openings has a velocity component only in the horizontal direction. For small openings, this has been confirmed experimentally. It is however known that this assumption gradually ceases to be valid as the opening area increases (38). When the height of the opening area increases in relation to the other dimensions of the fire compartment, a zone of increasing size is formed at the bottom of the opening in which the gas temperature is the same as the prevailing outside temperature. The vertical air and gas flow which is a consequence of the vertical temperature difference next to the opening reduces the horizontal pressure difference. This has the effect of reducing the interchange of gases between the fire compartment and the surroundings. There is no reliable theoretical model available at present for the flow configuration in these conditions, and approximate methods must be employed. An investigation of the effect on the gas temperature-time curve due to an increase in the openings in the fire compartment is described in (20). In Fig. 4.4a which is reproduced from this investigation, the dashed line curve shows the measured gas temperature-time

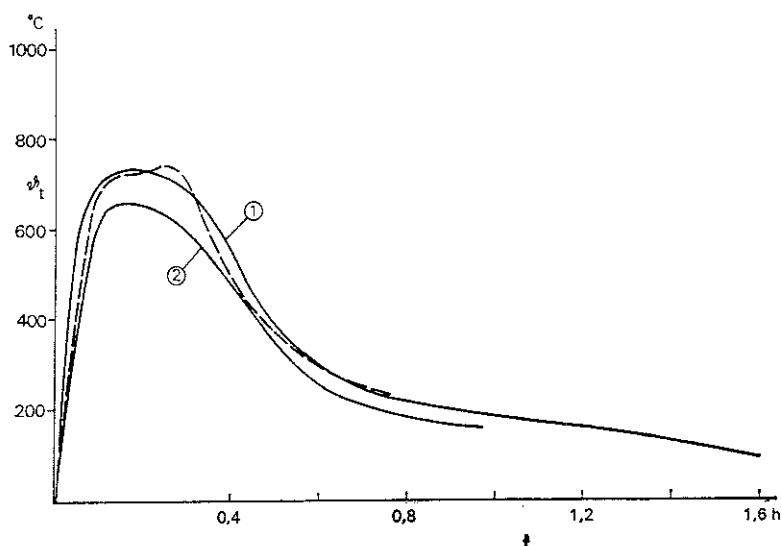


Fig. 4.4 a. Calculated (—) and measured (---) temperature-time curves for a fire compartment with a large opening. Curve 2 was calculated on the assumption that the heat removed by ventilation is given by Equation (4.2.2.4 e), and curve 1 on the assumption that the heat removed is 80% of that according to Equation (4.2.2.4 e)

curve for a fire compartment in which the opening is large in relation to the other dimensions, and the full lines 1 and 2 represent the calculated gas temperature-time curves. Both curve 1 and curve 2 were calculated on the assumption that the rate of combustion during the flame phase is 60% of the corresponding rate of combustion in a ventilation controlled fire. A further assumption made in calculating curve 2 was that a quantity of heat was being removed as set out in Equation (4.2.2.4 e), which implies a flow configuration according to Fig. 4.2.2.4 a. As will be seen in Fig. 4.4 a, agreement between the measured gas temperature-time curve and that calculated according to curve 2 is not too good. On the other hand, curve 1 is in good agreement with the measured gas temperature-time curve. In calculating curve 1, the gas interchange and thus the heat removed was assumed to be 80% of those under flow conditions according to Fig. 4.2.2.4 a.

Fire load controlled fires mainly occur in fire compartments with large openings in which the flow conditions are difficult to determine. The rate of combustion in fire load controlled fires is furthermore dependent on the method of storage and degree of distribution of the fire load, which are also difficult to define. Since, however, the assumption regarding ventilation controlled fire processes may be considered to produce steel temperatures on the safe side, it is natural that ventilation controlled fires should generally be assumed in the course of practical design.

The reason why the assumption that a fire is ventilation controlled produces results on the safe side is as follows.

It was seen in the example above that the interchange of air in a fire load controlled combustion process may remain at a level as high as 80% of the air interchange in a ventilation controlled fire, in spite of the fact that the rate of combustion during the flame phase is, for instance, only 60% of the rate of combustion in the ventilation controlled fire. This implies that the fire compartment is continually supplied with an excess of cool air which has no part in the combustion process, but only has a cooling effect. The greater duration of fire that is a consequence of the combustion process being fire load controlled is compensated for by the fact that, owing to this excess air, the temperature is lower than in a ventilation controlled fire. The maximum steel temperature in a fire load controlled process is therefore lower. This is also borne out by Fig. 4.4 b which shows the calculated maximum steel temperature  $\vartheta_{\max}$  as a function of the fire load  $q$  for an uninsulated steel structure and also for insulated steel structures with different insulation capacities  $d_i/\lambda_i$ . The dashed line curves relate to gas temperature-time processes calculated on the assumption of a ventilation controlled combustion process, with an opening factor  $A\sqrt{h}/A_t = 0.08 \text{ m}^{\frac{1}{2}}$ . The full line curves have been determined for fire load controlled combustion, the rate of combustion being assumed to be 50% of that in a ventilation controlled fire. In addition, the air interchange has been assumed to be 80% of that in a ventilation controlled fire. Fig. 4.4 b shows that the assumption concerning a ventilation controlled fire yields maximum steel temperatures on the safe side. In conjunction with high steel temperatures, which chiefly occur in uninsulated and lightly insulated steel structures, this is particularly pronounced.



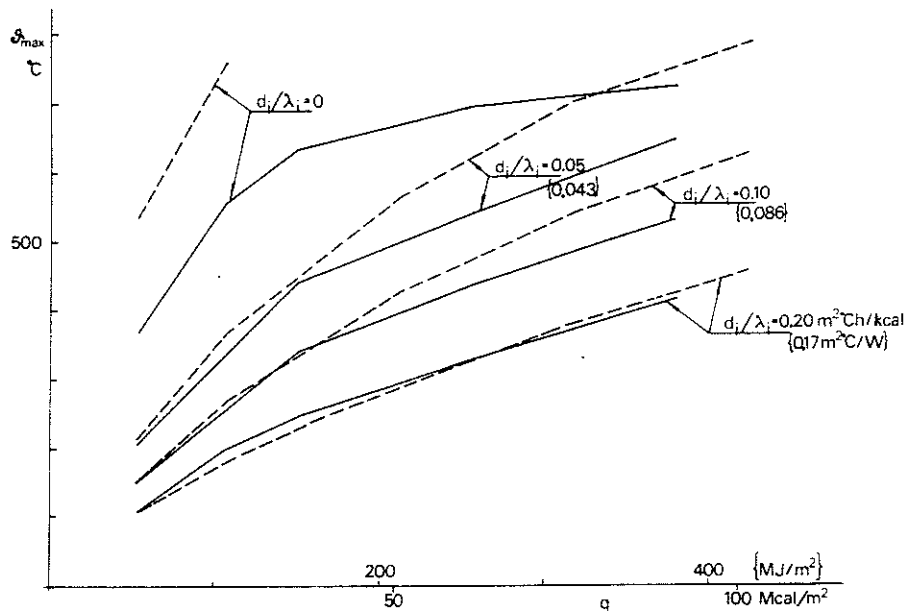


Fig. 4.4 b. Calculated maximum steel temperature  $\theta_{max}$  in steel structures with different insulation capacities  $d_i/\lambda_i$  as a function of the fire load  $q$ .  $d_i$  denotes the thickness of insulation and  $\lambda_i$  the thermal conductivity of the insulation. The dashed line curves were calculated on the assumption that the fire is ventilation controlled, the opening factor  $A\sqrt{h}/A_t$  being  $0.08\text{m}^{1/2}$ . The full line curves were calculated on the basis of a fire load controlled fire, the rate of combustion being 50% of that in a ventilation controlled fire. It was assumed that the air interchange in the fire load controlled fire is 80% of that in a ventilation controlled fire

## 5 TEMPERATURE - TIME CURVES FOR UNINSULATED STEEL STRUCTURES

### 5.1 The heat balance equation

The quantity of heat  $Q$  which passes through the boundary layer between the combustion gases and the steel section per unit length over a short interval of time  $\Delta t$  can be written (see Fig. 5.1 a)

$$Q = \alpha F_s (\vartheta_t - \vartheta_s) \Delta t \quad (\text{kcal/m}) \{ \text{J/m} \} \quad (5.1 \text{ a})$$

where  $\alpha$  = surface coefficient of heat transfer in the boundary layer between the combustion gases and the steel section ( $\text{kcal/m}^2 \text{ } ^\circ\text{C h}$ )  $\{ \text{W/m}^2 \text{ } ^\circ\text{C} \}$

$F_s$  = the surface of the steel section per unit length which is exposed to fire ( $\text{m}^2/\text{m}$ )

$\vartheta_t$  = the gas temperature in the fire compartment at time  $t$  ( $^\circ\text{C}$ )

$\vartheta_s$  = the temperature of the steel section at time  $t$  ( $^\circ\text{C}$ )

$\Delta t$  = the length of time interval ( $\text{h}$ )  $\{ \text{s} \}$

In order to increase the temperature of the steel section by  $\Delta \vartheta_s$   $^\circ\text{C}$ , a quantity of heat  $Q$  per unit length is required, the expression for this being

$$Q = c_{ps} \Delta \vartheta_s V_s \gamma_s \quad (\text{kcal/m}) \{ \text{J/m} \} \quad (5.1 \text{ b})$$

where  $c_{ps}$  = the specific heat capacity of the steel ( $\text{kcal/kg } ^\circ\text{C}$ )  $\{ \text{J/kg } ^\circ\text{C} \}$

$\Delta \vartheta_s$  = temperature rise in the steel section ( $^\circ\text{C}$ )

$V_s$  = volume per unit length of the steel section ( $\text{m}^3/\text{m}$ )

$\gamma_s$  = density of the steel ( $\text{kg/m}^3$ )

The quantity of heat supplied according to Equation (5.1. a) is equal to the quantity of heat required according to Equation (5.1 b) to increase the steel temperature by  $\Delta \vartheta_s$   $^\circ\text{C}$ . This gives the following expression for the rise in temperature  $\Delta \vartheta_s$  in the section over the time interval  $\Delta t$  during the fire

$$\Delta \vartheta_s = \frac{\alpha}{\gamma_s c_{ps}} \cdot \frac{F_s}{V_s} (\vartheta_t - \vartheta_s) \Delta t \quad (^\circ\text{C}) \quad (5.1 \text{ c})$$

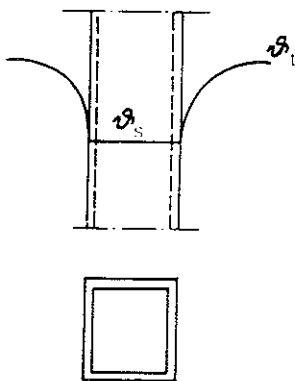


Fig. 5.1 a. Uninsulated steel section exposed to fire on all sides.  $\vartheta_t$  = gas temperature in fire compartment,  $\vartheta_s$  = temperature of steel section

Derivation of Equation (5.1 c) is based on the assumptions

- that, at every point of time, the steel temperature is uniformly distributed over the cross section of the steel member. The thinner the parts of the cross section, the greater the validity of this assumption.
- that heat flow is unidimensional. The smaller the corner effects, the greater the validity of this assumption

Owing to the high thermal conductivity of steel, these assumptions give satisfactory accuracy in ordinary cases. Sections of extremely thick walls constitute exceptions to the above.

If the gas temperature-time curve and thus  $\vartheta_t$  is known for a fire compartment, the maximum steel temperature can be determined by calculating the rise  $\Delta\vartheta_s$  in steel temperature for each time interval by means of Equation (5.1 c).

In Table 5 c in the Design Section, maximum steel temperatures  $\vartheta_{\max}$  calculated by computer are presented for different fire loads  $q$  and opening factors  $A'/h/A_t$  in the fire compartment. The calculations were performed by means of Equation (5.1 c), the different gas temperature-time curves for fire compartment type A (the standard fire compartment) according to Subsection 4.3.3 being used as the input data.

## 5.2 The quantities included in the heat balance equation

### 5.2.1 The length of the time interval $\Delta t$

Since the gas temperature  $\vartheta_t$  and the steel temperature  $\vartheta_s$  vary with time, the accuracy in calculating temperatures according to Equation (5.1 c) depends on the length of the time interval  $\Delta t$ . As a rule, a time interval  $\Delta t$  corresponding to one tenth to one twentieth of the duration of the whole fire process provides fully satisfactory accuracy.

### 5.2.2 The density of steel $\gamma_s$

The density of steel  $\gamma_s$  is  $7850 \text{ kg/m}^3$ .

### 5.2.3 The specific heat capacity $c_{ps}$ of steel

The specific heat capacity  $c_{ps}$  of steel varies with the temperature of steel and its composition. Representative values of the specific heat capacity for ordinary structural steels at different temperatures are given in Table 5.2.3 a.

Temp (°C)	$c_{ps}$ (kcal/kg °C)	$c_{ps}$ (kJ/kg °C)
0	0,115	0,482
100	0,115	0,482
200	0,125	0,522
300	0,134	0,560
400	0,143	0,600
500	0,153	0,640
600	0,163	0,682
700	0,166	0,695

Table 5.2.3 a. Representative values of the specific heat capacity  $c_{ps}$  for ordinary structural steels at different temperatures

#### 5.2.4 The surface coefficient of heat transfer $\alpha$ of the boundary layer

The surface coefficient of heat transfer  $\alpha$  of the boundary layer is made up of a convection portion and a radiation portion. With an accuracy that is sufficient in a fire engineering context, the convection portion  $\alpha_k$  can be put equal to 20 kcal/m<sup>2</sup> °C h { 23 W/m<sup>2</sup> °C }. The temperature dependent radiation portion  $\alpha_s$  is determined from the expression

$$\alpha_s = \frac{4.96\epsilon_r}{\vartheta_t - \vartheta_s} \left[ \left( \frac{\vartheta_t + 273}{100} \right)^4 - \left( \frac{\vartheta_s + 273}{100} \right)^4 \right] \quad (\text{kcal/m}^2 \text{ } ^\circ\text{C h}) \quad (5.2.4 \text{ a})$$

$$\alpha_s = \frac{5.77\epsilon_r}{\vartheta_t - \vartheta_s} \left[ \left( \frac{\vartheta_t + 273}{100} \right)^4 - \left( \frac{\vartheta_s + 273}{100} \right)^4 \right] \quad \{ \text{W/m}^2 \text{ } ^\circ\text{C} \}$$

where  $\epsilon_r$  = resultant emissivity

$\vartheta_t$  = gas temperature in the fire compartment at time  $t$  (°C)

$\vartheta_s$  = temperature of the steel section at time  $t$  (°C)

The total surface coefficient of heat transfer  $\alpha = \alpha_k + \alpha_s$  is thus

$$\alpha = 20 + \frac{4.96\epsilon_r}{\vartheta_t - \vartheta_s} \left[ \left( \frac{\vartheta_t + 273}{100} \right)^4 - \left( \frac{\vartheta_s + 273}{100} \right)^4 \right] \quad (\text{kcal/m}^2 \text{ } ^\circ\text{C h}) \quad (5.2.4 \text{ b})$$

$$\alpha = 23 + \frac{5.77\epsilon_r}{\vartheta_t - \vartheta_s} \left[ \left( \frac{\vartheta_t + 273}{100} \right)^4 - \left( \frac{\vartheta_s + 273}{100} \right)^4 \right] \quad \{ \text{W/m}^2 \text{ } ^\circ\text{C} \}$$

The resultant emissivity  $\epsilon_r$  is dependent on the emissivities  $\epsilon_t$  and  $\epsilon_s$  of the flames and the steel structure and on the sizes of the flames and the steel structure and their positions relative to one another. In the case of two infinitely large parallel surfaces, all radiation from the one surface impinges on the other surface, and vice versa. The expression for the resultant emissivity is then

$$\epsilon_r = \frac{1}{1/\epsilon_t + 1/\epsilon_s - 1} \quad (5.2.4 \text{ c})$$

where  $\epsilon_t$  = emissivity of the flames

$\epsilon_s$  = emissivity of the steel section

Equation (5.2.4 c) can be used for calculation of  $\epsilon_r$  for a column placed in the fire compartment which is exposed to fire on all sides, since if it is assumed that the flames completely surround the column, all radiation from these will impinge on the column, and vice versa. The emissivity of flames  $\epsilon_t$  which varies, inter alia, with the size of the flames, is usually in the range 0.6 - 0.9 (43). The emissivity of the steel structure  $\epsilon_s$  can normally be assumed to be 0.8 (43). Taking the emissivities of the flames and the steel structure as 0.85 and 0.8 respectively, Equation (5.2.4 c) gives a resultant emissivity of  $\epsilon_r = 0.7$ .

In the event of fire inside the building, a column placed outside the facade will be exposed to less radiation from the flames than a column placed inside the fire compartment. Furthermore, the cold outside air retards the temperature rise in the column. This can be approximately taken into consideration by using a lower value of the resultant emissivity  $\epsilon_r$  than that applicable to an internal column. An analysis of the conditions shows that a value of  $\epsilon_r = 0.3$  can be used

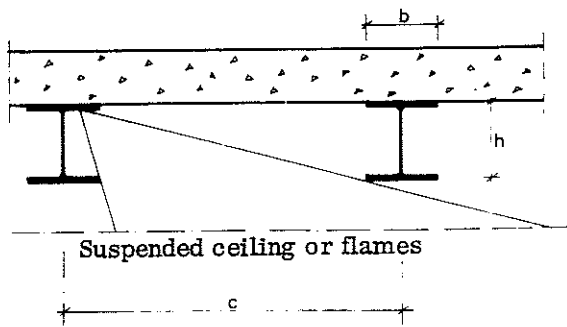


Fig. 5.2.4 a. Floor construction where the flames or suspended ceiling are in their entirety below the floor girders

for a rough assessment of the maximum steel temperature, which is on the safe side, in a column placed immediately outside a window opening (43).

In the case of floor girders situated in rooms of sufficient height and floor girders protected by a suspended ceiling, the whole of the heat emitting surface, i.e. the flames or the top of the suspended ceiling, is below the girders. Some parts of the girder surfaces will not be subjected to full radiation in such a case, since they are partly shielded from the flames by other parts of the girders (see Figure 5.2.4 a). The radiation to which the girders are subjected is dependent on the width-height ratio  $b/h$  of the girders and on the spacing-height ratio  $c/h$  of the girders. The resultant emissivity  $\epsilon_r$  as a function of these geometrical conditions is shown in Fig. 5.2.4 b for different values of the emissivity  $\epsilon_t$  for the flames or the suspended ceiling. The girder and floor emissivities  $\epsilon_s$  and  $\epsilon_{bj}$  have been taken as 0.8 throughout. Unless some other value is shown to be more correct, it is recommended that a value of 0.85 should be taken as the emissivity  $\epsilon_t$  of the flames in fire engineering design.

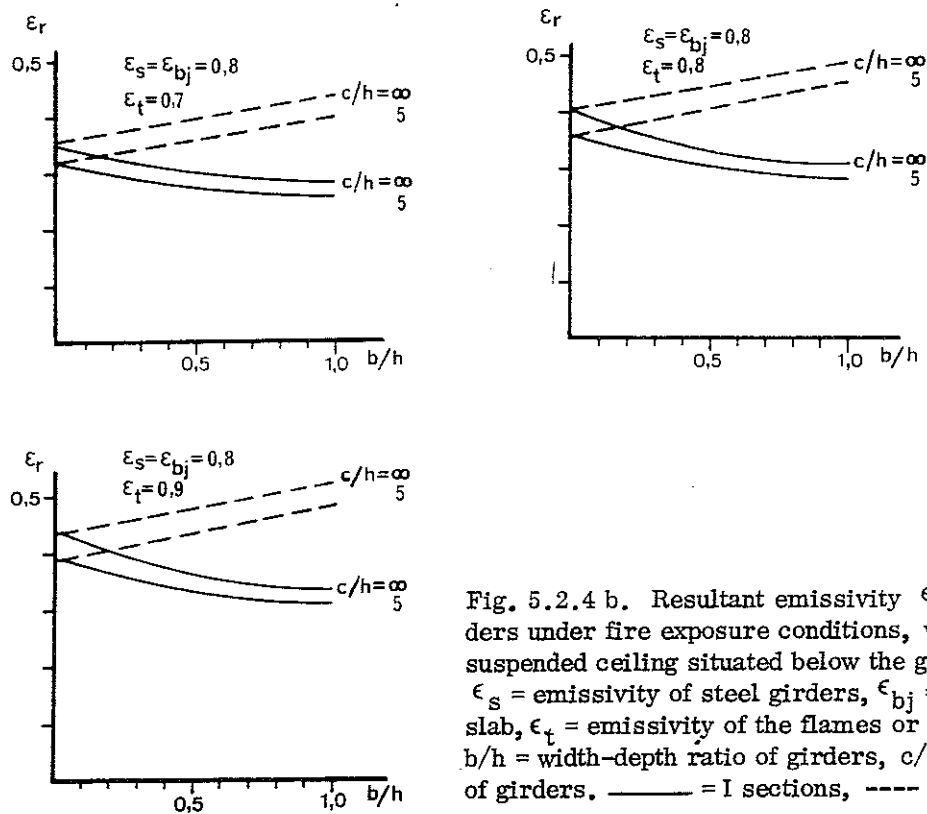


Fig. 5.2.4 b. Resultant emissivity  $\epsilon_r$  for steel floor girders under fire exposure conditions, with the flames or the suspended ceiling situated below the girders.

$\epsilon_s$  = emissivity of steel girders,  $\epsilon_{bj}$  = emissivity of floor slab,  $\epsilon_t$  = emissivity of the flames or suspended ceiling,  $b/h$  = width-depth ratio of girders,  $c/h$  = spacing-depth ratio of girders. — = I sections, ---- = box sections

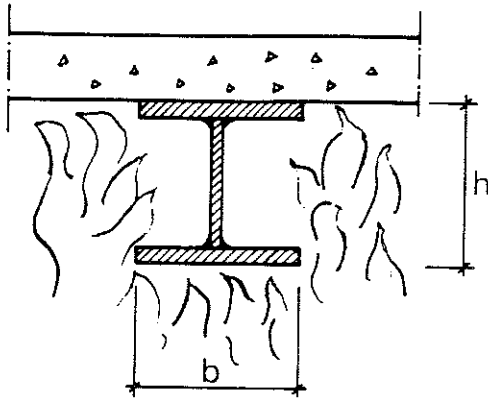


Fig. 5.2.4 c. Floor construction where the flames penetrate between the girders

Where the flames penetrate between the girders (see Fig. 5.2.4 c), the girders are exposed to greater radiation than floor girders which are situated completely above the flames. The resultant emissivity  $\epsilon_r$  for I girders carrying a floor slab on their top flanges, with the flames penetrating between the girders right up to the soffit of the slab, is given in Fig. 5.2.4 d as a function of the width-height ratio  $b/h$  of the girders, for different values of the flame emissivity  $\epsilon_t$ . The emissivity of the girders  $\epsilon_s$  was assumed to be 0.8. Unless some other value can be shown to be more correct, it is recommended that the value of the flame emissivity  $\epsilon_t$  is taken to be 0.85 in fire engineering design.

For floor girders of box section, the resultant emissivity  $\epsilon_r$  is to be calculated in the same way as for a column placed inside the fire compartment, if it is assumed that the flames reach the soffit of the floor slab. If the emissivities of the flames and the girders are taken as 0.85 and 0.8 respectively, Equation (5.2.4 c) gives a resultant emissivity of  $\epsilon_r = 0.7$ .

In the case of floor girders where the bottom flanges carry the concrete floor slab and it is consequently only the underside of the bottom flange that is directly exposed to fire, heat is conducted away from the flange up into the rest of the girder and the concrete slab. This condition can be approximately taken into account by basing the calculation of the steel temperature development on a value of the resultant emissivity that is lower than the value of 0.7 determined purely on the basis of radiation geometry. A value of  $\epsilon_r = 0.5$  of the resultant emissivity is recommended in this case, which gives a steel temperature on the safe side (43).

A summary of the recommended values of the resultant emissivity  $\epsilon_r$  to be used

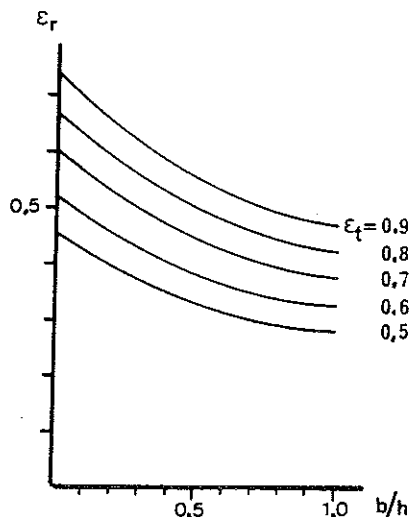


Fig. 5.2.4 d. Resultant emissivity  $\epsilon_r$  for I section floor girders where the flames penetrate up to the floor slab.  $\epsilon_t$  = emissivity of flames,  $b/h$  = width-depth ratio of girders. The emissivity of the girders is assumed to be 0.8

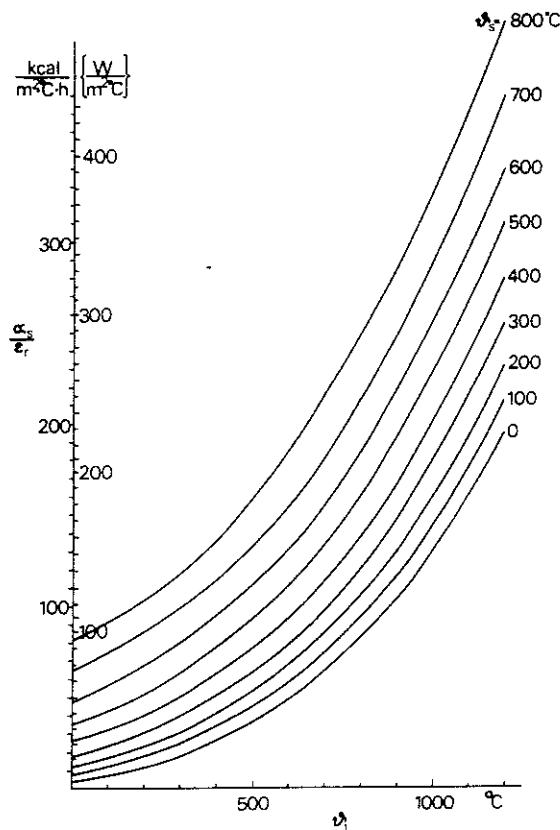


Fig. 5.2.4 e. The ratio  $\alpha_s/\epsilon_r$  as a function of the gas temperature  $\theta_t$  in the fire compartment and the temperature  $\theta_s$  of the steel section

in fire engineering design of different structures is given in Table 5 a in the Design Section. The values quoted give steel temperatures on the safe side.

When the value of  $\epsilon_r$  is known, the radiation portion  $\alpha_s$  of the surface coefficient of heat transfer according to Equation (5.2.4 a) can be calculated with the assistance of Fig. 5.2.4 e, after which the total surface coefficient of heat transfer  $\alpha$  is given by Equation (5.2.4 b).

#### 5.2.5 The $F_s/V_s$ ratio of the steel section

The ratio  $F_s/V_s$  between the fire exposed surface of the steel section and its volume per unit length varies as a function of the section dimensions and the method of construction.

For a floor girder where the floor slab is carried on the top of the top flange, the fire exposed surface  $F_s$  is equal to the total surface area of the section per unit length, less the area of the top of the top flange, and the volume  $V_s$  is equal to the total volume of the girder per unit length.

In the case of a floor girder where it is only the bottom of the bottom flange that is directly exposed to fire, only the volume of the bottom flange and not the whole volume of the girder is to be taken as  $V_s$ . This approximation, which yields results on the safe side, means that  $F_s/V_s$  is put equal to  $1/t$ , where  $t$  is the thickness of the flange in metres.

For a column placed inside a fire compartment and exposed to fire on all sides, the fire exposed area  $F_s$  is equal to the total surface area of the section per unit length, and the volume  $V_s$  equal to the total volume of the column per unit length.

In calculating the temperature in a fire exposed column placed outside the facade, it is best to put the fire exposed area  $F_s$  equal to the area of the flange facing the building plus the area of both sides of the web per unit length. The whole volume of the column per unit length is to be taken as  $V_s$  (43).

Examples of the way in which  $F_s/V_s$  is to be calculated for different structures are given in Fig. 5a in the Design Section. Table 5 b in the Design Section also gives values of the  $F_s/V_s$  ratio for rolled I girders for free-standing columns inside the fire compartment and for floor girders carrying a floor slab on the top of the top flange.

### 5.3 Dependence of the maximum steel temperature on $F_s/V_s$ , $\epsilon_r$ and $\theta_t$

As a rule, the ratio of the fire exposed surface  $F_s$  to the enclosed steel volume  $V_s$  exerts a great influence on the maximum steel temperature  $\theta_{\max}$ . The maximum steel temperature is further dependent on the value of the resultant emissivity  $\epsilon_r$ . Finally, the gas temperature-time relationship  $\theta_t$ , primarily determined on the basis of the opening factor  $A\sqrt{h}/A_t$  of the fire compartment and the fire load  $q$ , is of great significance for the value of the maximum steel temperature.

An example of the influence of the  $F_s/V_s$  ratio on the maximum steel temperature  $\theta_{\max}$  for two different values of the fire load  $q$ , a given resultant emissivity  $\epsilon_r$  and a given opening factor  $A\sqrt{h}/A_t$ , is given in Fig. 5.3 a.

An example of the influence of the resultant emissivity  $\epsilon_r$  on the maximum steel temperature  $\theta_{\max}$  at a given  $F_s/V_s$  ratio and a given opening factor  $A\sqrt{h}/A_t$  is given in Fig. 5.3 b.

An example of the influence of the opening factor  $A\sqrt{h}/A_t$  on the maximum steel temperature  $\theta_{\max}$  for a given resultant emissivity  $\epsilon_r$  and a given  $F_s/V_s$  ratio is given in Fig. 5.3 c.

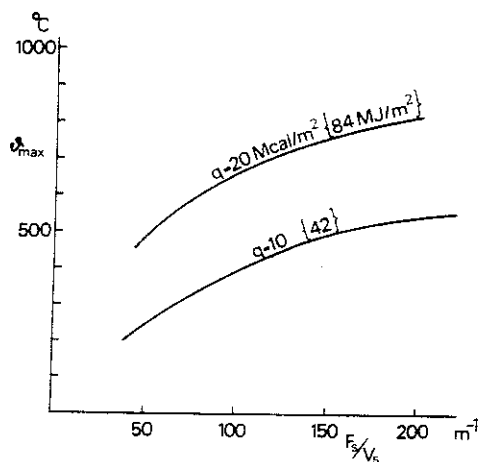


Fig. 5.3 a. Maximum steel temperature  $\theta_{\max}$  as a function of the  $F_s/V_s$  ratio of the steel section for fire loads of  $q = 10$  {42} and  $20 \text{ Mcal/m}^2$  {84  $\text{MJ/m}^2$ }. The resultant emissivity  $\epsilon_r = 0.5$  and the opening factor of the fire compartment  $A\sqrt{h}/A_t = 0.08 \text{ m}^{1/2}$



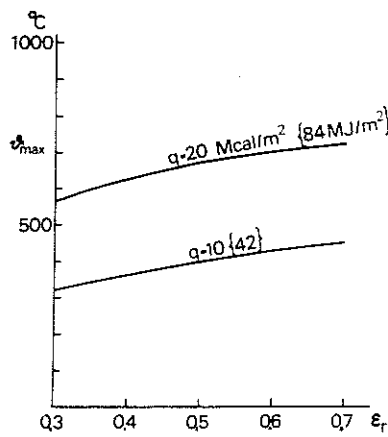


Fig. 5.3 b. Maximum steel temperature  $\vartheta_{max}$  as a function of the resultant emissivity  $\epsilon_r$  for fire loads  $q = 10 \{42\}$  and  $20 \text{ Mcal/m}^2 \{84 \text{ MJ/m}^2\}$ . The  $F_s/V_s$  ratio =  $100 \text{ m}^{-1}$  and the opening factor of the fire compartment  $Avh/A_t = 0.08 \text{ m}^{1/2}$

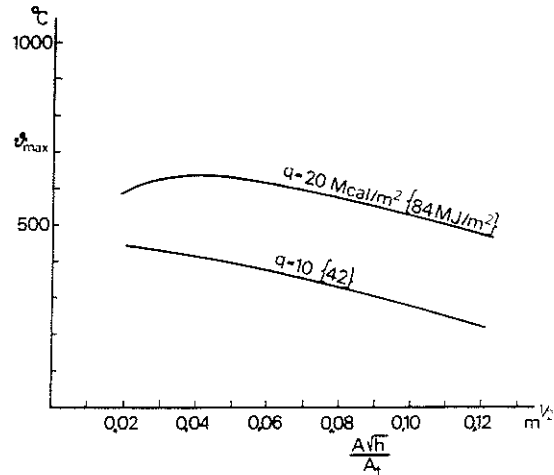


Fig. 5.3 c. Maximum steel temperature  $\vartheta_{max}$  as a function of the opening factor  $Avh/A_t$  of the fire compartment for fire loads  $q = 10 \{42\}$  and  $20 \text{ Mcal/m}^2 \{84 \text{ MJ/m}^2\}$ . The  $F_s/V_s$  ratio =  $100 \text{ m}^{-1}$  and the resultant emissivity  $\epsilon_r = 0.3$

#### 5.4 Worked example

Calculate the maximum steel temperature under fire exposure conditions for an uninsulated floor girder shown in Fig. 5.4 a which carries precast concrete floor units on its bottom flange. It is assumed that values of the gas temperature  $\vartheta_t$  in the fire compartment at various times are given in column 3 in Table 5.4 a.

According to Equation (5.1 c),

$$\Delta\vartheta_s = \frac{\alpha}{\gamma_s c_{ps}} \cdot \frac{F_s}{V_s} (\vartheta_t - \vartheta_s) \Delta t \quad (^\circ\text{C}) \quad (5.4 a)$$

According to Subsection 5.2.5, the  $F_s/V_s$  ratio for a girder as shown in Fig. 5.4 a can be calculated as  $1/t$ , where  $t$  is the flange thickness per metre. This gives  $F_s/V_s = 1/0.02 = 50 \text{ m}^{-1}$ . The density of steel  $\gamma_s = 7850 \text{ kg/m}^3$ . The specific heat capacity  $c_{ps}$  varies with the temperature according to Table 5.2.3 a. In this worked example, however,  $c_{ps}$  is assumed to be constant and equal to  $0.13 \text{ kcal/kg } ^\circ\text{C} \{0.54 \text{ kJ/kg } ^\circ\text{C}\}$ , which may be regarded as a reasonable mean

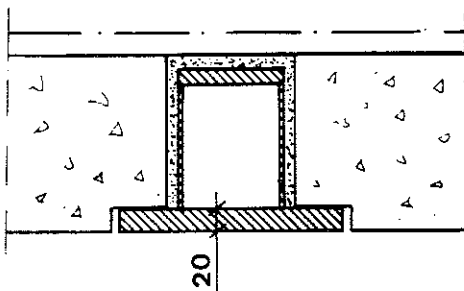


Fig. 5.4 a. Steel floor girder carrying precast concrete floor units on the bottom flange

Table 5.4 a. Calculation of the steel temperature-time curve for a floor girder of the configuration shown in Fig. 5.4 a

Line Rad (1)	Time (min) (2)	$\vartheta_t$ (°C) (3)	$\alpha$ (kcal/ $\text{m}^2\text{°C h}$ ) (4)	$(\vartheta_t - \vartheta_s)$ (°C) (5)	$\Delta\vartheta_s$ (°C) (6)	$\vartheta_s$ (°C) (7)
1	0					20
2		207	27,5	187	9	
3	2					29
4		622	47,5	593	46	
5	4					75
6		850	70	775	89	
7	6					164
8		894	83	730	100	
9	8					264
10		937	98	673	109	
11	10					373
12		900	102	527	88	
13	12					461
14		850	105	389	67	
15	14					528
16		734	95	206	32	
17	16					560
18		620	85	60	8	
19	18					568
20		540	75	-28	-4	
21	20					564

value of  $c_{ps}$  at the steel temperatures in question. The length of the time interval  $\Delta t$  is made 2 minutes, i.e.  $t = 1/30$  h.

With the above values substituted into Equation (5.4 a), we have

$$\Delta\vartheta_s = \frac{\alpha}{610} (\vartheta_t - \vartheta_s) \quad (\text{°C}) \quad (5.4 b)$$

The surface coefficient of heat transfer  $\alpha$  is calculated according to Equation (5.2.4 b) with the assistance of Fig. 5.2.4 e, the resultant emissivity  $\epsilon_r$  in accordance with the recommendation in Subsection 5.2.4 being put equal to 0.5. Calculation of the steel temperature-time curve by means of Equation (5.4 b) is illustrated in Table 5.4 a.

The steel temperature at the beginning of the fire is assumed to be  $\vartheta_s = 20$  °C (line 1, column 7). In the middle of the first time interval the temperature of the fire compartment,  $\vartheta_t$ , is given as 207°C (line 2, column 3). With these temperatures, Fig. 5.2.4 e gives a value of 15 kcal/m<sup>2</sup> °C h for  $\alpha_s/\epsilon_r$ . With  $\epsilon_r = 0.5$ , Equation (5.2.4 b) gives a value of  $\alpha = 27.5$  kcal/m<sup>2</sup> °C h (line 2, column 4). The difference between the temperature of the fire compartment  $\vartheta_t$  and the steel temperature  $\vartheta_s$  is 187°C (line 2, column 5). These values of  $\alpha$  and the difference in temperature give the rise in steel temperature  $\Delta\vartheta_s$  during the first time interval as 9°C (line 2, column 6). The steel temperature after 2 minutes is thus  $20 + 9 = 29$ °C (line 3, column 7). Calculation is to be continued in the same way for each time interval until the steel temperature has attained a maximum. As will be seen in the table, the maximum steel temperature of 568°C is reached after 18 minutes.

### 5.5 Comparison of the calculated steel temperature-time curve with that measured in fire tests

The calculated steel temperature-time curve is compared in Fig. 5.5 a with the temperature-time curve measured in fire tests for an uninsulated steel floor girder (43). With the exception of the top flange of the girder, agreement between the calculated and measured temperature-time curve for the section is good. The temperature in the top flange is consistently lower than in the rest of the girder. This is due to the fact that the top flange is exposed to less direct radiation than the bottom flange, and also that there is continuous conduction of heat away from the top flange into the cooler concrete slab. No account has been taken of this conduction in calculating the steel temperature-time curve.

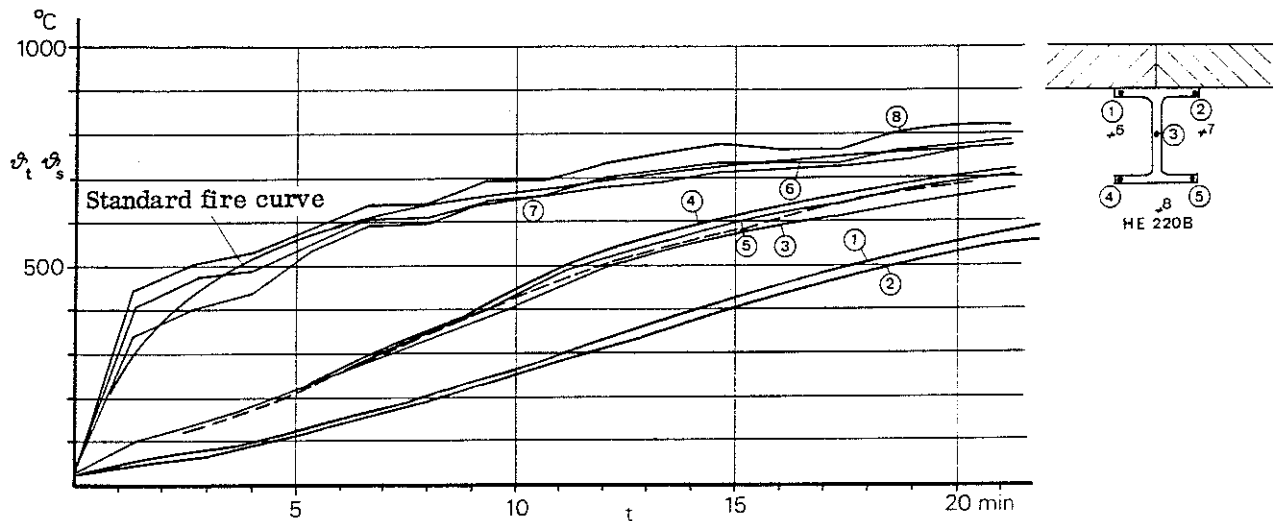


Fig. 5.5 a. Calculated(---) and measured (—) steel temperature-time ( $\vartheta_s - t$ ) curve for uninsulated HE 220 B steel girder

## 6 TEMPERATURE - TIME CURVES FOR INSULATED STEEL STRUCTURES

### 6.1 The heat balance equation

The quantity of heat  $Q$  which is supplied to unit length of an insulated steel section over a short time interval  $\Delta t$  of a fire can, on the assumption that the temperature gradient in the insulation is linear, be written (see Fig. 6.1 a)

$$Q = \frac{1}{1/\alpha + d_i/\lambda_i} A_i(\vartheta_t - \vartheta_s) \Delta t \quad (\text{kcal/m}) \{ \text{J/m} \} \quad (6.1 a)$$

where  $d_i$  = thickness of insulation (m)  
 $\lambda_i$  = thermal conductivity of the insulation material (kcal/m °C h) { W/m °C }  
 $\alpha$  = surface coefficient of heat transfer in the boundary layer between the combustion gases and the insulation (kcal/m<sup>2</sup> °C h) { W/m<sup>2</sup> °C }  
 $A_i$  = internal surface area of the insulation per unit length of the section (m<sup>2</sup>/m)  
 $\vartheta_t$  = gas temperature in the fire compartment at time  $t$  (°C)  
 $\vartheta_s$  = temperature of the steel section at time  $t$  (°C)  
 $\Delta t$  = length of time interval (h) { s }

In order to raise the temperature of the steel section by  $\Delta\vartheta_s$  °C, a quantity of heat  $Q$  per unit length is required according to the expression

$$Q = c_{ps} \Delta\vartheta_s V_s \gamma_s \quad (\text{kcal/m}) \{ \text{J/m} \} \quad (6.1 b)$$

where  $c_{ps}$  = specific heat capacity of the steel (kcal/kg °C) { J/kg °C }  
 $\Delta\vartheta_s$  = temperature rise in the steel section (°C)  
 $V_s$  = volume per unit length of the steel section (m<sup>3</sup>/m)  
 $\gamma_s$  = density of steel (kg/m<sup>3</sup>)

If the heat capacity of the insulation in comparison with that of the steel is ignored, the rise in temperatures  $\Delta\vartheta_s$  in the steel section over the time interval  $\Delta t$  of the fire is obtained by putting the quantity of heat supplied as set out in Equation (6.1 a) equal to the quantity of heat which, according to Equation (6.1 b), is required to raise the temperature of the steel section by  $\Delta\vartheta_s$  °C. It follows

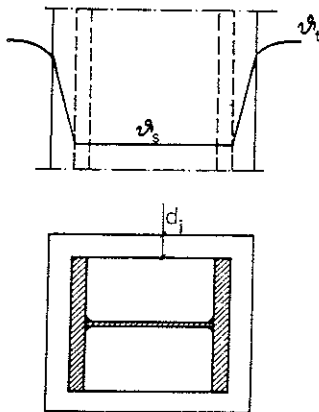


Fig. 6.1 a. Insulated steel section exposed to fire on all sides, with an assumed linear temperature gradient in the insulation.  $\vartheta_t$  = gas temperature in the fire compartment,  $\vartheta_s$  = temperature of steel section

from this that

$$\Delta\vartheta_s = \frac{A_i}{(1/\alpha + d_i/\lambda_i)\gamma_s c_{ps} V_s} (\vartheta_t - \vartheta_s) \Delta t \quad (^\circ\text{C}) \quad (6.1 \text{ c})$$

Derivation of Equation (6.1 c) is based on the assumptions

- that, at every point of time, the temperature is uniformly distributed over the cross section of the steel member. The thinner the parts of the cross section, the greater the validity of this assumption
- that the temperature gradient is linear and that the quantity of energy needed to heat the insulation is negligible. The smaller the insulation thickness, the greater the validity of this assumption
- that heat flow in the steel section and the insulation is unidimensional. The smaller the corner effects, the greater the validity of this assumption

At the temperatures which occur during a fire, the thermal surface resistance  $1/\alpha$  can normally be ignored in comparison with the thermal resistance  $d_i/\lambda_i$  of the insulation, and Equation (6.1 c) can therefore be written in the form

$$\Delta\vartheta_s = \frac{\lambda_i A_i \Delta t}{d_i V_s \gamma_s c_{ps}} (\vartheta_t - \vartheta_s) \quad (^\circ\text{C}) \quad (6.1 \text{ d})$$

In comparison with the heat capacity of the steel structure, the heat capacity of the lightweight insulation materials normally used today is very small. It is therefore generally justifiable to ignore completely the heat capacity of the insulation, as in Equations (6.1 c) and (6.1 d). In addition, this is an approximation on the safe side. If, however, heavier insulation with a greater heat capacity is used, there may be reason to take into account the quantity of heat stored in the insulation when the rise in temperature  $\Delta\vartheta_s$  in the steel is being calculated. In order to approximate this quantity of heat, it is assumed that the mean temperature rise in the insulation over the time interval  $\Delta t$  during the fire is equal to the mean of the rise in gas temperatures  $\Delta\vartheta_t$  and the rise in steel temperature  $\Delta\vartheta_s$  over the same interval of time, i.e.  $\frac{1}{2}(\Delta\vartheta_t + \Delta\vartheta_s)$ . The quantity of heat  $Q_i$  required per unit length to increase the mean temperature of the insulation by  $\frac{1}{2}(\Delta\vartheta_t + \Delta\vartheta_s)$  can be written

$$Q_i = c_{pi} \frac{1}{2} (\Delta\vartheta_t + \Delta\vartheta_s) d_i A_i \gamma_i \quad (\text{kcal/m}) \{ \text{J/m} \} \quad (6.1 \text{ e})$$

where  $c_{pi}$  = specific heat capacity of the insulation material (kcal/kg  $^\circ\text{C}$ ) { J/kg  $^\circ\text{C}$  }  
 $\Delta\vartheta_t$  = rise in gas temperature over the time interval  $\Delta t$  of the fire ( $^\circ\text{C}$ )  
 $\gamma_i$  = density of the insulation material (kg/m<sup>3</sup>)

If the quantity of heat supplied, as described in Equation (6.1 a), is put equal to the sum of the quantity of heat required, according to Equation (6.1 b), to raise the temperature of the steel by  $\Delta\vartheta_s$   $^\circ\text{C}$ , and the quantity of heat required according to Equation (6.1 e) to raise the temperature of the insulation by  $\frac{1}{2}(\Delta\vartheta_t + \Delta\vartheta_s)$   $^\circ\text{C}$ , the rise in temperature  $\Delta\vartheta_s$  in the steel section over a time interval  $\Delta t$  of the fire is given by the following expression (27), (32)

$$\Delta\vartheta_s = \frac{(\vartheta_t - \vartheta_s) \Delta t}{(1/\alpha + d_i/\lambda_i) \gamma_s c_{ps} \frac{V_s}{A_i} \left( 1 + \frac{d_i \gamma_i c_{pi} A_i}{2 \gamma_s c_{ps} V_s} \right)} - \frac{\Delta\vartheta_t}{\frac{2 \gamma_s c_{ps} V_s}{d_i \gamma_i c_{pi} A_i} + 1} \quad (6.1 \text{ f})$$

The influence of the heat capacity of the insulation is thus taken into account approximately in Equation (6.1 f).

When the gas temperature  $\vartheta_t$  in the fire compartment at a given time is known, the maximum steel temperature can be determined by calculating the rise in steel temperature  $\Delta\vartheta_s$  for each time interval by means of Equation (6.1 c), (6.1 d) or (6.1 f).

Tables 6 b and 6 c in the Design Section give values of the maximum steel temperatures  $\vartheta_{\max}$ , calculated by a computer, for different fire loads  $q$  and fire compartment opening factors  $A\sqrt{h}/A_t$ . For Table 6 b the calculations were performed in accordance with Equation (6.1 c), and for Table 6 c by means of a special computer program which takes into account the thermal data and their temperature dependence accurately and according to the principles set out in Subsection 4.2.2.3. The different gas temperature-time curves for fire compartment type A (standard fire compartment) according to Subsection 4.3.3 were used as input data.

## 6.2 The quantities included in the heat balance equation

With regard to  $\Delta t$ ,  $\gamma_s$ ,  $c_{ps}$  and  $\alpha$ , reference is to be made to Subsections 5.2.1 - 5.2.4.

### 6.2.1 Thermal conductivity $\lambda_i$ of the insulation

As a rule, the thermal conductivity  $\lambda_i$  of the insulation varies with the temperature. This can be taken into account when calculating the steel temperature by using the value of  $\lambda_i$  applicable for the actual insulation temperature for each step in the calculation.

Another possibility is to use a constant value of  $\lambda_i$  during the whole calculation. This value should be the mean value of  $\lambda_i$  for the entire fire process. Such a mean value can be estimated by assuming a value for  $\vartheta_{\max}$ , the maximum steel temperature during the fire (see Fig. 6.2.1 a). The gas temperature-time curve ( $\vartheta_t - t$ ) (see Subsection 4.3.3) is followed to the time during the cooling phase of the fire when the gas temperature has dropped to the assumed value of  $\vartheta_{\max}$ . This time is about the same as that for the maximum steel temperature, provided that this is the same as the assumed value of  $\vartheta_{\max}$ . The mean gas tempera-

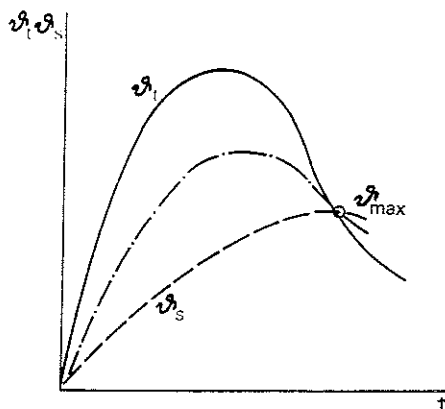


Fig. 6.2.1 a. Schematic representation of the gas temperature-time ( $\vartheta_t - t$ ) curve and the steel temperature-time ( $\vartheta_s - t$ ) curve. The chain line curve shows the temperature variation in time in the middle of the insulation

ture during the fire up to this time is determined by dividing the area underneath the gas temperature-time curve by the time. The mean value of steel temperature can be approximately estimated as the mean of the initial temperature of  $20^{\circ}\text{C}$  and the final temperature  $\vartheta_{\text{max}}$  (as assumed). The temperature at the outside of the insulation can be assumed to be the same as the gas temperature, and the temperature on the inside can be assumed to be the same as the steel temperature. If the temperature in the insulation is assumed to vary linearly from the outside to the inside, the mean temperature in the middle of the insulation can be determined from the calculated mean values, i.e. it will be the mean of the gas temperature and the steel temperature. The calculated mean value of the temperature in the middle of the insulation is used for the choice of the  $\lambda_i$  value. The value of  $\lambda_i$  at different temperatures is given for different insulation materials in Table 6 a in the Design Section. Using the chosen value of  $\lambda_i$ , the steel temperature-time curve and the maximum steel temperature are calculated. If it is found that the maximum steel temperature is substantially different from the assumed temperature  $\vartheta_{\text{max}}$ , it may be necessary to make a new estimate of the suitable value of  $\lambda_i$ .

Instead of calculating the mean temperature of the insulation, it is possible to use directly the value of  $\lambda_i$  which applies for a temperature equal to the maximum steel temperature, since calculations show that the mean temperature of the insulation is generally approximately the same as the maximum steel temperature.

#### 6.2.2 The specific heat capacity $c_{pi}$ of the insulation

As a rule, the specific heat capacity  $c_{pi}$  of the insulation varies with the temperature, but usually to a lesser extent than the thermal conductivity  $\lambda_i$ . If the heat capacity of the insulation is to be taken into account in calculating the steel temperature, as set out in Equation (6.1 f), a suitable value of  $c_{pi}$  can be determined in the same way as for  $\lambda_i$ .

#### 6.2.3 The $A_i/V_s$ ratio of the steel section

The ratio  $A_i/V_s$  of the inner surface area of the insulation to the volume of the steel section per unit length varies as a function of the dimensions of the section and the method of construction. Fig. 6 a in the Design Section gives examples of the calculation of the  $A_i/V_s$  ratio for different methods of construction.

### 6.3 Dependence of the maximum steel temperature on $A_i/V_s$ , $d_i/\lambda_i$ and $\vartheta_t$

The ratio of the inner surface area  $A_i$  of the insulation to the enclosed steel volume  $V_s$  generally exerts a great influence on the maximum steel temperature  $\vartheta_{\text{max}}$ . Furthermore, the maximum steel temperature is greatly dependent on the value of the insulation capacity  $d_i/\gamma_i$ . Finally, the gas temperature-time relationship  $\vartheta_t$ , primarily determined on the basis of the opening factor  $A\sqrt{h}/A_t$  of the fire compartment and the fire load  $q$ , is of great significance for the value of the maximum steel temperature.

An example of the influence of the  $A_i/V_s$  ratio on the maximum steel tempera-

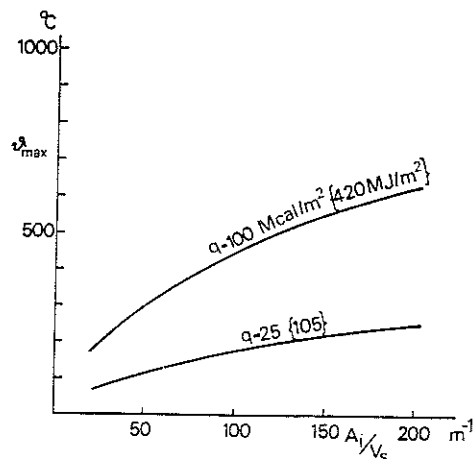


Fig. 6.3 a. Maximum steel temperature  $\vartheta_{max}$  as a function of the  $A_i/V_s$  ratio for fire loads of 25 {105} and 100  $\text{Mcal/m}^2$  {420  $\text{MJ/m}^2$ }. The insulation capacity  $d_i/\lambda_i = 0.20 \text{ m}^2 \text{ h } ^\circ\text{C/kcal}$  {0.172  $\text{m}^2 \text{ } ^\circ\text{C/W}$ } and the opening factor of the fire compartment  $A\sqrt{h}/A_t = 0.08 \text{ m}^{1/2}$

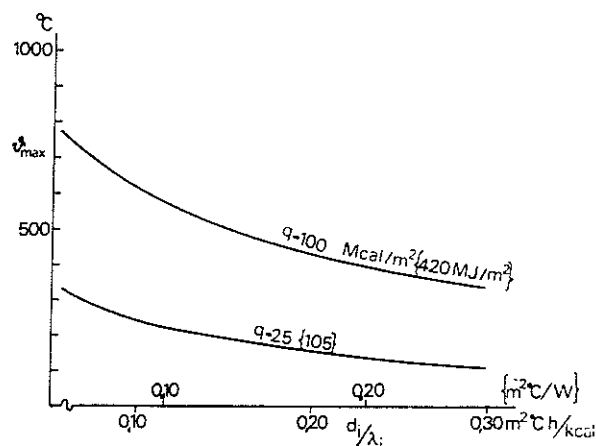


Fig. 6.3 b. Maximum steel temperature  $\vartheta_{max}$  as a function of the insulation capacity  $d_i/\lambda_i$  for fire loads  $q = 25 \{105\}$  and 100  $\text{Mcal/m}^2$  {420  $\text{MJ/m}^2$ }. The  $A_i/V_s$  ratio =  $100 \text{ m}^{-1}$  and the opening factor of the fire compartment  $A\sqrt{h}/A_t = 0.08 \text{ m}^{1/2}$

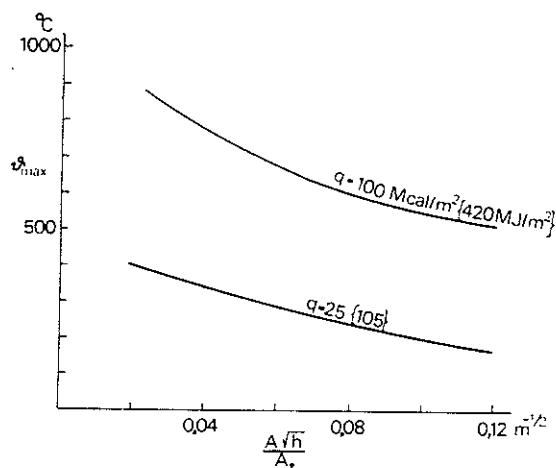


Fig. 6.3 c. Maximum steel temperature  $\vartheta_{max}$  as a function of the opening factor of the fire compartment  $A\sqrt{h}/A_t$  for fire loads  $q = 25 \{105\}$  and 100  $\text{Mcal/m}^2$  {420  $\text{MJ/m}^2$ }. The  $A_i/V_s$  ratio =  $100 \text{ m}^{-1}$  and the insulation capacity  $d_i/\lambda_i = 0.10 \text{ m}^2 \text{ h } ^\circ\text{C/kcal}$  {0.086  $\text{m}^2 \text{ } ^\circ\text{C/W}$ }

ture  $\vartheta_{max}$  for two different values of the fire load  $q$ , and given values of the ratio  $d_i/\lambda_i$  and the opening factor  $A\sqrt{h}/A_t$ , is given in Fig. 6.3 a.

An example of the influence of the insulation capacity  $d_i/\lambda_i$  on the maximum steel temperature  $\vartheta_{max}$  for a given  $A_i/V_s$  ratio and a given opening factor  $A\sqrt{h}/A_t$  is given in Fig. 6.3 b.

An example of the influence of the opening factor  $A\sqrt{h}/A_t$  on the maximum steel temperature  $\vartheta_{max}$  for a given  $A_i/V_s$  ratio and a given insulation capacity  $d_i/\lambda_i$  is given in Fig. 6.3 c.

#### 6.4 Worked example

Calculate the maximum steel temperature for an HE 200A column insulated as shown in Fig. 6.4 a with 15 mm slabs of a vermiculite based material and exposed to the action of fire on all sides. The values of the gas temperature  $\vartheta_t$  in the fire compartment at different times are given in column 3 in Table 6.4 a.



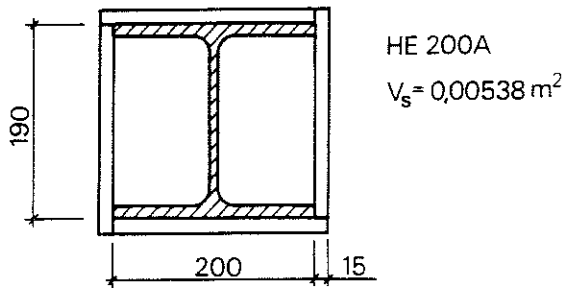


Fig. 6.4 a. Steel column insulated with 15 mm thick slabs of vermiculite based material

According to Equation (6.1 d),

$$\Delta\vartheta_s = \frac{\lambda_i A_i}{d_i V_s \gamma_s c_{ps}} (\vartheta_t - \vartheta_s) \Delta t \quad (^\circ\text{C}) \quad (6.4 a)$$

With dimensions as in Fig. 6.4 a, we have

$$A_i = 0.20 \cdot 2 + 0.19 \cdot 2 = 0.78 \text{ m}^2/\text{m}, \quad V_s = 0.00538 \text{ m}^3/\text{m}, \quad A_i/V_s = 145 \text{ m}^{-1}$$

The temperature dependence of the heat capacity is ignored, and  $c_{ps}$  is put equal to a constant value of  $0.13 \text{ kcal/kg}^\circ\text{C}$   $\{0.54 \text{ kJ/kg}^\circ\text{C}\}$ , which may be regarded as a reasonable mean value at the steel temperatures which obtain. The density  $\gamma_s = 7850 \text{ kg/m}^3$ . The length of the time interval  $\Delta t$  is made 6 minutes, i.e.  $\Delta t = 1/10 \text{ h}$ . The insulation thickness  $d_i = 0.015 \text{ m}$ .

The thermal conductivity  $\lambda_i$  of the insulation is a function of the temperature. In order to estimate a suitable mean value of  $\lambda_i$ , it is assumed that the maximum steel temperature is about  $550^\circ\text{C}$ . Column 3 of Table 6.4 a shows that the gas temperature  $\vartheta_t$  will have dropped to this value after about 50 minutes. The mean gas temperature over this period will be approximately

$$1/9 (622 + 937 + 973 + 1001 + 1024 + 872 + 732 + 625 + 569) = 820^\circ\text{C}$$

The mean temperature of the steel section over the same period will be approximately  $\frac{1}{2} (20 + 550) = 285^\circ\text{C}$ .

The mean temperature in the middle of the insulation will thus be approximately  $(285 + 820)/2 = 550^\circ\text{C}$ , i.e. about the same as the assumed maximum steel temperature.

It will be seen in Table 6 a in the Design Section that the thermal conductivity of slabs of vermiculite based material at  $550^\circ\text{C}$  is approximately  $0.12 \text{ kcal/m}^\circ\text{C h}$   $\{0.14 \text{ W/m}^\circ\text{C}\}$ .

When the above values are substituted into Equation (6.4 a), we have

$$\Delta\vartheta_s = \frac{\vartheta_t - \vartheta_s}{8.79} \quad (^\circ\text{C}) \quad (6.4 b)$$

Calculation of the steel temperature-time relationship using Equation (6.4 b) is illustrated in Table 6.4 a.

**Table 6.4 a.** Calculation of the temperature-time curve for the steel construction in Fig. 6.4a

Line (1)	Time (min) (2)	$\vartheta_t$ (°C) (3)	$(\vartheta_t - \vartheta_s)$ (°C) (4)	$\Delta\vartheta_s$ (°C) (5)	$\vartheta_s$ (°C) (6)
1	0				20
2		622	602	68	
3	6				88
4		937	849	97	
5	12				185
6		973	788	90	
7	18				275
8		1 001	726	83	
9	24				358
10		1 024	666	76	
11	30				434
12		872	438	50	
13	36				484
14		732	284	28	
15	42				512
16		625	113	13	
17	48				525
18		569	44	5	
19	54				530
20		509	- 21	- 2	
21	60				528

It is assumed that the steel temperature  $\vartheta_s = 20^\circ\text{C}$  at the beginning of the fire (line 1, column 6). In the middle of the first time interval, the temperature  $\vartheta_t$  of the fire compartment is given as  $622^\circ\text{C}$  (line 2, column 3). The difference between the temperature  $\vartheta_t$  of the fire compartment and the steel temperature  $\vartheta_s$  is  $602^\circ\text{C}$  (line 2, column 4). When these values are substituted into Equation (6.4 b), the rise  $\Delta\vartheta_s$  in steel temperature during the first time interval is given as  $68^\circ\text{C}$  (line 2, column 5). The steel temperature after 6 minutes' fire is thus  $20 + 68 = 88^\circ\text{C}$  (line 3, column 6). The calculation is to be continued in the same way step by step until the steel temperature reaches a maximum. It will be seen from the Table that the maximum steel temperature of approximately  $530^\circ\text{C}$  is reached after about 54 minutes. The calculated maximum steel temperature is in good agreement with the assumed temperature, and there is therefore no need to correct the assumed value of  $\lambda_i$ .

Instead of using a constant estimated mean value of  $\lambda_i$  as in the example, it is possible at each step in the calculation to use the value of  $\lambda_i$  which applies at the temperature that occurs in the middle of the insulation at the middle of each time interval. This temperature may be assumed to be equal to the mean value of the gas temperature  $\vartheta_t$  and the steel temperature  $\vartheta_s$ . Normally, these two methods give practically identical results with regard to the maximum steel temperature.

#### 6.5 Comparison of the calculated steel temperature-time curve with that measured in fire tests

Calculated steel temperature-time curves are compared in Figs. 6.5 a, 6.5 b and 6.5 c with curves measured in fire tests on steel sections insulated with slabs of mineral wool which were exposed to fire on all sides. There is consistently good agreement between calculated and measured temperature-time curves. The

calculations were performed using the more accurate one of the methods presented, which means that both the heat capacity of the insulation and the temperature variable thermal conductivity were taken into consideration.

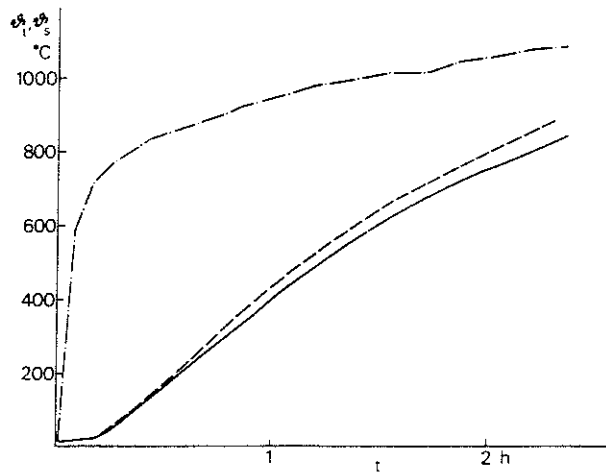


Fig. 6.5 a. Calculated (---) and measured (—) mean temperature-time ( $\bar{\theta}_s - t$ ) curve in a steel section insulated with 40 mm thick mineral wool slabs of density  $\gamma = 140 \text{ kg/m}^3$ . The  $A_i/V_s$  ratio of the section  $= 250 \text{ m}^{-1}$ . The chain line curve indicates the gas temperature-time ( $\bar{\theta}_t - t$ ) curve

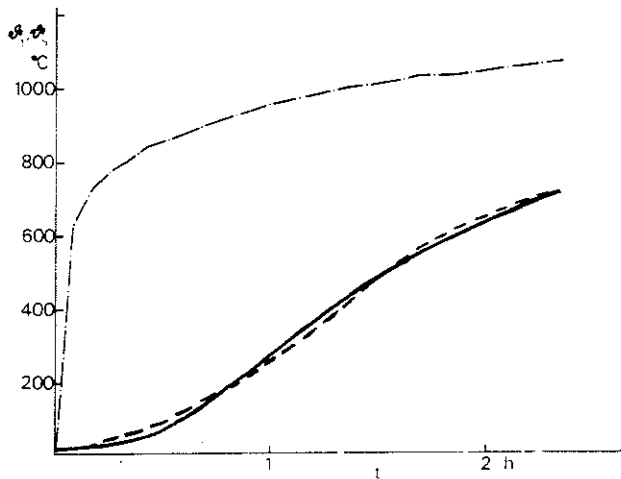


Fig. 6.5 b. Calculated (---) and measured (—) mean temperature-time ( $\bar{\theta}_s - t$ ) curve in a steel section insulated with 60 mm thick mineral wool slabs of density  $\gamma = 140 \text{ kg/m}^3$ . The  $A_i/V_s$  ratio of the section  $= 250 \text{ m}^{-1}$ . The chain line curve indicates the gas temperature-time ( $\bar{\theta}_t - t$ ) curve

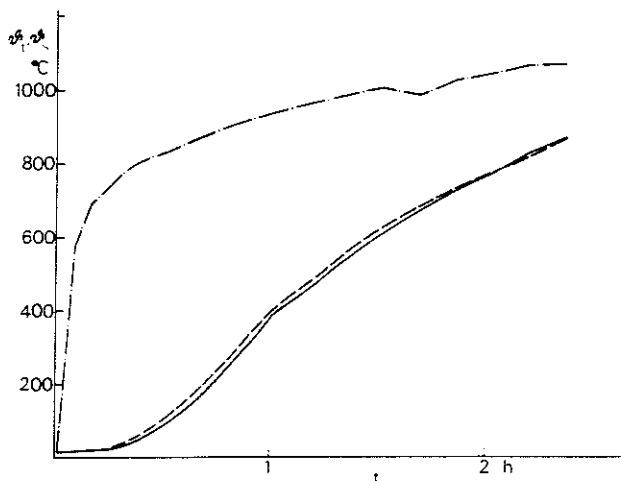


Fig. 6.5 c. Calculated (---) and measured (—) mean temperature-time ( $\bar{\theta}_s - t$ ) curve in a steel section insulated with 60 mm thick mineral wool slabs of density  $\gamma = 140 \text{ kg/m}^3$ . The  $A_i/V_s$  ratio of the section  $= 400 \text{ m}^{-1}$ . The chain line curve indicates the gas temperature-time ( $\bar{\theta}_t - t$ ) curve

## 7 TEMPERATURE - TIME CURVES FOR STEEL STRUCTURES WITH INSULATION IN THE FORM OF A SUSPENDED CEILING

### 7.1 The heat balance equation

Calculation of the steel temperature-time curve during a fire for a floor carried on steel girders which is insulated in the form of a suspended ceiling (see Fig. 7.1 a) is more complicated than the corresponding calculation for steel structures where the insulation is placed around the structural element itself. In the latter case, the gas temperature in the fire compartment is used directly in the course of calculations, while in the case of a structure with insulation in the form of a suspended ceiling it is necessary first of all to determine the surface temperature at the top of the suspended ceiling and at the soffit of the floor slab before the steel temperature can be calculated in a second calculation stage.

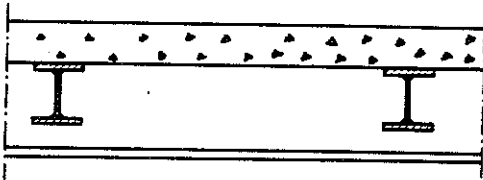


Fig. 7.1 a. Steel girder floor construction with insulation in the form of a suspended ceiling

#### 7.1.1 Calculation of the surface temperature of the floor slab and the suspended ceiling

Calculation of the surface temperature of the floor slab and the suspended ceiling can generally be carried out without considering the heat capacity of the steel girders, the air gap and the suspended ceiling. This approximation is a reasonable one, since it is usually the heat capacity of the floor slab which predominates. The approximation also yields calculated temperatures on the safe side. In the calculation the floor slab is divided into a number of elements as shown in Fig. 7.1.1. a. If the heat capacities are ignored, the temperature drops in the various surfaces and layers from the fire compartment to the floor slab are proportional to the thermal resistance of the surface or layer concerned. Using the symbols set out in Fig. 7.1.1. a, the following expressions therefore hold for the surface temperatures

$$\vartheta_{v1} = \vartheta_t - K \frac{1}{\alpha_1} (\vartheta_t - \vartheta_1) \quad (^\circ\text{C})$$

$$\vartheta_{s1} = \vartheta_t - K \left( \frac{1}{\alpha_1} + \frac{d_i}{\lambda_i} \right) (\vartheta_t - \vartheta_1) \quad (^\circ\text{C}) \quad (7.1.1 a)$$

$$\vartheta_{v2} = \vartheta_t - K \left( \frac{1}{\alpha_1} + \frac{d_i}{\lambda_i} + \frac{1}{\alpha_2} \right) (\vartheta_t - \vartheta_1) \quad (^\circ\text{C})$$

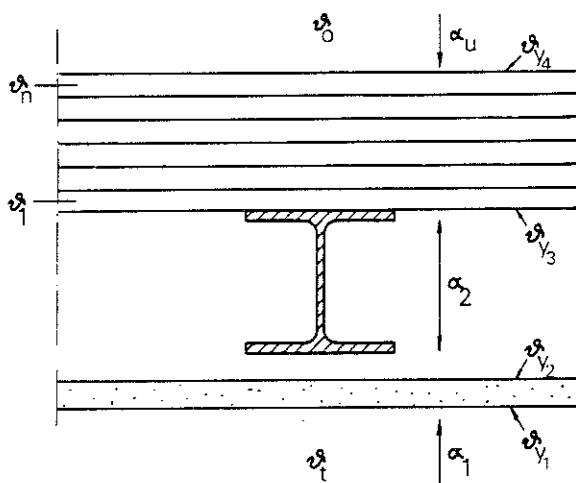


Fig. 7.1.1 a. Division of the floor slab into elements

- where  $\vartheta_t$  = gas temperature in the fire compartment at time  $t$  ( $^{\circ}\text{C}$ )  
 $\vartheta_1$  = temperature in the middle of the lowest strip of floor slab at time  $t$  ( $^{\circ}\text{C}$ )  
 $d_i$  = thickness of suspended ceiling  
 $\lambda_i$  = thermal conductivity of suspended ceiling ( $\text{kcal/m } ^{\circ}\text{C h}$ )  $\{\text{W/m } ^{\circ}\text{C}\}$   
 $\alpha_1$  = surface coefficient of heat transfer in the boundary layer between the combustion gases and the suspended ceiling ( $\text{kcal/m}^2 \text{ } ^{\circ}\text{C h}$ )  $\{\text{W/m}^2 \text{ } ^{\circ}\text{C}\}$   
 $\alpha_2$  = surface coefficient of heat transfer for radiation and convection between the suspended ceiling and the floor slab ( $\text{kcal/m}^2 \text{ } ^{\circ}\text{C h}$ )  $\{\text{W/m}^2 \text{ } ^{\circ}\text{C}\}$

The coefficient  $K$  can be written

$$K = \frac{1}{\frac{1}{\alpha_1} + \frac{d_i}{\lambda_i} + \frac{1}{\alpha_2} + \frac{\Delta x}{2\lambda_{bj}}} \quad (\text{kcal/m}^2 \text{ } ^{\circ}\text{C h}) \quad \{\text{W/m}^2 \text{ } ^{\circ}\text{C}\} \quad (7.1.1. b)$$

where  $\Delta x$  = thickness of the lowest floor slab strip (m)

$\lambda_{bj}$  = thermal conductivity of floor slab ( $\text{kcal/m } ^{\circ}\text{C h}$ )  $\{\text{W/m } ^{\circ}\text{C}\}$

The surface coefficient of heat transfer  $\alpha_1$  can, with sufficient accuracy, be considered composed of a constant convection portion and a temperature dependent radiation portion (see Subsection 4.2.2.3).

$$\alpha_1 = 20 + \frac{4.96\epsilon_r}{\vartheta_t - \vartheta_{y1}} \left[ \left( \frac{\vartheta_t + 273}{100} \right)^4 - \left( \frac{\vartheta_{y1} + 273}{100} \right)^4 \right] \quad (\text{kcal/m}^2 \text{ } ^{\circ}\text{C h}) \quad (7.1.1. c)$$

$$\alpha_1 = 23 + \frac{5.77\epsilon_r}{\vartheta_t - \vartheta_{y1}} \left[ \left( \frac{\vartheta_t + 273}{100} \right)^4 - \left( \frac{\vartheta_{y1} + 273}{100} \right)^4 \right] \quad \{\text{W/m}^2 \text{ } ^{\circ}\text{C}\}$$

The resultant emissivity  $\epsilon_r$  can be calculated from the formula

$$\epsilon_r = \frac{1}{1/\epsilon_t + 1/\epsilon_i - 1} \quad (7.1.1 d)$$

where  $\epsilon_t$  = emissivity of the flames

$\epsilon_i$  = emissivity of the surface of the suspended ceiling

With the emissivity of the flames  $\epsilon_t = 0.85$  and the suspended ceiling emissivity  $\epsilon_i = 0.8$ , Equation (7.1.1. d) gives a resultant emissivity  $\epsilon_r = 0.7$  (see Subsection 5.2.4).

As regards the surface coefficient of heat transfer  $\alpha_2$ , the convection portion can be assumed to be smaller than in the case of  $\alpha_1$ , since the surfaces involved are not exposed to the fire directly. A reasonable value for the convection portion of the surface coefficient of heat transfer in this instance is  $7.5 \text{ kcal/m}^2 \text{ }^\circ\text{C h}$   $\{8.7 \text{ W/m}^2 \text{ }^\circ\text{C}\}$  (19). Furthermore, the resultant emissivity can be calculated on the assumption that the emissivity of both the suspended ceiling surface and the slab surface is 0.8 (43). According to Equation (7.1.1 d), this gives the value  $\epsilon_r = 0.67$ . The surface coefficient of heat transfer  $\alpha_2$  can therefore be written

$$\alpha_2 = 7.5 + \frac{4.96 \cdot 0.67}{\vartheta_{ys} - \vartheta_{ys}} \left[ \left( \frac{\vartheta_{ys} + 273}{100} \right)^4 - \left( \frac{\vartheta_{ys} + 273}{100} \right)^4 \right] \quad (\text{kcal/m}^2 \text{ }^\circ\text{C h})$$

$$\alpha_2 = 8.7 + \frac{5.77 \cdot 0.67}{\vartheta_{ys} - \vartheta_{ys}} \left[ \left( \frac{\vartheta_{ys} + 273}{100} \right)^4 - \left( \frac{\vartheta_{ys} + 273}{100} \right)^4 \right] \quad \{ \text{W/m}^2 \text{ }^\circ\text{C} \} \quad (7.1.1 \text{ e})$$

In order to calculate the surface temperatures according to Equation (7.1.1 a), we must know the temperature  $\vartheta_1$  in the lowest strip of the floor slab according to Fig. 7.1.1 a, in addition to the combustion gas temperature  $\vartheta_t$  in the fire compartment. The temperature  $\vartheta_1$  is calculated from the heat balance equation of the floor slab elements by division of the fire into a number of short intervals  $\Delta t$ , in analogy with the calculation of the temperature field in the constructions surrounding a fire compartment (see Subsection 4.2.2.3). This gives a system of equations

$$\Delta x_1 c(x, \vartheta) \gamma \frac{\Delta \vartheta_1}{\Delta t} = \frac{1}{\frac{\Delta x_1}{2\lambda(x, \vartheta)}} (\vartheta_{ys} - \vartheta_1) - \frac{1}{\frac{\Delta x_1}{2\lambda(x, \vartheta)} + \frac{\Delta x_2}{2\lambda(x, \vartheta)}} (\vartheta_1 - \vartheta_2)$$

$$\Delta x_k c(x, \vartheta) \gamma \frac{\Delta \vartheta_k}{\Delta t} = \frac{1}{\frac{\Delta x_{k-1}}{2\lambda(x, \vartheta)} + \frac{\Delta x_k}{2\lambda(x, \vartheta)}} (\vartheta_{k-1} - \vartheta_k) - \frac{1}{\frac{\Delta x_k}{2\lambda(x, \vartheta)} + \frac{\Delta x_{k+1}}{2\lambda(x, \vartheta)}} (\vartheta_k - \vartheta_{k+1})$$

$$\Delta x_n c(x, \vartheta) \gamma \frac{\Delta \vartheta_n}{\Delta t} = \frac{1}{\frac{\Delta x_{n-1}}{2\lambda(x, \vartheta)} + \frac{\Delta x_n}{2\lambda(x, \vartheta)}} (\vartheta_{n-1} - \vartheta_n) - \frac{1}{\frac{\Delta x_n}{2\lambda(x, \vartheta)} + \frac{1}{\alpha_u(\vartheta)}} (\vartheta_n - \vartheta_0)$$

$$(7.1.1 \text{ f})$$

where  $c(x, \vartheta)$  = specific heat capacity at section  $x$  at temperature  $\vartheta$  (kcal/kg  $^\circ\text{C}$ )  
 $\{ \text{J/kg } ^\circ\text{C} \}$

$\gamma$  = density at section  $x$  (kg/m<sup>3</sup>)

- $\lambda(x, \vartheta)$  = thermal conductivity at section  $x$  at temperature  $\vartheta$  (kcal/m °C h)  
 $\{ \text{W/m } ^\circ\text{C} \}$   
 $\vartheta_k$  = temperature at the centre of layer  $k$  (°C)  
 $\Delta x_k$  = thickness of layer  $k$  (m)  
 $\alpha_u(\vartheta)$  = surface coefficient of heat transfer at the top of the floor slab  
 $(\text{kcal/m}^2 \text{ } ^\circ\text{C h}) \{ \text{W/m}^2 \text{ } ^\circ\text{C} \}$

For  $\alpha_u$ , the approximate expression is (19)

$$\begin{aligned}\alpha_u &= 7.5 + 0.028 \vartheta_{y_1} \quad (\text{kcal/m}^2 \text{ } ^\circ\text{C h}) \\ \alpha_u &= 8.7 + 0.033 \vartheta_{y_1} \quad \{ \text{W/m}^2 \text{ } ^\circ\text{C} \}\end{aligned} \quad (7.1.1 \text{ g})$$

When the expression for  $\vartheta_{y_3}$  according to Equation (7.1.1 a) is substituted into the system of equations (7.1.1 f), this can be solved by numerical integration, for instance according to the Runge-Kutta procedure. The surface temperatures  $\vartheta_{y_1}$ ,  $\vartheta_{y_2}$  and  $\vartheta_{y_3}$  are then obtained from Equation (7.1.1 a).

If the heat capacity of the suspended ceiling is also to be taken into account, the ceiling must also be split up into a number of strips, and the system of equations (7.1.1 f) must be extended by heat balance equations for these strips. This eliminates Equation (7.1.1 a). The required surface temperatures are then obtained from the extended system of equations.

#### 7.1.2 Calculation of the steel temperature

The quantity of heat  $Q$  per unit length of steel section which is required to raise the steel temperature by  $\Delta \vartheta_s$  °C is

$$Q = c_{ps} \Delta \vartheta_s V_s \gamma_s \quad (\text{kcal/m}) \{ \text{J/m} \} \quad (7.1.2 \text{ a})$$

where  $c_{ps}$  = specific heat capacity of the steel (kcal/kg °C) {J/kg °C}  
 (see Subsection 5.2.3)

$\Delta \vartheta_s$  = temperature rise in the steel section (°C)

$V_s$  = volume of the steel section per unit length (m<sup>3</sup>/m)

$\gamma_s$  = density of the steel (kg/m<sup>3</sup>) (see Subsection 5.2.2)

It is assumed that the steel section is exposed to heat radiation from the top of the suspended ceiling and the soffit of the floor slab, and to heat transfer by convection. If the air temperature in the space between the suspended ceiling and the floor slab is assumed to be the same as the mean of the surface temperatures  $\vartheta_{y_2}$  and  $\vartheta_{y_3}$  (see Subsection 7.1.1 a), then the quantity of heat  $Q$  which is supplied to the steel section per unit length over the time interval  $\Delta t$  can be written

$$Q = \alpha_{s_2} F_s (\vartheta_{y_2} - \vartheta_s) \Delta t + \alpha_{s_3} F_s (\vartheta_{y_3} - \vartheta_s) \Delta t + \alpha_k F_s \left( \frac{\vartheta_{y_2} + \vartheta_{y_3}}{2} - \vartheta_s \right) \Delta t \quad (\text{kcal/m}) \{ \text{J/m} \} \quad (7.1.2 \text{ b})$$

where  $F_s$  = surface area of the steel section per unit length, with the exception of the part carrying the floor slab ( $m^2/m$ )

$\vartheta_s$  = temperature of steel section at time  $t$  ( $^{\circ}C$ )

$\vartheta_{y2}$  = temperature of the top surface of the suspended ceiling at time  $t$  ( $^{\circ}C$ )

$\vartheta_{y3}$  = temperature of the surface of the floor slab soffit at time  $t$  ( $^{\circ}C$ )

$\alpha_{s2}, \alpha_{s3}$  = surface coefficients of heat transfer due to radiation ( $kcal/m^2 \cdot ^{\circ}C \cdot h$ )  
{ $W/m^2 \cdot ^{\circ}C$ }

$\alpha_k$  = surface coefficient of heat transfer due to convection ( $kcal/m^2 \cdot ^{\circ}C \cdot h$ )  
{ $W/m^2 \cdot ^{\circ}C$ }

The radiation portions  $\alpha_{s2}$  and  $\alpha_{s3}$  of the surface coefficients of heat transfer are obtained from the expressions

$$\alpha_{s2} = \frac{4.96 \epsilon_r}{\vartheta_{y2} - \vartheta_s} \left[ \left( \frac{\vartheta_{y2} + 273}{100} \right)^4 - \left( \frac{\vartheta_s + 273}{100} \right)^4 \right] \quad (kcal/m^2 \cdot ^{\circ}C \cdot h)$$

$$\alpha_{s3} = \frac{5.77 \epsilon_r}{\vartheta_{y3} - \vartheta_s} \left[ \left( \frac{\vartheta_{y3} + 273}{100} \right)^4 - \left( \frac{\vartheta_s + 273}{100} \right)^4 \right] \quad \{W/m^2 \cdot ^{\circ}C\}$$

(7.1.2 c)

$$\alpha_{s2} = \frac{4.96 \epsilon_r}{\vartheta_{y2} - \vartheta_s} \left[ \left( \frac{\vartheta_{y2} + 273}{100} \right)^4 - \left( \frac{\vartheta_s + 273}{100} \right)^4 \right] \quad (kcal/m^2 \cdot ^{\circ}C \cdot h)$$

$$\alpha_{s3} = \frac{5.77 \epsilon_r}{\vartheta_{y3} - \vartheta_s} \left[ \left( \frac{\vartheta_{y3} + 273}{100} \right)^4 - \left( \frac{\vartheta_s + 273}{100} \right)^4 \right] \quad \{W/m^2 \cdot ^{\circ}C\}$$

Calculation of the resultant emissivity  $\epsilon_r$  between two radiating surfaces, in accordance with Equation (7.1.1 d), presupposes that all radiation from one of the surfaces strikes the other surface, and vice versa. This does not occur in the case of steel girders in a construction as shown in Fig. 7.1.1 a. For this reason, apart from the emissivities of the surfaces, the value of  $\epsilon_r$  will also depend on the shapes and spacing of the girders. The value of  $\epsilon_r$  can be found from Fig. 5.2.4 b, a convenient assumption being that all surfaces on the suspended ceiling, floor slab and girders have an emissivity of 0.8.

The convection portion  $\alpha_k$  of the surface coefficient of heat transfer can, with sufficient accuracy, be put at a constant value of  $7.5 kcal/m^2 \cdot ^{\circ}C \cdot h$  { $8.7 W/m^2 \cdot ^{\circ}C$ } (see Subsection 7.1.1).

From Equations (7.1.2 a) and (7.1.2 b), the rise in temperature  $\Delta \vartheta_s$  in the steel section over the time interval  $\Delta t$  is obtained as

$$\Delta \vartheta_s = \frac{F_s \Delta t}{V_s \gamma_s c_{ps}} \left[ \left( \frac{\alpha_k}{2} + \alpha_{s2} \right) (\vartheta_{y2} - \vartheta_s) + \left( \frac{\alpha_k}{2} + \alpha_{s3} \right) (\vartheta_{y3} - \vartheta_s) \right] \quad (7.1.2 d)$$



## 7.2 Comparison of the calculated steel temperature-time curve with that measured in fire tests

Calculated steel temperatures in girders insulated with a suspended ceiling are compared with those measured in the course of fire tests in Figs. 7.2 a - 7.2 c. In Fig. 7.2 a the suspended ceiling consists of mineral wool slabs, and in Figs. 7.2 b and 7.2 c of gypsum plasterboard.

In all cases, the floor slab is of concrete. Consideration was given in the calculation to the possibility that the plasterboard may disintegrate. The assumption made was that disintegration occurs when the temperature on the unexposed side reaches a calculated value of  $550^{\circ}\text{C}$ . Agreement between the calculated steel temperature-time curve and the measured one is satisfactory.

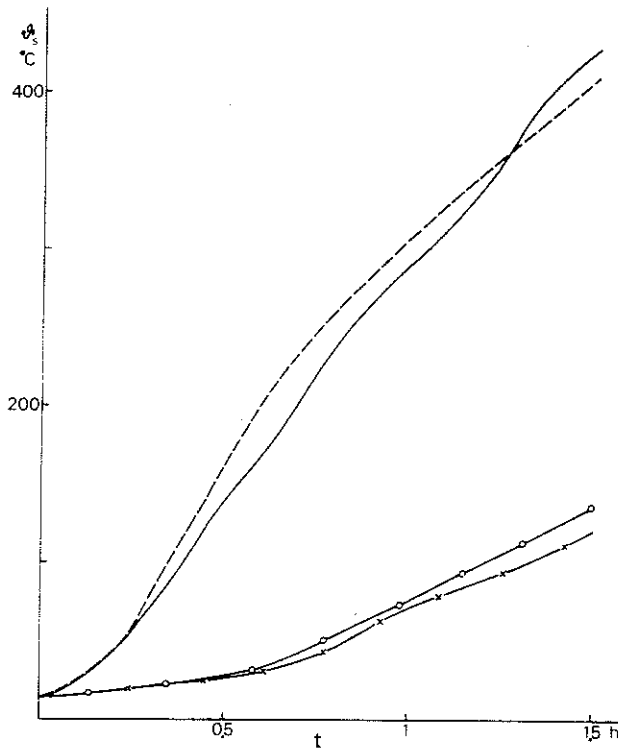


Fig. 7.2 a. Calculated (---) and measured (—) steel temperature-time ( $\theta_s - t$ ) curve for a floor girder IPE 140 with insulation in the form of a suspended ceiling of 40 mm thick mineral wool slabs of density  $\gamma = 150 \text{ kg/m}^3$ . The figure also gives the calculated (- o -) and measured (- x -) temperature-time curve for the top of the 50 mm thick concrete floor slab. The curves are drawn on the assumption that the gas temperature-time curve conforms to the standard fire curve

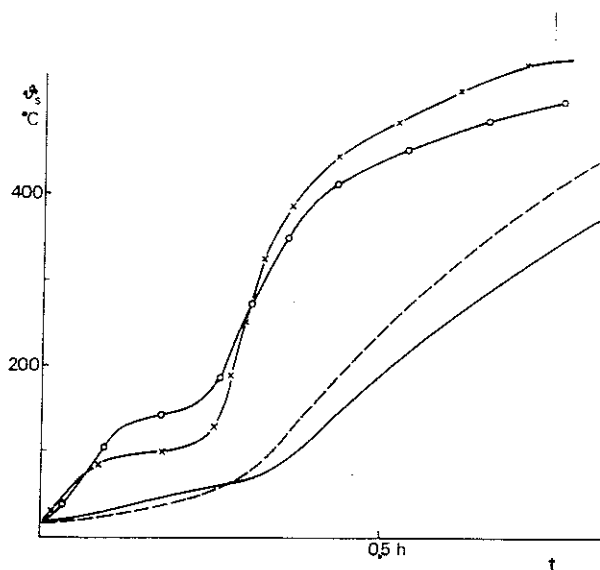


Fig. 7.2 b. Calculated (---) and measured (—) steel temperature-time ( $\theta_s - t$ ) curve for a floor girder IPE 270 with insulation in the form of a suspended ceiling of one 13 mm thick slab of gypsum plaster of density  $\gamma = 790 \text{ kg/m}^3$ . The floor slab is of concrete. The figure also gives the calculated (- o -) and measured (- x -) temperature-time curve for the top of the suspended ceiling. The curves are drawn on the assumption that the gas temperature-time curve conforms to the standard fire curve

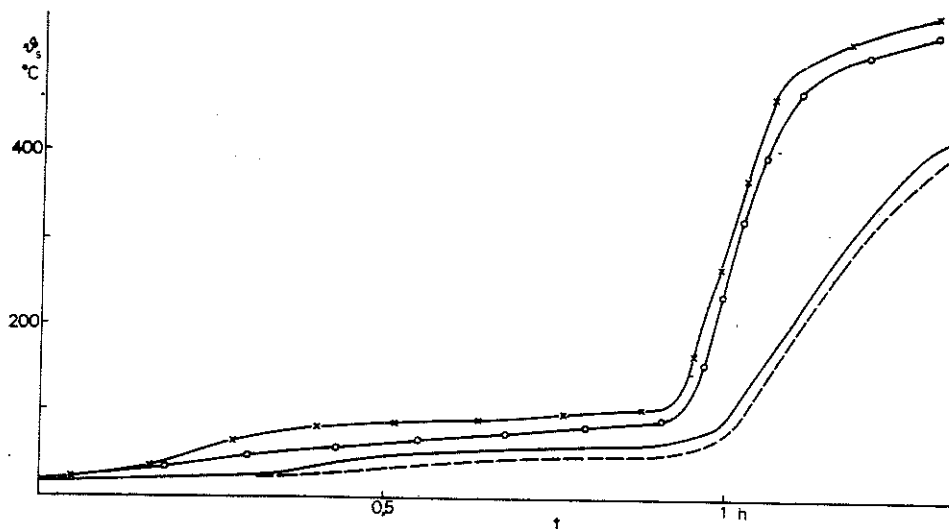


Fig. 7.2 c. Calculated (---) and measured (—) steel temperature-time ( $\theta_s - t$ ) curve for a floor girder IPE 270 with insulation in the form of a suspended ceiling of three 13 mm thick slabs of gypsum plaster of density  $\gamma = 790 \text{ kg/m}^3$ . The floor slab is of concrete. The figure also gives the calculated (- o -) and measured (- x -) temperature-time curve for the top of the suspended ceiling. The curves are drawn on the assumption that the gas temperature-time curve conforms to the standard fire curve

### 7.3 Influence of the material and thickness of the floor slab on the steel temperature

The heat capacity of the floor slab has a great influence on the surface temperatures on the suspended ceiling and the slab (see Subsection 7.1.1), and consequently on the steel temperature, in the event of fire. This is illustrated in Fig. 7.3 in which the calculated steel temperature-time curves are compared for floor slabs of concrete and lightweight concrete with a density of  $\gamma = 500 \text{ kg/m}^3$ . The steel sections and the suspended ceiling are identical in the two cases. When the floor slab consists of lightweight concrete, the heat capacity of which is considerably less than that of ordinary concrete, the steel temperature is appreciably higher than when the floor slab is of ordinary concrete.

It appears from the calculations that the thickness of floor slabs made of concrete and lightweight concrete has very little influence on the steel temperature-time curve, at any rate in the range which is of practical interest for floor slabs. The reason for this is that it is only the lower portions of the floor slab which are heated to any appreciable extent, and thus contribute to the storage of heat, during the relatively short periods in a fire. This is illustrated in Fig. 7.3 b in which the calculated steel temperature-time curve has been plotted for different thicknesses of the floor slab.

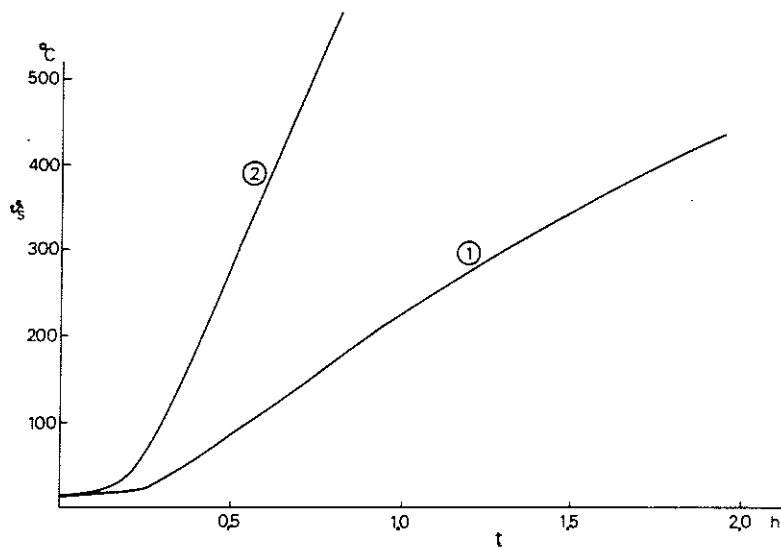


Fig. 7.3 a. Calculated steel temperature-time ( $\theta_s - t$ ) curve for a floor girder IPE 330 with insulation in the form of a suspended ceiling, carrying a floor slab of concrete ① and light-weight concrete of density  $\gamma = 500 \text{ kg/m}^3$  ②. The suspended ceiling consists of a 25mm thick slab of Rockwool mineral wool of a density  $\gamma = 150 \text{ kg/m}^3$ . The thickness of the floor slab is in both cases 85 mm. The curves are drawn for a gas temperature-time curve for a standard fire

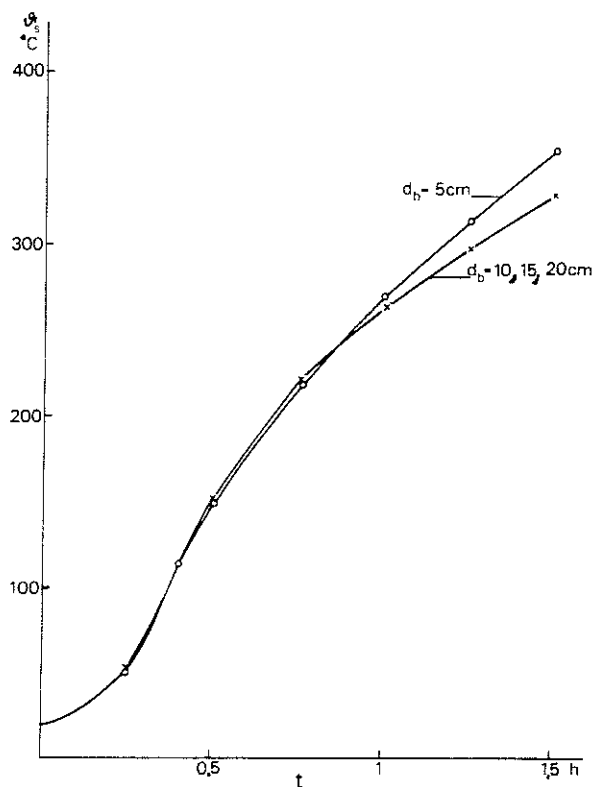


Fig. 7.3 b. Calculated steel temperature time ( $\theta_s - t$ ) curve for a floor girder IPE 140 with insulation in the form of a suspended ceiling, carrying a floor slab of concrete of different thicknesses  $d_b$ . The suspended ceiling consists of a 40 mm thick slab of Rockwool mineral wool of a density  $\gamma = 75 \text{ kg/m}^3$ . The curves are drawn for a gas temperature-time curve for a standard fire

#### 7.4 Practical design and the need for fire tests

The maximum steel temperatures under fire exposure conditions in girders insulated by a suspended ceiling have been calculated and set out in Table 7 b in the Design Section. With regard to fire exposure, the input data used are those relating to the gas temperature-time curve for fire compartment Type A (standard fire compartment) according to Subsection 4.3.3. The maximum steel temperature  $\theta_{\max}$  is given as a function of the fire load  $q$ , the opening factor  $\sqrt{A_f}/A_t$ , and the  $F_s/V_s$  ratio of the steel section for different values of the insulation capacity  $d_i/\lambda_i$  of the suspended ceiling. The maximum temperature in the middle of the suspended ceiling is also given in Table 7 b. The values set out are applicable to floors comprising a slab of concrete.

Fire tests performed on suspended ceilings have shown that, for many suspended ceiling constructions, it is not the maximum steel temperature which is critical, but the resistance to fire of the suspended ceiling and the suspension devices. The suspended ceiling may, for instance, deform so much after a relatively short exposure to fire that substantial cracking occurs or the ceiling wholly or partially falls down after a time. In such suspended ceiling constructions it is obviously impossible to assess the maximum steel temperature purely on the basis of the insulation capacity  $d_i/\lambda_i$  determined by the thickness and thermal conductivity of the suspended ceiling. However, the results of fire tests on such suspended ceilings permit the determination of fictive values of  $d_i/\lambda_i$  for such ceilings, the effect due to the ceiling not remaining intact during the entire fire being included in these fictive values. Determination of these  $d_i/\lambda_i$  values can be carried out using Fig. 7.4 a. This gives the calculated steel temperature-time curve for girders insulated by means of a suspended ceiling when exposed to a fire which gives rise to a gas temperature-time curve corresponding to that used in standard fire tests. The steel temperature is given for different values of the  $F_s/V_s$  ratio of the girders and for different values of the insulation capacity  $d_i/\lambda_i$ . Fig. 7.4 a also shows the calculated temperature-time curve in the middle of the suspended ceiling. The steel temperature-time curve determined in the course of fire tests is to be compared to the calculated temperature curve plotted in Fig. 7.4 a, and the suspended ceiling given a fictive  $d_i/\lambda_i$  value corresponding to the value for that curve in the figure which agrees most closely with the measured steel temperature-time curve. Fire tests also frequently provide information on the length of time that elapses before the strength of the suspended ceiling is appreciably impaired. By reading off the temperature corresponding to this time in the appropriate curve in Fig. 7.4 a, it is possible to determine the critical temperature for the suspended ceiling in question from the calculated temperature-time curve for the suspended ceiling.

Fictive  $d_i/\lambda_i$  values and critical temperatures have been determined for a number of types of suspended ceilings in a fire test series performed at the National Swedish Institute for Testing and Metrology in Stockholm (44). The compositions of these suspended ceilings and the results obtained are set out in Table 7 a in the Design Section. The fictive  $d_i/\lambda_i$  value and the critical temperature are given for each suspended ceiling type. In all cases, assessment of the  $d_i/\lambda_i$  value and the critical temperature for the suspended ceiling was on the safe side. With the assistance of these fictive  $d_i/\lambda_i$  values, the maximum steel temperature under fire exposure conditions in a girder insulated with one of the suspended ceilings listed can be determined from Table 7 b in the Design Section as a function of the fire load  $q$  and the opening factor  $\sqrt{A_f}/A_t$ . This Table also gives the maximum temperature in the suspended ceiling. This temperature must be checked against the critical temperature of the suspended ceiling as set out in Table 7 a in the Design Section.

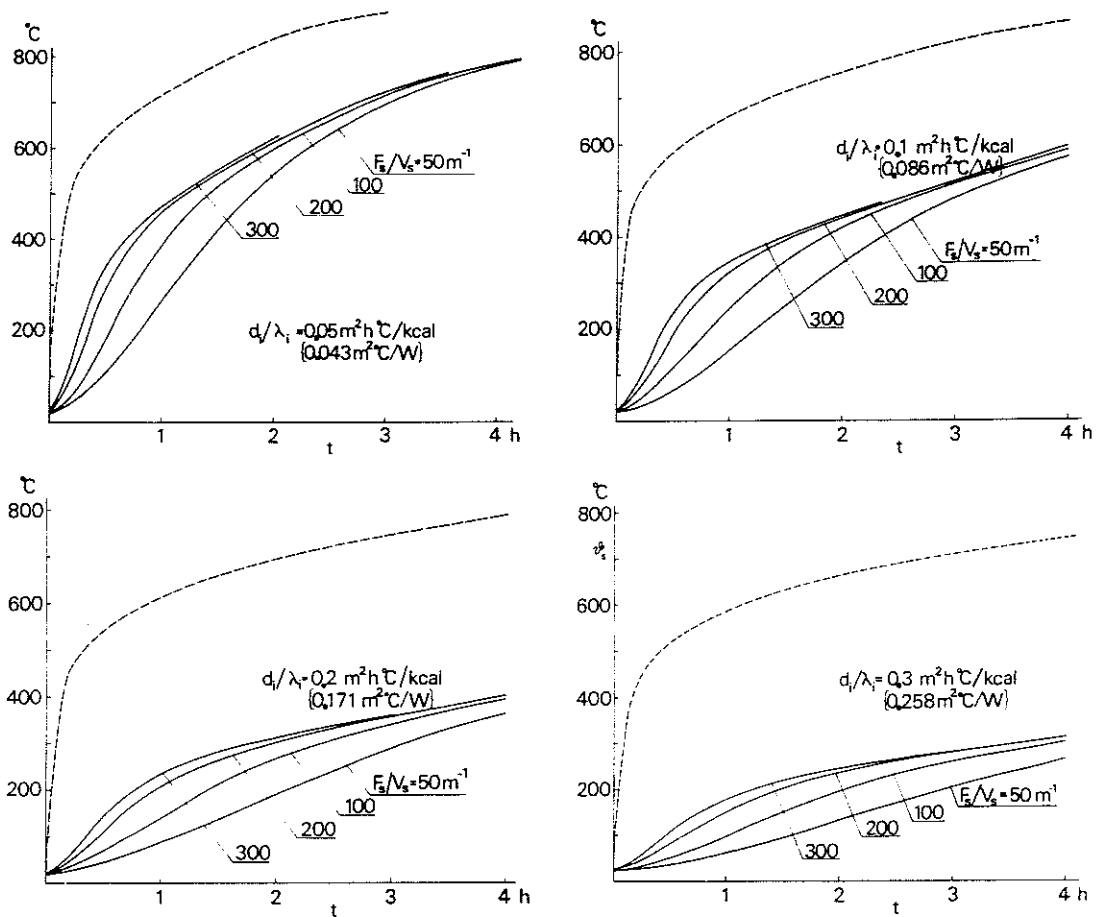


Fig. 7.4 a. Calculated steel temperature-time ( $\theta_s - t$ ) curves for floor girders of different  $F_s/V_s$  ratios with insulation in the form of a suspended ceiling, when exposed to action according to the temperature-time curve for a standard fire.  $F_s$  denotes the surface area of the steel girder per metre, excluding the part covered by the floor slab ( $\text{m}^2/\text{m}$ ), and  $V_s$  denotes the volume of the girder per m ( $\text{m}^3/\text{m}$ ).  $d_i$  denotes the thickness of the suspended ceiling and  $\lambda_i$  its thermal conductivity ( $\text{kcal}/\text{m } ^{\circ}\text{C h}$ ) [ $\text{W}/\text{m } ^{\circ}\text{C}$ ]. The dashed curve shows the calculated variation with time of the temperature in the middle of the suspended ceiling

## 8 TEMPERATURE - TIME CURVES FOR PARTITIONS

The requirements imposed on a partition are that it should be impervious to the penetration of flames and also that it should limit the rise in temperature on the unexposed side. A construction which constitutes the boundary of a fire compartment may include functionally necessary components such as doors and windows which have a fire resistance lower than that required of the rest of the construction. The assumption made in relation to these components is that spread of fire through them is prevented by the action of the fire brigade, arriving within the normal time, or by some other means.

According to requirements in regulations (see Subsection 2.4.2), the rise in temperature on the unexposed side of the partition must not exceed an average value of  $140^{\circ}\text{C}$ , nor  $180^{\circ}\text{C}$  over limited areas of the surface. Generally approved constructions which meet these requirements are listed in a schedule of products of fire engineering classification which is published and annually revised by the National Swedish Board of Physical Planning and Building. The limitation of the rise in temperature to  $140^{\circ}\text{C}$  and  $180^{\circ}\text{C}$  respectively is related to the heating phase of a standardised fire. Furthermore, these values are chosen in such a way as to allow for an estimated reasonable rise in temperature during the cooling phase of the fire. In a rational fire engineering design process based on the complete fire process which also includes the cooling phase, it is therefore reasonable to modify these figures. On the side not exposed to fire, a maximum temperature (not rise in temperature) of  $200^{\circ}\text{C}$  on average, and  $240^{\circ}\text{C}$  over limited areas, can therefore be accepted.

The temperature on the side of a partition which is not exposed to fire can be calculated using a heat balance equation in analogy with Equation (4.2.2.3 b), by dividing the construction into a suitable number of strips. The input data used in the calculation is the combustion gas temperature  $\theta_t$  in the fire compartment, determined according to Section 4.

If a partition contains materials which attain temperatures critical with regard to disintegration during a fire, this must be taken into account in calculating the temperature field of the construction. The flow chart for the calculation of the variation in time of the temperature field, under fire exposure conditions, in a partition of steel stud with sheets of plasterboard, which takes into account the disintegration of the plasterboard, is shown in Fig. 8 a (26).

The calculation method indicated has been experimentally verified by means of fire engineering tests. By way of example, Fig 8 b shows measured and calculated temperature-time curves in different parts of a partition consisting of a lightweight steel frame insulated with two 13 mm sheets of plasterboard on each side. The positions of the temperature gauges are shown in the inset figure. On the basis of results obtained in fire tests on plasterboard, it is assumed that the plasterboard disintegrates when the temperature on the side of a sheet which is facing away from the fire has reached  $550^{\circ}\text{C}$ .

The calculation method has been used for systematic calculation of the temperature-time field in a steel stud-plasterboard wall, for different gas temperature-

$n$  = number of first order  
 ordinary differential equations  
 $t$  = time  
 $\Delta t$  = integration stage  
 test temp. = temperature on the side of the  
 sheet which is not exposed to  
 fire

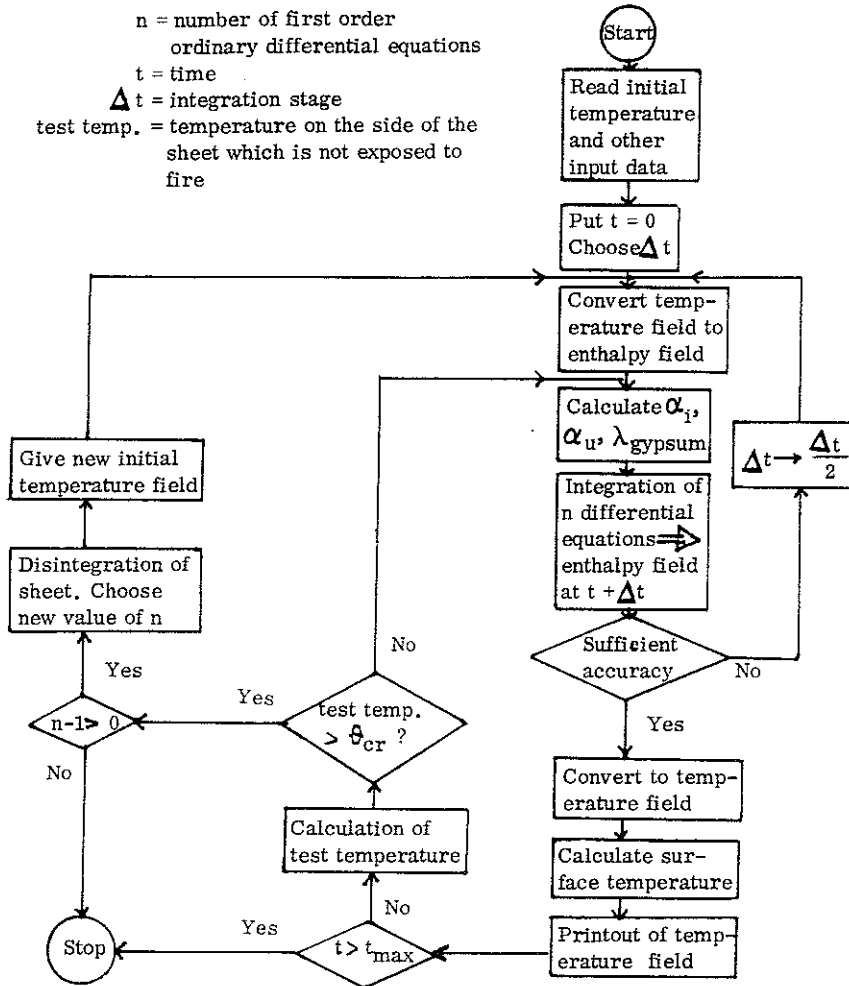


Fig 8 a. Flow chart for calculation of the variation with time of the temperature field for a steel stud wall insulated with gypsum plaster sheets and exposed to fire on one side (26)

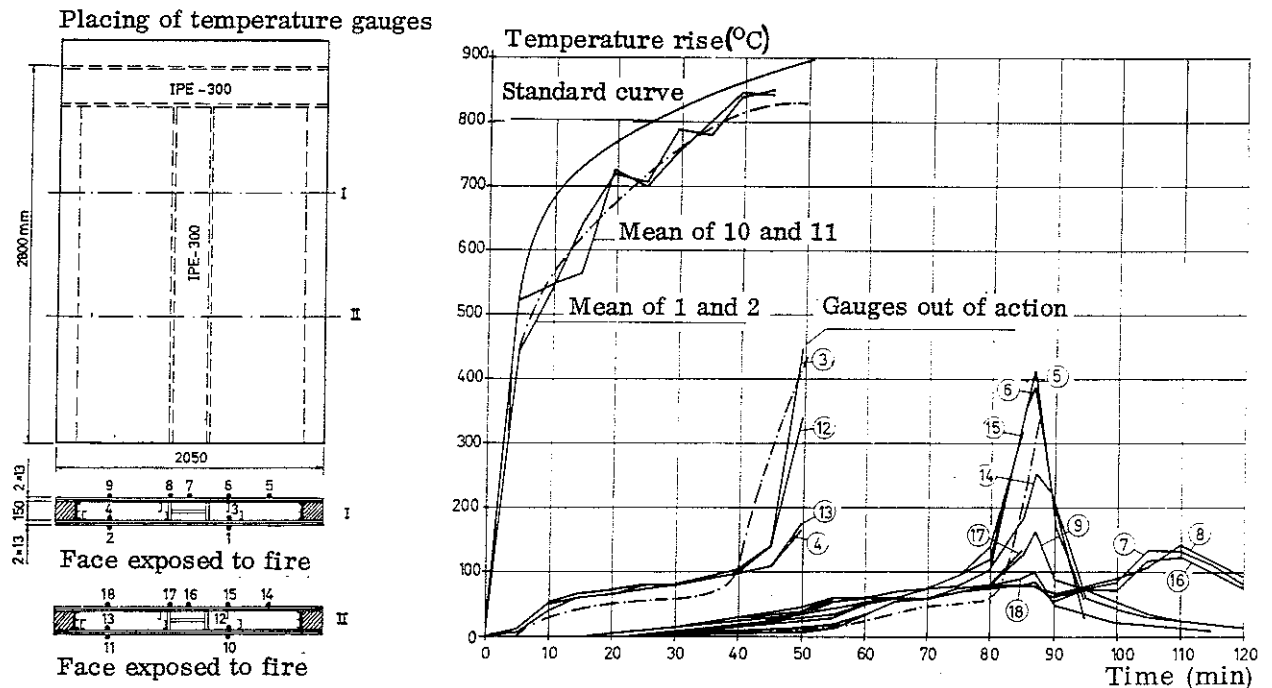


Fig. 8 b. Calculated (---) and measured (—) temperature-time field for a steel stud wall, insulated on each side with two 13 mm gypsum plaster sheets of density  $\gamma = 790 \text{ kg/m}^3$ , and exposed to fire on one side. The positions of the temperature gauges are shown on the wall cross sections. The curves are drawn on the assumption that the gas temperature-time curve conforms to the standard fire curve

time curves in the fire compartment. The results are set out in Figs. 8 c and 8 d in which the maximum temperature  $\vartheta_{\max}$  on the side of the wall, which is not exposed to fire is given for the complete fire process as a function of the fire load  $q$  for different values of the opening factor  $A\sqrt{h}/A_t$  of the fire compartment. Fig. 8 c relates to a wall with two 13 mm sheets of plasterboard on each side, and Fig. 8 d to a wall with one 13 mm sheet of plasterboard on each side. With regard to fire exposure, the input data used was the gas temperature-time curve for fire compartment Type A (standard fire compartment) according to Subsection 4.3.3.

Corresponding calculations of the maximum temperature  $\vartheta_{\max}$  on the side not exposed to fire have been made for a wall with slabs of mineral wool 50, 100 and 150 mm thick respectively between arbitrarily chosen incombustible external layers. The results are shown in Fig. 8 e. No account has been taken of the heat capacity and thermal insulation capacity of the external layer in calculating the surface temperature of the wall. This implies that, the higher the heat capacity and heat resistance of the external layer, the more the temperatures given in the figures are on the safe side, and the greater the underestimation of the real fire separating capacity of the wall in question.

In the Design Section, Fig. 8 a gives a summary of the results set out in Figs. 8 c - 8 e. This figure contains the combinations of fire load  $q$  and opening factor  $A\sqrt{h}/A_t$  for which the maximum temperature  $\vartheta_{\max}$  on the sides of the different types of wall which are not exposed to fire, does not exceed  $200^\circ\text{C}$ , i.e. the conditions under which the partitions meet the stipulated temperature requirements.

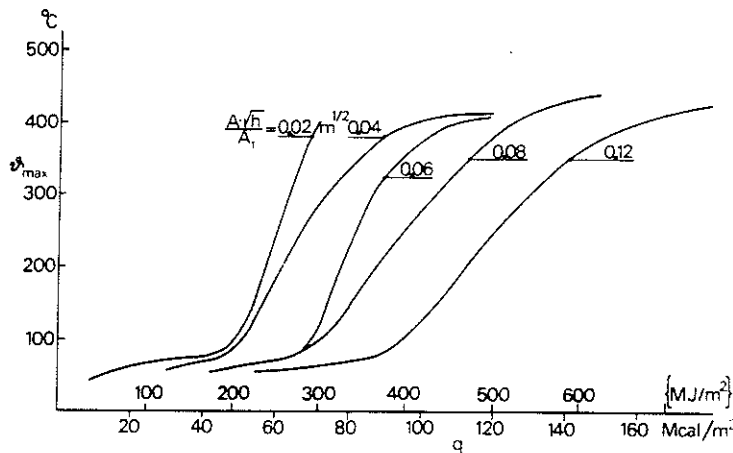


Fig. 8 c. Calculated maximum temperature  $\vartheta_{\max}$  during a complete fire process on the unexposed side of a steel stud-gypsum plaster sheeting wall as a function of the fire load  $q$  and the opening factor of the fire compartment  $A\sqrt{h}/A_t$ . The wall is insulated on each side with two 13 mm gypsum plaster sheets of density  $\gamma = 790 \text{ kg/m}^3$

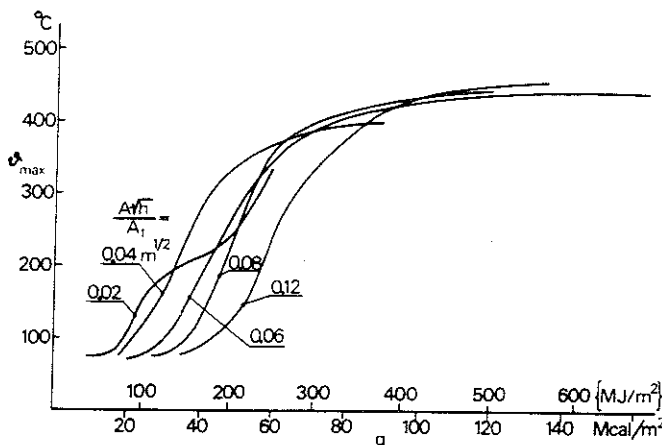


Fig. 8 d. Calculated maximum temperature  $\vartheta_{\max}$  during a complete fire process on the unexposed side of a steel stud-gypsum plaster sheeting wall as a function of the fire load  $q$  and the opening factor of the fire compartment  $A\sqrt{h}/A_t$ . The wall is insulated on each side with one 13 mm gypsum plaster sheet of density  $\gamma = 790 \text{ kg/m}^3$



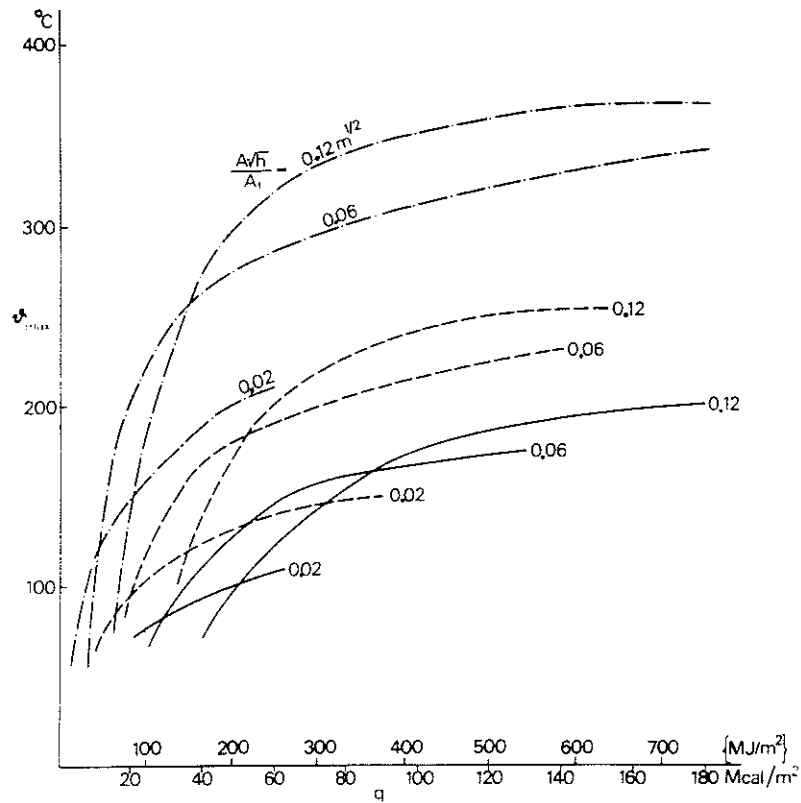


Fig. 8 e. Calculated maximum temperature  $\theta_{\max}$  during a complete fire process on the unexposed side of a wall insulated with mineral wool as a function of the fire load  $q$  and the opening factor of the fire compartment  $A_v \bar{h}/A_t$ . The external layers of the wall may be of any incombustible material. The wall is made with mineral wool of an approximate density of 45 kg/m<sup>3</sup>, of 50 (---), 100(---) and 150 mm thickness(—). No account has been taken of the heat capacity and thermal resistance of the external layers

## 9 CRITICAL LOAD UNDER FIRE EXPOSURE CONDITIONS FOR A STEEL STRUCTURE SUBJECT TO A FLEXURAL, TENSILE OR COMPRESSIVE LOADING WITHOUT THE CONCOMITANT RISK OF INSTABILITY

### 9.1 Determination of the critical load on the basis of the yield stress at elevated temperatures or the 0.2% proof stress

Determination of the loadbearing capacity of a steel structure under fire exposure conditions requires knowledge of the deformation and strength properties of the steel over the temperature range covered during a fire. In the case of structures subject to flexural, tensile or compressive loading without the concomitant risk of instability, such determination is often based on the 0.2% proof stress of the steel, i.e. the stress which produces a residual strain of 0.2%. This proof stress is employed instead of the yield stress, since there is no real yield region in usual structural steels at elevated temperatures. A relationship between the 0.2% proof stress  $\sigma_{0.2}$ , as a percentage of the yield stress at room temperature, and the steel temperature  $\theta_s$  is shown in Fig. 9.1 a (45). This relationship has been determined for tensile test specimens loaded at the temperature concerned at such a slow rate that the values include a considerable influence of short-term creep at high temperatures.

If the 0.2% proof stress is employed as the design stress under fire exposure conditions for a steel structure subject to flexural, tensile or compressive loading without the concomitant risk of instability, it is suitable to base assessment of the loadbearing capacity of the structure on the limit state theory (46). The stipulation is made that the shape of the cross section is such, or the structure is braced in such a way, that instability failure in the form of buckling or lateral buckling is not of critical significance for the loadbearing capacity. If the shape of the cross section is such, or the structure is braced in such a way, that the permissible bending stress according to Steel Construction Code 70 (54) need not be reduced in view of the risk of buckling or lateral buckling at room temperatures, then it may be supposed that there is no risk of such instability failure at elevated temperatures. If, however, the permissible bending stress at room temperatures must be reduced in view of the risk of buckling or lateral buckling, limit state design should not normally be employed for the determination of the critical load of the structure under fire exposure conditions. The critical load under fire exposure conditions should instead be calculated in the same way in

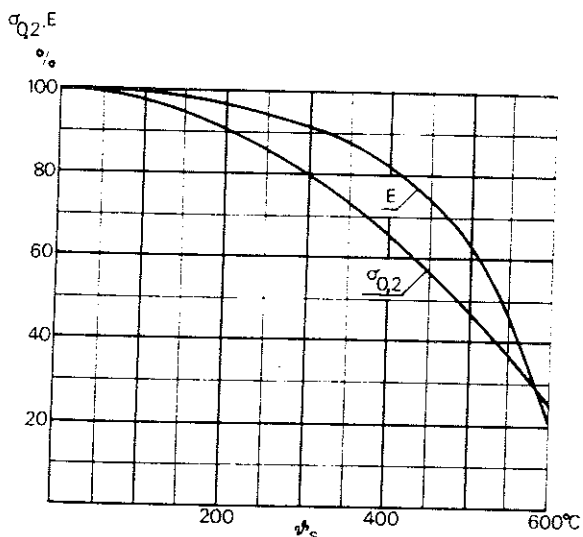


Fig. 9.1 a. The 0.2% proof stress  $\sigma_{0.2}$  and the modulus of elasticity  $E$  as a function of the steel temperature  $\theta_s$  for a mild structural steel (45)

principle as at room temperatures, with the difference that the values of the modulus of elasticity and the yield stress (0.2% proof stress) used must be those which apply at the steel temperature concerned according to Fig. 9.1 a.

For a continuous beam of I section, the risk of flange buckling at different temperatures can be determined directly from Equation (9.1 a). In this connection, it may be supposed that there is no risk of flange buckling if (see (54))

$$\frac{b}{t} \leq 0,38 \sqrt{\frac{E}{\sigma_{0,2}}} \quad (9.1 a)$$

where  $b$  = width of flange

$t$  = thickness of flange

$E$  = modulus of elasticity at the steel temperature concerned

(see Fig. 9.1 a)

$\sigma_{0,2}$  = 0.2% proof stress at the steel temperature concerned (see Fig. 9.1 a)

The requirement according to Equation (9.1 a) is satisfied by all rolled sections available in Sweden.

Examples of the application of the limit state theory under fire exposure conditions are given in the following for a statically determinate structure, a simply supported beam carrying a uniformly distributed load, as well as for a statically indeterminate structure, a beam rigidly restrained at one end and carrying a point load.

The ultimate bending moment  $M$  for a simply supported beam of length  $L$  (cm) {m} which is carrying a uniformly distributed load  $q$  (kgf/cm) {MN/m} is

$$M = \frac{qL^2}{8} \quad (\text{kgfcm}) \{ \text{MNm} \} \quad (9.1 b)$$

The ultimate load of the beam is reached when the beam is in a state of full plasticity at the section where the maximum moment occurs. The moment capacity of a section in a state of full plasticity, which is at the temperature  $\vartheta_s$ , can be written as

$$M = \sigma_{0,2} W_p \quad (\text{kgfcm}) \{ \text{MNm} \} \quad (9.1 c)$$

where  $W_p$  = plastic modulus of section for the beam ( $\text{cm}^3$ ) { $\text{m}^3$ }

$\sigma_{0,2}$  = yield stress or 0.2% proof stress at the steel temperature  $\vartheta_s$  concerned ( $\text{kgf/cm}^2$ ) {MPa} (Fig. 9.1 a)

If the maximum moment in the beam, as in Equation (9.1 b), is put equal to the maximum moment capacity of the cross section as in Equation (9.1 c), the critical load  $q_{cr}$  of the beam is given by

$$q_{cr} = \frac{8\sigma_{0,2} W_p}{L^2} = \frac{8\sigma_{0,2} W_{\alpha_p}}{L^2} \quad (\text{kgf/cm}) \{ \text{MN/m} \} \quad (9.1 d)$$

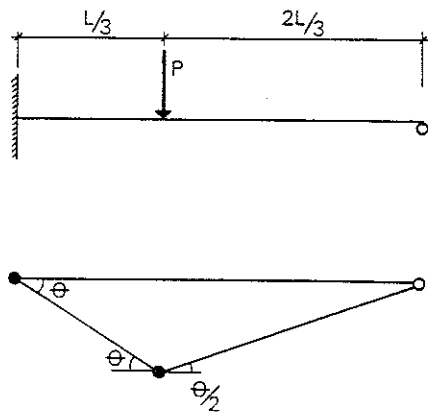


Fig. 9.1 b. Sketch showing procedure for determination of the ultimate bending moment in a beam rigidly restrained at one end and acted upon by a point load

where  $W$  = elastic modulus of section ( $\text{cm}^3$ )  $\{\text{m}^3\}$   
 $\alpha_p$  = degree of plasticity of the cross section

For ordinary I sections,  $\alpha_p = 1.13 - 1.15$ , and for rectangular cross sections,  $\alpha_p = 1.50$ .

For a beam of constant cross section which is rigidly restrained at one end and carrying a point load as in Fig. 9.1 b, plastic hinges are formed at the section of end restraint and at the section below the point load, before the ultimate load is reached. The relationship between the moments  $M$  at these sections and the external load  $P$  when the ultimate load has been reached can be written, using the symbols according to Fig. 9.1 b, as

$$M\theta + M(\theta + \theta/2) = P \frac{L\theta}{3} \quad (9.1 e)$$

which gives

$$M = \frac{PL}{7.5} \quad (\text{kgfcm}) \{\text{MNm}\} \quad (9.1 f)$$

If the moment according to Equation (9.1 f) is put equal to the maximum moment capacity of the cross section as in Equation (9.1 a), the critical load  $P_{cr}$  of the beam is given as

$$P_{cr} = 7.5 \frac{\sigma_{0.2} W \alpha_p}{L} \quad (\text{kgf}) \{\text{MN}\} \quad (9.1 g)$$

One advantage in determining the loadbearing capacity of a steel structure under fire exposure conditions on the basis of the 0.2% proof stress is that the same principles of calculation can be used as those employed in design at normal temperatures. All that need be done is to replace the value of the yield stress at room temperature with the 0.2% proof stress at the temperature concerned. One disadvantage in using the 0.2% proof stress is that, often, this is not the significant critical stress. Stress-strain curves obtained in tensile tests at elevated temperatures namely have a very rounded shape, and an increase in stress to a value higher than the 0.2% proof stress does not, therefore, result in immediate collapse of the structure. Furthermore, it is difficult in determining the loadbearing capacity on the basis of the 0.2% proof stress to give due consideration to the effect of the creep strain in the material at elevated temperatures. The influence on the loadbearing capacity of the softly rounded shape of the stress-strain

curves at elevated temperatures, and the effect of the creep strain in the material, can however be taken into account when the loadbearing capacity is determined on the basis of the deformations in the structure during the fire.

## 9.2 Determination of the critical load for beams on the basis of the calculated deformation curve

### 9.2.1 Deformation curve and failure criterion

By calculating the deformation curve of a steel girder under fire exposure conditions, account can be taken of the softly rounded shape of the stress-strain curve at elevated temperatures, and also of the influence of creep strain. An analytical model for this purpose has been proposed in (47) - (49).

According to this analytical model, the fire process is divided into a number of time intervals, and the midspan deflection of the girder at the beginning of each time interval is calculated at the temperature which obtains during this interval, on the basis of the stress-strain curves for the material. These curves have been determined in tensile tests at elevated temperatures performed at such a high rate of loading that the effect of the creep strain in the material can be considered to be negligible (48). The effect of the creep strain on the strain and the deflection is calculated separately by means of certain creep equations (50) - (52). The applicability of these creep equations for the calculation of the creep strain in steel structures under fire exposure conditions has been verified in creep tests on test specimens (52). The analytical model has also been verified by means of some twenty fire tests on loaded simply supported steel girders (48). An example of the close agreement between the calculated and measured deformation-time curves in these fire tests is given in Fig. 9.2.1 a.

In principle, the loadbearing capacity of a steel girder acted upon by fire can be considered exhausted when its rate of deformation is infinitely large. From the practical point of view, however, it is necessary to apply a failure criterion related to a finite deformation or to a finite rate of deformation. The results of experimental and theoretical investigations indicate that the following failure criterion, related to the magnitude of the deflection, is suitable for use in conjunction with steel girders under fire exposure conditions (48), (53)

$$y_{cr} = \frac{L^2}{800h} \quad (9.2.1 a)$$

where  $y_{cr}$  = critical midspan deflection (cm)  
 $L$  = span of the girder (cm)  
 $h$  = depth of the girder (cm)

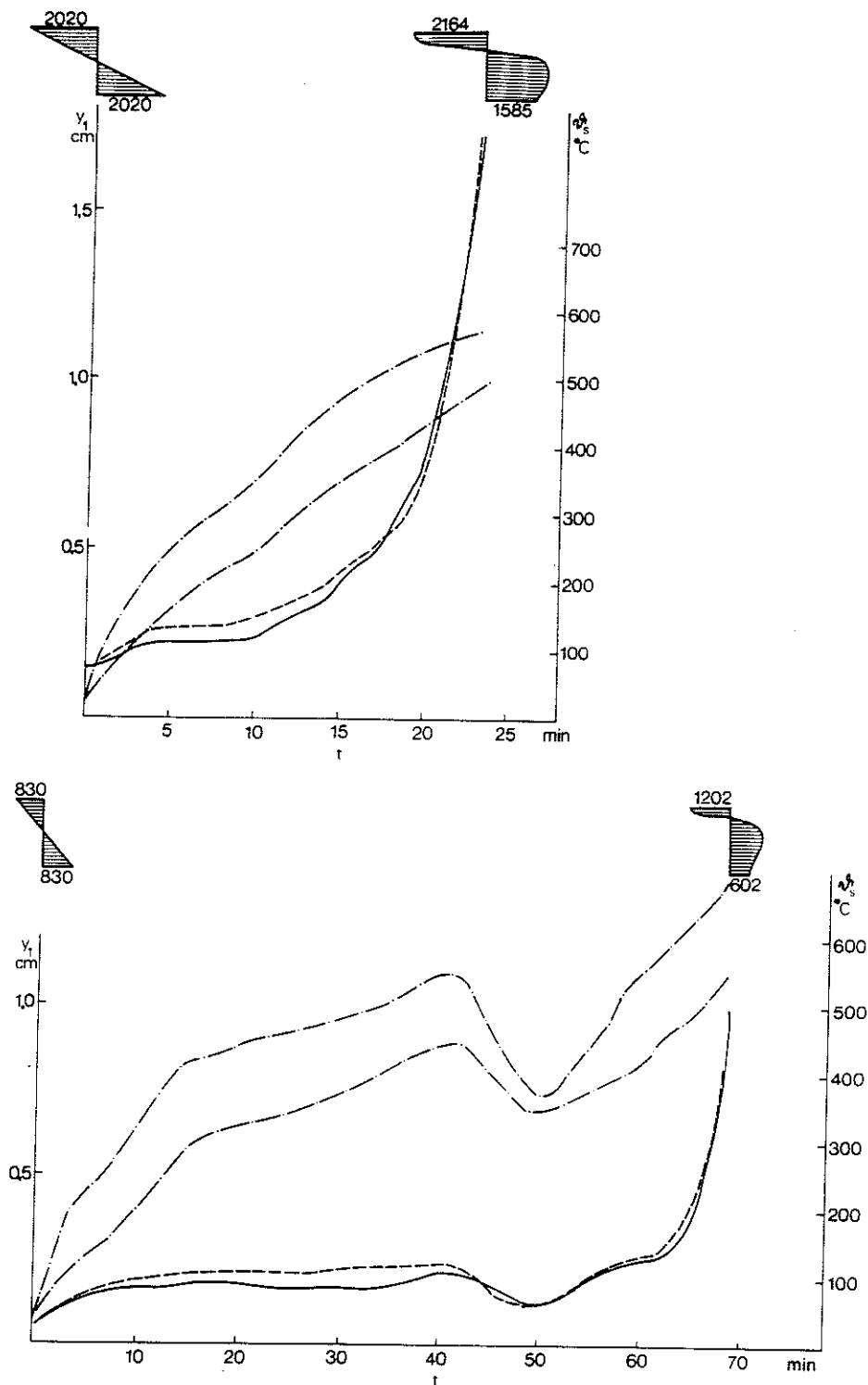


Fig. 9.2.1 a. Measured (—) and calculated (---) deflection-time ( $y_1 - t$ ) curves for two simply supported steel girders during fire tests (48). The upper chain line is the temperature-time ( $\theta_s - t$ ) curve for the bottom flange at the midpoint of the girder, and the lower one the corresponding curve for the top flange. The calculated stress distributions at the beginning and end of each test are given in the figure. The span of the girders was 2.50 m. The load consisted of two point loads symmetrically placed about the midpoint of the girder at a spacing of 0.76 m. The deflection  $y_1$  is the midspan deflection calculated for the part of the girder between the load points. The upper figure relates to a rapid fire process and the lower one to a slow fire process

### 9.2.2 Evaluation of the critical load under certain given conditions

The deformation curve of a steel girder under fire exposure conditions, and consequently its loadbearing capacity, are dependent on the type of loading and the

statical system, etc. By means of systematic calculations of the deformation curve for steel girders acted upon by a fire, and by application of the failure criterion according to Equation (9.2.1 a), it has been possible to determine the critical load for different types of loading and statical systems. The results have been shown in the form of a diagram (49). An example of this is given in Fig. 9.2.2 a for a simply supported beam with a uniformly distributed load. The coefficient  $\beta$  for calculation of the critical load according to the formula in the diagram is given as a function of the maximum steel temperature  $\vartheta_{\max}$  during the fire. By definition,  $\beta$  is the ratio of the load which, under fire exposure conditions, causes a midspan deflection according to Equation (9.2.1 a), to the load which, at room temperature, causes the yield stress to be attained in the most highly stressed cross section. In Chapter 9 in the Design Section, the coefficient  $\beta$  is also given for other types of loading and statical systems.

Owing to the creep strain, the rate of heating and cooling of the beam influences the deformation process and consequently the critical load, at temperatures over about  $450^{\circ}\text{C}$ . For this reason, the coefficient  $\beta$  has been given for a number of rates of heating, viz. 100, 20 and  $4^{\circ}\text{C}/\text{min}$ . On the basis of the results of fire tests and calculations of the temperature-time curves of steel girders under fire exposure conditions, the rate of cooling has been assumed throughout to be one third of the rate of heating (49). A rough estimate of the average rate of heating of a steel structure under fire exposure conditions can easily be made with the aid of Fig. 9 a in the Design Section, in which the average rate of heating is given as a function of the fire load  $q$ , the opening factor  $A\sqrt{h}/A_t$ , and the maximum steel temperature  $\vartheta_{\max}$ .

Apart from the assumption that the rate of cooling is one third of the rate of heating, the values of  $\beta$  in Fig. 9.2.2 a and in the Design Section have been calculated on the assumption that the material of the girders is ordinary mild structural steel, i. e. steel with an analysis and strength values corresponding to those in the 13 and 14 Series in conformity with the appropriate Swedish Standards (see Table 9.2.2 a). It has further been assumed that the girders have a constant I section of such shape that there is no risk of instability failure in the form of buckling or lateral buckling.

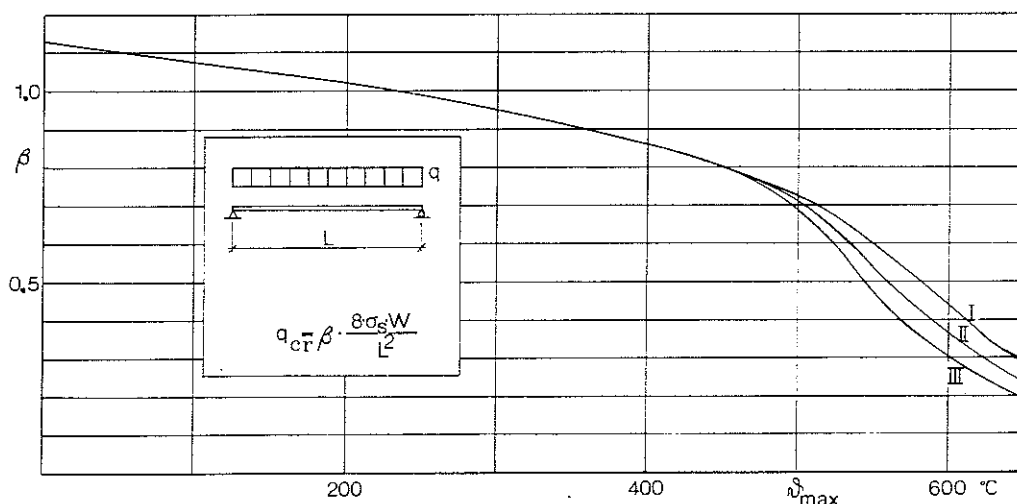


Fig. 9.2.2 a. The coefficient  $\beta$  for determination of the critical load  $q_{cr}$  for a fire exposed simply supported beam of constant I section acted upon by a uniformly distributed load. The coefficient  $\beta$  is given as a function of the maximum steel temperature  $\vartheta_{\max}$  for three different rates of heating and cooling, curves I, II, III. The rates of heating for these curves are 100, 20 and  $4^{\circ}\text{C}/\text{min}$  respectively, the rate of cooling being assumed in all cases to be one third of the rate of heating. The yield stress at room temperature is denoted  $\sigma_s$  and the elastic modulus of section  $W$

Table 9.2.2 a. Some characteristics of certain structural steels according to Swedish Standards

Serie No.	Steel group	Examples of steel	Nominal yield stress		Analysis (%)	Mn	Si	P(max)	S(max)
			kgf/cm <sup>2</sup>	[Mpa]					
13	Carbon steel	1311, 1312	2200	220	0.12-0.20	0.3-0.7	0.05-0.25	0.06-0.08	0.05-0.06
14	Carbon steel	1411, 1412	2600	260	0.15-0.20	0.4-1.1	0.05-0.25	0.05-0.08	0.05-0.06
21	Carbon-manganese steel	2172, 2173, 2174	3200	320	0.18-0.20	1.0-1.8	0.05-0.5	0.04-0.05	0.04-0.05
	Grain refined steel	2132, 2133, 2134	3600	360	0.14-0.20	< 1.6	< 0.5	0.035	0.035
	Grain refined steel	2142, 2143, 2144	4000	400	0.16-0.20	< 1.8	< 0.5	0.035	0.035

Finally, it has been assumed that the temperature is uniform over the entire girder, and that there is nothing to prevent longitudinal expansion. With regard to deviations from these assumptions, reference is to be made to Subsection 9.2.3.

### 9.2.3 Evaluation of the critical load under conditions different from those in Subsection 9.2.2

The diagrams in Chapter 9 in the Design Section which are provided for the determination of the critical load in steel girders under fire exposure conditions can in many cases also be used in conditions different from those set out in Subsection 9.2.2, in order to yield approximate values of the critical load on the safe side (49).

Details are given below of the way in which these diagrams can be used for

- other types of loading
- continuous beams
- other steel grades
- other cross sections
- uneven temperature distribution in the beam
- restraint on longitudinal expansion

#### 9.2.3.1 Other types of loading

When the types of loading are different from those specified in the diagrams in Chapter 9 in the Design Section, the value of  $\beta$  applicable to constant bending moment and the temperature in the actual case can be used for an assessment of the critical load on the safe side. The critical load is obtained by multiplying this value of  $\beta$  by the load level which, for the type of loading in the case under consideration, causes the yield stress to occur in the most highly stressed section at room temperature.

#### 9.2.3.2 Continuous beams

An assessment of the critical load on the safe side for a continuous beam of constant I section acted upon by a uniformly distributed load or a central point load can be based on the values of  $\beta$  for a beam rigidly restrained at both ends which



is subject to a uniformly distributed load or a central point load. The value of  $\beta$  applicable to the temperature and type of loading in the actual case is to be multiplied by that load which causes the yield stress to be attained at room temperature in the most highly stressed section in the continuous beam.

### 9.2.3.3 Other steel grades

The diagrams in Chapter 9 in the Design Section are primarily valid for girders of structural steel with analyses and strengths corresponding to those of an ordinary mild carbon steel, i.e. steels in the 13 and 14 Series in conformity with the appropriate Swedish Standards. Investigations show, however, that these diagrams can also be used with satisfactory accuracy for fine grained steels of higher strengths with a basic analysis corresponding to that of ordinary carbon-manganese steels, e.g. a basic analysis corresponding to that of Steel 2 172 in conformity with Swedish Standard SIS 14 21 72 (see Table 9.2.2 a) (49), (52).

For steels of the carbon-manganese type which have not received grain refinement treatment, the diagrams give calculated critical loads which, in many cases, are not substantially below the actual critical loads. Examples of this are given in Figs. 9.2.3.3 a and 9.2.3.3 b, in which the values of  $\beta$  for a simply supported beam and a beam rigidly restrained at both ends, respectively, both of carbon-manganese steel and carrying a uniformly distributed load, are compared with the values of  $\beta$  applicable to corresponding beams of ordinary carbon steel.

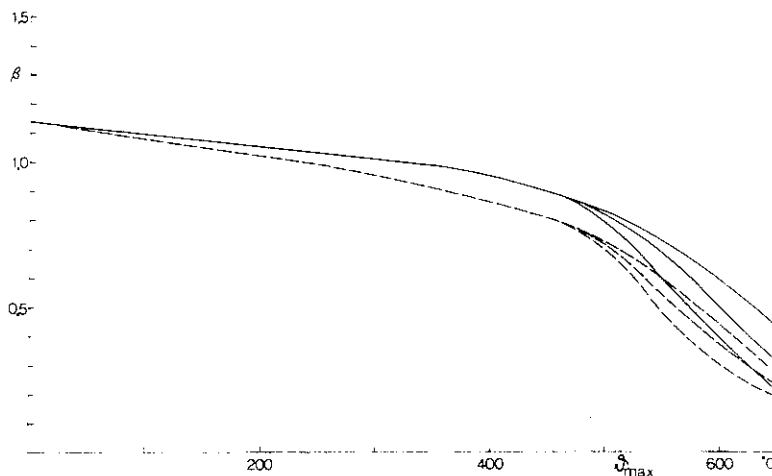


Fig. 9.2.3.3 a. The coefficient  $\beta$  for simply supported beams of carbon-manganese steel (—) and carbon steel (---) of constant I section which are acted upon by a uniformly distributed load. It is assumed in both cases that the temperature  $\theta_{\max}$  is uniform in the entire beam, and that the beam is free to expand. The curve branches correspond to the different rates of heating and cooling according to curves I, II and III in Fig. 9.2.2 a. The expression used for calculation of the critical loads is  $q_{cr} = \beta 8\sigma_s W/L^2$ , where  $\sigma_s$  is the yield stress of the material at room temperature.  $W$  = elastic modulus of section and  $L$  = span of the beam

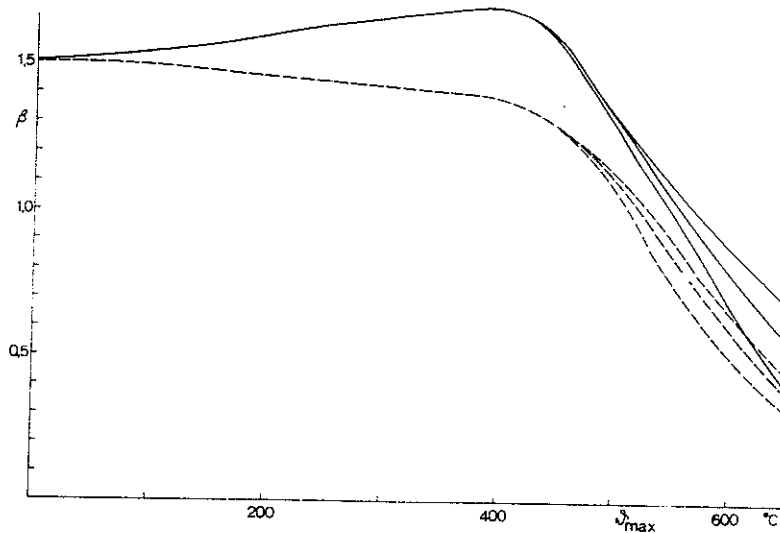


Fig. 9.2.3.3 b. The coefficient  $\beta$  for beams of carbon-manganese steel (—) and carbon steel (---) of constant I section which are rigidly restrained at each end and acted upon by a uniformly distributed load. It is assumed in both cases that the temperature  $\theta_{\max}$  is uniform in the entire beam, and that the beam is free to expand. The curve branches correspond to the different rates of heating and cooling according to curves I, II and III in Fig. 9.2.2 a. The expression used for calculation of the critical load is  $q_{cr} = \beta 12 \sigma_s W/L^2$ , where  $\sigma_s$  is the yield stress of the material at room temperature.  $W$  = elastic modulus of section and  $L$  = span of the beam

#### 9.2.3.4 Other cross sections

The diagrams in Chapter 9 in the Design Section have been calculated on the assumption that the degree of plasticity of the cross section, i.e. the ratio of the plastic to the elastic modulus of section, is 1.13. This degree of plasticity is representative for ordinary I sections when bending occurs about the major axis. In the case of cross sections with a higher degree of plasticity, the corresponding deformation will be less and the loadbearing capacity consequently higher. However, the increase in loadbearing capacity is not in direct proportion to the degree of plasticity. The reason for this is that the design cross section of a steel girder under fire exposure conditions is not fully plastic at the deflection corresponding to the failure criterion according to Equation (9.2.1 a), due to the softly rounded shape of the stress-strain curves at high temperatures. In Figs. 9.2.3.4 a and 9.2.3.4 b the values of  $\beta$  for a simply supported beam and a beam rigidly restrained at each end, respectively, each of rectangular cross section (degree of plasticity = 1.50) and carrying a uniformly distributed load, are compared with the values of  $\beta$  for corresponding beams of I section (degree of plasticity = 1.13).

Another assumption on which the diagrams in Chapter 9 in the Design Section are based is that there is no risk of instability failure in the form of buckling or lateral buckling. As regards the material properties, the risk of instability failure is essentially determined by the modulus of elasticity, the percentage reduction in which, as the temperature rises, is however less than the reduction in the yield stress or the 0.2% proof stress. As the temperature rises, therefore, the risk of instability failure should diminish in relation to the risk of flexural failure. This implies that, provided that the shape of the cross section is such, or the construction is braced in such a way, that the permissible bending stress according to the Steel Construction Code 70 (54) need not be reduced in view of the risk of buckling or lateral buckling at room temperature,

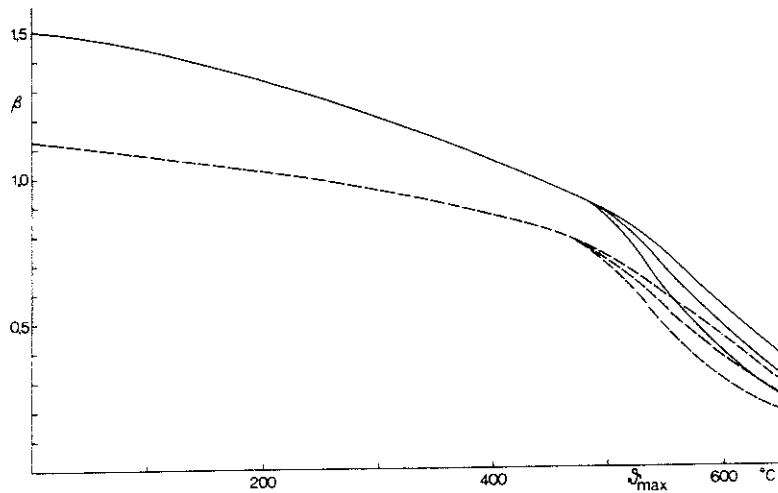


Fig. 9.2.3.4 a. The coefficient  $\beta$  for a simply supported beam of carbon steel acted upon by a uniformly distributed load, the cross section being rectangular (—) or I-shaped (---). It is assumed in both cases that the temperature  $t_{max}$  is uniform in the entire beam, and that the beam is free to expand. The curve branches correspond to the different rates of heating and cooling according to curves I, II and III in Fig. 9.2.2 a. The expression used for calculation of the critical load is  $q_{cr} = \beta 8 \sigma_s W / L^2$ , where  $\sigma_s$  is the yield stress of the material at room temperature.  $W$  = elastic modulus of section and  $L$  = span of the beam

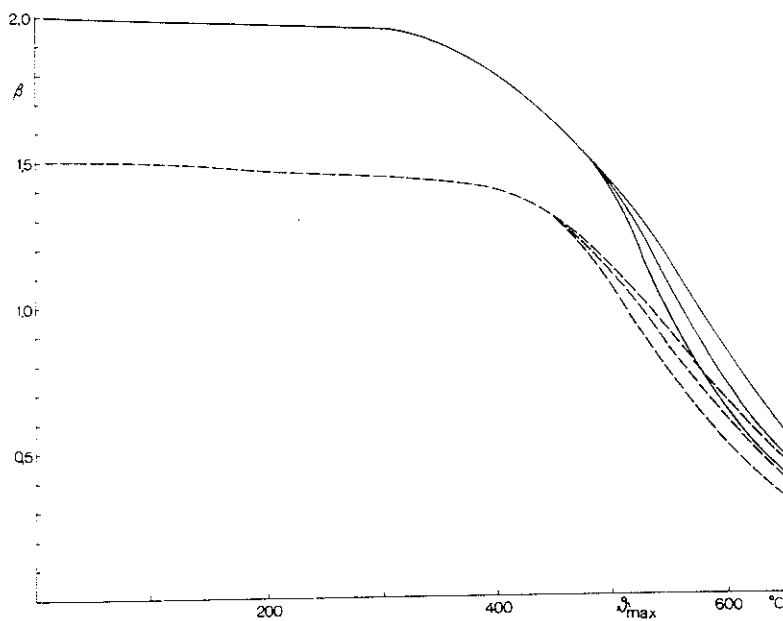


Fig. 9.2.3.4 b. The coefficient  $\beta$  for a beam of carbon steel which is rigidly restrained at each end and acted upon by a uniformly distributed load, the cross section being rectangular (—) and I-shaped (---). It is assumed in both cases that the temperature  $t_{max}$  is uniform in the entire beam, and that the beam is free to expand. The curve branches correspond to the different rates of heating and cooling according to curves I, II and III in Fig. 9.2.2 a. The expression used for calculation of the critical load is  $q_{cr} = \beta 12 \sigma_s W / L^2$ , where  $\sigma_s$  is the yield stress of the material at room temperature.  $W$  = elastic modulus of section and  $L$  = the span of the beam

then it may be supposed that there is no risk of buckling or lateral buckling in the event of fire. For continuous beams of I section, the risk of flange buckling at different temperatures can be directly determined from Equation (9.1 a).

If there is a risk of buckling or lateral buckling, the loadbearing capacity of the girder under fire exposure conditions should be calculated in the same principal way as at room temperature, with the difference that the values of the modulus

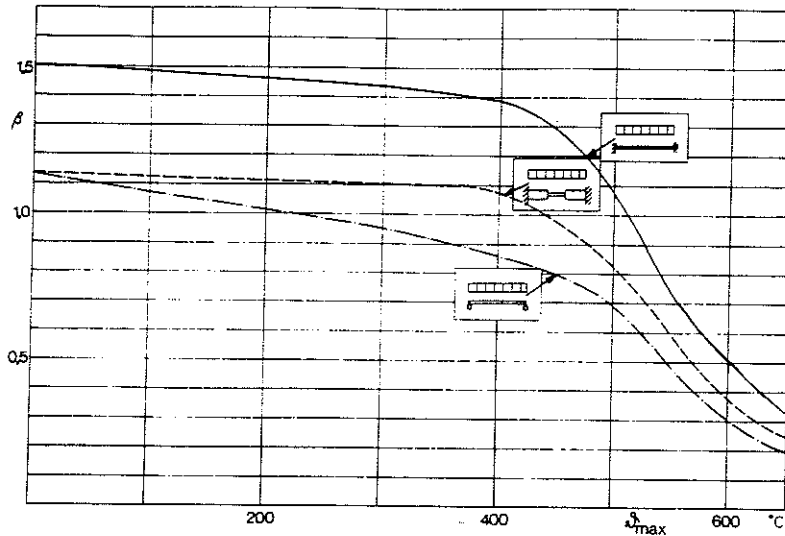


Fig. 9.2.3.4 c. The coefficient  $\beta$  for a simply supported beam of constant I section (— · —), a beam of I section rigidly restrained at each end in which the modulus of section at midspan is only half as much as at the ends (---), and a beam of constant I section rigidly restrained at each end (—). It is assumed in all cases that the load is uniformly distributed and that the beam is free to expand. It is also assumed that the temperature  $\theta_{max}$  is uniform in the entire beam. The values of  $\beta$  are those for the lowest rate of heating according to curve III in Fig. 9.2.2 a. The expression used for calculation of the critical load in the simply supported beam is  $q_{cr} = \beta 8 \sigma_s W/L^2$ , and in the beams with rigidly restrained ends  $q_{cr} = \beta 12 \sigma_s W/L^2$ , where  $\sigma_s$  is the yield stress of the material at room temperature.  $W$  = elastic modulus of section (for the beam of variable section, that at the ends) and  $L$  = span of the beam

of elasticity and yield stress (0.2% proof stress) employed must be those which apply at the actual steel temperatures according to Fig. 9.1 a.

For a simply supported beam of variable cross section, the value of  $\beta$  applicable to the loading type of constant bending moment can always be used for an assessment, on the safe side, of the critical load. The value of  $\beta$  applicable to the actual temperature must be multiplied by that load level which, for the actual beam and type of loading, causes the yield stress to occur at room temperature in the most highly stressed cross section.

For a rigidly restrained beam of variable cross section, an assessment of the critical load can always be based on the value of  $\beta$  applicable for a simply supported beam carrying the same type of loading. However, this often results in an assessment of the risk of failure which is rather too much on the safe side. This is illustrated in Fig. 9.2.3.4 c where the values of  $\beta$  for a beam rigidly restrained at both ends, with a modulus of section at midspan that is only half as much as at the ends, are compared with the values of  $\beta$  for a rigidly restrained beam of constant cross section and also with the values of  $\beta$  for a simply supported beam of constant cross section. In all cases, a uniformly distributed load is assumed.

#### 9.2.3.5 Uneven temperature distribution in the beam

As a rule, the temperature in the top flange of a steel girder which is exposed to the action of fire is lower than in the bottom flange. This is due to the fact that there is less direct heat applied to the top flange than to the bottom flange, and also that there is conduction of heat from the top flange to the floor slab or the roof. The results of fire tests show that the temperature difference between

the top and bottom flange can often be as much as  $100-200^{\circ}\text{C}$ . This difference in temperature causes the beam to deflect. On the other hand, since the top flange has a lower temperature, this can take up higher stresses and thus reduce the stresses in the hotter bottom flange. In consequence, the total deflection is less and the loadbearing capacity is greater than if the whole beam had had the same temperature as the bottom flange. Calculations of the critical load for beams in which there is an uneven distribution of temperature over the cross section show that this increase in loadbearing capacity is of the order of 5-20% (49).

In many cases, the temperature at the ends of a beam is lower than near the centre. This also results in an increase in the loadbearing capacity compared with the case where the whole beam has the same temperature as the central portion. Particularly in the case of statically indeterminate beams, this rise in loadbearing capacity can be considerable (49).

#### 9.2.3.6 Restraint on longitudinal expansion

If thermal longitudinal expansion of a steel girder under fire exposure conditions is wholly or partially prevented, for instance due to limited provision for movement at the supports, forces are imposed on the girder. There are several factors which govern the magnitudes of these imposed forces, such as the temperature conditions, the degree of restraint on longitudinal expansion, the stiffness of the girder, the size of transverse load, etc.

Forms of construction in which there are very limited facilities for movement at the supports often occur in practice. An example of this is a stiff floor slab which limits horizontal movement of the supporting columns and thus the beam supports. It is probable that some movement occurs in spite of this, for instance as a result of end play or plastic deformation at the junctions.

The greater the deflection is in a beam whose supports can move in the horizontal direction, the more the ends of the beam will tend to move closer to one another, due to the difference in length between the centroidal axis of the beam and the corresponding chord (see Fig. 9.2.3.6 a). On the other hand,

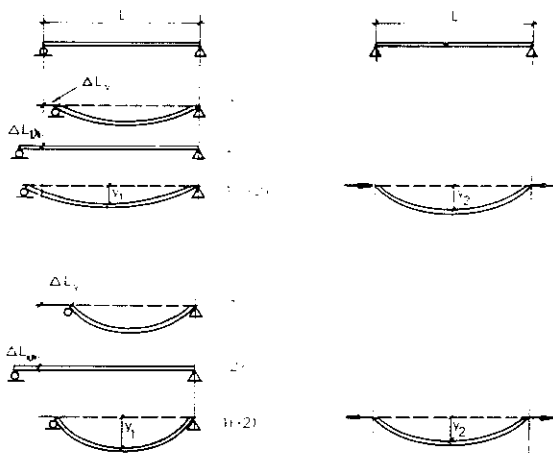


Fig. 9.2.3.6 a. Expansion and imposed forces in a beam which is free to expand longitudinally (to the left) and in a beam in which there is no provision at all for horizontal movement at the supports (to the right)

a rise in temperature in the beam causes longitudinal expansion. At the beginning of a fire process, when deflection of the beam is still relatively small, the thermal longitudinal expansion  $\Delta L_\theta$  takes precedence over the contraction  $\Delta L_y$  due to the deflection. The ends of the beam thus endeavour to move away from one another through a distance  $\Delta L = \Delta L_\theta - \Delta L_y$ . If the supports of the beam are rigid, an axial compressive force is imposed on the beam. If it is assumed that the resultant of this compressive force coincides with, or lies above, the line joining the centroids of the two end cross sections, then the moment increases over the whole beam, causing increased deflection. At this stage, therefore, the deflection  $y_2$  in this beam is greater than the deflection  $y_1$  in a similar beam whose longitudinal expansion is not prevented. Later on during the fire, when the deflection has assumed sufficiently large values, the contraction  $\Delta L_y$  due to the deflection takes precedence over the thermal longitudinal expansion  $\Delta L_\theta$ . Due to this, the distance between the ends of a beam with movable supports will be less than the original distance between the supports. In a beam in which longitudinal expansion is prevented there is instead an imposed tensile force which reduces the moment along the beam. As a result, the deflection in such a beam is less than that in a beam which is free to expand longitudinally, i.e. at this stage  $y_2$  is smaller than  $y_1$  (see Fig. 9.2.3.6 a).

If the resultant of the compressive force in the beam in which longitudinal expansion is prevented is instead below the line joining the centroids of the end cross sections, then at the beginning of the fire when the deflection is small, the compressive force reduces the moment along the beam, and the deflection  $y_2$  is consequently smaller than the deflection  $y_1$ . However, as the deflection gradually increases during the fire, the moment becomes greater along the beam and at last exceeds the moment in a beam which is free to expand in the longitudinal direction. The situation after this is the same as in a beam where the resultant of the compressive force coincides with, or lies above, the line joining the centroids of the end cross sections. The deflection  $y_2$  in the beam with restraints on expansion will be greater initially, but later on, when the deflection again increases and gives rise to tensile forces which reduce the moment, will be smaller than the deflection  $y_1$  in the beam which is free to expand longitudinally.

If the deflection criterion  $y_{cr} = L^2/800 h$  according to Equation (9.2.1 a) is applied as the failure criterion also for a beam which is wholly incapable of horizontal movement at the supports, the critical temperature for this beam may be either higher or lower than for a beam which is free to expand longitudinally, depending, inter alia, on the magnitude of the load and the stiffness of the beam. The greater the load and the more slender the beam, the greater the probability that the critical temperature will be higher in a beam that has no movement facilities at the supports than in a beam which is free to expand (49).

One condition which must be satisfied in order that the deflection criterion in accordance with Equation (9.2.1 a) should be applicable as the criterion of failure for a steel girder under fire exposure conditions is that the deflection of the girder should increase very rapidly as the temperature rises once the deflection according to Equation (9.2.1 a) has been reached. Normally, this does not occur in beams in which longitudinal expansion is prevented. The increase in deflection after the attainment of a deflection large enough for tensile forces to be formed is at a considerably slower rate than the increase in deflection in a corresponding beam which is free to expand longitudinally. Some

modification of the failure criterion may therefore be justified in beams which have no axial movement facility. In practice, however, it is difficult to make a quantitative assessment of any great accuracy of the ability of a beam to move under fire exposure conditions. Owing, inter alia, to end play and plastic flow at the end junctions, the actual state of affairs is in many cases probably intermediate between that applicable to a beam which is wholly incapable of movement at the support and one which is completely free to expand. Owing to the difficulty of making a relevant assessment of the ability of a beam to move at the supports, it would therefore appear to be appropriate from the practical point of view generally to base the determination of the loadbearing capacity of a steel girder under fire exposure conditions on the assumption that the girder is free to expand longitudinally. It is true that the deflection in a beam in which the movements at the supports is subject to restraint may be somewhat larger than that given by the deflection criterion  $y_{cr} = L^2/800 h$ , especially if the depth of the beam is large in relation to its length and the load is small. However, the failure load in such a beam, if the failure load is taken to mean the greatest load which a beam is able to carry at a certain temperature without consideration of the magnitude of the deflection, will always be greater than the failure load in a similar beam which is free to expand longitudinally (49).

If movement of a beam which is exposed to fire is subject to some restraint at the ends and it is in addition sufficiently slender in the direction of the minor axis, then there is a risk that the beam will deflect laterally due to the forces imposed in it. There is however no question of instability failure in the actual sense of the term, since the compressive force diminishes as the beam deflects and attains a new position of equilibrium. This is a fundamental difference in relation to the state of affairs in a vertically loaded column in which, owing to the fact that the column is subject to an axial compressive force during the whole of the deflection process, an increased deflection gives rise to an increase in moment.

Even if it is impossible for buckling in a horizontal direction to take place in a fire exposed steel girder which is subject to imposed compressive forces as a result of a restraint on longitudinal expansion, a deflection in the lateral direction may result in the girder being subjected to torsion. If, however, the restraint on longitudinal expansion is due to a stiff floor slab, then the girder will at the same time, as a rule, be effectively braced laterally by the slab, and lateral deflection is therefore impossible or very limited.

The risk of lateral deflection in a girder under fire exposure conditions which has no axial movement facilities at the supports and is not supported laterally by a floor slab or similar structural elements is not directly comparable with the risk of buckling in a column. In spite of this, a comparison with a column may give an idea of the factors which have a bearing on the risk of lateral deflection in such a girder. For this reason, the variation in the imposed force under fire exposure conditions in simply supported beams acted upon by a uniformly distributed load and restrained against horizontal displacement at the level of the centroids of the end sections was determined at the same time as the deformations in the beams were calculated. The calculation has been carried out for beams of different stiffnesses and load levels. From the results, the imposed stress  $\sigma_t$ , i.e. the imposed force divided by the area of the beam, has been determined as a function of the steel temperature. This imposed stress has then been compared with the buckling stress  $\sigma_k$  at the same temperature, calculated according to Section 10.1 for columns of the same slenderness ratio as that of the beams in the direction of the minor axis. In calculating the slenderness ratio, it was assumed that the beams are pinjointed at both ends.

The ratio  $\sigma_t / \sigma_k$  of the imposed stress calculated as above to the buckling stress is plotted in Fig. 9.2.3.6 b as a function of the steel temperature  $\vartheta_s$ . It will be seen from the curves in the figure that the risk of lateral deflection in a steel girder under fire exposure conditions, which has no movement facilities at the ends and is not supported laterally, appears to increase as the value of the slenderness ratio  $\lambda$  increases, and decrease as the vertical load  $q$  increases. It is also evident from the figure that the risk of lateral deflection is greatest in the temperature range 100–200°C. The fundamental difference in this context between a beam and a column, i.e. that a column buckles at a stress equal to  $\sigma_k$  while the beam, owing to its lateral deflection, is gradually relieved of the stress imposed in it, must however be emphasised.

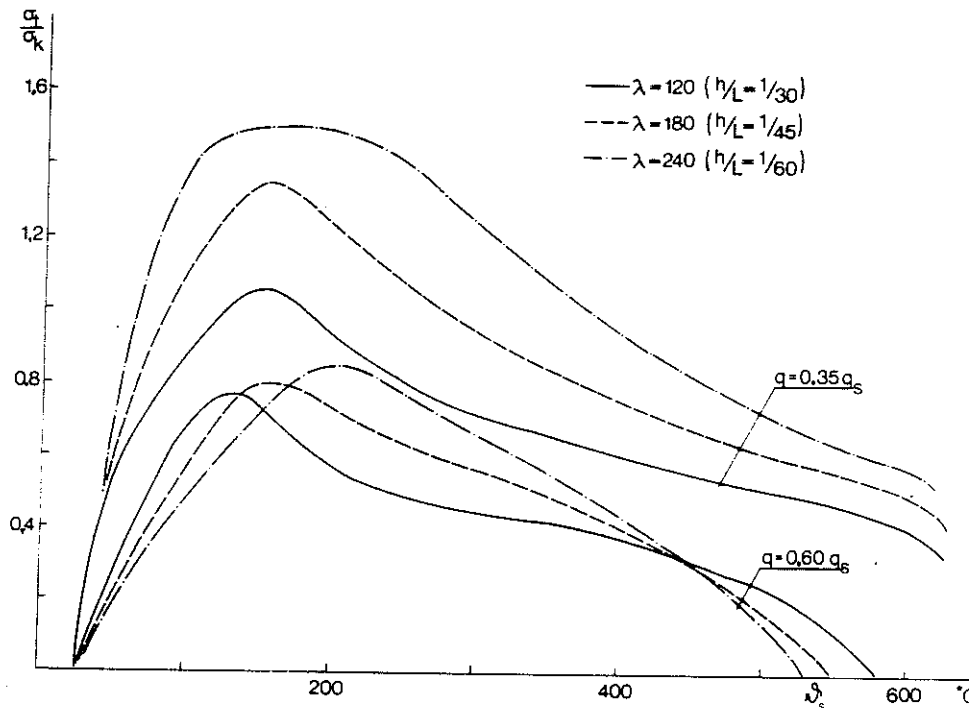


Fig. 9.2.3.6 b. The ratio of the imposed stress  $\sigma_t$  in beams in which there is no provision at all for movement at the supports, to the buckling stress  $\sigma_k$  in columns of the same slenderness ratio, as a function of the steel temperature  $\vartheta_s$  for different slenderness ratios and different transverse loads. In calculating  $\sigma_k$ , the slenderness ratio of the column was assumed to be the same as that of the beam with respect to lateral deflection perpendicular to the minor axis, and it was also assumed that both ends of the column are pinjointed. The transverse load on the beam is denoted  $q$  and the load which causes the yield stress to occur at room temperature in the most highly stressed section is denoted  $q_s$ . The depth of the beam is denoted  $h$  and its length  $L$ .



## 10 CRITICAL LOAD UNDER FIRE EXPOSURE CONDITIONS FOR A STEEL STRUCTURE SUBJECT TO AN AXIAL COMPRESSIVE FORCE

### 10.1 Determination of the buckling load under in-plane instability conditions when there is no restraint on longitudinal expansion

The methods employed in designing steel columns acted upon by an axial compressive load with regard to buckling at ordinary temperatures may be classified in two principal groups.

In principle, the method of approach used for one of these groups is as follows. The buckling load  $N_k$  is first of all determined for the ideal case of an initially straight column subject to a central compressive load, account being taken of the actual stress-strain curve of the material in question. The ideal buckling load is usually determined according to the tangent modulus theory. The compressive load  $N_{k,per}$  which is permissible with regard to buckling is then obtained by dividing the load  $N_k$  by a safety factor  $s$ . This safety factor allows for the effects of the initial curvature and unintentional load eccentricity which are unavoidable in practice. This implies that the safety factor  $s$  is dependent on the slenderness ratio of the column.

According to the other principal group the buckling load  $N_k$  is determined on the basis of a column of representative initial curvature and unintentional load eccentricity. The maximum compressive stress  $\sigma_{max}$  in the column is determined for this case, consideration being given to the effect of additional deflections. The critical axial compressive force is defined as the compressive force  $N_k$  which causes  $\sigma_{max}$  to attain a value, usually the yield stress  $\sigma_s$  or the 0.2% proof stress  $\sigma_{0.2}$  of the material, which is critical in this context. The permissible compressive force  $N_{k,per}$  is then obtained from the buckling load  $N_k$  by dividing this by a safety factor  $s_0$  which is independent of the slenderness ratio of the column.

Steel Construction Code 70 specifies a procedure for design with regard to buckling which is closely related to the first type of method (54). A design procedure in accordance with the latter type of method is specified in the Draft Code for Aluminium Constructions (55), (56).

It is natural to base approximate treatment of in-plane buckling in axially loaded steel structures under fire exposure conditions directly on the methods in the latter principal group, particularly for the case in Section 10.2 which deals with in-plane buckling in columns under fire exposure conditions when longitudinal expansion is partially prevented.

For a column which is free to expand on being heated, the buckling stress

$$\sigma_k = \frac{N_k}{A} \quad (\text{kgf/cm}^2) \text{ (MPa)} \quad (10.1 \text{ a})$$

can be calculated from the following expression (26), (27), (32)

$$\sigma_k^2 - \sigma_k \left[ \sigma_{0.2} + \pi^2 E \left( 4.8 \cdot 10^{-5} + \frac{1}{\lambda^2} \right) \right] = -\sigma_{0.2} \frac{\pi^2 E}{\lambda^2} \quad (10.1 \text{ b})$$

where  $N_k$  = buckling load of the column (kgf) {MN}  
 $A$  = area of cross section of the column (cm<sup>2</sup>) { m<sup>2</sup>}  
 $\sigma_{0.2}$  = yield stress or 0.2% proof stress at the actual steel temperature (kgf/cm<sup>2</sup>) {MPa}  
 $E$  = modulus of elasticity at the actual steel temperature (kgf/cm<sup>2</sup>) {MPa}

The fictive slenderness ratio  $\lambda$  of the column in Equation (10.1 b) is defined by the expression

$$\lambda = \frac{\beta L}{i} \quad (10.1 c)$$

where  $L$  = length of column (cm) {m}  
 $\beta$  = nondimensional coefficient which is a function of the end fixity conditions of the column, the variation of cross section and the variation of the axial compressive force along the column, and which can in a large number of cases be obtained directly from manuals (57)  
 $i$  = the radius of gyration of the cross section with respect to the neutral axis through the centroid (cm) {m}

In Equation (10.1 b) the sum of initial curvature and unintentional eccentricity of the load is described by a pure initial curvature which has the same mathematical form as the ideal buckling deflection and has a maximum value  $f$  of (58)

$$f = 4.8 \cdot 10^{-5} \cdot \frac{(\beta L)^2}{d} \quad (10.1 d)$$

where  $d$  = distance from the neutral axis to the extreme fibre of the cross section in compression at the section which governs design (m)

With the actual stress-strain curves of the steel material in question at different steel temperatures approximated by the associated elasto-plastic stress-strain curves, as defined by the modulus of elasticity and the 0.2% proof stress  $\sigma_{0.2}$  at the temperatures concerned, the buckling stress  $\sigma_k$  during fire exposure conditions can be calculated from Equation (10.1 b). Owing to the softly rounded shape of the stress-strain curve at elevated temperatures, however (see Section 9.1), functionally better substantiated values of the buckling stress will be obtained if the initial modulus of elasticity  $E$  in Equation (10.1 b) is replaced by the secant modulus, and the 0.2% proof stress  $\sigma_{0.2}$  by the 0.5% proof stress  $\sigma_{0.5}$ . This latter stress is more significant as critical stress at elevated temperatures than  $\sigma_{0.2}$  (47), (48). Examples of design diagrams calculated in this way are given in Fig. 10.1 a (27), (59), (60). The diagrams give  $\sigma_k - \lambda$  curves for different steel temperatures  $\vartheta_s$  for steel columns of material grades with yield stresses of  $\sigma_s = 2200$  {220}, 2600 {260} and 3200 kgf/cm<sup>2</sup> {320 MPa} at ordinary room temperatures.

With the action of fire defined according to Chapter 4, the maximum steel temperature  $\vartheta_{\max}$  for uninsulated columns can be determined from Table 5 c and for insulated columns from Table 6 a or 6 b in the Design Section. The minimum loadbearing capacity  $N_k$  of the column, with regard to in-plane buckling due to a complete undisturbed fire process, can then be obtained from the diagrams in Fig. 10.1 a. The requirement with regard to the loadbearing function of the steel column is satisfied if this minimum loadbearing capacity is not less than the value of the axial force pertaining to the load factor and safety factor specifications set out in Subsection 2.4.1.

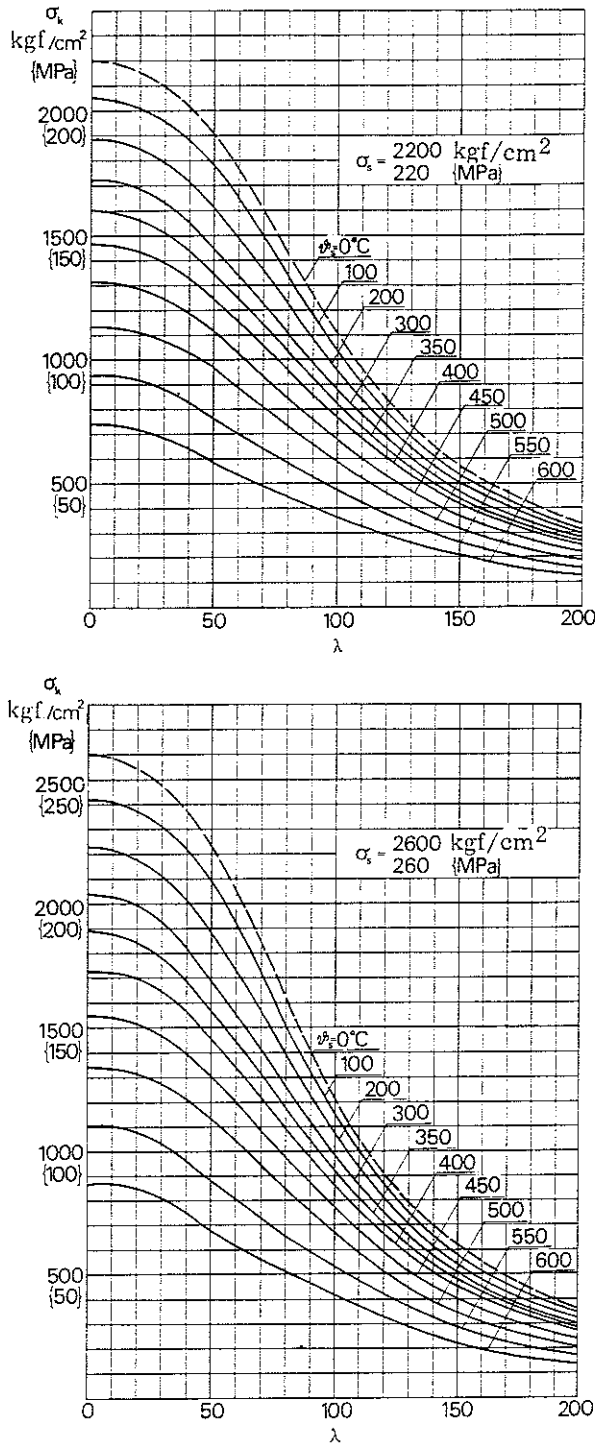
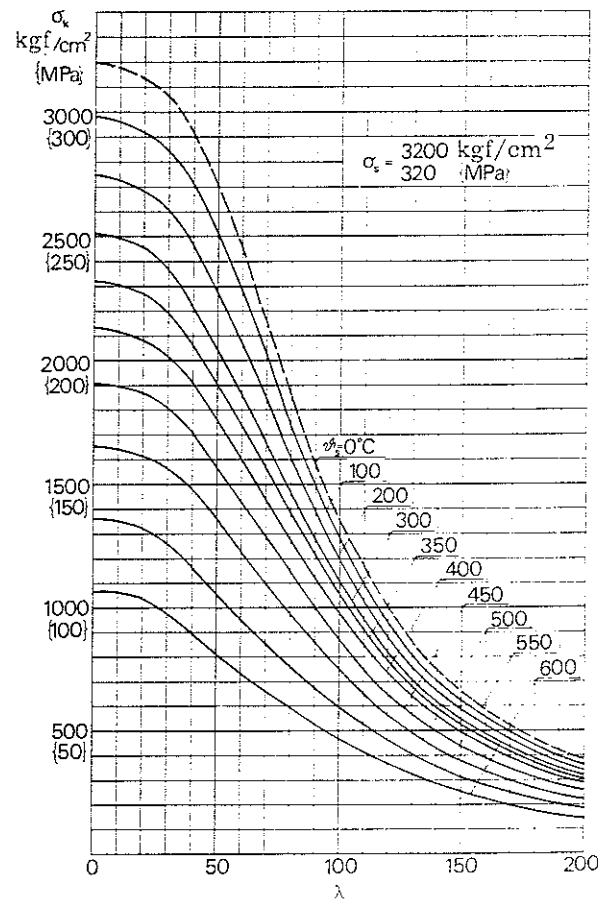


Fig. 10.1 a. Calculated relationships between the buckling stress  $\sigma_k$  and slenderness ratio  $\lambda$  for steel columns made of materials with yield stresses at room temperature of  $\sigma_s = 2200 \{220\}$ ,  $2600 \{260\}$  and  $3200 \text{ kgf/cm}^2 \{320 \text{ MPa}\}$  at different temperatures  $\theta_s$ . The diagram apply to columns which are free to expand longitudinally



The  $\sigma_k - \lambda$  curves given in Fig. 10.1 a have a somewhat different background in principle than the design diagrams and tables given in Steel Construction Code 70 for buckling at ordinary temperatures. This deviation does not give rise to any differences of decisive practical significance in buckling stress, either at room temperatures or elevated temperatures. For buckling at ordinary temperatures, the design data in Steel Construction Code 70 are recommended to be used, and for this reason the  $\sigma_k - \lambda$  curves for  $\sigma_s = 0^\circ\text{C}$  in Fig. 10.1 a have been marked by a dashed line.

The calculated  $\sigma_k - \lambda$  curves in Fig. 10.1 a are based on the temperature dependence of the 0.5% proof stress  $\sigma_{0.5}$  and on the temperature and stress dependence of the secant modulus  $E$  as set out in Fig. 10.1 b. These material quantities

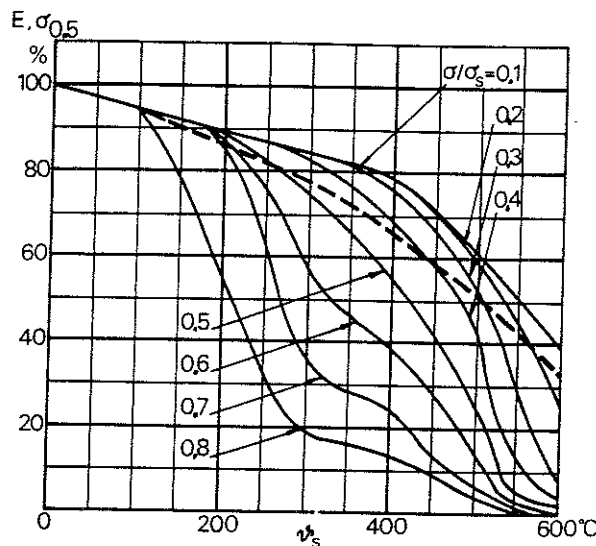


Fig. 10.1 b. The modulus of elasticity (secant modulus)  $E$  as a function of the steel temperature  $\theta_s$  for different values of the ratio of the stress  $\sigma$  to the yield stress at room temperature  $\sigma_s$ . The dashed curve indicates the variation with temperature of the 0.5% proof stress

have been determined on tensile test specimens which were loaded to failure at the appropriate temperature level at a constant rate of loading of  $18 \text{ kgf/cm}^2/\text{min}$  [ $1.8 \text{ MPa/min}$ ], i.e. at such a slow rate of load increase that a considerable effect due to short-term creep at high temperatures has been included.

By comparing the results of full-scale fire engineering tests, it has been found that the diagrams presented in Fig. 10.1 a constitute a satisfactory basis, in the normal case, for practical fire engineering design (60). If a more accurate set of design data is to be produced, the deflection curve of the steel column due to the action of fire must be calculated on the basis of the actual temperature dependent stress-strain curves, account being taken of short-term creep at high temperatures. Such a refined treatment will yield  $\sigma_k - \lambda$  curves which, apart from the maximum steel temperature, will also be dependent on the rates of heating and cooling. Work on the production of such more accurate design data is in progress.

## 10.2 Determination of the buckling load under in-plane instability conditions when longitudinal expansion is partially prevented

If there is no restraint on longitudinal expansion, the expansion of an unloaded steel column under fire exposure conditions is given by the expression

$$\Delta L_1 = \alpha \theta_s L \quad (\text{cm}) \{ \text{m} \} \quad (10.2 \text{ a})$$

where  $\alpha$  = coefficient of linear expansion ( $^{\circ}\text{C}^{-1}$ )  
 $\theta_s$  = steel temperature ( $^{\circ}\text{C}$ )  
 $L$  = original length of the column (cm) {m}

If the column is at the same time subjected to an axial compressive force  $N$ , the expansion is reduced owing to the drop in the value of the modulus of elasticity of the steel as the steel temperature  $\theta_s$  rises. This reduction of the expansion is

$$\Delta L_2 = \frac{NL}{A} \left( \frac{1}{E} - \frac{1}{E_0} \right) \quad (\text{cm}) \{ \text{m} \} \quad (10.2 \text{ b})$$

where  $E$  = modulus of elasticity (secant modulus) of the steel at the stress and steel temperature in question according to Fig. 10.1 b (kgf/cm<sup>2</sup>) {MPa}.

$E_0$  = modulus of elasticity of the steel at ordinary room temperatures (kgf/cm<sup>2</sup>) {MPa}.

$A$  = area of cross section of the column (cm<sup>2</sup>) {m<sup>2</sup>}.

$N$  = magnitude of the compressive force (kgf) {MN}.

The resultant expansion  $\Delta L$  of the column when this is completely free to expand is therefore

$$\Delta L = \Delta L_1 - \Delta L_2 = \alpha \vartheta_s L - \frac{NL}{A} \left( \frac{1}{E} - \frac{1}{E_0} \right) \quad (\text{cm}) \{ \text{m} \} \quad (10.2 \text{ c})$$

If adjacent structural elements partially prevent longitudinal expansion of the column under fire exposure conditions, the expansion is reduced. This reduced expansion  $\Delta L_r$  can be written

$$\Delta L_r = \gamma \Delta L \quad (\text{cm}) \{ \text{m} \} \quad (10.2 \text{ d})$$

where  $\gamma$  = degree of expansion, a nondimensional coefficient which has a value between 0 and 1

The value  $\gamma = 0$  is equivalent to the case where expansion is completely prevented, and  $\gamma = 1$  to the case where there is no restraint on expansion. In Subsection 10.2.1 an account is given of the way in which the degree of expansion  $\gamma$  of a column due to the action of fire can be determined in practical cases. Further, in Chapter 10 in the Design Section there is a diagram which makes possible easy calculation of the value of  $\gamma$  for some cases which are of common practical occurrence.

When longitudinal expansion is partially prevented, exposure to fire causes the axial compressive force in the column to increase. In turn, this causes the column to buckle at a lower initially imposed external load than in the case where expansion is not restrained.

With the same assumptions in principle as those made in the treatment presented in Section 10.1, calculation of the buckling stress in a steel column exposed to fire whose longitudinal expansion is partially prevented gives design diagrams of the same type as those shown in Fig. 10.1 a. Apart from the degree of expansion  $\gamma$ , there is the further parameter of the cross sectional factor  $i/d$ . The effect of this latter parameter is however relatively limited.

Apart from design diagrams for columns which are free to expand longitudinally ( $\gamma = 1$ ), Chapter 10 in the Design Section also presents design diagrams which permit approximate determination of the buckling stress  $\sigma_k$  for in-plane buckling of a steel column under fire exposure conditions in which longitudinal expansion is partially restrained. These diagrams give  $\sigma_k - \lambda$  curves for different steel temperatures  $\vartheta_s$  and degrees of expansion  $\gamma$  for steel columns of materials with a yield stress  $\sigma_s = 2200$  {220; 2600 {260; and 3200 kgf/cm<sup>2</sup> {320 MPa} at ordinary room temperatures. The curves have been calculated for  $i/d = 0.5$ , which yields design values on the safe side for steel sections of the usual shapes.

As regards the accuracy of data, the comments relating to the design diagrams for the case when longitudinal expansion is partially prevented are essentially the same as those made in Section 10.1 with regard to the analogous diagrams for columns which are completely free to expand longitudinally ( $\gamma = 1$ ).

### 10.2.1 Determination of the degree of expansion $\gamma$

More accurate determination of the degree of expansion  $\gamma$  which, according to Equation (10.2 d), describes the degree of expansion in a steel column under fire exposure conditions when the longitudinal expansion is subject to restraint, is a comparatively complicated process. A worked example of such more accurate determination is given in (59) and (60). The presentation here will be confined to an approximate procedure which makes for ease of calculation and consistently yields values somewhat on the safe side. The procedure is illustrated by means of the case shown in Fig. 10.2.1 a in which a steel column CD which is exposed to fire is hinged at its top end into a simply supported girder AB. The column and girder may either have the same or different temperatures.

At ordinary room temperatures, the axial compressive force in the column is  $N$ . Under fire exposure conditions, there is an increase of  $\Delta N$  in the compressive force due to the connection between the column and the girder AB. This is accompanied by an upwards bending deformation  $y_1$  in the girder AB at the junction point. Assuming elastic conditions, using the symbols in the figure,

$$y_1 = \frac{\Delta N a^2 b^2}{3E_b I_b L_b} \quad (\text{cm}) \{ \text{m} \} \quad (10.2.1 \text{ a})$$

where  $\Delta N$  = additional force in column (kgf) {MN};

$E_b$  = modulus of elasticity of the girder at the temperature concerned according to Fig. 9.1 a (kgf/cm<sup>2</sup>) {MPa};

$I_b$  = moment of inertia of the girder with respect to vertical deflection (cm<sup>4</sup>) {m<sup>4</sup>}.

The deformation condition which must be satisfied is that vertical displacement  $y_1$  of the girder shall be equal to the partially restrained longitudinal expansion  $\Delta L_r = \gamma L$  of the column, i.e.

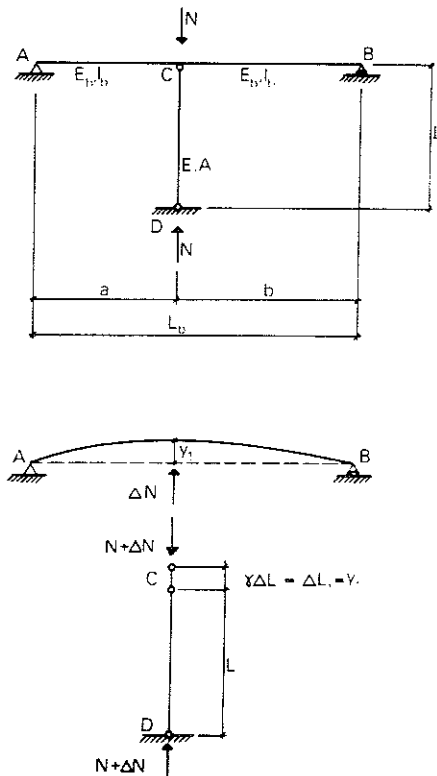


Fig. 10.2.1 a. Fire exposed structure made up of a column CD hinged at its top end into a simply supported girder AB

$$\frac{\Delta N a^2 b^2}{3 E_b I_b L_b} = \gamma \Delta L \quad (10.2.1 \text{ b})$$

This partially restrained longitudinal expansion  $\Delta L_r$  is determined by

- the free thermal longitudinal expansion  $\alpha \vartheta_s L$  of the column
- contraction of the column due to the axial force  $N$ , as a result of the decrease in the modulus of elasticity (secant modulus) consequent upon the increase in temperature (see Equation 10.2 b)
- elastic contraction of the column due to the additional axial force  $\Delta N$
- reduction of the distance between the ends of the column due to increased deflection

As an approximation somewhat on the safe side, the last of the above deformation components can be ignored, and  $\Delta L_r = \gamma \Delta L$  can therefore be written

$$\gamma \Delta L = \alpha \vartheta_s L - \frac{NL}{A} \left( \frac{1}{E} - \frac{1}{E_0} \right) - \frac{\Delta NL}{EA} = \Delta L - \frac{\Delta NL}{EA} \quad (10.2.1 \text{ c})$$

If  $\Delta N$  is found from the first and last terms of this equation and this expression for  $\Delta N$  is substituted into Equation (10.2.1 b), we have

$$\gamma = \frac{1}{1 + \frac{3 E_b I_b L_b L}{E A a^2 b^2}} \quad (10.2.1 \text{ d})$$

Alternatively, Equation (10.2.1 d) can be written in the form

$$\gamma = \frac{1}{1 + \frac{L}{E A y_{1\Delta N=1}}} \quad (10.2.1 \text{ e})$$

$$\text{where } y_{1\Delta N=1} = \frac{a^2 b^2}{3 E_b I_b L_b} \quad (\text{cm}) \{ \text{m} \} \quad (10.2.1 \text{ f})$$

denotes upwards deflection in the girder at the point where the column is connected for the unit load  $\Delta N = 1$ .

In calculating  $\gamma$  using Equation (10.2.1 d) or (10.2.1 e), the secant modulus of the column according to Fig. 10.1 b shall be used. This modulus is dependent on the temperature of the column and its actual stress as made up of an initial stress and an additional stress due to the longitudinal expansion of the column being partially restrained. The latter stress component is unknown. As an approximation on the safe side, however, it is possible to use the value of the secant modulus  $E$  which corresponds to a stress equal to the buckling stress of the column at the temperature concerned, its actual slenderness ratio and unrestrained longitudinal expansion, i.e. at a value  $\gamma = 1$ . The approximation this entails in the calculation of the value of  $\gamma$  will be the greater, the less highly stressed the column. If the stress in the column is low, there may therefore be reason to determine the actual stress by means of an iteration procedure (59), (60).

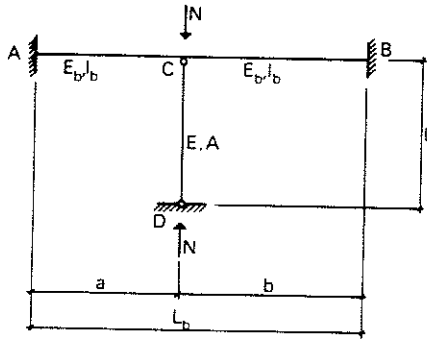


Fig. 10.2.1 b. Fire exposed structure made up of a column CD hinged at its top end into a girder AB which is rigidly fixed at both ends

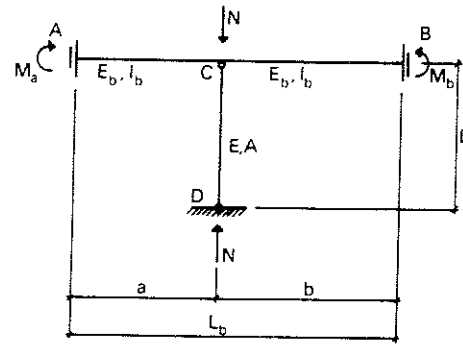


Fig. 10.2.1 c. Fire exposed structure made up of a column CD hinged at its top end into a girder AB which is elastically fixed at its end

For the case where the girder AB, as shown in Fig. 10.2.1 b, is rigidly fixed at both ends, an analogous treatment will show that  $\gamma$  can be determined from Equation (10.2.1 e) by putting

$$y_{1\Delta N=1} = \frac{a^2 b^3}{3E_b I_b L_b^3} \quad (\text{cm}) \{ \text{m} \} \quad (10.2.1 \text{ g})$$

For the more general case where the girder AB is elastically fixed at its ends as shown in Fig. 10.2.1 c, Equation (10.2.1 e) still holds, but the deflection  $y_{1\Delta N=1}$  due to unit load must be determined from the expression

$$y_{1\Delta N=1} = \frac{1}{3E_b I_b L_b} \left\{ a^2 b^2 - \frac{L_b^2 \left[ a^2 \left( 1 - \frac{a^2}{L_b^2} \right)^2 (1 + 3k_a) + b^2 \left( 1 - \frac{b^2}{L_b^2} \right)^2 (1 + 3k_b) - ab \left( 1 - \frac{a^2}{L_b^2} \right) \left( 1 - \frac{b^2}{L_b^2} \right) \right]}{4(1 + 3k_a)(1 + 3k_b) - 1} \right\} \quad (\text{cm}) \{ \text{m} \} \quad (10.2.1 \text{ h})$$

It has been assumed in this context that elastic fixity of the ends A and B of the girder in adjacent structures can be described by the expressions

$$\left. \begin{aligned} \theta_a &= k_a \frac{L_b}{E_b I_b} M_a \\ \theta_b &= k_b \frac{L_b}{E_b I_b} M_b \end{aligned} \right\} \quad (10.2.1 \text{ i})$$

where

- $\theta_a$  and  $\theta_b$  = rotations at the ends A and B
- $M_a$  and  $M_b$  = fixing moments at ends A and B (kgf cm) {MNm}
- $k_a$  and  $k_b$  = nondimensional coefficients which describe the degree of elastic fixity. For the special case when the girder is simply supported,  $k = \infty$ , and for the special case when the girder is rigidly fixed,  $k = 0$ .



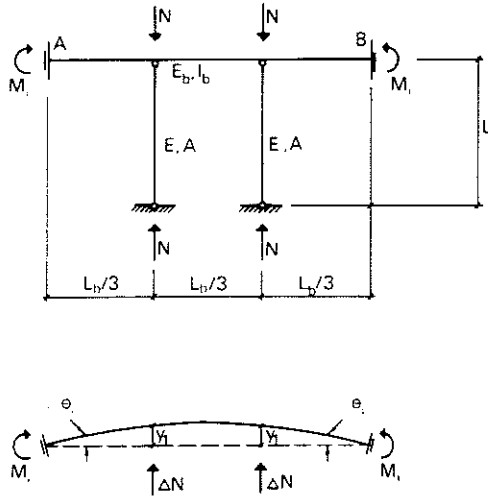


Fig. 10.2.1 d. Fire exposed structure made up of two symmetrically placed columns hinged at their top ends into a girder AB which is elastically fixed at its ends

A procedure according to Equation (10.2.1 e) can also be used for the case shown in Fig. 10.2.1 d where a symmetrical structure is made up of two columns hinged at their top ends into a girder AB elastically fixed at both its ends. Using the symbols in the Figure, the following expression holds for the deflection  $y_1$  due to the two symmetrically acting unit loads  $\Delta N = 1$

$$y_{1\Delta N=1} = \frac{5L_b^3}{162E_b I_b} \left[ 1 - \frac{4}{5(1+2k_i)} \right] \quad (\text{cm}) \{ \text{m} \} \quad (10.2.1 j)$$

The nondimensional elastic fixity coefficient  $k_i$  is determined from the condition, analogous to that in Equation (10.2.1 i), that

$$\theta_i = k_i \frac{L_b}{E_b I_b} M_i \quad (10.2.1 k)$$

For the case where the girder is simply supported,  $k_i = \infty$ , and

$$y_{1\Delta N=1} = \frac{5L_b^3}{162E_b I_b} \quad (\text{cm}) \{ \text{m} \} \quad (10.2.1 l)$$

For the case where the girder is rigidly fixed,  $k_i = 0$ , and

$$y_{1\Delta N=1} = \frac{L_b^3}{162E_b I_b} \quad (\text{cm}) \{ \text{m} \} \quad (10.2.1 m)$$

Finally, in order to complete the treatment, a description will be given of the approximate procedure for the determination of the coefficient  $\gamma$  in a somewhat more complicated case. The structure considered is that in Fig. 10.2.1 e where three columns are hinged at their top ends into a girder elastically fixed at both its ends A and B. The three columns have different initial axial compressive forces  $N_1$ ,  $N_2$  and  $N_3$ , different cross sectional areas  $A_1$ ,  $A_2$  and  $A_3$ , and different moduli of elasticity (secant moduli)  $E_1$ ,  $E_2$  and  $E_3$  due, for instance, to differences

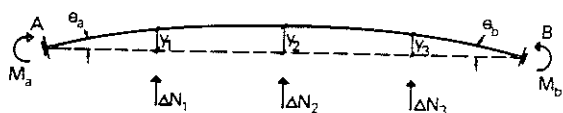
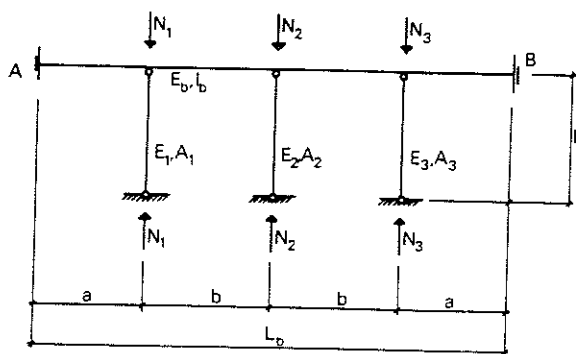


Fig. 10.2.1 e. Fire exposed structure made up of three columns hinged at their top ends into a girder AB which is elastically fixed at its ends, the fixity characteristics being given by Equation (10.2.1 f)

in column temperatures. On being exposed to fire, the three columns expand through the distances  $y_1$ ,  $y_2$  and  $y_3$  respectively. These expansions are related to the corresponding free longitudinal expansions  $\Delta L_1$ ,  $\Delta L_2$  and  $\Delta L_3$  in columns in which there is no restraint on longitudinal expansion by the expressions

$$\left. \begin{aligned} y_1 &= \gamma_1 \Delta L_1 \\ y_2 &= \gamma_2 \Delta L_2 \\ y_3 &= \gamma_3 \Delta L_3 \end{aligned} \right\} \quad (\text{cm}) \quad \{ \text{m} \} \quad (10.2.1 \text{ n})$$

The partial restraint on longitudinal expansion of the columns owing to their being connected to the girder AB gives rise in them to the additional axial forces  $\Delta N_1$ ,  $\Delta N_2$  and  $\Delta N_3$  respectively. The resulting displacements  $y_1$ ,  $y_2$  and  $y_3$  can then be written as

$$\left. \begin{aligned} y_1 &= \gamma_1 \Delta L_1 = \Delta L_1 - \frac{\Delta N_1 L}{E_1 A_1} \\ y_2 &= \gamma_2 \Delta L_2 = \Delta L_2 - \frac{\Delta N_2 L}{E_2 A_2} \\ y_3 &= \gamma_3 \Delta L_3 = \Delta L_3 - \frac{\Delta N_3 L}{E_3 A_3} \end{aligned} \right\} \quad (\text{cm}) \quad \{ \text{m} \} \quad (10.2.1 \text{ o})$$

The imposed forces  $\Delta N_1$ ,  $\Delta N_2$  and  $\Delta N_3$  give rise to the following vertical displacements at the points in the girder AB where the columns are attached

$$\left. \begin{aligned} y_1 &= \Delta N_1 y_{1\Delta N_1-1} + \Delta N_2 y_{1\Delta N_2-1} + \Delta N_3 y_{1\Delta N_3-1} \\ y_2 &= \Delta N_1 y_{2\Delta N_1-1} + \Delta N_2 y_{2\Delta N_2-1} + \Delta N_3 y_{2\Delta N_3-1} \\ y_3 &= \Delta N_1 y_{3\Delta N_1-1} + \Delta N_2 y_{3\Delta N_2-1} + \Delta N_3 y_{3\Delta N_3-1} \end{aligned} \right\} \quad (\text{cm}) \quad \{ \text{m} \} \quad (10.2.1 \text{ p})$$

where  $y_1 \Delta N_1 = 1$  = displacement at section  $y_1$  due to the unit load  $\Delta N_1 = 1$

$y_1 \Delta N_2 = 1$  = displacement at section  $y_1$  due to the unit load  $\Delta N_2 = 1$ , and so on

The elementary displacements  $y_1 \Delta N_1 = 1$ , etc, can, for ordinary practical applications, be calculated from data given in handbooks.

If the associated displacements  $y_1$ ,  $y_2$  and  $y_3$  according to Equations (10.2.1 o) and (10.2.1 p) are put equal, a system of equations is obtained from which  $\Delta L_1$ ,  $\Delta L_2$  and  $\Delta L_3$ ,  $\Delta N_1$ ,  $\Delta N_2$  and  $\Delta N_3$  can be eliminated and the nondimensional coefficients  $\gamma_1$ ,  $\gamma_2$  and  $\gamma_3$  obtained.

For a single column connected to a simply supported or rigidly restrained beam, the coefficient  $\gamma$  can be easily determined with the assistance of Fig. 10 a in the Design Section.

### 10.3 Determination of the critical load in a structure subject to simultaneous flexure and axial compressive force

Hardly any studies have been performed so far concerning the problem of carrying out a fire engineering design for a slender beam or column which is subject to axial force and transverse load at the same time. It appears most appropriate at this initial stage to make treatment of this problem as simple and approximate as possible. A procedure based on modified interaction formulae of the type used in Steel Construction Code 70 is therefore the obvious choice as a temporary solution (54).

In such an approximate procedure, the minimum loadbearing capacity of a structure under fire exposure conditions, which is subject to simultaneous flexure and axial compression, is determined as a function of the ratios

$$K = \frac{N}{N_k} \quad (10.3 a)$$

$$B = \frac{Q}{Q_{cr}} \quad (10.3 b)$$

where  $N$  = the axial compressive force in the event of fire (see the load and safety regulations set out in Subsection 2.4.1)

$N_k$  = buckling load of the structure under in-plane instability conditions, determined according to Section 10.1 when the structure is free to expand, and according to Section 10.2 when expansion is partially restrained at the maximum temperature  $\hat{\vartheta}_{\max}$  of the steel structure

$Q$  = transverse load in the event of fire (see the load and safety regulations set out in Subsection 2.4.1)

$Q_{cr}$  = critical load of the structure when acted upon by the transverse load alone, determined according to Section 9.2 for the maximum temperature  $\hat{\vartheta}_{\max}$  of the steel structure.

The ratios  $K$  and  $B$  give an idea of the stress levels in the structure under fire ex-

posure conditions with regard to buckling only and moment capacity, respectively.

By reference to Steel Construction Code 70, certain approximate conditions can be laid down to ensure that the loadbearing function is satisfied in the structure under fire exposure conditions. The expression which holds for a box section irrespective of the direction of deflection, and for other sections of normal shape when deflection occurs in the direction of maximum stiffness, is

$$K+B \leq 1 \quad (10.3 \text{ c})$$

When deflection occurs in the direction of minimum stiffness in sections of normal shape, with the exception of box sections, the value of  $\alpha$  must first be calculated. This is given by the expression

$$\alpha = \sqrt{\frac{\sigma_{0.2}}{\sigma_{el}}} \quad (10.3 \text{ d})$$

where  $\sigma_{0.2}$  = yield stress or 0.2% proof stress at maximum steel temperature  $\vartheta_{\max}$  (see Fig. 9.1 a) (kgf/cm<sup>2</sup>) {MPa}  
 $\sigma_{el}$  = ideal buckling stress calculated according to the elastic theory (the Euler critical stress) for the modulus of elasticity  $E$  at the maximum steel temperature  $\vartheta_{\max}$  (see Fig. 9.1 a) (kgf/cm<sup>2</sup>) {MPa}

For a large number of loading and support conditions, the ideal buckling stress  $\sigma_{el}$  can be directly determined from handbooks, e.g. (57).

If  $\alpha$  is in the range  $0.8 < \alpha < 1.6$ , we have that

$$\begin{aligned} 1.1K+B &\leq 1 \quad \text{f\"or } K \leq 3B \\ K+1.3B &\leq 1 \quad \text{f\"or } K > 3B \end{aligned} \quad (10.3 \text{ e})$$

For other values of  $\alpha$ , Equation (10.3 c) holds even when deflection is in the direction of minimum stiffness.

#### 10.4 Determination of the buckling load under out-of-plane instability conditions

No studies have been made so far of the problem involved in designing a column subject to an axial compressive force with regard to out-of-plane instability under fire exposure conditions. In view of this, a simple approximate treatment is recommended which, by means of a fictive comparative slenderness ratio  $\lambda_{fj}$ , converts the out-of-plane instability problem into an in-plane instability problem.

In such an approximate treatment, the expression for the fictive comparative slenderness ratio  $\lambda_{fj}$  is (56)

$$\lambda_{fj} = \pi \sqrt{\frac{E}{\sigma_{klR}}} \quad (10.4 \text{ a})$$

where  $E$  = modulus of elasticity at the maximum steel temperature  $\vartheta_{\max}$  according to Fig. 9.1 a (kgf/cm<sup>2</sup>){MPa}  
 $\sigma_{kiR}$  = the greatest compressive stress in the column cross section due to the ideal out-of-plane buckling load  $N_{kiR}$  at the maximum steel temperature  $\vartheta_{\max}$ , calculated for an initially straight structure according to the elastic theory (kgf/cm<sup>2</sup>){MPa}

For commonly occurring loading and support conditions, the ideal out-of-plane buckling load  $N_{kiR}$  can be directly determined from handbooks, e.g. (56) and (61). In this context, the value of  $E$  is taken from Fig. 9.1 a, and the shear modulus  $G$  is determined approximately from the expression

$$G = \frac{1}{2}E \quad (10.4 \text{ b})$$

With the value of  $\lambda_{fj}$  calculated from Equation (10.4 a), the greatest compressive stress  $\sigma_{kR} = \sigma_k$  in the column cross section under fire exposure conditions, corresponding to the actual out-of-plane buckling load  $N_{kR}$ , is obtained from diagrams applicable to in-plane buckling given in Chapter 10 in the Design Section.

In practice, a check with regard to in-plane instability is relevant to be carried out when a column subject to an axial compressive force is braced by adjacent structural elements against deflection at right angles to the plane of bending. When buckling deformation can freely occur out of the plane of bending, pure in-plane buckling will only occur if the line of action of the axial compressive force coincides with the shear centre of the cross section. In all other cases, a slender column acted upon by an axial compressive force must be checked for out-of-plane instability.

## 11 PROTECTION OF STRUCTURAL STEELWORK

### 11.1 Materials and methods

In recent years, there has been intensive development of materials and methods for the protection of structural steelwork under fire exposure conditions (62). New materials and methods are being developed and old ones are being modified or improved. A description of the various materials and methods used for structural fire insulation purposes will therefore remain up-to-date for a considerably shorter time than the information given in the other Chapters of this handbook. In spite of this, it has been considered essential to give a detailed account of the present situation in Sweden.

Protection in the form of insulation is applied to structural steelwork in order to limit the rate of heating and the rise in temperature, and consequently the reduction in the strength of the construction, in the event of fire. The materials used for structural fire insulation should have good thermal insulation capacity and a good resistance to fire. Earlier, it was common to provide fire protection for steel structures by encasing the steel member in brickwork, or by casting concrete round it. Nowadays, these methods are regarded as quite antiquated and uneconomic. They also detracted from the advantages of using steel in construction, such as its low weight, small dimensions and rapidity of erection. Encasement in brickwork or concrete is applied at present only in very special cases, the endeavour being to employ lighter and more easily applied insulation materials.

One of the factors which govern the extent of fire protection is the form of construction. Parts of the steelwork can often be provided with fire protection more or less automatically. For instance, floor girders can often be incorporated in, and partially insulated by, the floor slab. See Fig. 11.1 a.

With regard to the method of application, a distinction can be made between wet and dry methods of insulation. The wet methods comprise fire insulation using

- sprayed mineral wool
- sprayed asbestos
- fire retardant plasters
- fire retardant paints

The dry methods comprise fire insulation in the form of slabs and prefabricated sections such as

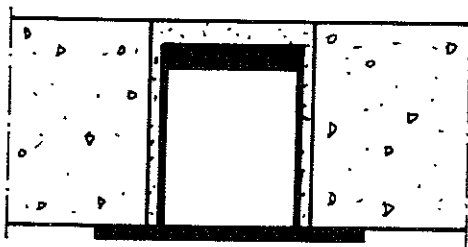


Fig. 11.1 a. Floor girder partially built into, and insulated by, the floor slab

- mineral wool slabs
- vermiculite slabs
- gypsum plaster slabs
- prefabricated gypsum plaster sections

The fire insulation is usually applied directly onto the construction or part thereof which is to be protected. Another, more indirect, form of structural fire insulation is constituted by fire resistant suspended ceilings and fire division partitions which can be used to isolate adjacent constructions wholly or partially.

#### 11.1.1 Sprayed mineral wool

Sprayed mineral wool consists of mineral wool fibres mixed with cement or gypsum plaster as the binder. The composition is sprayed in an atomized form, together with water, to the desired thickness directly onto the steel surface which is to be provided with fire insulation. The thickness of the finished insulation is normally between 10 and 30 mm, depending on the insulation capacity to be achieved. The composition must be sprayed at temperatures above freezing. Prior to application, grease and loose mill scale should be removed from the surface, but a light covering of rust does not prevent satisfactory adhesion. The surface of the insulation can be spray painted.

The insulation can also be sprayed onto metal lathing. This is done if the external shape of the section is to be altered, for instance if a column of I section is to have the shape of a closed rectangle after application of the insulation. A metal lathing is then attached to the flanges, for instance by spot welding, after which the composition is sprayed onto the lathing.

Depending on the make, the density  $\gamma_i$  of sprayed mineral wool varies between 250 and 370 kg/m<sup>3</sup>. The insulation is relatively soft, and this must be borne in mind if it is used on constructions which are subject to direct mechanical damage. The mechanical strength can be increased by gluing a glass fibre fabric onto the surface. When requirements concerning mechanical strength are very stringent, the surface can be given a coat of hard plaster. Mechanical protection can also be achieved by encasement with a suitable slab material. The thermal conductivity  $\lambda_i$  and enthalpy  $I$  of sprayed mineral wool, as a function of the insulation temperature  $\vartheta_i$ , are given in Figs. 11.1.1 b, c and d.



Fig. 11.1.1 a. Fire insulation of steel girder by sprayed mineral wool

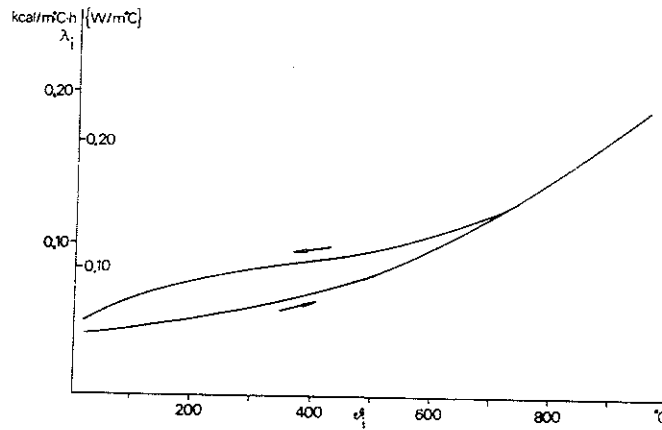


Fig. 11.1.1 b. Thermal conductivity  $\lambda_i$  as a function of the insulation temperature  $\theta_i$  for sprayed mineral wool Type Cafco Blaze-Shield DC/F of density  $\gamma_1 = 300\text{--}370 \text{ kg/m}^3$ . (According to the National Swedish Institute for Testing and Metrology)

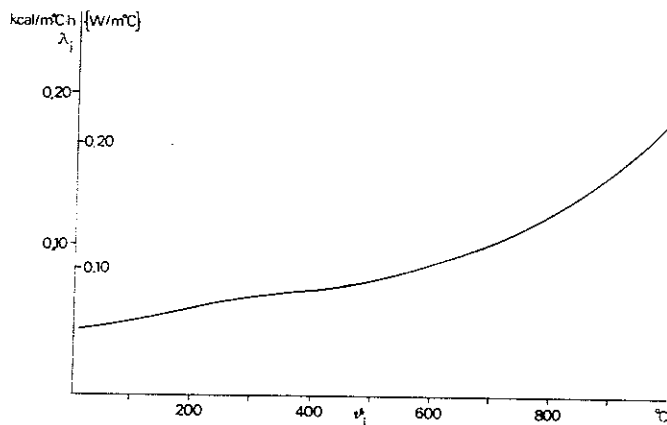


Fig. 11.1.1 c. Thermal conductivity  $\lambda_i$  as a function of the insulation temperature  $\theta_i$  for sprayed mineral wool Type Pyroguard 101 of density  $\gamma_1 = 250 \text{ kg/m}^3$ . (According to the National Swedish Institute for Testing and Metrology)

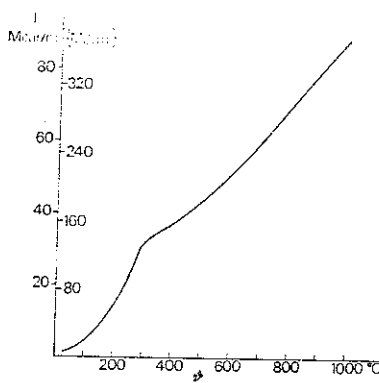


Fig. 11.1.1 d. Enthalpy  $I$  as a function of the insulation temperature  $\theta_i$  for sprayed mineral wool Type Pyroguard 101 of density  $\gamma_1 = 250 \text{ kg/m}^3$ . (According to the National Swedish Institute for Testing and Metrology)

### 11.1.2 Sprayed asbestos

Sprayed asbestos consists of asbestos fibres mixed with cement. In the same way as sprayed mineral wool, the composition is sprayed in an atomized form, together with water, directly onto the steel surface which is to be provided with fire insulation. Sprayed asbestos was a forerunner to sprayed mineral wool, and the two materials have very similar thermal and mechanical properties. Sprayed asbestos was used very extensively before, but has been mainly superseded by sprayed mineral wool. The reason for this is that the health hazards in conjunction with the use of sprayed asbestos have been realized lately. These hazards and the occupational safety requirements imposed when asbestos is being sprayed, as well as the availability of substitute materials such as sprayed mineral wool, lead to a prohibition of the use of sprayed asbestos in Sweden.



### 11.1.3 Fire retardant plasters

The term fire retardant plaster is a generic name for insulation materials for steelwork in the form of plaster in which the aggregate consists of vermiculite or perlite. Cement, lime or gypsum are usually employed as binders. Vermiculite is an expanded mica, and perlite an expanded volcanic material. These plasters are sprayed or applied by hand onto the steel construction. The thickness normally varies between 10 and 40 mm, depending on the type of plaster and the required insulation capacity. For certain plasters, the maximum recommended coat thickness is 10–15 mm. Before a coat is applied, the previous one must be completely dry. Application must take place at temperatures above freezing. Some plasters can be applied directly to the steel surface, while others require metal lathing as the base in order that adhesion should be satisfactory. The finished surface can be painted or floated. The surface of some plasters is relatively uneven, and it is recommended that these are given a coat of filler before being painted.

The density  $\gamma_i$  normally varies between 300 and 800 kg/m<sup>3</sup> depending on the type of plaster. Plasters of densities at the lower end of the range are relatively soft, and this must be borne in mind when they are used in constructions where there is a risk of mechanical damage. It is possible to achieve some increase in mechanical strength by covering the surface with fabric. Some kind of corner protection is also recommended at times. When the requirements concerning mechanical strength are very stringent, the surface can be given a coat of hard plaster. Plasters of densities at the higher end of the range have surfaces which are themselves often relatively hard.

The thermal conductivity  $\lambda_i$  for two types of fire retardant plaster, as a function of the insulation temperature  $\vartheta_i$ , is given in Figs. 11.1.3 a and b.

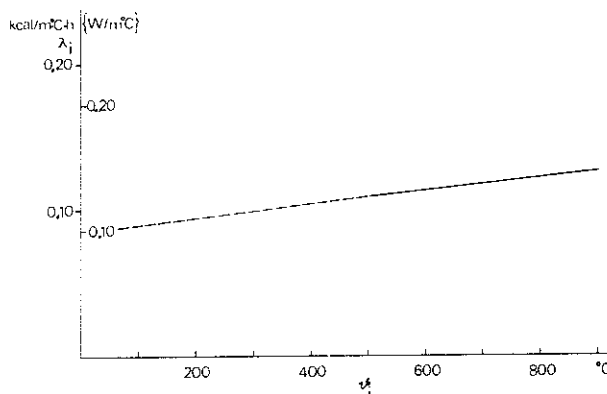


Fig. 11.1.3 a. Thermal conductivity  $\lambda_i$  as a function of the insulation temperature  $\vartheta_i$  for fire retardant plaster Type Pyrodur of density  $\gamma_i = 300 \text{ kg/m}^3$ . (According to the National Swedish Institute for Testing and Metrology)

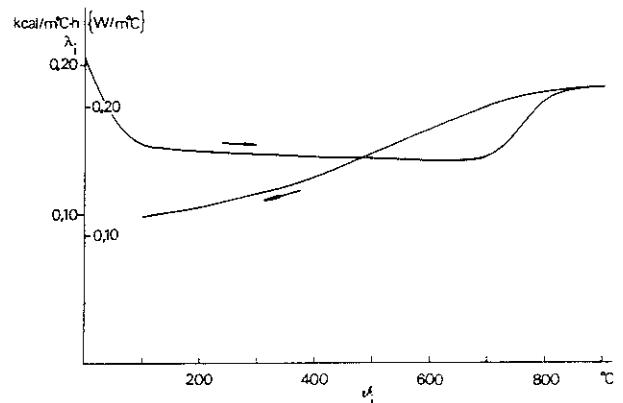


Fig. 11.1.3 b. Thermal conductivity  $\lambda_i$  as a function of the insulation temperature  $\vartheta_i$  for fire retardant plaster Type Jimoterm of density  $\gamma_i = 800 \text{ kg/m}^3$ . (According to the National Swedish Institute for Testing and Metrology)

### 11.1.4 Fire retardant paints

A relatively new method of providing protection for structural steelwork is presented by fire retardant paints which are applied to the surface to be protected by spraying, in the same way as ordinary paints. The finished surface is sometimes quite rough and can be smoothed down by rolling. The coat thickness is normally of the order of 0.5 – 3 mm. It is a characteristic property of these fire retardant

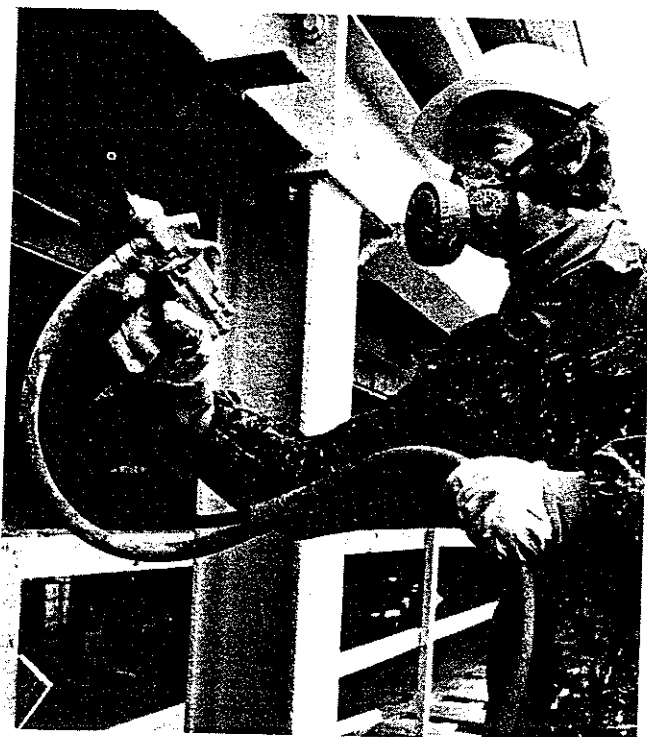


Fig. 11.1.4 a. Fire insulation of steel structure with fire retardant paints

paints that they intumesce when heated to around 100-150°C and form a foam-like layer which acts as thermal insulation. Some types of paints also bind considerable quantities of heat in the form of energy of sublimation.

Some types are applied to full thickness in one spraying operation, either onto a coat of primer or directly onto the steel surface. In the latter case the steel surface must be absolutely clean, preferably sand blasted. Other types of paint are built up in a number of layers, the components of which are somewhat different. Before a coat is applied, the previous one must be dry. In conjunction with these paint types, a zinc chromate primer is usually employed. The number of coats in which a fire retardant paint is to be applied depends on the required insulation capacity. Most types of fire retardant paint are generally provided with some form of varnish finish.

#### 11.1.5 Mineral wool slabs

Mineral wool slabs with a minimum density  $\gamma_i$  of about 150 kg/cm<sup>3</sup> are used for the fire insulation of structural steelwork. The slabs can be attached to the steel surface with temperature resistant glue or with stud-welded pins and lock washers. The latter method is the cheapest and is used most frequently. See Fig. 11.1.5 a.

The thickness of the slabs varies according to the required thermal insulation capacity. Standard thicknesses ranging between 30 and 70 mm are normally used. Even if slabs thinner than 30 mm would in many cases provide sufficient insulation capacity, they cannot be used in practice owing to their low stiffness. In I sections with deep webs, it is usual for the slabs to be attached directly to the web, while in sections with a shallower web it is usual for the slabs to be attached to the edges of the flanges, so that a rectangular section is obtained. The slabs of mineral wool must be provided with some form of surface protection where enhanced resistance to mechanical damage is required.

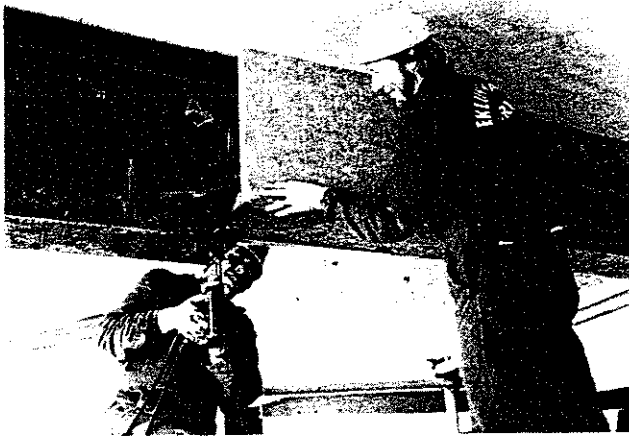


Fig. 11.1.5 a. Fire insulation of steel girders with slabs of mineral wool

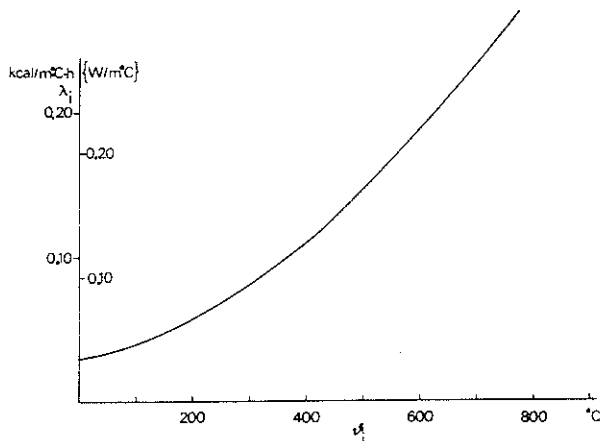


Fig. 11.1.5 b. Thermal conductivity  $\lambda_i$  as a function of the insulation temperature  $\theta_i$  for slabs of mineral wool Type Minwool 3060 or Rockwool 337, of density  $\gamma_i = 150 \text{ kg/m}^3$ . (According to the National Swedish Institute for Testing and Metrology)

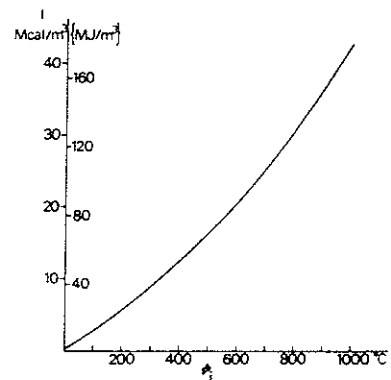


Fig. 11.1.5 c. Enthalpy I as a function of the insulation temperature  $\theta_i$  for slabs of mineral wool Type Minwool 3060 or Rockwool 337, of density  $\gamma_i = 150 \text{ kg/m}^3$ . (According to the National Swedish Institute for Testing and Metrology)

The thermal conductivity  $\lambda_i$  and the enthalpy I for slabs of mineral wool, as a function of the insulation temperature  $\theta_i$ , are given in Figs. 11.1.5 b and c.

#### 11.1.6 Vermiculite slabs

Vermiculite slabs are made of a material with a composition similar to that of some fire retardant plasters, viz. a silicate binder and vermiculite. The material is pressed into slabs with a density  $\gamma_i$  varying between 350 and 500  $\text{kg/m}^3$ . The slabs are attached to the steel surface with a fire resistant adhesive. The surface must be free from rust and loose millscale. Individual slabs are also joined together by means of adhesive and screws. The adhesive must be applied at temperatures above freezing. The slabs need not always be glued to the steel surface. On providing encasement for columns, the slabs can be joined at the corners with adhesive and screws, so that a freestanding box is formed around the column.

Vermiculite slabs are made in a number of standard thicknesses. The thicknesses normally employed vary between 10 and 30 mm. The thickness required varies in

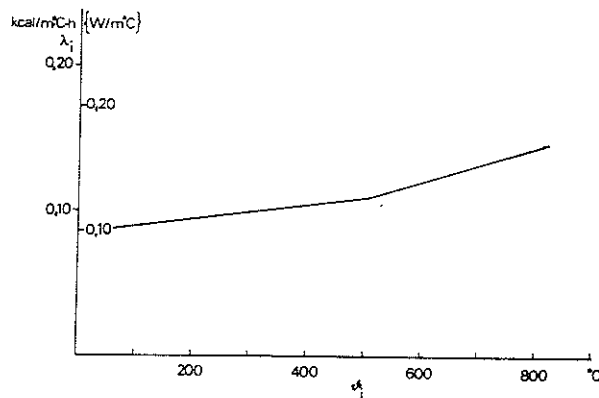


Fig. 11.1.6 a. Thermal conductivity  $\lambda_1$  as a function of the insulation temperature  $\theta_1$  for slabs of vermiculite based material Type Vermit fire insulation slab of density  $\gamma_1 = 400 \text{ kg/m}^3$ . (According to Forschungsheim für Wärmeschutz, Munich)

accordance with the stipulated insulation capacity. The slabs, which can be worked with usual woodworking tools, have a smooth surface which can be painted or covered with fabric. Vermiculite slabs are also made into prefabricated angles and channels.

The thermal conductivity  $\lambda_1$  of one type of vermiculite slab, as a function of the insulation temperature  $\theta_1$ , is given in Fig. 11.1.6 a.

#### 11.1.7 Gypsum plaster slabs

Encasement with gypsum plaster slabs with the density  $\gamma_1$  of around  $800 \text{ kg/m}^3$  is employed for the fire insulation of structural steelwork. See Fig. 11.1.7 a. Gypsum contains relatively large quantities of water in both the free and bound forms. When gypsum is being heated, this water evaporates, with consequent storage of large quantities of energy. This, together with the thermal insulation effect of the gypsum plaster slabs, retards the rise in temperature in the insulated construction. When all the water has evaporated, the slabs disintegrate. By admixing small quantities of glass fibre reinforcement into the material, the disintegration temperature can be raised, thereby increasing the fire resistance of the slabs. Sufficient fire resistance can however be provided by means of standard slabs not reinforced with glass fibre.

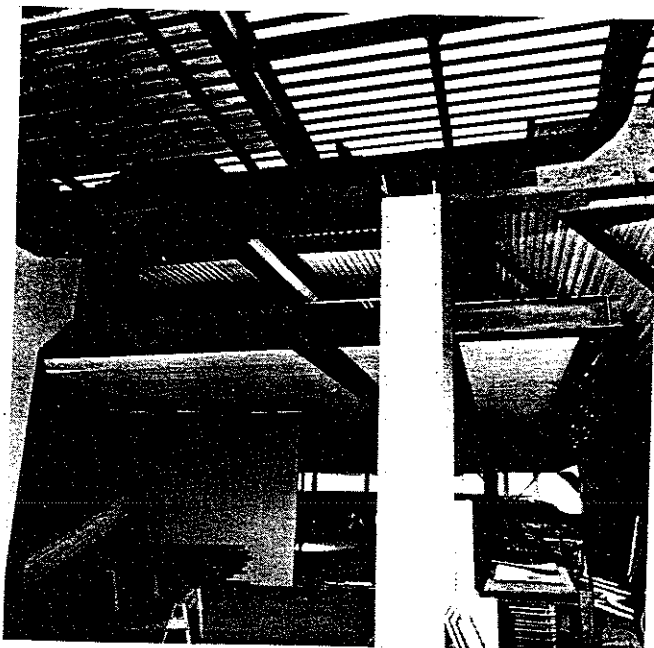


Fig. 11.1.7 a. Steel columns with fire insulation in the form of gypsum plaster slabs. The girders are insulated with slabs of mineral wool

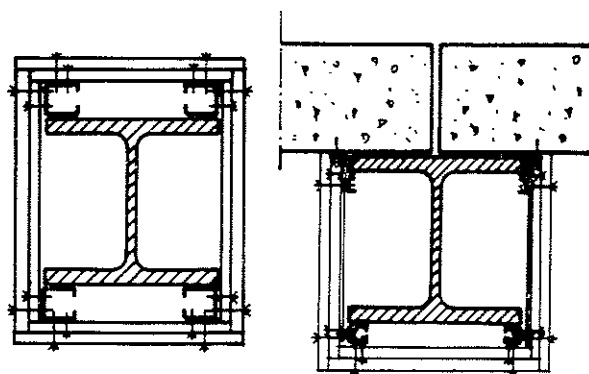


Fig. 11.1.7 b. Sketch showing fire insulation of columns and floor girders with two layers of 13 mm gypsum plaster slabs. On the girder, the sections of metal sheeting are suspended on steel straps attached to special sections fixed in the precast floor units

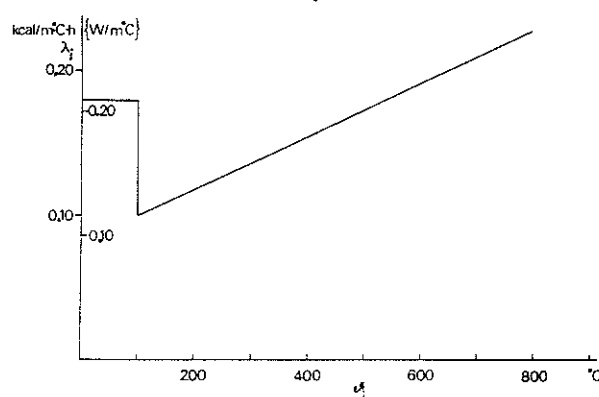


Fig. 11.1.7 c. Thermal conductivity  $\lambda_i$  as a function of the insulation temperature  $\theta_i$  for gypsum plaster slabs Type Gyproc of density  $\gamma_i = 790 \text{ kg/m}^3$ . (According to (26))

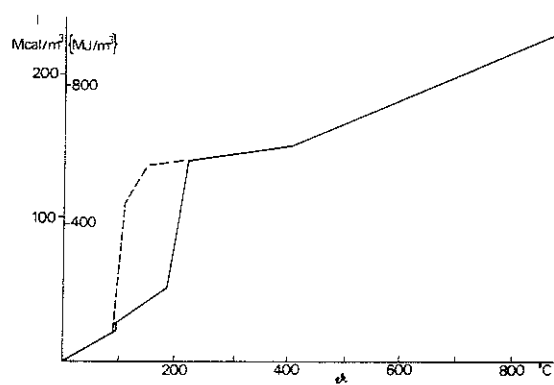


Fig. 11.1.7 d. Enthalpy  $I$  as a function of the insulation temperature  $\theta_i$  for gypsum plaster slabs Type Gyproc of density  $\gamma_i = 790 \text{ kg/m}^3$ . (According to (26)). The full line refers to rapid heating (gypsum plaster slab directly exposed to fire) and the dashed line to slow heating (gypsum plaster slab not directly exposed to fire)

Gypsum plaster slabs 13 mm in thickness are normally used in one, two or three layers depending on the required insulation capacity. The slabs are usually mounted around the steel member with the assistance of cold-bent sections of metal sheeting and thread-cutting screws. Typical sketches of columns and floor girders of steel with fire insulation in the form of two layers of gypsum plaster slabs are shown in Fig. 11.1.7 b.

The thermal conductivity  $\lambda_i$  and enthalpy  $I$  of gypsum plaster slabs, as a function of the insulation temperature  $\theta_i$ , are shown in Figs. 11.1.7 c and d.

### 11.1.8 Prefabricated gypsum plaster sections

Precast sections made up of a mixture of gypsum, perlite and glass fibre are used for the encasement and fire insulation of structural steelwork. These sections are usually made the height of a storey and are channel shaped. When columns placed against an external wall are to be provided with fire insulation, the sections

are positioned around the columns and attached to the wall by means of fixing devices set into the wall for which holes had been provided in the sections. See Fig. 11.1.8 a. The holes are subsequently filled with gypsum plaster. When free standing columns are insulated with channel sections, a cover in the form of a flat slab, which is glued to the channel section, is normally used. This provides a freestanding box around the column. See Fig. 11.1.8 b.

The density  $\gamma_i$  of the gypsum plaster sections varies between 670 and 800 kg/m<sup>3</sup>. The required thickness depends on the stipulated insulation capacity and is normally in the 20–40 mm range. The surface is hard and can be painted directly.

The thermal conductivity  $\lambda_i$  for two types of gypsum plaster section, as a function of the insulation temperature  $\vartheta_i$ , is given in Fig. 11.1.8 c and d.



Fig. 11.1.8 a. Facade columns with fire insulation in the form of prefabricated gypsum plaster sections

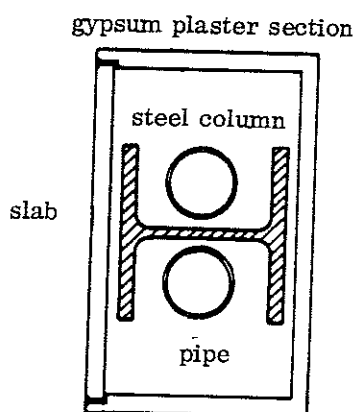


Fig. 11.1.8 b. Freestanding column with fire insulation in the form of prefabricated gypsum plaster sections

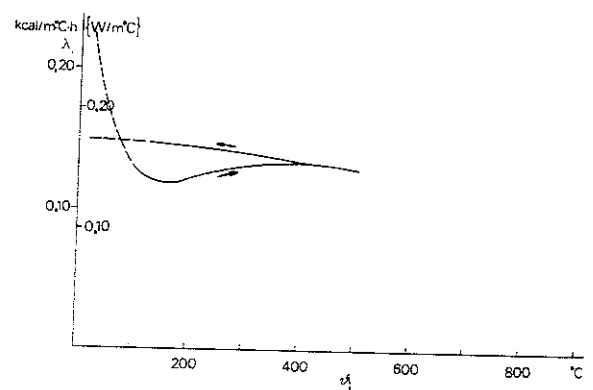


Fig. 11.1.8 c. Thermal conductivity  $\lambda_i$  as a function of the insulation temperature  $\vartheta_i$  for prefabricated gypsum plaster sections Type GPG of density  $\gamma_i = 750 - 800 \text{ kg/m}^3$ . (According to the National Swedish Institute for Testing and Metrology)

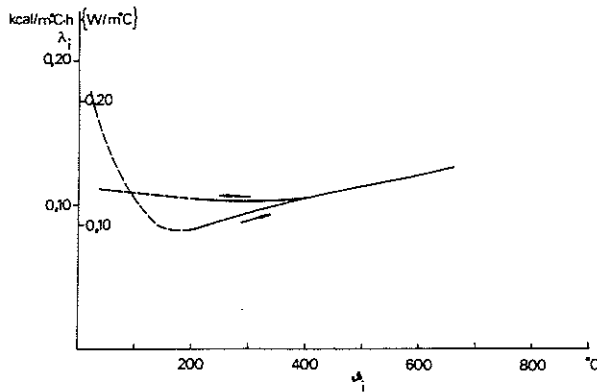


Fig. 11.1.8 d. Thermal conductivity  $\lambda_1$  as a function of the insulation temperature  $\theta_1$  for prefabricated gypsum plaster sections Type Perlitgips of density  $\lambda_1 = 670 \text{ kg/m}^3$ . (According to the National Swedish Institute for Testing and Metrology)

#### 11.1.9 Suspended ceilings and partitions

Suspended ceilings are often required in buildings for acoustic and aesthetic reasons and for installation purposes. If this suspended ceiling is made of a material that is resistant to fire and the suspension devices are designed in the appropriate manner, then the suspended ceiling can also be used to provide fire insulation for the steel construction placed above it (see Chapter 7). As a rule, the insulation capacity of a suspended ceiling need not be particularly high in order that the temperature of the steel girders above this should be limited to acceptable values in the event of fire. The reason for this is that most of the heat which penetrates through the suspended ceiling is used up in heating the floor slab which is usually quite thick. In most cases, it is therefore not the temperature rise in the steel girders but the suspension devices for the ceiling which are critical with regard to the fire resistance of the suspended ceiling. This is also borne out by the results of a series of fire tests on a number of suspended ceiling types, carried out by the National Swedish Institute for Testing and Metrology (44). The most important results are tabulated in Chapter 7 in the Design Section. The table gives the fire resistance times of suspended ceilings in standard fire tests, the insulation capacity of the suspended ceiling, and the temperatures which were considered to be critical for the suspended ceilings and their suspension devices.

Lightweight fire resistant partitions can sometimes be used to provide columns with fire insulation protection. When the column dimensions and the design of the partition are suitable, the columns can be wholly or partially incorporated into the partition. In this way, the columns are more or less automatically provided with fire protection. See Fig. 11.1.9 a.

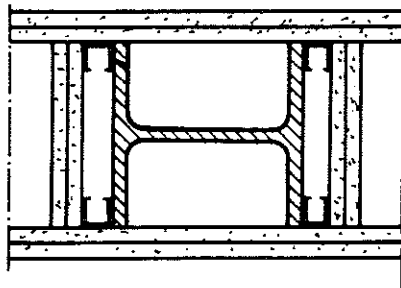


Fig. 11.1.9 a. Steel column built into fire resistant partition

### 11.1.10 Other methods

By providing a steel construction with fire insulation protection in the form of plaster or slabs applied directly to the construction or indirectly in the form of a suspended ceiling or partitions, a limitation of the temperature rise in the construction in the event of fire is achieved. Another way in which the temperature rise in a steel construction can be limited under fire exposure conditions is to raise its heat capacity instead of providing it with fire protection. The higher the heat capacity of the construction, the lower the temperature rise for a certain additional heat quantity. For columns and beams of closed hollow sections, the heat capacity can be increased by filling the hollow sections with water (63), (64). This limits the steel temperature in the event of fire, since most of the energy supplied is used up in heating and evaporating the water. The construction can be connected to a tank which continually replenishes the water as it evaporates from the hollow sections. In this way, very long fire resistance times can be provided. Systems have also been used in which the closed hollow sections have been directly connected to the municipal water supply. During a fire, the water circulates through the construction and cools this. If the rate of flow through the system is higher than the rate of evaporation of the water, fire resistance times of practically unlimited length can be obtained.

Another way of increasing the heat capacity of hollow sections is to fill them with concrete (65). The increase in fire resistance is however limited. Owing to the concrete fill, the temperature of the steel during a fire will normally be 50-200°C lower than in a section of the same dimensions without concrete fill.

### 11.2 Costs

The costs of providing a steel construction with fire insulation will vary according to the type of construction, type of fire protection, thickness of protection, surface finish and the required resistance to mechanical damage. Obviously, modifications and improvements of present materials, and the development of new methods of fire protection, can also affect costs. Some rough values, which are intended only to give an approximate idea of the costs of providing fire insulation under Swedish conditions, and the relationships between the costs of different fire protection methods, are however given in Table 11.2 a.

Table 11.2 a Approximate cost levels in the normal case, under Swedish conditions, for some fire insulation methods. The lower values apply for insulation layers of smaller thickness and the higher values for thicker insulations. The costs relate to the finished insulation and the level of costs in 1974. With the exception of fire retardant paints, the costs given do not include the costs of painting or other treatment of the surface layer

Type of insulation	Cost in Skr. /m <sup>2</sup> of external insulation surface
Sprayed mineral wool	25-35
Fire retardant plasters	30-70
Fire retardant paints	45-105
Mineral wool slabs	20-30
Vermiculite slabs	35-55
Gypsum plaster slabs	35-60
Prefabricated gypsum plaster sections	60-75



In assessing the costs, it must also be borne in mind that different methods of fire protection offer different types of surface finish and different degrees of resistance to mechanical damage, etc. It must also be emphasised that the costs quoted relate to normal conditions, and that costs can be greatly affected by the scope and difficulty of the work and by the efficiency of the working methods.

The costs of fire resistant suspended ceilings naturally also vary according to the type of ceiling, the required protection capacity and surface finish, etc. The normal range of costs, in Swedish conditions, for fire resistant suspended ceilings inclusive of mounting is Skr. 30-70 per m<sup>2</sup>.

### 11.3 Classification of fire insulation materials

The materials used in providing structural steelwork with fire protection are subject to fire engineering classification. The classifying authority is the National Swedish Board of Physical Planning and Building, which regularly publishes a list of products with a fire engineering classification, and general approvals of methods of providing fire protection for steelwork. In order that a classification may be assigned to a fire insulation material, fire engineering testing according to a standard testing procedure is generally required. The classification presupposes that the material is affixed in the approved manner. Classification is accompanied by some production control. The period of validity of a classification is normally 5 years, after which an application must be made for new classification.



## DESIGN SECTION

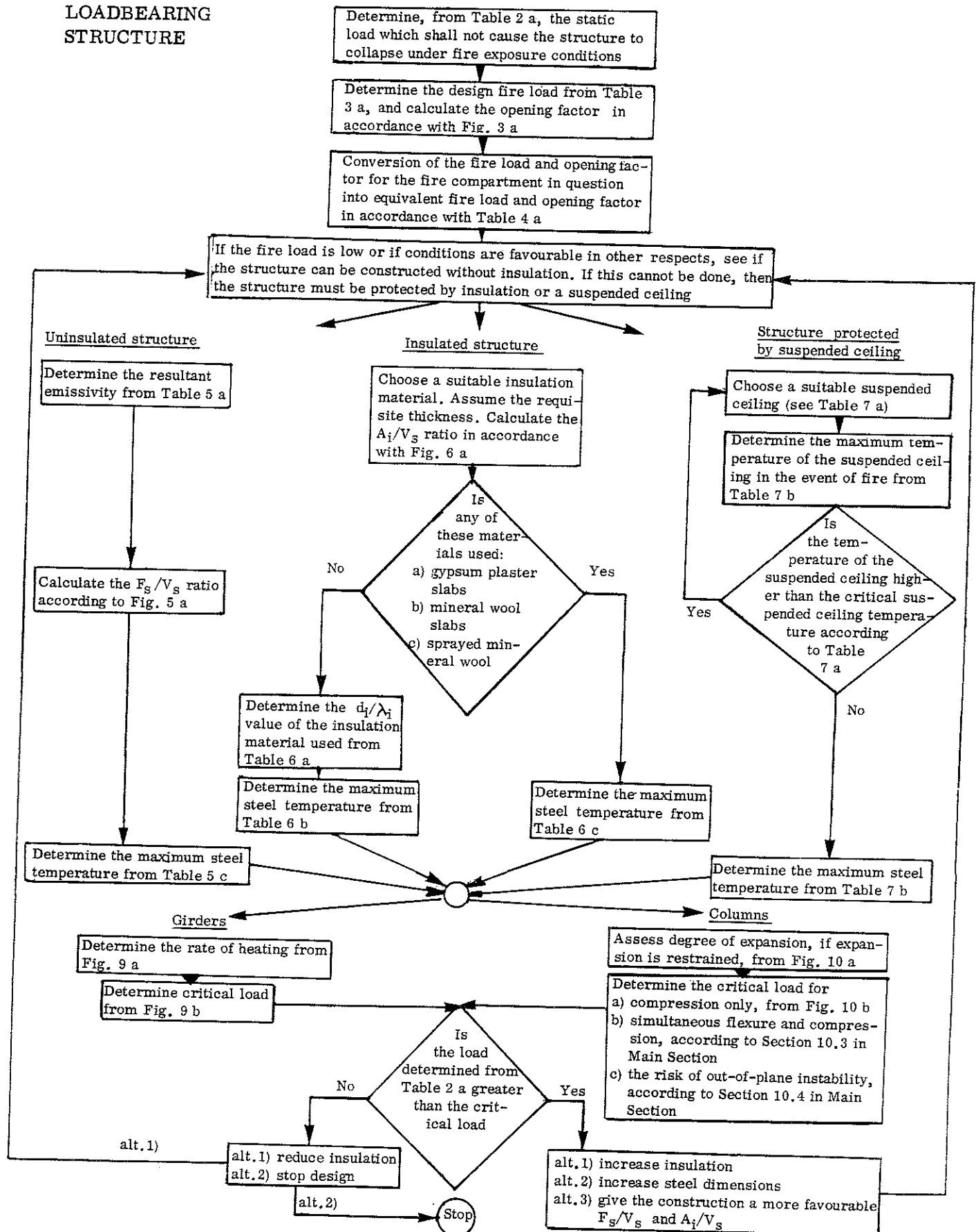
Tables and diagrams  
for structural fire  
engineering design



## CONTENTS

- 1 Flow chart which illustrates the design procedure
- 2 Determination of the design static load in the event of fire
- 3 Determination of the design fire load and opening factor
- 4 Conversion to equivalent fire load and opening factor
- 5 Determination of the maximum temperature in the event of fire in uninsulated steel structures
- 6 Determination of the maximum temperature in the event of fire in insulated steel structures
- 7 Determination of the maximum temperature in the event of fire in steel structures with insulation in the form of a suspended ceiling
- 8 Check on the function of partitions
- 9 Determination of the critical load for steel girders under fire exposure conditions
- 10 Determination of the critical load for steel columns under fire exposure conditions

## 1 FLOW CHART WHICH ILLUSTRATES THE DESIGN PROCEDURE

LOADBEARING  
STRUCTURE

## PARTITION

The fire load, opening factor and equivalent fire load and opening factor are to be determined as above according to Table 3 a, Fig. 3 a and Table 4 a. The separating capacity of the construction is to be checked for the equivalent fire load and opening factor with the assistance of e.g. Fig. 8 a

## 2 DETERMINATION OF THE DESIGN STATIC LOAD IN THE EVENT OF FIRE

Table 2 a. Static load which shall not cause a loadbearing structure to collapse under fire exposure conditions (Main Section, Subsection 2.4.1)

It shall be shown that, during a complete fire process, the structure will not collapse due to the most dangerous combination of

1. dead load
2. snow load, multiplied by the load factor 1.2
3. live load, multiplied by the load factor 1.4

Calculation:

1. The dead load is to be calculated in the conventional way
2. For the snow load, the values to be applied for the static and mobile constituents are to be 80% of the values according to current building regulations
3. The following values are to be applied for the live load

Type of premises	Static load		Mobile load	
	kgf/m <sup>2</sup>	{ kN/m <sup>2</sup> }	kgf/m <sup>2</sup>	{ kN/m <sup>2</sup> }
<u>Buildings in which complete evacuation of people in the event of fire cannot be assumed with absolute certainty</u>				
Dwelling and hotel rooms, hospital wards, etc	35	{ 0.35 }	70	{ 0.70 }
Offices and schools(classrooms and group study rooms)	35	{ 0.35 }	100	{ 1.00 }
Shops, department stores, assembly halls (excl. records rooms and warehouses containing compact stacked loading)	35	{ 0.35 }	250	{ 2.50 }
<u>Buildings in which complete evacuation of people in the event of fire can be assumed with absolute certainty</u>				
Dwelling and hotel rooms, hospital wards, etc	35	{ 0.35 }	35	{ 0.35 }
Offices and schools (classrooms and group study rooms)	35	{ 0.35 }	55	{ 0.55 }
Shops, department stores, assembly halls (excl. records rooms and warehouses with compact stacked loading)	35	{ 0.35 }	70	{ 0.70 }

## 3 DETERMINATION OF THE DESIGN FIRE LOAD AND OPENING FACTOR

Table 3 a. Fire loads in various types of buildings and premises determined by means of statistical investigations. The values are referred to the total internal surface area of the fire compartments. (Main Section, Section 3.1 and 3.2)

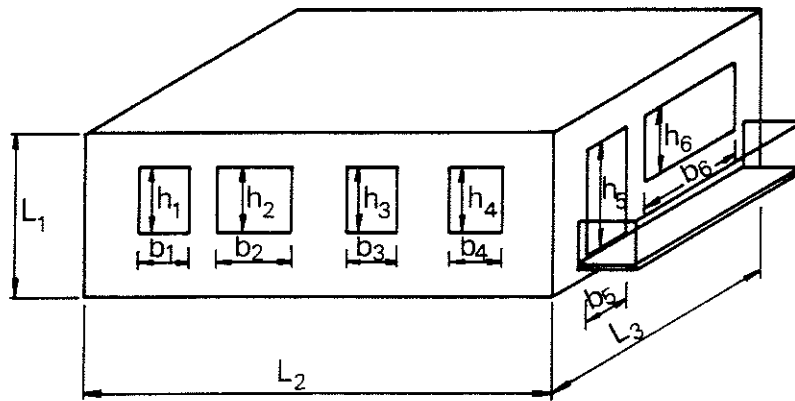
Type of building or premises	Fire load mean value	Fire load standard deviation	Design fire load. Fire load denoting the 80% level
	Mcal/m <sup>2</sup> {MJ/m <sup>2</sup> }	Mcal/m <sup>2</sup> {MJ/m <sup>2</sup> }	Mcal/m <sup>2</sup> {MJ/m <sup>2</sup> }
1 Dwellings <sup>a</sup>			
2 rooms + kitchen	35.8 {149.9}	5.9 {24.7}	40.0 {167.5}
3 rooms + kitchen	33.1 {138.6}	4.8 {20.1}	35.5 {148.6}
2 Office buildings <sup>b, c</sup>			
Technical offices (architects' offices etc)	29.7 {124.4}	7.5 {31.4}	34.5 {144.5}
Economic and ad- ministrative offices (banks, insurance companies, etc)	24.3 {101.7}	7.7 {32.2}	31.5 {131.9}
All the investigated offices taken together	27.3 {114.3}	9.4 {39.4}	33.0 {138.2}
3 Schools <sup>b</sup>			
Junior level schools	20.1 {84.2}	3.4 {14.2}	23.5 {98.4}
Intermediate level schools	23.1 {96.7}	4.9 {20.5}	28.0 {117.2}
Seniors level schools	14.6 {61.1}	4.4 {18.4}	17.0 {71.2}
All the investigated schools taken together	19.2 {80.4}	5.6 {23.4}	23.0 {96.3}
4 Hospitals	27.6 {115.6}	8.6 {36.0}	35.0 {146.5}
5 Hotels <sup>b</sup>	16.0 {67.0}	4.6 {19.3}	19.5 {81.6}

<sup>a</sup> The fire load due to floor coverings is not included in the values quoted.

<sup>b</sup> The values quoted apply only to the fire load due to furniture and fittings. Any additional fire load is to be calculated according to Equation (3.1 a) in the Main Section.

<sup>c</sup> According to Swedish regulations, an entire office apartment is defined as a fire compartment. Since there were difficulties during the statistical investigation in determining the sizes of the fire compartments, the quoted values of the fire load apply to each office room. Furthermore, it is to be noted that office buildings are often constructed in such a way that each office room can be designated as an individual fire compartment. In Subsection 3.2.2 in the Main Section, distribution curves are also given for the fire load with reference to the floor area. These values can be used in determining the fire load per m<sup>2</sup> of the total internal surface area when division into fire compartments is arbitrary.





$$A = A_1 + A_2 + \dots + A_6 = b_1 h_1 + b_2 h_2 + \dots + b_6 h_6$$

$$h = \frac{1}{A} [A_1 h_1 + A_2 h_2 + \dots + A_6 h_6]$$

$$A_t = 2 [L_1 L_2 + L_1 L_3 + L_2 L_3]$$

OPENING  
FACTOR  
 $\frac{A\sqrt{h}}{A_t}$

Fig. 3 a. Calculation of the opening factor for a fire compartment with vertical openings.  $L_1$ ,  $L_2$  and  $L_3$  denote the internal dimensions of the fire compartment (Main Section, Subsection 4.3.2)

## 4 CONVERSION TO EQUIVALENT FIRE LOAD AND OPENING FACTOR

Table 4 a. Factors for the conversion of the actual fire load and opening factor for different types of fire compartment<sup>a</sup> to equivalent fire load and opening factor applicable to fire compartment Type A (standard fire compartment) (Main Section, Subsection 4.3.4)

Equivalent fire load =  $k_f \cdot$  actual fire load

Equivalent opening factor =  $k_f \cdot$  actual opening factor

Fire compartment		Factor $k_f$					
		Actual opening factor ( $m^{1/2}$ )					
Type	Description of enclosing construction	0.02	0.04	0.06	0.08	0.10	0.12
A	Thermal properties corresponding to average values for concrete, brick and lightweight concrete (standard fire compartment)	1.0	1.0	1.0	1.0	1.0	1.0
B	Concrete	0.85	0.85	0.85	0.85	0.85	0.85
C	Lightweight concrete	3.0	3.0	3.0	3.0	3.0	2.5
D	50 % concrete 50 % lightweight concrete	1.35	1.35	1.35	1.50	1.55	1.65
E	50 % lightweight concrete 33 % concrete	1.65	1.50	1.35	1.50	1.75	2.00
	17 % { from the inside outwards, 13 mm gypsum plaster-board 100 mm mineral wool brickwork						
F <sup>b</sup>	80 % uninsulated steel sheeting 20 % concrete	1.0-0.5	1.0-0.5	0.8-0.5	0.7-0.5	0.7-0.5	0.7-0.5
G	20 % concrete	1.50	1.45	1.35	1.25	1.15	1.05
	80 % { 2x13 mm gypsum plaster-board 100 mm air gap 2x13 mm gypsum plaster-board						
H	100 % { steel sheeting 100 mm mineral wool steel sheeting	3.0	3.0	3.0	3.0	3.0	2.5

<sup>a</sup>For types of fire compartment not listed in the Table, the conversion factor  $k_f$  is to be determined by linear interpolation between the appropriate fire compartment types in the Table, or the value of the conversion factor  $k_f$  chosen in such a way that it will give results on the safe side. In the case of fire compartments with enclosing constructions of lightweight concrete and concrete in certain proportions, different values of the conversion factor  $k_f$  can be obtained depending on which of the compartment types B, C and D is used for interpolation. This is due to the fact that the relationships which determine the conversion factor  $k_f$  are not linear. However, the values of  $k_f$  tabulated above have been chosen in such a way that linear interpolation will always yield results on the safe side, irrespective of the fire compartments used for interpolation. In order that overestimation of the value of  $k_f$  should not be unnecessarily large, it is recommended that the fire compartment types used in interpolation should be those which yield the lowest value of  $k_f$ . At the interpolation, the different fire compartment types may not be combined in such a way, that any of the types gives a negative contribution to the  $k_f$  value.

<sup>b</sup>The higher values apply in the case of an actual fire load less than  $15 \text{ Mcal/m}^2 \{63 \text{ MJ/m}^2\}$ . The lower values apply in the case of an actual fire load greater than  $120 \text{ Mcal/m}^2 \{500 \text{ MJ/m}^2\}$ . Interpolation is to be applied for intermediate values of the fire load.

Example:

Fire compartment with 22% concrete and 78% gypsum plasterboard walls.  
Actual design fire load  $q = 20 \text{ Mcal/m}^2 \{84 \text{ MJ/m}^2\}$ .

Actual opening factor  $A\sqrt{h}/A_t = 0.10 \text{ m}^{1/2}$ .

The fire compartment is most nearly equivalent to fire compartment Type G.

Factor  $k_f = 1.15$

Equivalent fire load  $= 1.15 \cdot 20 = 23 \text{ Mcal/m}^2 \{96 \text{ MJ/m}^2\}$

Equivalent opening factor  $= 1.15 \cdot 0.10 = 0.115 \text{ m}^{1/2}$

# 5 DETERMINATION OF THE MAXIMUM TEMPERATURE IN THE EVENT OF FIRE IN UNINSULATED STEEL STRUCTURES

## Calculation procedure:

- Determine the resultant emissivity  $\epsilon_r$
- Determine the  $F_s/V_s$  ratio
- Determine the maximum temperature  $\theta_{\max}$

Table 5 a. Resultant emissivity  $\epsilon_r$  for different constructions. The values yield results on the safe side (Main Section, Subsection 5.2.4)

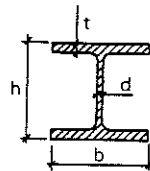
Type of construction	Resultant emissivity $\epsilon_r$
1 Column exposed to fire on all sides	0.7
2 Column outside facade	0.3
3 Floor girder with floor slab of concrete, only the underside of the bottom flange being directly exposed to fire	0.5
4 Floor girder with floor slab on the top flange <sup>a</sup>	
Girder of I section for which the width-depth ratio is not less than 0.5	0.5
Girder of I section for which the width-depth ratio is less than 0.5	0.7
Box girder and lattice girder	0.7

<sup>a</sup> More accurate values of  $\epsilon_r$  which take into account the width-depth ratio  $b/h$  and spacing-depth ratio  $c/h$  of the girders are given in Fig. 5.2.4 b in the Main Section.

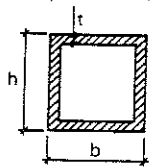
Table 5 b. The ratio  $F_s/V_s$  ( $m^{-1}$ ) for rolled I girders for two different cases of exposure to radiation (Main Section, Subsection 5.2.5)

Steel section	All surfaces of the steel section exposed to radiation	One side of one flange not exposed to radiation
<b>HEA</b>		
100	275	227
120	277	229
140	260	215
160	240	199
180	232	192
200	217	180
220	200	166
240	183	152
260	175	146
280	169	140
300	157	130
320	145	121
340	138	115
360	132	110
400	123	104
<b>HEB</b>		
100	226	188
120	208	173
140	192	160
160	174	144
180	163	135
200	151	126
220	143	119
240	134	111
260	130	108
280	126	105
300	119	99
320	112	94
340	109	91
360	105	88
400	100	85
<b>IPE</b>		
80	440	380
100	400	346
120	369	321
140	343	299
160	317	277
180	298	260
200	277	242
220	260	227
240	242	212
270	231	203
300	220	193
330	205	180
360	190	167
400	178	157

Column within a  
fire compartment

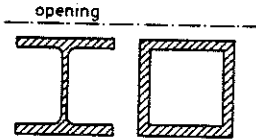


$$\frac{F_s}{V_s} = \frac{2h + 4b - 2d}{\text{cross section area}}$$



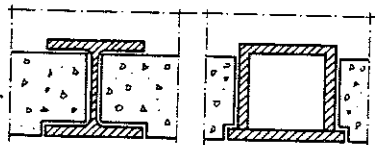
$$\frac{F_s}{V_s} = \frac{2h + 2b}{\text{cross section area}}$$

Column, immediately  
outside a window  
opening



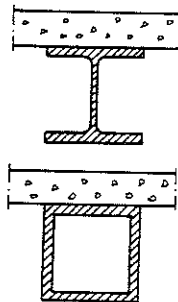
$$\frac{F_s}{V_s} = \frac{2h + b}{\text{cross section area}}$$

Floor structure, com-  
posed of steel beams  
with a concrete slab,  
supported on the lower  
flange of the beams



$$\frac{F_s}{V_s} = \frac{b}{bt} = \frac{1}{t}$$

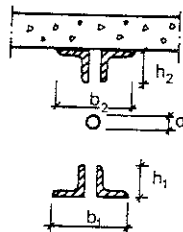
Beams with a floor  
slab, supported on  
the upper flange of  
the beams



$$\frac{F_s}{V_s} = \frac{2h + 3b - 2d}{\text{cross section area}}$$

$$\frac{F_s}{V_s} = \frac{2h + b}{\text{cross section area}}$$

Floor slab beams of  
truss type ( $F_s/V_s$  is  
determined for each  
part of the truss)



$$\frac{F_s}{V_s} \text{ (lower flange)} = \frac{2b_1 + 2h_1}{\text{cross section area of lower flange}}$$

$$\frac{F_s}{V_s} \text{ (upper flange)} = \frac{b_2 + 2h_2}{\text{cross section area of upper flange}}$$

$$\frac{F_s}{V_s} \text{ (diagonal)} = \frac{h}{d}$$

Fig. 5 a. Examples of calculating  $F_s/V_s$  ( $m^{-1}$ ), the ratio of the area per unit length exposed to fire ( $m^2/m$ ) to the enclosed steel volume per unit length ( $m^3/m$ ) for different types of construction. See also Table 5 b (Main Section, Subsection 5.2.5)

Table 5 c. Maximum steel temperature  $\vartheta_{\max}$  ( $^{\circ}\text{C}$ ) for uninsulated steel structure as a function of the equivalent fire load  $q$  ( $\text{Mcal/m}^2$ )  $\{\text{MJ/m}^2\}$ , equivalent opening factor  $AV_h/A_t$  ( $\text{m}^{1/2}$ ) and the  $F_s/V_s$  ratio of the construction ( $\text{m}^{-1}$ ) for different resultant emissivities  $\epsilon_r$  (Main Section, Chapter 5)

q	$\frac{A\sqrt{h}}{A_t}$	$\frac{F_s}{V_s}$	$\vartheta_{\max}$			q	$\frac{A\sqrt{h}}{A_t}$	$\frac{F_s}{V_s}$	$\vartheta_{\max}$			q	$\frac{A\sqrt{h}}{A_t}$	$\frac{F_s}{V_s}$	$\vartheta_{\max}$			q	$\frac{A\sqrt{h}}{A_t}$	$\frac{F_s}{V_s}$	$\vartheta_{\max}$		
			$\epsilon_r$	$\epsilon_r$	$\epsilon_r$				$\epsilon_r$	$\epsilon_r$	$\epsilon_r$				$\epsilon_r$	$\epsilon_r$	$\epsilon_r$				$\epsilon_r$		
																						0,3	0,5
10 {12}	0,01	50	325	345	370	0,01	50	400	420	440	0,01	25	390	425	445	0,01	25	455	490	500			
		75	365	385	405		75	435	445	460		50	465	480	490		50	510	525	530			
		100	395	410	425		100	450	460	470		75	485	500	500		75	525	530	535			
		125	410	425	435		125	460	470	475		100	495	505	505		100	530	535	535			
		150	425	435	440		150	470	475	480		125	500	505	510		125	530	535	540			
		200	435	445	445		200	475	480	480		150	505	510	510		150	535	540	540			
	0,02	400	450	450	450	400	480	485	485	200	505	510	515	200	535	540	540						
		50	335	380	410	0,02	50	425	480	515	0,02	50	500	550	575	0,02	50	555	600	625			
		75	410	445	475		75	500	540	565		75	560	600	620		75	610	640	650			
		100	445	490	520		100	540	575	595		100	595	620	630		100	640	650	655			
		125	480	520	545		125	565	600	610		125	615	630	640		125	650	655	660			
		150	500	540	555		150	585	605	615		150	625	640	645		150	670	675	680			
	200	540	560	575	200		605	620	625	200		635	645	650	200		680	685	690				
	0,04	400	575	585	585	400	625	630	630	0,04	400	650	650	650	0,04	400	650	650	650				
		50	285	320	365	0,04	50	400	455	510	0,04	50	495	565		625	0,04	50	570	645	700		
		75	350	400	450		75	490	550	600		75	585	650		700		75	640	690	730		
		100	405	460	510		100	550	610	655		100	650	700		740		100	700	750	780		
		125	450	515	555		125	600	655	690		125	700	740		775		125	750	780	770		
		150	495	555	595		150	635	680	710		150	740	775		800		150	790	810	830		
	0,06	200	550	605	645		0,06	200	605	630		630	0,06	200	630	645		650	0,06	200	630	645	650
		300	625	660	690	300		675	700	700	300	700		715	720	300	700	715		720			
		50	235	275	330	0,08		50	300	375	430	0,08		50	390	490	550	0,08		50	480	590	655
		75	305	370	425			75	380	465	535			75	485	590	670			75	580	700	770
		100	365	410	485			100	450	550	630			100	565	670	735			100	660	775	-
		125	415	455	515			125	500	595	670			125	610	700	755			125	710	780	800
	150	450	485	530	150		535	650	710	150	640		730	780	150	740	810		830				
	0,08	200	520	550	600		0,12	200	600	690	750		0,12	200	630	645	650		0,12	200	630	645	650
300		615	680	735	300	650		700	750	300	680	715		790	300	715	750	800					
50		200	250	300	0,12	50		260	290	400	0,01	25		430	460	480	0,01	25		505	525	540	
75		270	330	400		75		340	380	500		50		490	565	615		50		545	555	560	
100		330	400	460		100		390	460	600		75		510	515	520		75		560	560	560	
125		360	450	510		125		450	540	675		100		520	520	520		100		560	560	560	
150	410	510	580	150		500	600	750	125	530		530	530	125	560	565		565					
0,12	200	480	590	660		0,12	200	575	680	-		0,01	25	430	460	480		0,01	25	505	525	540	
	300	600	700	760	300		650	700	750	300	680		715	790	300	715	750		800				
	50	170	200	260	0,02		50	230	260	350	0,02		50	310	375	500	0,02		50	400	460	590	
	75	220	260	350			75	280	320	400			75	340	380	500			75	430	460	590	
	100	240	310	400			100	300	375	430			100	320	320	320			100	400	460	590	
	125	260	380	540			125	340	400	500			125	360	360	360			125	430	460	590	
150	310	430	620	150		380	480	600	150	400		400	400	150	460	540		650					
12,5 {32,5}	0,01	200	380	500		700	0,01	200	450	550		550	0,02	25	320	380		460	0,02	25	320	380	460
		300	450	620	800	300		520	600	650	50	480		550	645	50	360	440		520			
		50	365	385	405	50		460	515	550	75	585		650	740	75	430	555		640			
		75	410	425	435	75		530	570	595	100	635		645	645	100	535	650		720			
		100	430	445	450	100		565	600	615	125	625		635	635	125	595	735		790			
		125	440	450	460	125		585	610	630	150	645		650	655	150	660	675		675			
	0,02	150	450	455	460	0,02	150	585	610	630	0,04	200	630	645	650	0,04	200	630	645	650			
		200	455	460	465		200	600	660	705		50	525	600	660		50	290	-	440			
		400	465	470	470		400	630	645	645		75	620	690	735		75	460	540	650			
		50	380	435	470		50	460	515	550		100	680	740	760		100	665	740	-			
		75	455	500	535		75	530	570	595		125	630	645	650		125	660	675	-			
		100	500	540	560		100	565	600	615		150	645	650	655		150	660	675	-			
	0,04	125	525	555	575	0,04	125	600	660	705	0,06	200	650	660	665	0,06	200	650	660	665			
		150	550	570	580		150	610	620	635		50	525	600	660		50	290	-	440			
		200	570	590	600		200	625	635	645		75	630	645	650		75	460	540	650			
		400	600	605	605		400	635	645	645		100	650	660	665		100	665	740	-			
		50	340	400	450		50	460	515	550		125	625	635	635		125	590	730	790			
		75	415	455	540		75	530	570	595		150	645	650	655		150	660	675	-			
	0,06	100	485	550	600	0,06	100	600	660	705	0,08	200	650	660	665	0,08	200	650	660	665			
		125	535	600	640		125	635	645	645		50	525	600	660		50	290	-	440			
		150	570	625	665		150	660	670	750		75	640	650	655		75	460	540	650			
		200	630	665	700		200	670	750	750		100	680	740	760		100	665	740	-			
		50	340	400	450		50	460	515	550		125	625	635	635		125	590	730	790			
		75	415	455	540		75	530	570	595		150	645	650	655		150	660	675	-			
	0,08	100	485	550	600	0,08	100	600	660	705	0,12	200	650	660	665	0,12	200	650	660	665			
		125	535	600	640		125	635	645	645		50	525	600	660		50	290	-	440			
		150	570	625	665		150	660	670	750		75	640	650	655		75	460	540	650			
200		630	665	700	200		670	750	750	100		680	740	760	100		665	740	-				
50		340	400	450	50		460	515	550	125		625	635	635	125		590	730	790				
75		415	455	540	75		530	570	595	150		645	650	655	150		660	675	-				
0,12	100	485	550	600	0,12	100	600	660	705	0,12	200	650	660	665	0,12	200	650	660	665				
	125	535	600	640		125	635	645	645		50	525	600	660		50	290	-	440				
	150	570	625	665		150	660	670	750		75	640	650	655		75	460	540	650				
	200	630	665	700		200	670	750	750		100	680	740	760		100	665	740	-				
	50	340	400	450		50	460	515	550		125	625	635	635		125	590	730	790				
	75	415	455	540		75	530	570	595		150	645	650	655		150	660	675	-				
0,06	100	485	550	600	0,06	100	600	660	705	0,12	200	650	660	665	0,12	200	650	660	665				
	125	535	600	640		125	635	645	645		50	525	600	660		50	290	-	440				
	150	570	625	665		150	660	670	750		75	640	650	655		75	460	540	650				
	200	630	665	700		200	670	750	750		100	680	740	760		100	665	740	-				
	50	340	400	450		50	460	515	550		125	625	635	635		125	590	730	790				
	75	415	455	540		75	530	570	595		150	645	650	655		150	660	675	-				
0,08	100	485	550	600	0,08	100	600	660	705	0,12	200	650	660	665	0,12	200	650	660	665				
	125	535	600	640		125	635	645	645		50	525	600	660		50	290	-	440				
	150	570	625	665		150	660	670	750		75	640	650	655		75	460	540	650				
	200																						

# 6 DETERMINATION OF THE MAXIMUM TEMPERATURE IN THE EVENT OF FIRE IN INSULATED STEEL STRUCTURES

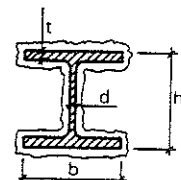
## Calculation procedure:

Determine the  $A_i/V_s$  ratio

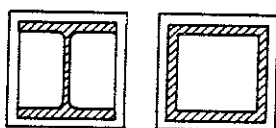
Determine the insulation capacity  $d_i/\lambda_i$  or, for specific materials, the insulation thickness  $d_i$

Determine the maximum temperature  $\theta_{\max}$

Column in a fire compartment

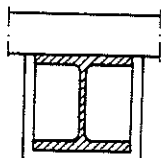


$$\frac{A_i}{V_s} = \frac{2h + 4b - 2d}{\text{steel cross section area}}$$



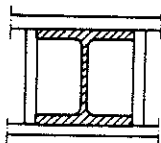
$$\frac{A_i}{V_s} = \frac{2h + 2b}{\text{steel cross section area}}$$

Column against a wall with a sufficient fire resistance



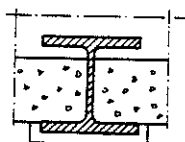
$$\frac{A_i}{V_s} = \frac{2h + b}{\text{steel cross section area}}$$

Column within a wall with a sufficient fire resistance



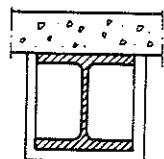
$$\frac{A_i}{V_s} = \frac{b}{bt} = \frac{1}{t}$$

Floor structure, composed of steel beams with a concrete slab, supported on the lower flange of the beams



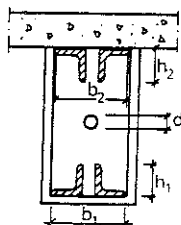
$$\frac{A_i}{V_s} = \frac{b}{bt} = \frac{1}{t}$$

Beams with a floor slab, supported on the upper flange of the beams



$$\frac{A_i}{V_s} = \frac{2h + b}{\text{steel cross section area}}$$

Floor slab beams of truss type ( $A_i/V_s$  is determined for each part of the truss)



$$\frac{A_i}{V_s} (\text{lower flange}) = \frac{2b_2 + 2h_2}{\text{cross section area of lower flange}}$$

$$\frac{A_i}{V_s} (\text{upper flange}) = \frac{b_2 + 2h_2}{\text{cross section area of upper flange}}$$

$$\frac{A_i}{V_s} (\text{diagonal}) = \frac{4}{d}$$

Fig. 6 a. Examples of calculating  $A_i/V_s$  ( $\text{m}^{-1}$ ), the ratio of the inner surface area of the insulation per unit length ( $\text{m}^2/\text{m}$ ) to the enclosed steel volume per unit length ( $\text{m}^3/\text{m}$ ) for different types of construction (Main Section, Subsection 6.2.3)



Table 6 a. The thermal conductivity  $\lambda_i$  (kcal/m °Ch) {W/m °C} of some insulation materials as a function of the insulation temperature (Main Section, Chapter 11)

	Temperature °C <sup>a</sup>										
	0	100	200	300	400	500	600	700	800	900	1000
Sprayed mineral wool Cafco Blaze-Shield Type DC/F	0,045 {0,053}	0,047 {0,055}	0,050 {0,058}	0,058 {0,068}	0,066 {0,077}	0,077 {0,090}	0,095 {0,110}	0,120 {0,140}	0,145 {0,170}	0,170 {0,198}	0,210 {0,245}
Sprayed mineral wool Type Pyroguard 101	0,044 {0,051}	0,055 {0,064}	0,059 {0,069}	0,066 {0,077}	0,071 {0,083}	0,079 {0,092}	0,089 {0,104}	0,103 {0,120}	0,123 {0,144}	0,150 {0,175}	0,190 {0,220}
Fire retardant plaster Type Jimoterm	0,203 {0,236}	0,145 {0,169}	0,144 {0,168}	0,143 {0,167}	0,141 {0,165}	0,138 {0,161}	0,138 {0,161}	0,156 {0,182}	0,182 {0,212}	0,186 {0,217}	—
Fire retardant plaster Type Pyrodur	0,085 {0,099}	0,090 {0,105}	0,095 {0,110}	0,100 {0,116}	0,105 {0,122}	0,110 {0,128}	0,115 {0,134}	0,115 {0,134}	0,120 {0,140}	0,125 {0,146}	0,130 {0,152}
Slabs of vermiculite based material Type Vermit fire insulation slab	0,077 {0,090}	0,085 {0,099}	0,092 {0,108}	0,100 {0,116}	0,112 {0,130}	0,117 {0,137}	0,125 {0,146}	0,133 {0,155}	0,145 {0,169}	0,157 {0,183}	0,171 {0,199}
Mineral wool slabs with a density of $\gamma \approx 150 \text{ kg/m}^3$ Type Minwool slab 3060 or Rockwool slab 337	0,030 {0,035}	0,044 {0,051}	0,058 {0,068}	0,081 {0,094}	0,109 {0,127}	0,149 {0,173}	0,187 {0,218}	0,235 {0,275}	0,280 {0,325}	0,365 {0,425}	0,470 {0,550}
Gypsum plaster slabs Type Gyproc	0,180 {0,210}	0,180 {0,210}	0,120 {0,140}	0,135 {0,157}	0,155 {0,181}	0,170 {0,198}	0,190 {0,220}	0,205 {0,240}	0,225 {0,260}	0,250 {0,290}	0,275 {0,320}
Prefabricated gypsum plaster sections Type GPG	0,250 {0,290}	0,130 {0,152}	0,124 {0,145}	0,133 {0,155}	0,135 {0,157}	0,130 {0,152}	—	—	—	—	—
Prefabricated gypsum plaster sections Type Perlitgips	0,180 {0,210}	0,105 {0,122}	0,084 {0,098}	0,106 {0,123}	0,115 {0,134}	0,122 {0,142}	—	—	—	—	—

Fire retardant paints Most fire retardant paints change in thickness on exposure to fire. Information relating only to the variation of the thermal conductivity with temperature does not therefore provide a sufficient basis for design. The insulation capacity of the paint, expressed in terms of a fictive  $d_i/\lambda_i$  value, must be known. For Unitherm fire retardant paint, the following values can be used in determining the maximum steel temperature. Two-coat Unitherm application,  $d_i/\lambda_i = 0,075 \text{ m}^2 \text{ °C h/kcal}$  {0,064  $\text{m}^2 \text{ °C/W}$ }. Three-coat Unitherm application,  $d_i/\lambda_i = 0,10 \text{ m}^2 \text{ °C h/kcal}$  {0,086  $\text{m}^2 \text{ °C/W}$ }. These values have been determined using the results of standard fire tests. The values are clearly on the safe side and should be applicable also to other types of paint which are found in fire tests to exhibit at least the same fire resistance as Unitherm fire retardant paint.

<sup>a</sup>In determining the maximum steel temperature from Table 6b, the value of  $\lambda_i$  used for the insulation is to be that corresponding to an insulation temperature approximately equal to the maximum steel temperature. Normally, therefore, a value of  $\lambda_i$  corresponding to a temperature of 400–600°C is to be used (see Main Section, Subsection 6.2.1).

Table 6 b. Maximum steel temperature  $\vartheta_{\max}$  ( $^{\circ}\text{C}$ ) for an insulated steel structure as a function of the equivalent fire load  $q$  ( $\text{Mcal/m}^2$ ) [ $\text{MJ/m}^2$ ], equivalent opening factor  $AV\bar{h}/A_t$  ( $\text{m}^{1/2}$ ) and the  $A_i/V_s$  ratio ( $\text{m}^{-1}$ ) of the construction for different values of the thermal resistance  $d_i/\lambda_i$  ( $\text{m}^2 \text{ }^{\circ}\text{C h/kcal}$ ) of the insulation.  $d_i$  denotes the insulation thickness (m) (Main Section, Chapter 6)

	$\frac{AV\bar{h}}{A_t}$	$\frac{A_i}{V_s}$	$\vartheta_{\max}$					$q$	$\frac{AV\bar{h}}{A_t}$	$\frac{A_i}{V_s}$	$\vartheta_{\max}$					$q$	$\frac{AV\bar{h}}{A_t}$	$\frac{A_i}{V_s}$	$\vartheta_{\max}$					$q$	$\frac{AV\bar{h}}{A_t}$	$\frac{A_i}{V_s}$	$\vartheta_{\max}$									
			$d_{ji}/\lambda_i$	$d_{ji}/\lambda_i$	$d_{ji}/\lambda_i$	$d_{ji}/\lambda_i$	$d_{ji}/\lambda_i$				$d_{ji}/\lambda_i$	$d_{ji}/\lambda_i$	$d_{ji}/\lambda_i$	$d_{ji}/\lambda_i$	$d_{ji}/\lambda_i$				$d_{ji}/\lambda_i$	$d_{ji}/\lambda_i$	$d_{ji}/\lambda_i$	$d_{ji}/\lambda_i$	$d_{ji}/\lambda_i$				$d_{ji}/\lambda_i$	$d_{ji}/\lambda_i$	$d_{ji}/\lambda_i$	$d_{ji}/\lambda_i$	$d_{ji}/\lambda_i$	$d_{ji}/\lambda_i$	$d_{ji}/\lambda_i$	$d_{ji}/\lambda_i$	$d_{ji}/\lambda_i$	$d_{ji}/\lambda_i$
15 [63]	0,01	100	380	325	255	215	0,01	50	430	360	275	230	0,02	25	360	260	185	145	0,02	25	445	330	230	180	0,02	25	445	330	230	180						
		125	405	350	280	240		75	470	410	330	275		50	490	380	270	225		50	570	460	340	275		50	570	460	340	275						
		150	420	365	300	260		100	495	445	370	320		75	550	445	340	280		75	640	540	415	340		75	640	540	415	340						
		200	440	395	335	290		125	505	465	395	350		100	595	490	385	325		100	670	580	470	395		100	670	580	470	395						
		300	460	430	375	335		150	515	480	420	375		125	625	535	425	360		125	695	620	510	440		125	695	620	510	440						
		400	470	445	405	370		200	525	500	450	410		150	645	555	460	395		150	710	650	550	475		150	710	650	550	475						
	0,02	100	390	300	220	180	0,02	50	395	300	225	180	0,04	25	275	200	130	100	0,04	25	330	245	160	125	0,04	25	330	245	160	125						
		125	420	340	250	205		75	455	360	280	230		50	410	300	205	160		50	480	360	250	195		50	480	360	250	195						
		150	450	360	275	225		100	500	405	310	260		75	500	380	265	210		75	565	440	315	250		75	565	440	315	250						
		200	500	400	310	260		125	540	445	350	300		100	560	440	310	250		100	630	500	370	300		100	630	500	370	300						
		300	550	460	370	320		150	595	515	420	360		125	610	480	350	280		125	680	550	410	340		125	680	550	410	340						
		400	575	505	415	355		200	635	570	490	435		150	650	565	455	370		150	715	590	450	370		150	715	590	450	370						
20 [84]	0,01	100	420	355	280	235	0,01	50	450	380	270	220	0,02	25	380	275	185	145	0,02	25	465	355	245	195	0,02	25	465	355	245	195						
		125	440	385	315	270		75	470	405	305	275		50	490	385	280	225		50	510	380	260	205		50	510	380	260	205						
		150	460	415	340	290		100	495	445	370	320		75	510	405	305	275		75	530	410	300	240		75	530	410	300	240						
		200	480	435	365	320		125	515	465	395	355		100	530	425	310	250		100	550	430	310	250		100	550	430	310	250						
		300	500	460	400	340		150	535	485	415	365		125	555	455	330	260		125	575	465	330	260		125	575	465	330	260						
		400	505	490	460	430		200	565	515	445	405		150	585	505	350	280		150	605	495	350	280		150	605	495	350	280						
	0,02	100	430	315	240	190	0,02	50	435	315	240	190	0,04	25	390	285	190	145	0,04	25	475	365	255	205	0,04	25	475	365	255	205						
		125	450	335	260	210		75	455	335	260	210		50	455	335	260	210		50	475	365	255	205		50	475	365	255	205						
		150	480	360	290	220		100	485	365	290	220		75	485	365	290	220		75	505	385	270	210		75	505	385	270	210						
		200	510	415	325	275		125	515	405	325	275		100	515	405	325	275		100	535	415	325	275		100	535	415	325	275						
		300	550	470	370	310		150	555	470	370	310		125	555	470	370	310		125	575	495	370	310		125	575	495	370	310						
		400	615	560	475	410		200	615	560	475	410		150	615	560	475	410		150	635	580	475	410		150	635	580	475	410						
30 [126]	0,01	100	400	300	210	160	0,01	50	400	300	210	160	0,02	25	400	300	210	165	0,02	25	485	385	275	215	0,02	25	485	385	275	215						
		125	450	340	240	190		75	450	340	240	190		50	450	340	240	190		50	485	385	275	215		50	485	385	275	215						
		150	480	365	260	210		100	480	365	260	210		75	480	365	260	210		75	510	410	300	240		75	510	410	300	240						
		200	540	420	310	250		125	540	420	310	250		100	540	420	310	250		100	565	440	310	250		100	565	440	310	250						
		300	620	500	380	310		150	620	500	380	310		125	620	500	380	310		125	645	520	380	310		125	645	520	380	310						
		400	670	555	440	360		200	670	555	440	360		150	670	555	440	360		150	695	585	440	360		150	695	585	440	360						
	0,02	100	350	250	175	135	0,02	50	350	250	175	135	0,04	25	350	250	175	135	0,04	25	435	335	245	195	0,04	25	435	335	245	195						
		125	390	280	200	155		75	390	280	200	155		50	390	280	200	155		50	435	335	245	195		50	435	335	245	195						
		150	430	320	220	175		100	430	320	220	175		75	430	320	220	175		75	465	365	260	210		75	465	365	260	210						
		200	490	370	260	210		125	490	370	260	210		100	490	370	260	210		100	515	405	280	220		100	515	405	280	220						
		300	580	450	325	260		150	580	450	325	260		125	580	450	325	260		125	615	495	325	260		125	615	495	325	260						
		400	640	505	380	310		200	640	505	380	310		150	640	505	380	310		150	665	545	380	310		150	665	545	380	310						
0,04	100	370	260	185	150	0,04	50	370	260	185	150	0,06	25	370	260	185	150	0,06	25	455	355	265	215	0,06	25	455	355	265	215							
	125	400	290	210	175		75	400	290	210	175		50	400	290	210	175		50	455	355	265	215		50	455	355	265	215							
	150	440	310	225	175		100	440	310	225	175		75	440	310	225	175		75	485	385	275	215		75	485	385	275	215							
	200	530	400	280	215		125	530	400	280	215		100	530	400	280	215		100	565	440	310	245		100	565	440	310	245							
	300	600	450	340	260		150	600	450	340	260		125	600	450	340	260		125	635	495	340	260		125	635	495	340	260							
	400	660	510	390	290		200	660	510	390	290		150	660	510	390	290		150	685	555	390	290		150	685	555	390	290							
40 [168]	0,01	100	340	240	165	130	0,01	50	340	240	165	130	0,02	25	340	240	165	130	0,02	25	425	325	235	185	0,02	25	425	325	235	185						
		125	380	280	200	155		75	380	280	200	155		50	380	280	200	155		50	425	325	235	185		50	425	325	235	185						
		150	420	320	220	175		100	420	320	220	175		75	420	320	220	175		75	465	365	260	210		75	465	365	260	210						
		200	480	380	280	220		125	480	380	280	220		100	480	380	280	220		100	515	415	310	240		100	515	415	310	240						
		300	580	480	380	320		150	580	480	380	320		125	580	480	380	320		125	615	515	415	310		125	615	515	415	310						
		400	640	540	440	340		200	640	540	440	340		150	640	540	440	340		150	665	565	465	360		150	665	565	465	360						
	0,02	100	360	260	185	140	0,02	50	360	260	185	140	0,04	25	360	260	185	140	0,04	25	445	345	255	195	0,04	25	445	345	255	195						
		125	400	300	210	175		75	400	300	210	175		50	400	300	210	175		50	445	345	255	195		50	445	345	255	195						
		150	440	340	240	190		100	440	340	240	190		75	440	340	240	190		75	485	385	275	215		75	485	385	275	215						
		200	500	400	300	220		125	500	400	300	220		100	500	400	300	220		100	535	435	310	240		100	535	435	310	240						
		300	600	500	400	300		150	600	500	400	300		125	600	500	400	300		125																

q	$\frac{A\sqrt{h}}{A_t}$	$\frac{A_i}{V_s}$	$\vartheta_{max}$					q	$\frac{A\sqrt{h}}{A_t}$	$\frac{A_i}{V_s}$	$\vartheta_{max}$					q	$\frac{A\sqrt{h}}{A_t}$	$\frac{A_i}{V_s}$	$\vartheta_{max}$																
			$d_{ij}\lambda_i$ 0,05	$d_{ij}\lambda_i$ 0,10	$d_{ij}\lambda_i$ 0,20	$d_{ij}\lambda_i$ 0,30	$d_{ij}\lambda_i$ 0,05				$d_{ij}\lambda_i$ 0,10	$d_{ij}\lambda_i$ 0,20	$d_{ij}\lambda_i$ 0,30	$d_{ij}\lambda_i$ 0,05	$d_{ij}\lambda_i$ 0,10				$d_{ij}\lambda_i$ 0,20	$d_{ij}\lambda_i$ 0,30															
30 {210}	0,02	25	480	355	250	200	60 {250}	0,02	25	530	420	295	235	75 {315}	0,04	25	525	395	270	205	120 {500}	0,04	25	660	500	350	270								
		50	605	490	375	300			50	665	560	430	350			50	665	540	400	320			50	-	670	520	420								
		75	665	570	450	380			75	715	640	515	435			75	735	625	490	400			75	-	760	620	520								
		100	700	620	510	435			100	745	675	570	495			100	790	680	550	435			100	-	-	695	595								
		125	720	650	550	475			125	760	705	610	540			125	-	710	600	505			125	-	-	745	650								
		150	730	675	585	510			150	770	725	640	575			150	-	750	640	550			150	-	-	-	-								
	0,04	200	745	700	630	565			200	780	750	690	625			200	-	800	695	605			200	-	-	-	-								
		250	755	735	680	635			250	805	800	740	680			250	400	280	185	140			250	550	395	265	200								
		300	-	-	-	-			300	-	-	-	-			300	565	415	285	225			300	735	570	400	320								
		400	-	-	-	-			400	-	-	-	-			400	670	510	365	290			400	-	-	675	500	405							
		500	-	-	-	-			500	-	-	-	-			500	740	585	425	345			500	-	-	750	575	475							
		600	-	-	-	-			600	-	-	-	-			600	790	640	480	390			600	-	-	800	635	535							
	0,06	25	300	210	135	105			25	345	240	155	120		0,06	25	350	240	160	120		0,08	25	390	250	165	130	0,08	25	390	250	165	130		
		50	445	320	215	170			50	500	360	240	195			50	510	365	250	190			50	565	390	260	210		50	565	390	260	210		
		75	540	400	275	220			75	600	450	315	250			75	615	455	320	250			75	690	495	340	270		75	690	495	340	270		
		100	610	465	330	260			100	670	515	375	300			100	700	530	375	300			100	760	565	400	320		100	760	565	400	320		
		125	665	515	375	300			125	725	570	415	340			125	750	585	425	340			125	-	-	640	450		370	125	-	-	640	450	370
		150	710	560	410	330			150	765	615	460	375			150	800	640	470	385			150	-	-	690	500		410	150	-	-	690	500	410
	0,08	200	775	625	475	395			200	-	-	685	525	435		200	-	-	650	550	200		-	-	740	560	450	200	-	-	740	560	450		
		300	-	-	-	-			300	-	-	775	625	530		300	-	-	730	625	300		-	-	780	610	500	300	-	-	780	610	500		
		400	-	-	-	-			400	-	-	-	695	600		400	-	-	730	625	400		-	-	-	-	400	-	-	-	-	580			
		500	-	-	-	-			500	-	-	-	-	-		500	420	290	190	150	500		435	300	195	150	500	435	300	195	150				
		600	-	-	-	-			600	-	-	-	-	-		600	525	375	250	200	600		510	355	235	180	600	510	355	235	180				
		700	-	-	-	-			700	-	-	-	-	-		700	600	440	300	240	700		575	410	270	210	700	575	410	270	210				
	0,12	25	260	180	115	90			25	300	200	135	100	0,12	25	305	205	135	105	0,30	25	305	205	135	110	0,30	25	305	205	135	110				
		50	400	275	180	140			50	450	315	210	160		50	470	330	210	170		50	480	345	225	175		50	480	345	225	175				
		75	500	350	240	190			75	550	400	275	210		75	550	400	275	210		75	550	400	275	210		75	550	400	275	210				
		100	555	410	290	225			100	615	460	325	255		100	615	460	325	255		100	615	460	325	255		100	615	460	325	255				
		125	615	460	325	255			125	680	515	365	290		125	680	515	365	290		125	680	515	365	290		125	680	515	365	290				
		150	665	505	355	295			150	725	560	400	330		150	725	560	400	330		150	725	560	400	330		150	725	560	400	330				
90 {380}	0,02	200	775	625	475	395			200	-	-	685	525		435	200	-	-	650		550	200	-	-	690	500	410	200	-	-	690	500	410		
		300	-	-	-	-			300	-	-	775	625		530	300	-	-	730		625	300	-	-	740	560	450	300	-	-	740	560	450		
		400	-	-	-	-			400	-	-	-	695		600	400	-	-	730		625	400	-	-	-	-	400	-	-	-	-	580			
		500	-	-	-	-			500	-	-	-	-		-	500	420	290	190		150	500	435	300	195	150	500	435	300	195	150				
		600	-	-	-	-			600	-	-	-	-		-	600	525	375	250		200	600	510	355	235	180	600	510	355	235	180				
		700	-	-	-	-			700	-	-	-	-		-	700	600	440	300		240	700	575	410	270	210	700	575	410	270	210				
	0,04	25	260	180	115	90			25	300	200	135	100	0,04	25	305	205	135	105	0,06	25	305	205	135	110	0,06	25	305	205	135	110				
		50	400	275	180	140			50	450	315	210	160		50	470	330	210	170		50	480	345	225	175		50	480	345	225	175				
		75	500	350	240	190			75	550	400	275	210		75	550	400	275	210		75	550	400	275	210		75	550	400	275	210				
		100	555	410	290	225			100	615	460	325	255		100	615	460	325	255	100	615	460	325	255	100	615	460	325	255						
90 {380}	0,06	125	615	460	325	255	125	680	515	365	290	0,06	125	680	500	350	275	0,08	125	725	550	390	300	0,08	125	725	550	390	300						
		150	665	505	355	295	150	725	560	400	330		150	725	560	400	330		150	725	560	400	330		150	725	560	400	330						
		200	750	580	425	350	200	800	640	475	390		200	800	640	475	390		200	800	640	475	390		200	800	640	475	390						
		300	-	-	-	-	300	-	-	750	580		480	300	-	-	750		580	300	-	-	730		625	400	-	-	730	625	400				
		400	-	-	-	-	400	-	-	-	650		550	400	-	-	-		650	550	400	-	-		-	-	400	-	-	-	-	580			
		500	-	-	-	-	500	-	-	-	-		-	500	420	290	190		150	500	435	300	195		150	500	435	300	195	150					
	0,12	25	320	220	140	105	25	345	235	155	125		0,12	25	350	240	160		120	0,12	25	390	250	165	130	0,12	25	390	250	165	130				
		50	475	330	220	175	50	570	415	285	220			50	680	510	360		285		50	680	510	360	285		50	680	510	360	285				
		75	590	425	285	225	75	590	425	285	225			75	590	425	285		225		75	590	425	285	225		75	590	425	285	225				
		100	670	495	340	275	100	670	495	340	275			100	670	495	340		275		100	670	495	340	275		100	670	495	340	275				
90 {380}	0,12	125	740	550	395	305	125	740	550	395	305		0,12	125	740	550	395		305	0,12	125	740	550	395	305	0,12	125	740	550	395	305				
		150	800	600	440	350	150	800	600	440	350			150	800	600	440		350		150	800	600	440	350		150	800	600	440	350				
		200	-	690	500	405	200	-	690	500	405	200		-	690	500	405	200	-		690	500	405	200	-		690	500	405						
		300	-	800	605	505	300	-	800	605	505	300		-	800	605	505	300	-		800	605	505	300	-		800	605	505						
		400	-	-	700	595	400	-	-	700	595	400		-	-	700	595	400	-		-	700	595	400	-		-	700	595	400					
		500	-	-	-	-	500	-	-	-	-	-		500	420	290	190	150	500		435	300	195	150	500		435	300	195	150					
	0,30	75	355	245	160	125	75	355	245	160	125	0,30		75	355	245	160	125	0,30		75	355	245	160	125	0,30	75	355	245	160	125				
		100	425	290	195	150	100	425	290	195	150			100	425	290	195	150			100	425	290	195	150		100	425	290	195	150				
		125	480	335	225	175	125	480	335	225	175			125	480	335	225	175			125	480	335	225	175		125	480	335	225	175				
		150	530	375	250	195	150	530	375	250	195			150	530	375	250	195			150	530	375	250	195		150	530	375	250	195				

Table 6 c. Maximum steel temperature  $\vartheta_{\max}$  ( $^{\circ}\text{C}$ ) for a steel structure insulated with gypsum plaster slabs, mineral wool slabs or sprayed mineral wool as a function of the equivalent fire load  $q$  ( $\text{Mcal/m}^2$ ) [ $\text{MJ/m}^2$ ], equivalent opening factor  $A\sqrt{h}/A_t$  ( $\text{m}^{1/2}$ ) and the  $A_l/V_s$  ratio of the construction ( $\text{m}^{-1}$ ) for different insulation thickness  $d_l$  (mm) (Main Section, Chapter 6)

Table 6 c:1 Gypsum plaster slabs Type Gyproc ( $\gamma \approx 790 \text{ kg/m}^3$ )

$q$	$A\sqrt{h}/A_t$	$A_l/V_s$	$\vartheta_{\max}$		$q$	$A\sqrt{h}/A_t$	$A_l/V_s$	$\vartheta_{\max}$		$q$	$A\sqrt{h}/A_t$	$A_l/V_s$	$\vartheta_{\max}$		$q$	$A\sqrt{h}/A_t$	$A_l/V_s$	$\vartheta_{\max}$	
			$d_l$ 13	$d_l$ 26				$d_l$ 13	$d_l$ 26				$d_l$ 13	$d_l$ 26				$d_l$ 13	$d_l$ 26
15 {63}	0,01	0,01	125	315 200	30 {126}	0,01	0,01	25	315 210	40 {168}	0,02	0,02	25	305 195	50 {210}	0,02	0,02	25	390 250
			150	335 215				50	415 305				50	435 290				50	550 370
			200	365 235				75	465 360				75	525 345				75	655 500
			300	395 260				100	495 395				100	600 390				100	725 570
	0,02	0,02	400	415 275		0,02	0,02	125	510 420		0,04	0,04	125	640 425		0,04	0,04	125	755 615
			150	325 165				150	525 440				150	675 500				150	765 680
			200	350 200				200	535 465				200	700 585				200	775 550
			300	405 215				300	550 495				300	720 650				300	775 550
	0,04	0,04	400	435 230		0,04	0,04	400	560 510		0,06	0,06	400	720 650		0,06	0,06	400	775 550
			150	300 120				50	350 215				50	350 200				50	410 275
			400	330 125				75	410 265				75	425 260				75	500 330
								100	460 305				100	485 300				100	575 380
20 {84}	0,01	0,01	75	345 230	30 {126}	0,02	0,02	125	495 335	40 {168}	0,04	0,04	125	535 325	50 {210}	0,04	0,04	150	745 455
			100	380 260				150	520 365				150	605 355				200	- 500
			125	405 280				200	570 400				200	690 400				300	- 635
			200	440 325				300	640 450				300	780 495				400	- 635
	0,02	0,02	300	465 355		0,04	0,04	400	665 470		0,06	0,06	400	800 560		0,06	0,06	50	350 205
			400	480 375				75	345 185				75	365 185				75	435 265
								100	400 215				100	420 215				100	510 310
								125	435 245				125	450 235				125	570 345
	0,04	0,04	150	420 300		0,06	0,06	150	470 260		0,08	0,08	150	485 260		0,08	0,08	150	600 375
			200	460 325				200	520 300				200	600 300				200	750 425
			300	445 355				300	630 350				300	730 355				300	- 495
			400	480 375				400	695 380				400	800 385				400	- 535
	0,06	0,06	100	300 180		0,08	0,08	100	330 140		0,12	0,12	100	315 115		0,12	0,12	50	300 200
			100	345 200				125	365 155				125	315 115				75	375 245
			125	375 220				150	395 175				150	350 120				100	440 280
			200	440 265				200	445 200				200	400 200				125	490 300
	0,08	0,08	300	490 300		0,12	0,12	300	550 235		0,12	0,12	300	510 250		0,12	0,12	150	550 330
			400	520 320				400	600 255				400	600 295				200	650 375
								125	305 120				125	315 115				300	770 415
								150	345 125				150	350 120				400	- 500
25 {105}	0,01	0,01	50	360 250	35 {147}	0,02	0,02	50	390 255	45 {190}	0,04	0,04	50	380 230	60 {250}	0,04	0,04	50	400 295
			75	410 300				75	465 305				75	460 290				75	490 375
			100	440 335				100	520 345				100	525 330				100	610 425
			125	470 360				125	560 380				125	585 385				125	710 455
	0,02	0,02	150	480 375		0,04	0,04	150	595 420		0,06	0,06	150	675 400		0,06	0,06	150	760 490
			200	500 410				200	640 490				200	775 445				200	860 525
			300	520 440				300	690 540				300	800 500				300	900 550
			400	530 465				400	705 570				400	815 555				400	- 600
	0,04	0,04	50	300 175		0,06	0,06	50	310 170		0,08	0,08	50	320 173		0,08	0,08	50	340 200
			75	355 225				75	385 230				75	400 220				75	445 250
			100	400 255				100	445 265				100	460 255				100	500 365
			125	430 285				125	490 295				125	505 290				125	555 400
	0,06	0,06	150	455 300		0,08	0,08	150	535 315		0,12	0,12	150	670 360		0,12	0,12	150	780 500
			200	500 335				200	600 355				200	700 315				200	800 500
			300	550 375				300	710 425				300	815 455				300	900 550
			400	585 400				400	775 475				400	865 500				400	- 660
	0,08	0,08	100	335 150		0,12	0,12	100	315 140		0,12	0,12	100	305 125		0,12	0,12	100	340 195
			125	375 180				125	355 150				125	345 125				100	400 220
			150	400 200				150	395 160				150	375 130				125	450 250
			200	455 225				200	450 180				200	420 155				150	500 280

Table 6 c:2 Mineral wool slabs Type Minwool slab 3060 or Rockwool slab 337 ( $\gamma \approx 150 \text{ kg/m}^3$ )

$q$	$\frac{A\sqrt{h}}{A_t}$	$\frac{A_i}{V_s}$	$\vartheta_{\max}$			$q$	$\frac{A\sqrt{h}}{A_t}$	$\frac{A_i}{V_s}$	$\vartheta_{\max}$			$q$	$\frac{A\sqrt{h}}{A_t}$	$\frac{A_i}{V_s}$	$\vartheta_{\max}$			$q$	$\frac{A\sqrt{h}}{A_t}$	$\frac{A_i}{V_s}$	$\vartheta_{\max}$		
			$d_i$	$d_j$	$d_i$				$d_i$	$d_j$	$d_i$				$d_i$	$d_j$	$d_i$				$d_i$	$d_j$	$d_i$
			30	50	70				30	50	70				30	50	70				30	50	70
20 {84}	0.01	200	325	250	200	40 {168}	0.02	100	370	275	215	60 {250}	0.02	50	400	285	220	90 {380}	0.04	50	415	295	220
		300	380	300	245			125	415	310	245			75	500	375	295			75	540	390	300
		400	415	335	275			150	455	345	270			100	565	440	350			100	620	465	365
	0.02	200	295	215	165		0.04	200	515	400	320		0.04	125	610	495	400		0.06	125	680	530	420
		300	355	265	210			300	585	475	390			150	640	530	440			150	725	580	465
		400	400	300	240			400	625	525	435			200	690	595	505			200	785	650	540
	0.04	300	300	205	150		0.06	100	300	205	155		0.08	300	735	660	580		0.12	300	-	745	635
		400	350	250	180		0.08	125	340	240	180		0.12	400	760	695	625			400	-	800	690
		400	320	200	135		0.12	150	380	270	205		0.12	75	355	250	190			75	320	220	165
	0.06	125	330	250	200		0.12	200	450	320	240		0.12	100	425	305	230		0.12	75	425	295	220
		150	355	270	225		0.12	300	535	400	300		0.12	125	485	350	270			100	510	360	270
25 {105}	0.01	200	395	315	260	45 {190}	0.02	125	295	195	140	75 {315}	0.04	150	525	390	300	120 {500}	0.08	125	570	410	315
		300	450	370	310			150	330	220	165			200	600	450	350			150	625	460	355
		400	480	405	340			400	600	450	350			300	690	550	430			200	710	530	420
	0.02	150	300	225	175		0.04	200	400	265	200		0.06	75	300	200	150		0.12	300	-	635	510
		200	350	260	205		0.06	300	495	340	240		0.06	100	360	250	185			400	-	700	570
		300	415	315	250		0.08	400	550	395	285		0.08	125	415	285	215			75	375	250	190
	0.04	200	300	210	150		0.08	200	350	225	155		0.12	150	465	325	240		0.12	100	450	310	230
		300	375	265	195		0.12	300	440	280	200		0.12	200	540	385	285			125	515	365	270
		400	430	310	225		0.12	400	500	340	230		0.12	300	650	475	360			150	570	400	300
	0.06	300	330	210	150		0.12	75	365	265	205		0.12	400	710	540	415			200	650	480	360
30 {126}	0.01	75	310	230	175	50 {210}	0.02	100	430	315	250	75 {315}	0.04	125	480	360	290	120 {500}	0.08	125	375	275	200
		100	355	270	215			125	480	360	290			150	520	400	320			150	425	305	230
		125	390	305	245			200	580	460	370			200	500	340	250			200	500	365	275
	0.02	150	420	335	270		0.04	300	645	540	450		0.06	300	605	435	305		0.12	300	765	585	450
		200	460	375	315		0.06	400	680	590	500		0.06	400	680	500	350			400	-	655	515
		300	500	425	365		0.08	100	325	230	175		0.08	125	370	250	180			100	325	230	175
	0.04	400	520	460	405		0.08	125	415	300	225		0.12	150	415	285	200			125	375	275	200
		125	320	235	185		0.12	200	485	350	270		0.12	200	500	340	250			150	425	305	230
		150	355	260	205		0.12	300	580	435	335		0.12	300	605	435	305			200	500	365	275
	0.06	200	405	305	240		0.12	400	640	495	385		0.12	400	680	500	350			300	765	585	450
35 {147}	0.01	150	300	210	155	50 {210}	0.02	125	325	220	160	75 {315}	0.04	150	340	240	180	120 {500}	0.08	125	355	240	190
		200	350	250	185			150	365	250	185			200	385	250	175			75	560	410	315
		300	440	315	235			200	405	305	240			300	480	370	300			75	680	525	420
	0.02	400	530	420	335		0.06	125	325	220	160		0.06	125	340	240	180		0.12	100	750	610	495
		150	300	210	155		0.08	150	365	250	185		0.08	150	385	250	175			125	-	670	560
		200	350	250	185		0.12	200	435	300	220		0.12	200	465	325	240			150	-	715	610
	0.04	300	440	315	235		0.12	300	535	375	275		0.12	300	540	385	285			200	-	785	685
		400	500	365	270		0.12	400	600	430	320		0.12	400	680	500	350			300	-	-	765
	0.06	200	305	200	140		0.12	150	320	210	150		0.12	75	360	250	185			400	-	-	-
		300	395	250	180		0.12	200	385	250	175		0.12	100	440	300	225			25	260	175	130
		400	450	300	210		0.12	300	480	315	225		0.12	125	500	350	260			50	430	300	225

Table 6 c:3 Sprayed mineral wool Type Cafco Blaze-Shield D C/F ( $\gamma \approx 300\text{--}370 \text{ kg/m}^3$ ) or Pyroguard 101 ( $\gamma \approx 250 \text{ kg/m}^3$ )

q	$\frac{AV\sqrt{h}}{A_t}$	$\frac{A_i}{V_s}$	$\vartheta_{\max}$			q	$\frac{AV\sqrt{h}}{A_t}$	$\frac{A_i}{V_s}$	$\vartheta_{\max}$			q	$\frac{AV\sqrt{h}}{A_t}$	$\frac{A_i}{V_s}$	$\vartheta_{\max}$			q	$\frac{AV\sqrt{h}}{A_t}$	$\frac{A_i}{V_s}$	$\vartheta_{\max}$		
			$d_i$ 10	$d_i$ 20	$d_i$ 30				$d_i$ 10	$d_i$ 20	$d_i$ 30				$d_i$ 10	$d_i$ 20	$d_i$ 30				$d_i$ 10	$d_i$ 20	$d_i$ 30
15 {63}	0.01	150	310	235	190	30 {126}	0.01	50	350	250	195	40 {168}	0.02	50	355	235	185	50 {210}	0.02	25	300	190	140
		200	350	265	215			75	415	310	250			75	435	305	240			50	440	300	230
		300	390	305	255			100	450	355	290			100	500	355	280			75	535	380	300
		400	415	335	280			125	480	385	325			125	535	400	320			100	595	445	350
	0.02	150	300	205	160		0.02	150	495	410	350		0.02	150	570	435	350		0.02	125	635	490	395
		200	345	240	185			200	520	450	385			200	615	490	400			150	665	530	430
		300	400	285	225			300	540	490	435			300	665	555	475			200	700	585	485
		400	450	325	255			400	550	515	470			400	690	600	520			300	735	655	565
	0.04	200	300	190	145		0.04	75	350	240	185		0.04	75	350	225	180		0.04	50	330	210	165
		300	365	240	180			100	400	280	220			100	415	270	215			75	415	275	215
		400	425	275	210			125	435	315	250			125	470	310	250			125	485	325	255
								150	470	350	275			150	510	345	275			150	590	400	325
20 {84}	0.01	75	295	215	170	40 {168}	0.02	100	340	215	170	50 {210}	0.04	100	345	225	170	60 {250}	0.06	75	355	220	175
		100	335	245	200			125	380	250	200			125	405	255	200			100	420	265	210
		125	365	275	225			150	420	275	215			150	450	280	225			125	480	310	240
		150	390	295	245			200	490	320	255			200	520	330	265			150	525	345	275
	0.02	200	405	295	235		0.04	300	580	395	315		0.06	300	625	415	325		0.06	200	600	405	325
		300	475	350	285			400	645	445	360			400	700	475	385			300	715	495	400
		400	515	390	320			125	320	200	160			125	360	210	170			400	785	565	455
								150	360	220	175			150	400	240	190			100	375	225	175
	0.04	150	315	200	150		0.06	200	425	265	210		0.08	200	480	290	225		0.08	125	435	260	200
		200	365	235	185			300	525	325	260			300	585	355	285			150	480	300	230
		300	450	295	225			400	590	375	300			400	665	410	330			200	560	350	275
		400	505	335	260			150	305	185	150			125	300	165	130			300	675	435	345
0.06	200	300	190	150	0.08	200	370	215	175	0.12	200	385	225	175	0.12	100	300	170	135				
	300	375	240	190		300	465	275	215		300	480	280	225		125	350	200	155				
	400	435	280	215		400	545	310	250		400	565	330	260		150	400	225	175				
						150	295	155	115		150	340	190	150		200	465	275	210				
0.08	300	350	200	155	0.12	200	320	190	145	0.12	300	480	280	225	0.12	300	580	340	265				
	400	400	225	190		300	405	240	175		400	565	330	260		400	675	400	310				
						400	500	285	200		50	400	275	215		300	305	170	125				
											100	490	345	275		400	380	200	155				
25 {105}	0.01	50	300	210	165	35 {147}	0.02	50	315	210	160	45 {190}	0.02	50	305	195	150	60 {250}	0.02	25	365	235	175
		75	360	260	210			75	390	270	210			75	390	250	200			50	525	365	285
		100	400	300	245			100	450	315	250			100	460	300	240			75	615	455	370
		125	425	330	270			125	485	355	280			125	515	345	275			100	665	520	430
	0.02	150	450	355	295		0.02	150	520	390	310		0.04	150	560	380	300		0.04	125	700	570	480
		200	480	395	330			200	570	440	360			200	630	440	350			150	725	610	520
		300	510	445	380			300	625	505	475			300	715	530	430			200	750	660	580
		400	525	475	415			400	655	550	465			400	765	595	485			300	775	710	645
	0.04	75	310	210	165		0.04	75	315	200	160		0.06	75	325	200	160		0.06	50	385	245	190
		100	355	250	195			100	380	245	195			100	460	300	240			75	480	315	250
		125	390	280	225			125	425	275	220			125	515	345	275			100	665	520	430
		150	420	305	245			150	465	310	250			150	560	380	300			125	700	570	480
0.06	200	470	350	280	0.06	200	540	365	290	0.08	200	630	440	350	0.08	150	725	610	520				
	300	535	405	335		300	635	440	350		300	715	530	430		200	750	660	580				
	400	570	450	375		400	685	495	400		400	765	595	485		300	775	710	645				
0.08	100	295	180	145	0.08	100	315	195	155	0.12	100	325	190	150	0.12	50	315	195	155				
	125	340	210	165		125	370	225	180		125	410	240	190		75	410	250	205				
	150	370	235	185		150	400	250	200		150	455	275	215		100	485	310	245				
	200	430	275	220		200	475	300	240		200	540	320	255		125	550	360	280				
0.12	300	510	340	270	0.12	300	575	370	295	0.12	300	650	405	325	0.12	150	600	400	315				
	400	575	390	305		400	650	425	350		400	675	455	365		200	675	465	380				
																300	755	560	455				
																400	-	680	585				
30 {126}	0.01	150	300	205	160	40 {168}	0.02	150	495	410	350	50 {210}	0.04	150	570	435	350	60 {250}	0.06	150	665	530	430
		200	345	240	185			200	520	450	385			200	615	490	400			150	665	530	430
		300	400	285	225			300	540	490	435			300	665	555	475			200	700	585	485
		400	450	325	255			400	550	515	470			400	690	600	520			300	735	655	565
	0.02	200	300	190	145		0.04	75	350	240	185		0.06	75	350	225	180		0.06	50	330	210	165
		300	365	240	180			100	400	280	220			100	415	270	215			75	415	275	215
		400	425	275	210			125	435	315	250			125	470	310	250			125	485	325	255
								150	470	350	275			150	510	345	275			150	590	400	325
	0.04	200	300	190	145		0.06	100	340	215	170		0.08	100	345	225	170		0.08	75	355	220	175
		300	365	240	180			125	380	250	200			125	405	255	200			100	420	265	210
		400	425	275	210			150	420	275	215			150	450	280	225			125	480	310	240
								200	490	320	255			200	520	330	265			150	525	345	275
0.06	200	405	295	235	0.08	300	580	395	315	0.12	300	625	415	325	0.12	200	600	405	325				
	300	475	350	285		400	645	445	360		400	700	475	385		300	715	495	400				
	400	515	390	320		125	320	200	160		125	360	210	170		400	785	565	455				
						150	360	220	175		150	400	240	190		100	375	225	175				
0.08	300	350	200	155	0.12	200	320	190	145	0.12	200	385	225	175	0.12	125	435	260	200				
	400	400	225	190		300	405	240	175		300	480	290	225		150	480	300	230				
						400	500	285	200		400	565	330	260		200	560	350	275				
																300	675	435	345				
35 {147}	0.01	50	300	210	165	45 {190}	0.02	50	315	210	160	50 {210}	0.04	50	305	195	150	60 {250}	0.06	25	365	235	175
		75	360	260	210			75	390	270	210			75	390	250	200			50	525	365	285
		100	400	300	245			100	450	315	250			100	460	300	240			75	615	455	370
		125	425	330	270			125	485	355	280			125	515	345	275			100	665	520	430
	0.02	150	450	355	295		0.04	150	520	390	310		0.06	150	560	380	300		0.06	125	700	570	480
		200	480	395	330			200	570	440	360			200	630	440	350			150	725	610	520
		300	510	445	380			300	625	505	475			300	715	530	430			200	750	660	580

$q$	$\frac{A\sqrt{h}}{A_t}$	$\frac{A_j}{V_s}$	$\vartheta_{\max}$			$q$	$\frac{A\sqrt{h}}{A_t}$	$\frac{A_j}{V_s}$	$\vartheta_{\max}$			$q$	$\frac{A\sqrt{h}}{A_t}$	$\frac{A_j}{V_s}$	$\vartheta_{\max}$		
			$d_j$ 10	$d_j$ 20	$d_i$ 30				$d_j$ 10	$d_j$ 20	$d_i$ 30				$d_j$ 10	$d_j$ 20	$d_i$ 30
75 {315}	0.04	25	300	185	145	90 {380}	0.04	25	360	220	175	120 {500}	0.04	25	490	300	235
		50	460	300	235			50	535	360	285			50	695	485	385
		75	570	390	305			75	675	470	365			75	-	605	490
		100	650	455	365			100	750	550	440			100	-	685	575
		125	710	515	420			125	-	610	500			125	-	740	635
		150	740	555	460			150	-	655	550			25	365	220	175
	0.06	200	-	635	525		0.06	200	-	730	625		0.06	50	570	365	285
		300	-	725	615			50	440	275	215			75	695	475	375
		50	375	235	185			75	555	360	285			100	780	560	455
		75	485	300	245			100	635	430	345			125	-	630	515
		100	570	365	295			125	705	490	395			150	-	690	570
		125	635	425	335			150	755	540	435		25	300	180	140	
	0.08	150	685	475	375		0.08	200	-	620	510		0.08	50	485	300	230
		200	760	545	440			300	-	725	615			75	610	395	305
		300	-	650	540			50	385	235	185			100	700	470	370
		400	-	720	605			75	500	310	240			125	775	535	425
		50	335	200	155			100	585	370	290			150	-	585	470
		75	435	265	205			125	655	430	335		200	-	675	550	
	0.12	100	515	325	255		0.12	150	710	475	375		0.12	50	385	230	180
		125	580	370	290			200	-	555	445			75	505	305	235
		150	635	410	325			300	-	665	550			100	600	375	285
		200	725	485	385			400	-	745	615			125	665	430	335
		300	-	590	475			50	310	185	140			150	730	480	375
		400	-	660	540			75	415	250	185		200	-	560	445	
	0.30	75	350	205	160		0.12	100	495	300	225		0.30	300	-	685	550
		100	425	250	200			125	560	345	260			400	-	765	630
		125	495	295	225			150	620	380	300			100	335	190	150
		150	550	325	250			200	715	450	350			125	400	220	170
		200	650	395	300			300	-	555	450			150	445	250	190
300		770	490	390	400	-		630	515	200	545	295	230				
0.30	400	-	555	450	0.30	125	310	180	135		300	685	385	295			
	150	300	165	130		150	350	200	155		400	785	450	350			
	200	345	195	155		200	415	230	185								
	300	470	245	195		300	550	295	230								
	400	555	290	230		400	640	345	275								

# 7 DETERMINATION OF THE MAXIMUM TEMPERATURE IN THE EVENT OF FIRE IN STEEL STRUCTURES WITH INSULATION IN THE FORM OF A SUSPENDED CEILING

## Calculation procedure:

Choose a suitable suspended ceiling

Determine the fictive insulation capacity  $(d_i/\lambda_i)_{fict}$  of the suspended ceiling

Determine the maximum steel temperature  $\theta_{max}$

Check the maximum temperature of the suspended ceiling

Table 7 a. Summary of results of fire tests on some suspended ceilings (Main Section, Section 7.4)

No	Make	Material	Resistance time in standard fire test (min)	Remarks	Estimated $(d_i/\lambda_i)_{fict}$ $\left(\frac{m^2 \cdot ^\circ C \cdot h}{kcal}\right)$	Estimated $(d_i/\lambda_i)_{fict}$ $\left(\frac{m^2 \cdot ^\circ C}{W}\right)$	Estimated critical suspended ceiling tempera- ture( $^\circ C$ )
1	Gyproc	2x13 mm gypsum plaster slabs no glass fibre reinforcement	30-40	All tests were discontinued because the suspended ceiling fell down. The critical temperature had not been reached in the steel girders	0,075	0,064	625
2		1x13 mm gypsum plaster slabs 0.25% g f r	48		0,075	0,064	650
3		1x16 mm gypsum plaster slabs 0.25% g f r	49		0,10	0,086	650
4		2x13 mm gypsum plaster slabs 0.25% g f r	60		0,15	0,129	650
5		3x13mm gypsum plaster slabs 0.25% g f r	75-80		0,25	0,215	625
6		2x20 mm gypsum plaster slabs 0.25% g f r	80		0,30	0,258	625
7	WST	2x13 mm gypsum plaster slabs with 13 mm mineral wool between them	45	All tests were discontinued for the same reason as above. The gypsum plaster slabs were not reinforced	0,30	0,258	550
8		2x13 mm gypsum plaster slabs with 13 mm mineral wool between them	50		0,30	0,258	550
9		2x13 mm gypsum plaster slabs with 43 mm straw between them	47		0,30	0,258	550
10		2x13mm gypsum plaster slabs with 43 mm straw between them	54		0,30	0,258	550
11	Ingenjörss- firma Zero	Soundex special suspended ceiling tiles. Cast glass fibre reinforced gypsum plaster tiles with "ridges" in a grid pattern. Tile thickness 18 mm, at the ridges 38 mm	90	Parts of the ceiling fell down after 90 minutes. Max. steel temperature approx. 440 $^\circ C$	0,15	0,129	700
12	Consensus	Armstrong 13 mm thick	30	No visible damage to suspended ceiling. Max steel temperature about 450 $^\circ C$	0,05	0,043	550
13		Mineral wool acoustic 16 mm thick	80		0,075	0,064	>(725) <sup>a</sup>
14		Type minaboard 13 mm thick	85	No visible damage to suspended ceiling. Max steel temperature about 300 $^\circ C$	0,075	0,064	>(725) <sup>a</sup>
15	Dansk Eternitfabrik	Deflamit-Asbestolux (9 mm Deflamit + 15 mm mineral wool + 8 mm eternit)	50		0,20	0,172	>(675) <sup>a</sup>
16	Nordakustik	Celotex Acoustiformat 15 mm thick glass fibre slab	90		0,10	0,086	(725) <sup>a</sup>
17	Rockwool	Rockfon Decor 85l (15 mm thick mineral wool slab)	60	No visible damage to suspended ceiling. Max steel temperature about 450 $^\circ C$ . The test was dis- continued because the suspended ceiling fell down. The critical temperature had not been reached in the steel girders.	0,20	0,172	600

<sup>a</sup> No damage to the suspended ceiling. Calculated temperature in the suspended ceiling when the test was discontinued.



Table 7 b. Maximum steel temperature  $\vartheta_{\max}$  ( $^{\circ}\text{C}$ ) for a steel structure with insulation in the form of a suspended ceiling as a function of the equivalent fire load  $q$  ( $\text{Mcal}/\text{m}^2$ )  $\{\text{MJ}/\text{m}^2\}$ , the equivalent opening factor  $A\sqrt{h}/A_t$  ( $\text{m}^{1/2}$ )<sup>a</sup> and the  $F_s/V_s$  ratio of the construction ( $\text{m}^{-1}$ )<sup>b</sup> for different values of the thermal resistance  $(d_i/\lambda_i)_{\text{fict}}$  ( $\text{m}^2 \text{ }^{\circ}\text{Ch}/\text{kcal}$ )<sup>c</sup> of the suspended ceiling. The maximum temperature in the suspended ceiling is given in brackets. The given values of temperature assume that the floor slab is of concrete (Main Section, Chapter 7)

<sup>a</sup>When the opening factor  $A\sqrt{h}/A_t$  is greater than  $0.12 \text{ m}^{1/2}$ , the value of  $0.12 \text{ m}^{1/2}$  shall be used

<sup>b</sup> $F_s$  denotes the surface area of the girder per metre run of girder, less the part covered by the floor slab.  $V_s$  denotes the volume of the girder per metre run of the girder (see Chapter 5 in the Design Section)

$$^c \begin{cases} 0,05 \text{ m}^2 \text{ }^{\circ}\text{Ch}/\text{kcal} = 0,043 \text{ m}^2 \text{ }^{\circ}\text{C}/\text{W} \\ 0,10 \text{ } \gg \gg = 0,086 \text{ } \gg \\ 0,20 \text{ } \gg \gg = 0,172 \text{ } \gg \\ 0,30 \text{ } \gg \gg = 0,258 \text{ } \gg \end{cases}$$

q	$\frac{A\sqrt{h}}{A_t}$	$\frac{F_s}{V_s}$	Maximum steel temperature $\vartheta_{\max}$ and ( ) maximum suspended ceiling temperature				q	$\frac{A\sqrt{h}}{A_t}$	$\frac{F_s}{V_s}$	Maximum steel temperature $\vartheta_{\max}$ and ( ) maximum suspended ceiling temperature				
			$(d_i/\lambda_i)_{\text{fict}}$							$(d_i/\lambda_i)_{\text{fict}}$				
			0,05	0,10	0,20	0,30				0,05	0,10	0,20	0,30	
15 {63}	0,02	50	130	90	65	50	60 {250}	0,02	50	435	315	200	160	
		100	180	(470)	130 (440)	90 (410)			70 (390)	100	450 (615)	340 (570)	240 (530)	185 (500)
		200	230		170	115			90	200	455	350	250	200
		300	260		190	130			100	300	455	350	250	200
	0,04	50	100	70	45	40		0,04	50	340	225	145	110	
		100	150	(565)	100 (530)	65 (500)			50 (475)	100	400 (680)	285 (630)	185 (590)	140 (560)
		200	200		140	90			70	200	435	320	220	165
		300	240		170	110			80	300	445	330	230	180
	0,08	50	65	50	35	25		0,08	50	250	160	100	75	
		100	95	(675)	70 (630)	50 (590)			40 (570)	100	340 (750)	225 (700)	130 (650)	100 (625)
		200	150		100	65			50	200	415	285	185	135
		300	190		125	90			60	300	445	315	210	155
	0,12	50	40	35	30	25		0,12	50	190	120	75	60	
		100	60	(735)	45 (690)	40 (650)			30 (620)	100	285 (780)	185 (725)	110 (680)	80 (660)
		200	120		70	50			40	200	375	250	155	110
		300	155		100	60			45	300	420	290	185	130
25 {105}	0,02	50	200	140	95	75	90 {380}	0,02	50	475	330	205	150	
		100	260	(510)	185 (470)	125 (435)			100 (420)	100	510 (740)	370 (680)	250 (630)	190 (600)
		200	300		225	155			120	200	515	385	270	210
		300	320		245	170			130	300	515	385	270	215
	0,04	50	160	110	75	55		0,04	50	345	225	130	100	
		100	230	(600)	150 (565)	100 (530)			75 (515)	100	430 (790)	290 (730)	180 (675)	130 (650)
		200	290		205	135			100	200	480	340	225	170
		300	325		235	155			115	300	495	360	250	190
	0,08	50	115	75	50	40		0,08	50	560	400	260	200	
		100	160	(680)	110 (635)	70 (595)			55 (570)	100	570 (780)	420 (715)	290 (660)	220 (630)
		200	240		160	100			75	200	575	425	300	230
		300	285		195	120			90	300	575	425	300	230
	0,12	50	80	60	40	30		0,12	50	425	280	160	120	
		100	130	(740)	80 (690)	60 (650)			45 (620)	100	495 (810)	345 (750)	210 (695)	160 (670)
		200	190		125	80			60	200	520	375	250	195
		300	235		160	100			75	300	525	385	260	205
40 {168}	0,02	50	300	220	145	110	120 {500}	0,02	50	300	220	145	110	
		100	360	(560)	260 (520)	175 (480)			135 (460)	100	360	260	175	135
		200	380		290	200			160	200	380	290	200	160
		300	385		295	210			165	300	385	295	210	165
	0,04	50	240	160	105	80		0,04	50	315	220	140	100	
		100	315	(645)	220 (600)	140 (560)			100 (535)	100	375	270	180	135
		200	375		270	180			135	200	375	270	180	135
		300	390		290	195			150	300	390	290	195	150
	0,08	50	170	110	70	55		0,08	50	170	110	70	55	
		100	245	(715)	160 (665)	100 (625)			75 (600)	100	245	160	100	75
		200	335		220	140			105	200	335	220	140	105
		300	380		260	165			120	300	380	260	165	120
	0,12	50	130	85	55	45		0,12	50	130	85	55	45	
		100	200	(750)	130 (700)	85 (660)			60 (630)	100	200	130	85	60
		200	290		190	115			85	200	290	190	115	85
		300	340		225	145			100	300	340	225	145	100

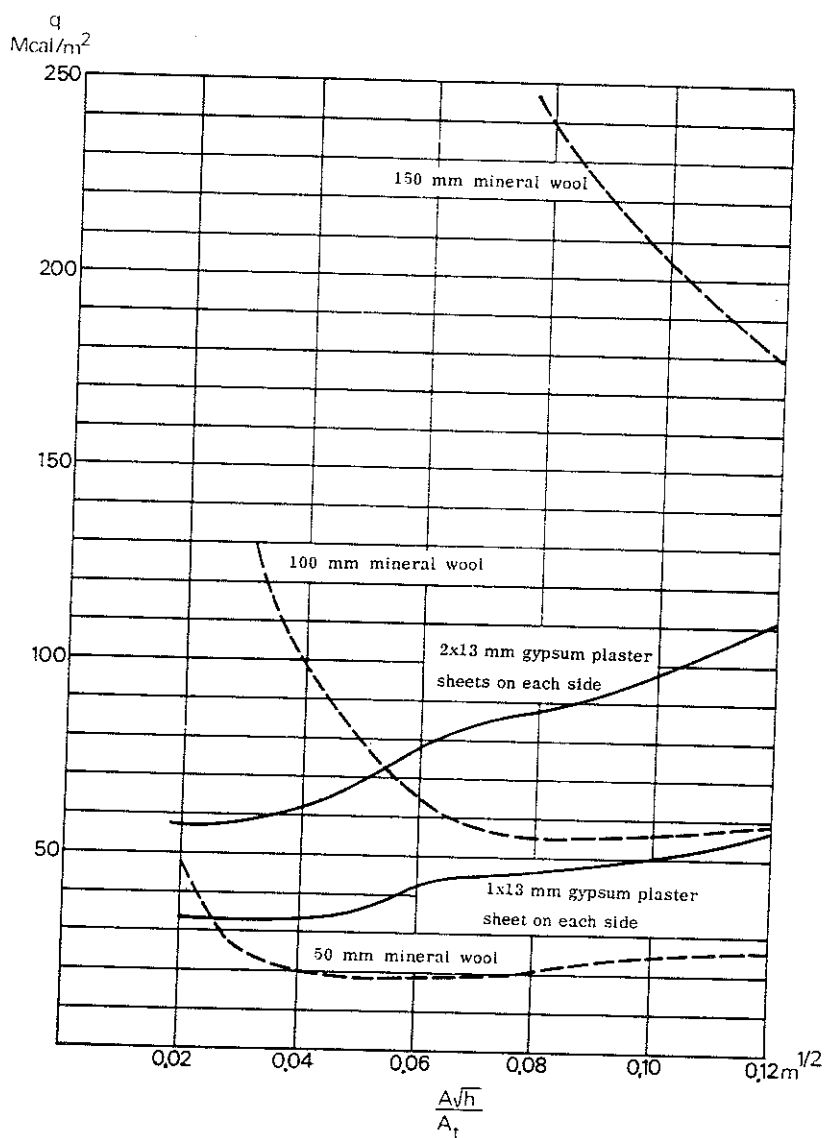
## 8 CHECK ON THE FUNCTION OF PARTITIONS

Fig. 8 a. Curves showing the maximum values of the equivalent fire load  $q$  for which some types of wall satisfy the temperature requirements stipulated for partitions at varying equivalent opening factor  $A\sqrt{h}/A_t$ .

— Wall of steel studs with one or two 13 mm sheets of gypsum plasterboard, of density  $\gamma \approx 790 \text{ kg/m}^3$ , on each side

---- Wall consisting of mineral wool insulation of 50, 100 and 150 mm thickness and of density  $\gamma \approx 45 \text{ kg/m}^3$  between arbitrarily chosen incombustible external layers.

If the opening factor  $A\sqrt{h}/A_t$  is greater than  $0.12 \text{ m}^{1/2}$ , the value of  $0.12 \text{ m}^{1/2}$  shall be used. { The fire load in  $\text{MJ/m}^2$  is obtained by multiplying the fire load values in the figure by the factor 4.2 } (Main Section, Chapter 8)



## 9 DETERMINATION OF THE CRITICAL LOAD FOR STEEL GIRDERS UNDER FIRE EXPOSURE CONDITIONS

### Calculation procedure:

Determine the rate of heating

Determine the critical load

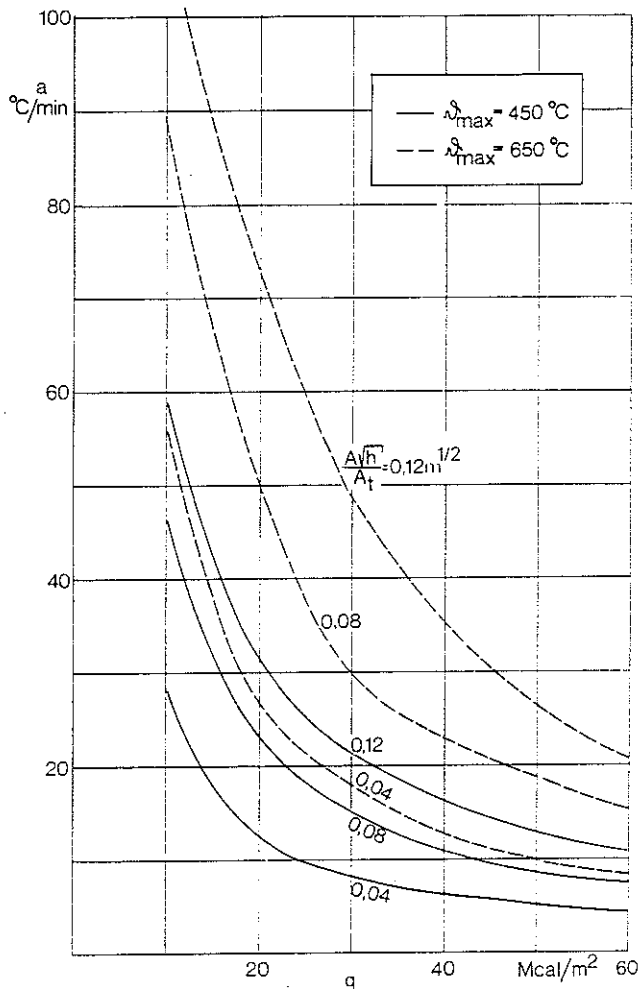


Fig. 9 a. Average rate of heating  $\dot{a}$  as a function of the equivalent fire load  $q$  for different values of the equivalent opening factor  $\frac{A_v h}{A_t}$  of the fire compartment and for different maximum steel temperatures  $\theta_{max}$ . {The fire load expressed in MJ/m² is obtained by multiplying the fire load values in the figure by the factor 4.2} (Main Section, Subsection 9.2.2)

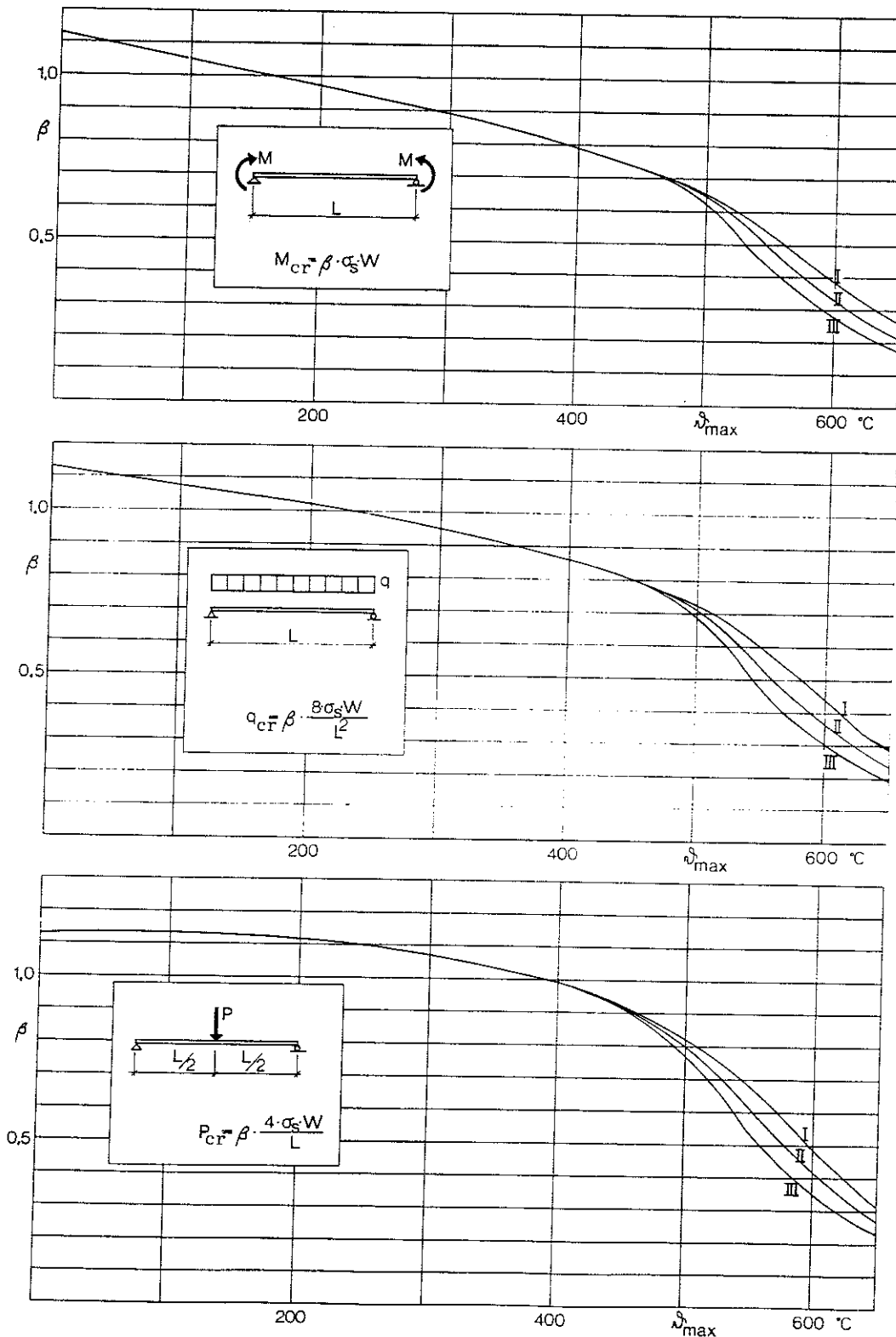
Fig. 9 b. The coefficient  $\beta$  for determination of the critical load, under fire exposure conditions, for steel girders of mild structural steel for different types of loading and statical system, as a function of the maximum steel temperature  $\vartheta_{\max}$  for different rates of heating and associated rates of cooling (I, II, III) (Main Section, Subsections 9.2.2 and 9.2.3)

Curve rate of heating ( $^{\circ}\text{C}/\text{min}$ ) rate of cooling ( $^{\circ}\text{C}/\text{min}$ )

I	100	33.3
II	20	6.67
III	4	1.33

Symbols

$M_{cr}, q_{cr}, P_{cr}$  = critical load (kgf cm) {MNm}, (kgf/cm) {MN/m}, (kgf) {MN}  
 $W$  = elastic modulus of section ( $\text{cm}^3$ ) { $\text{m}^3$ }  
 $\sigma_s$  = yield stress of material at room temperature (kgf/cm<sup>2</sup>) {MPa}  
 $L$  = span of girder (cm) {m}



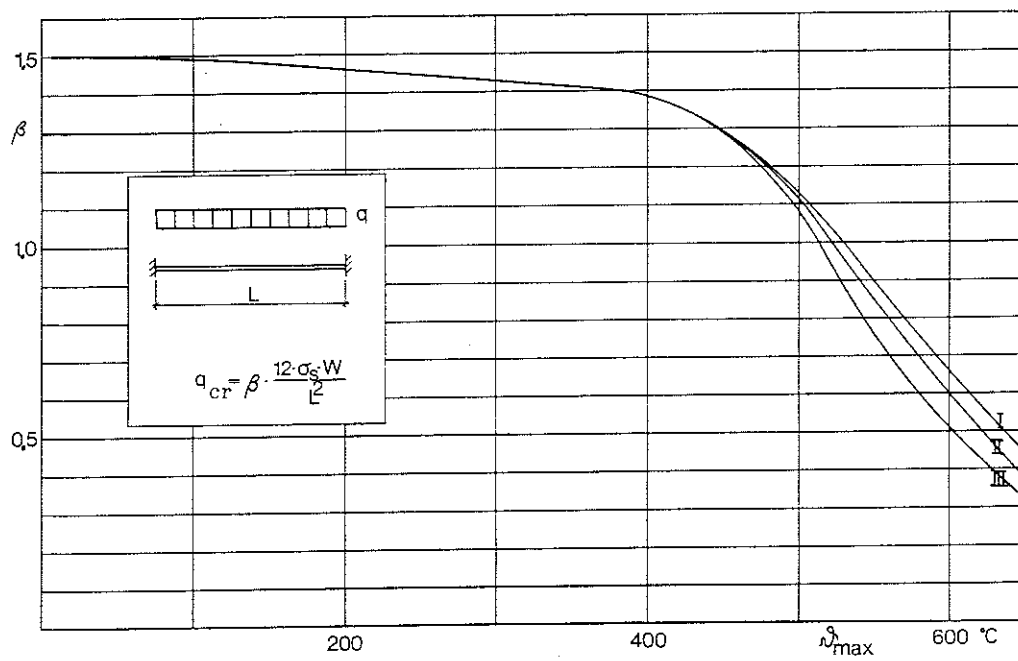
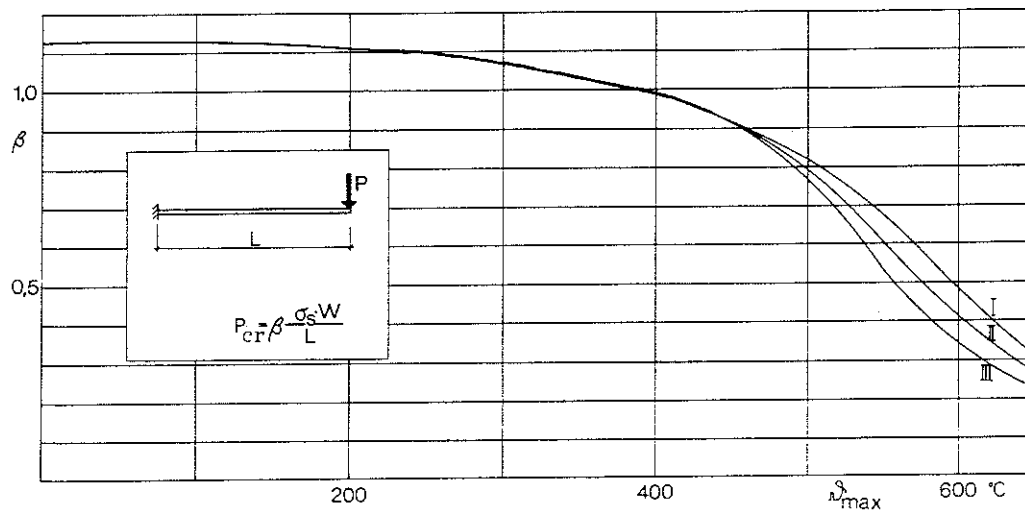
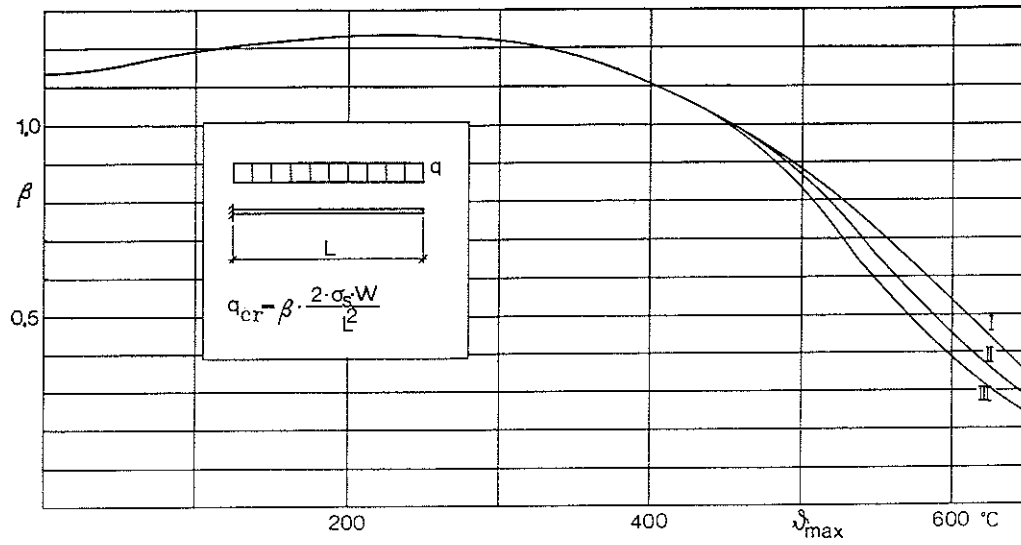
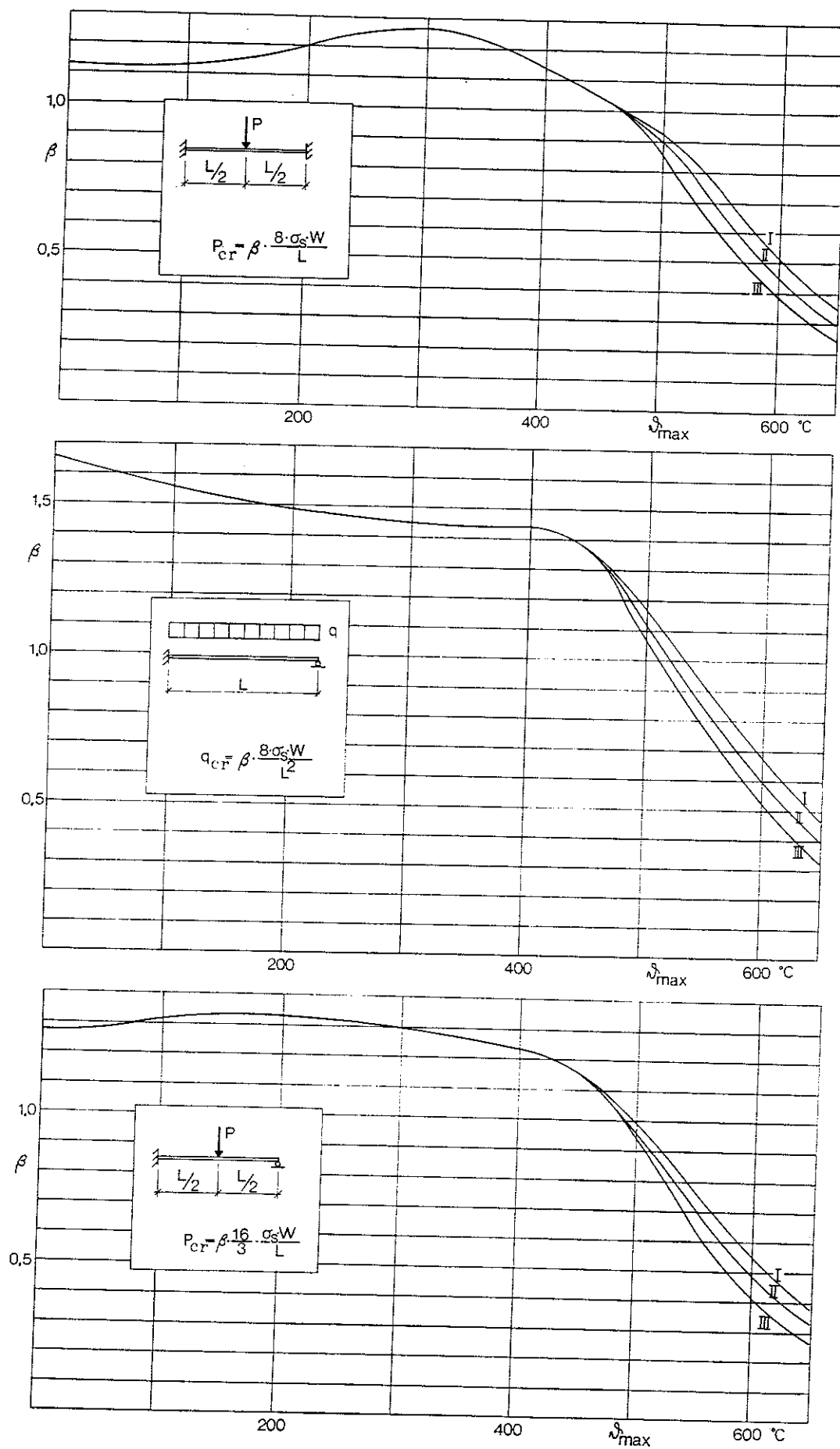


Fig.9b



# DETERMINATION OF THE CRITICAL LOAD FOR STEEL COLUMNS UNDER FIRE EXPOSURE CONDITIONS

## Calculation procedure:

Determine the degree of expansion if longitudinal expansion is restrained  
Determine the critical load

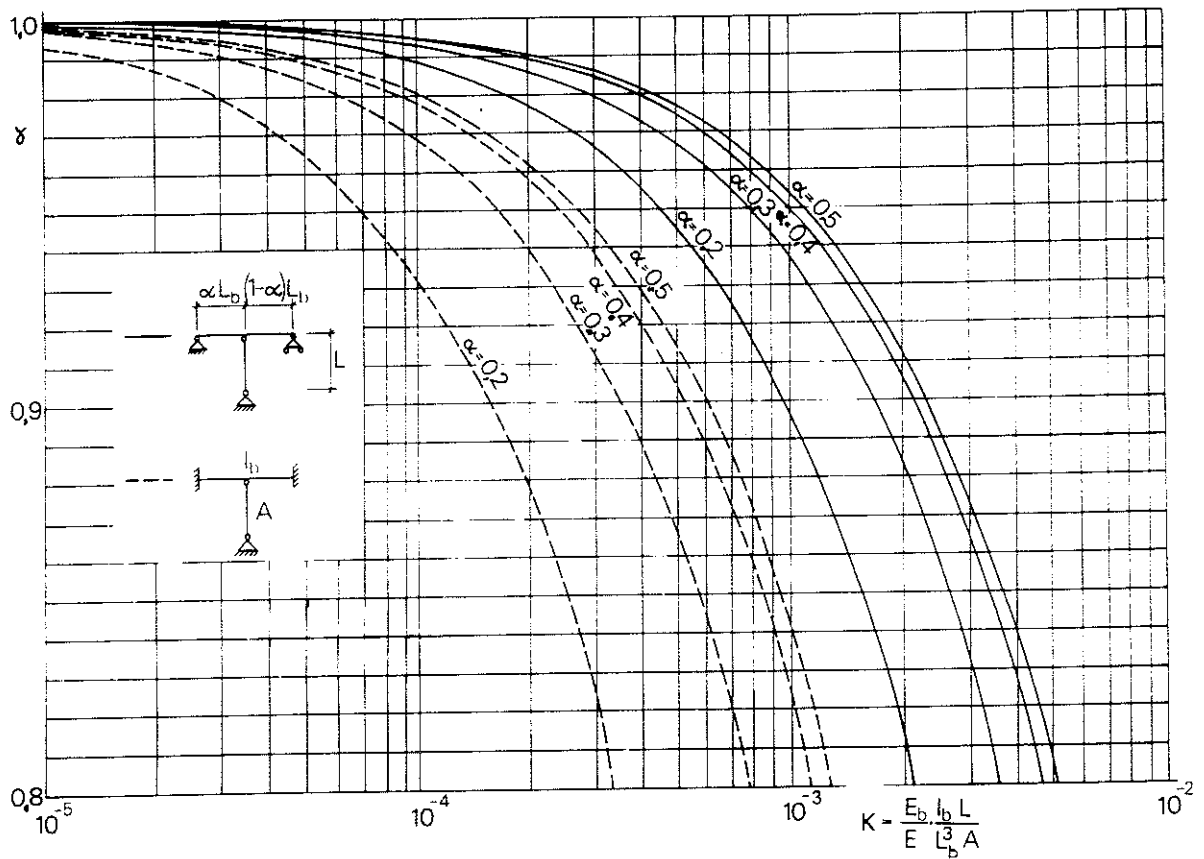
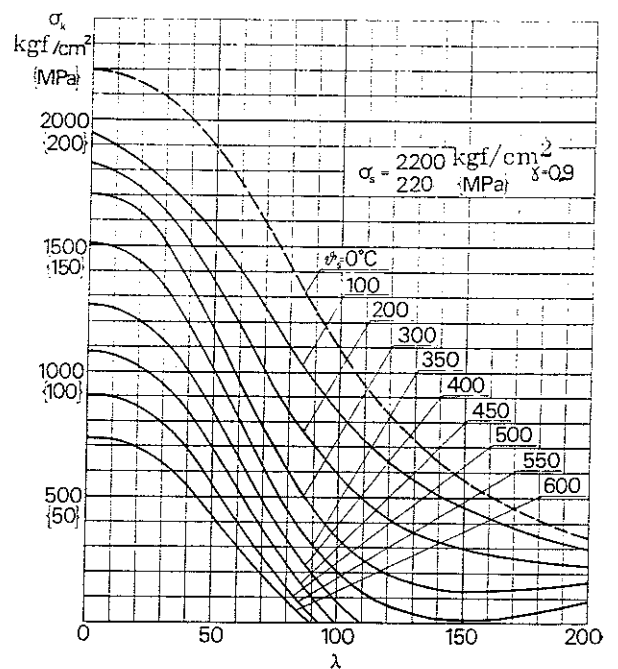
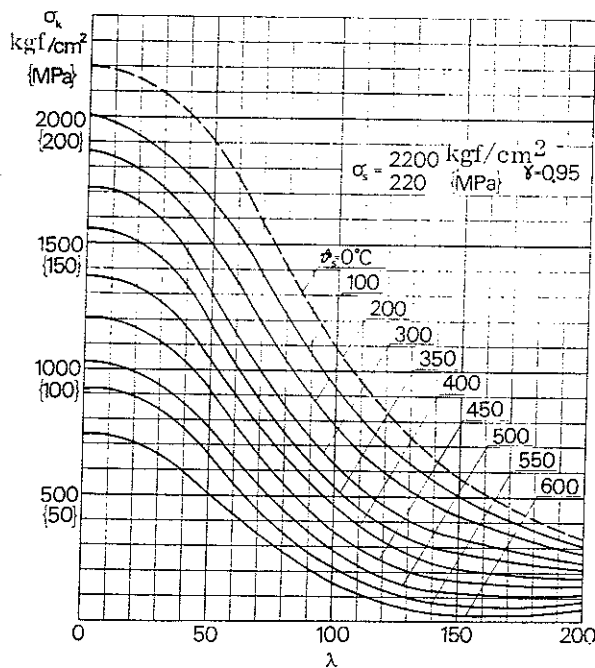
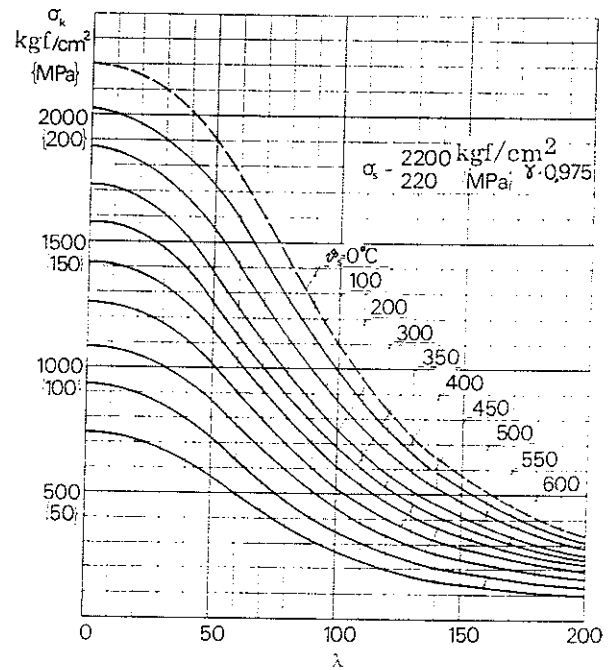
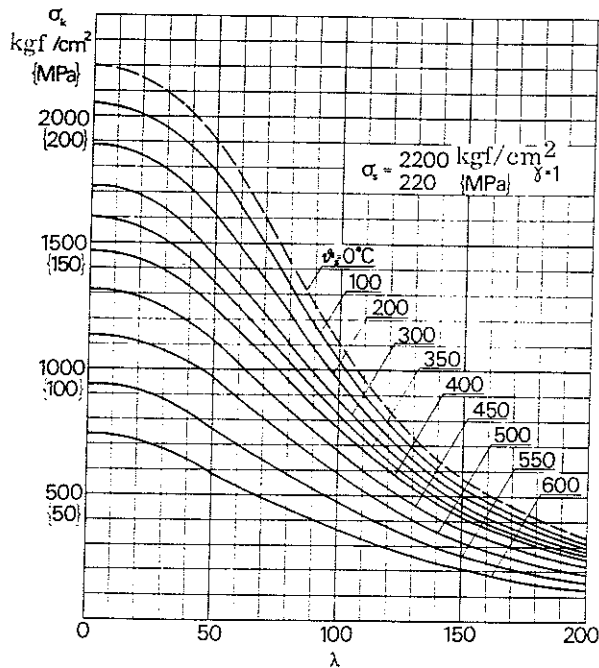


Fig. 10 a. The coefficient  $\gamma$  which indicates the degree of expansion under fire exposure conditions in columns connected to a simply supported beam and a beam rigidly restrained at both ends, respectively, as a function of the nondimensional parameter  $K$ . In the expression for  $K$ ,  $E_b$  denotes the modulus of elasticity of the beam at the temperature concerned, (see Fig. 9.1 a in the Main Section), and  $E$  denotes the modulus of elasticity (secant modulus) of the column at the temperature and stress concerned, inclusive of the additional stress due to partial restraint on longitudinal expansion of the column (see Fig. 10.1 b in the Main Section).  $L_b$  and  $L$  denote the lengths of the beam and column, and  $I_b$  and  $A$  the moment of inertia of the beam and the area of column cross section, respectively (Main Section, Subsection 10.2.1)

Fig. 10 b. Critical buckling stress  $\sigma_k$  as a function of the steel temperature  $\theta_s$  and slenderness ratio  $\lambda$  for a column under fire exposure conditions, made of structural steel with a nominal yield stress at room temperature of  $\sigma_s = 2200$  {220}, 2600 {260} and 3200 kgf/cm<sup>2</sup> {320 MPa}.  $\gamma$  = coefficient indicating degree of expansion. When  $\gamma \neq 1$ , the cross sectional factor  $i/d$  influences the shape of the curves, but this influence is comparatively limited. The curves given have therefore been generally determined for  $i/d = 0,5$ , which for normal types of section results in design on the safe side. For determination of the critical load in a structure subject to simultaneous flexure and compression, see Section 10.3 in the Main Section. For determination of the critical load in a structure where there is a risk of out-of-plane buckling, see Section 10.4 in the Main Section





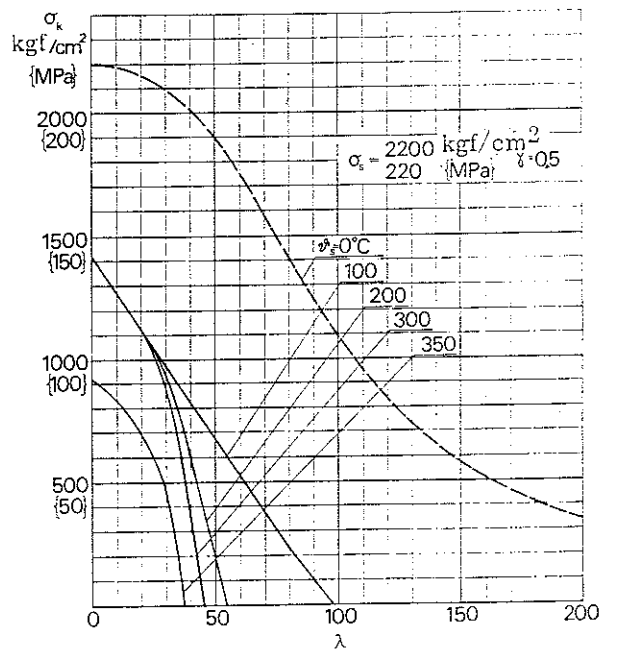
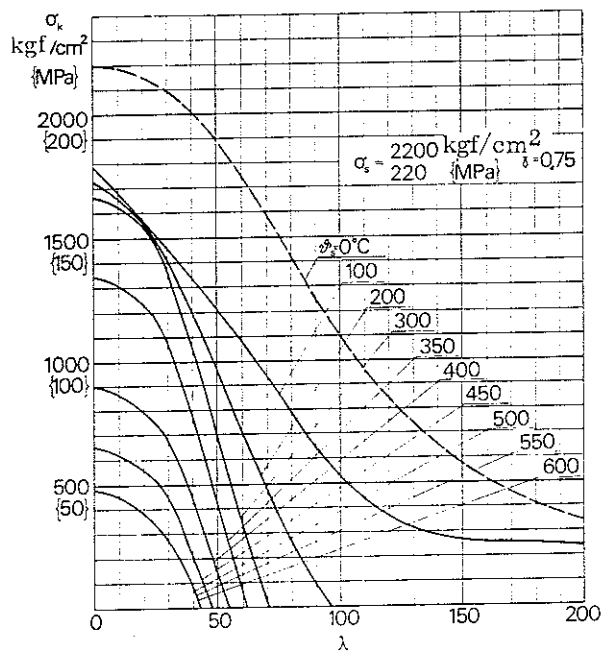
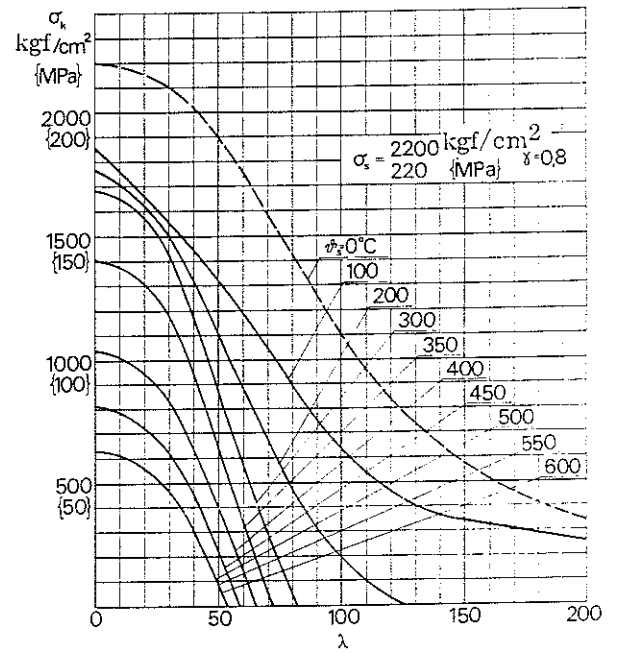
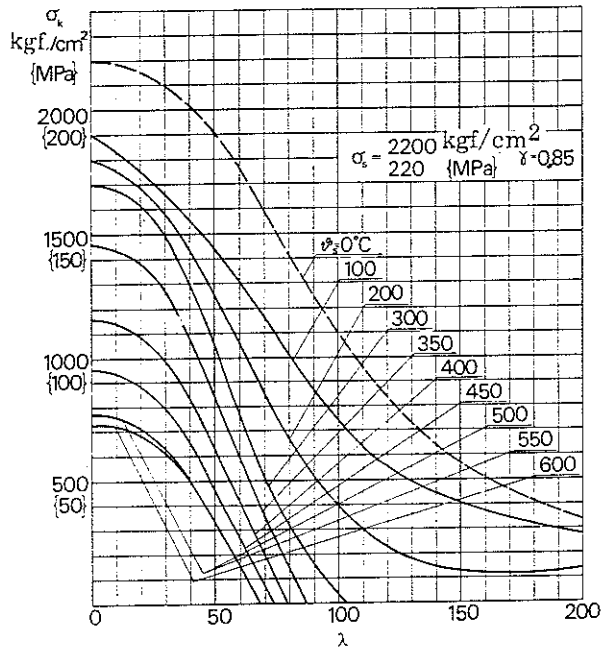
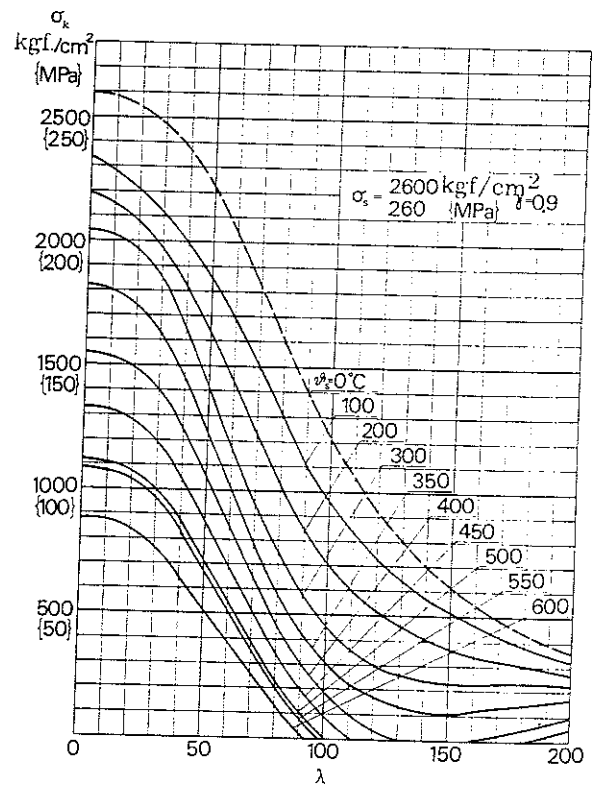
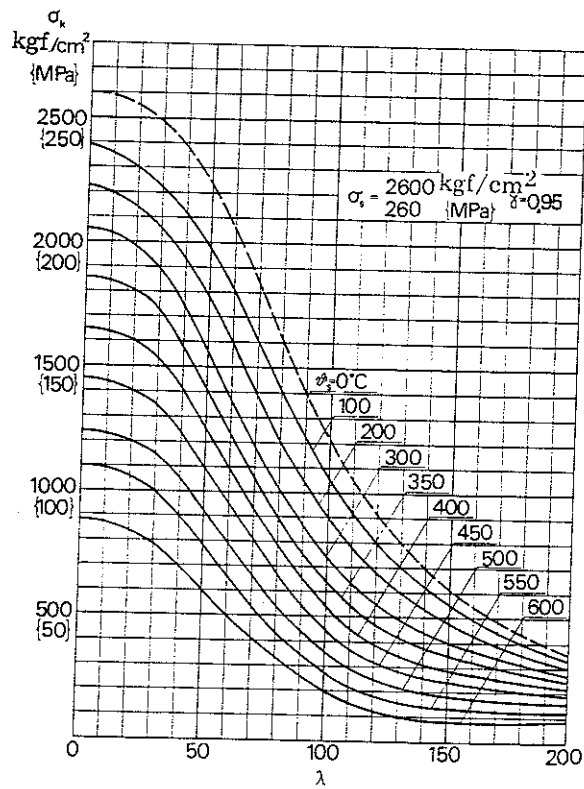
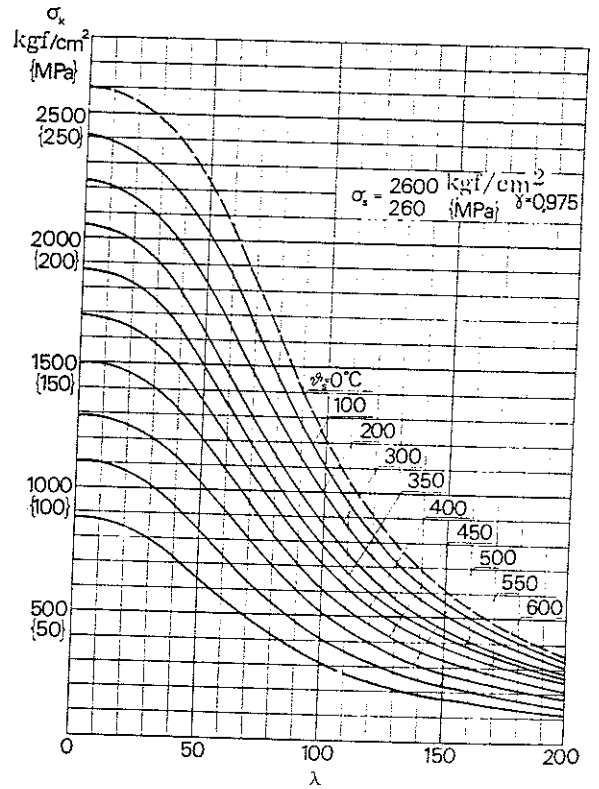
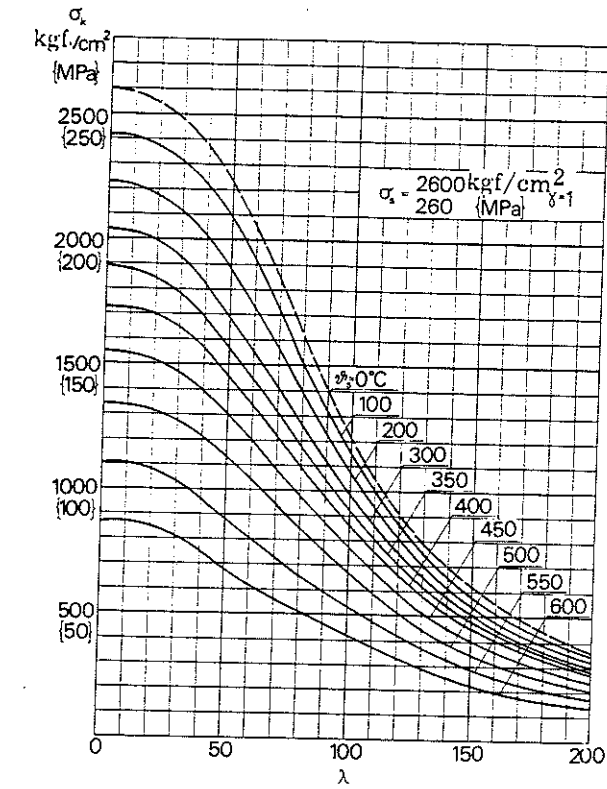
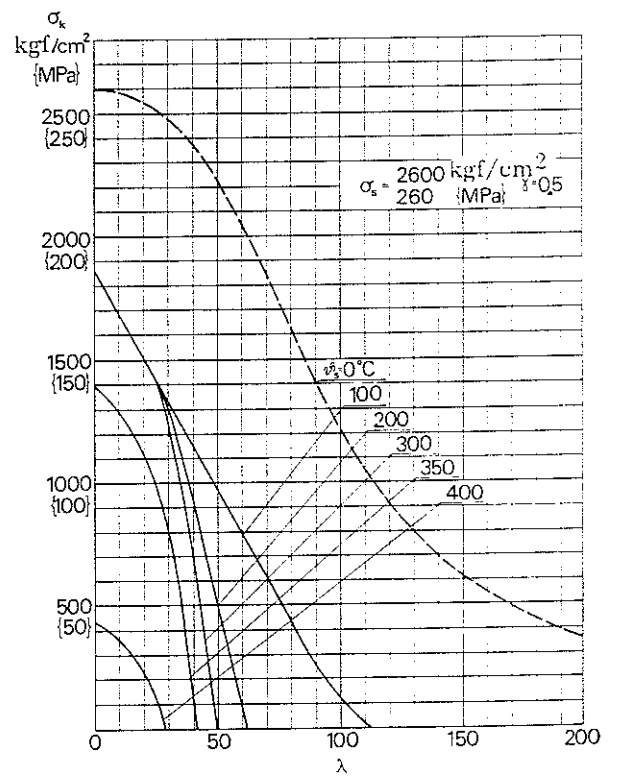
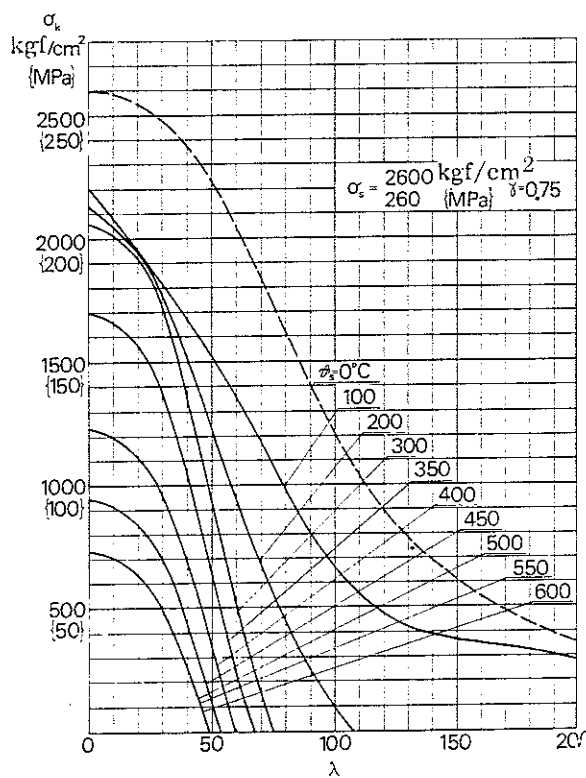
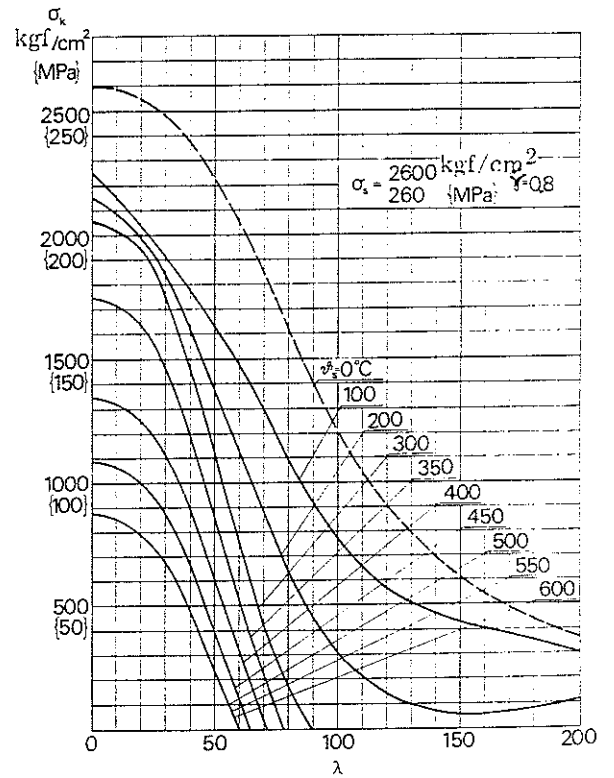
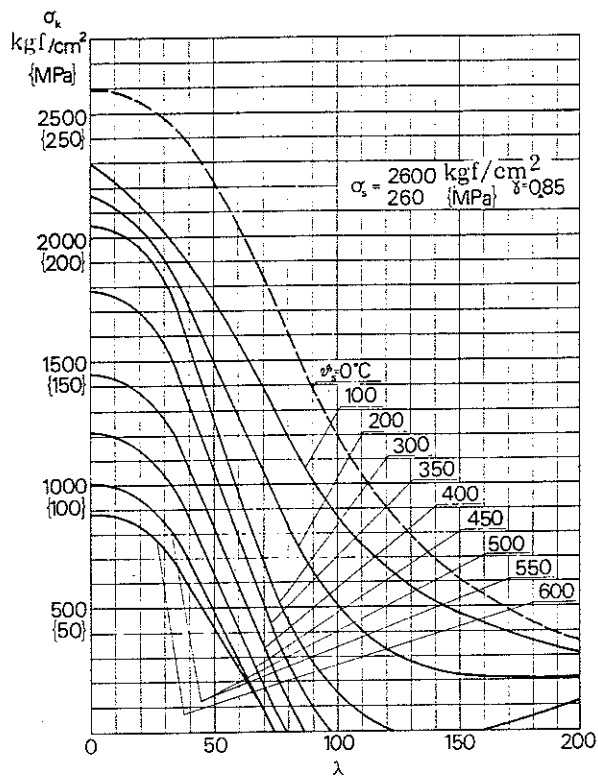
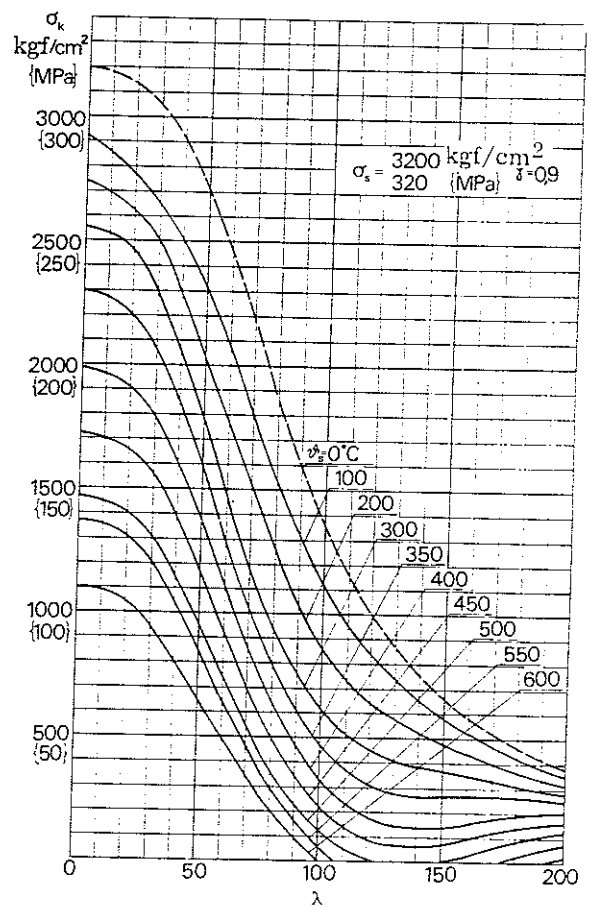
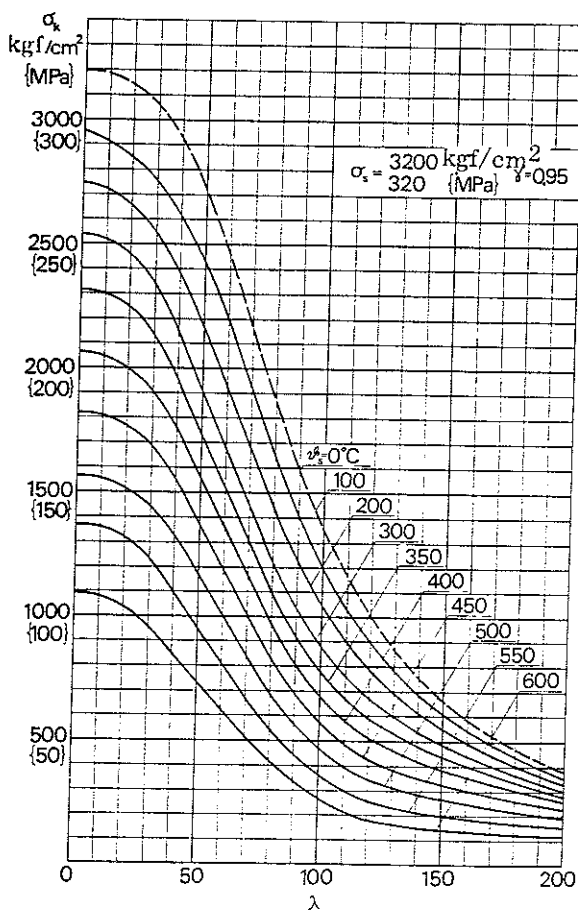
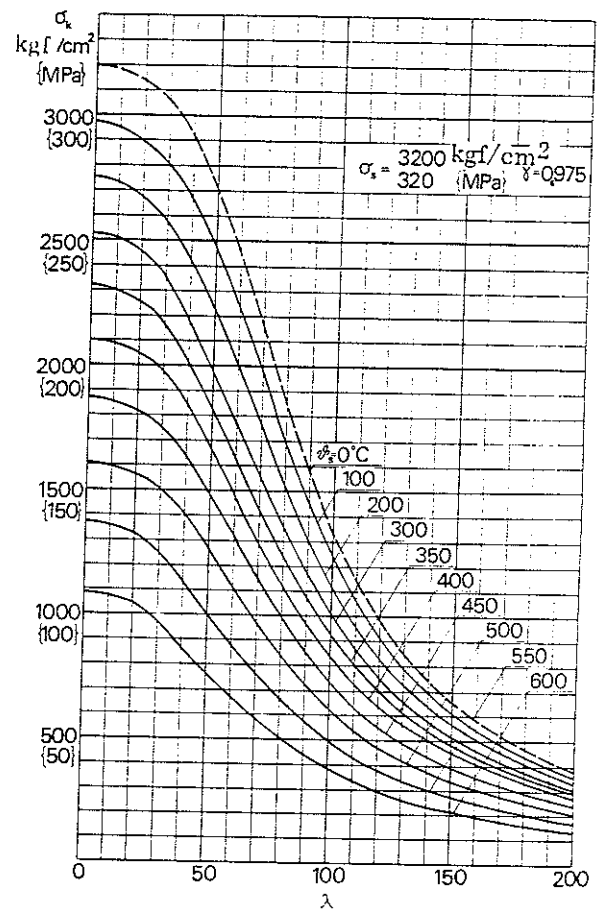
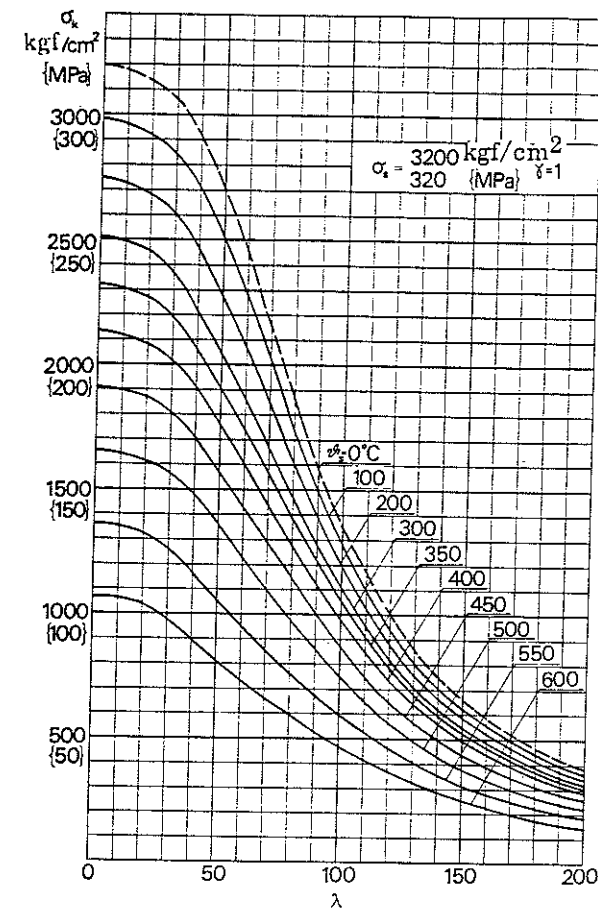
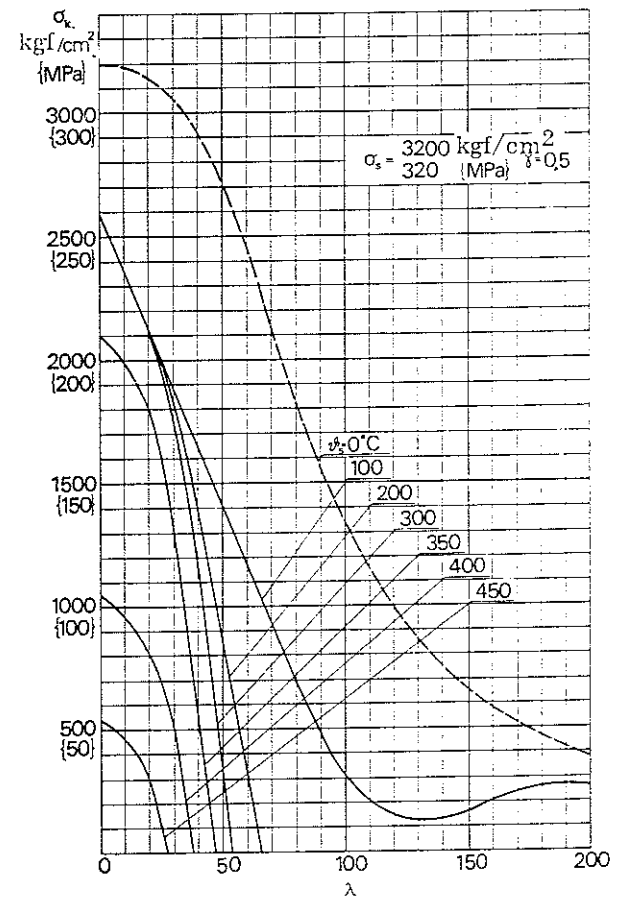
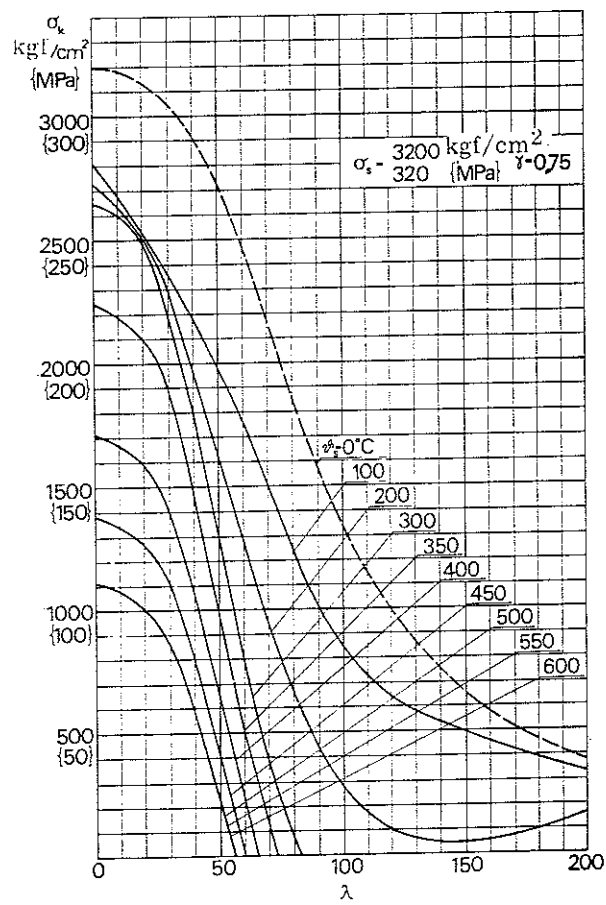
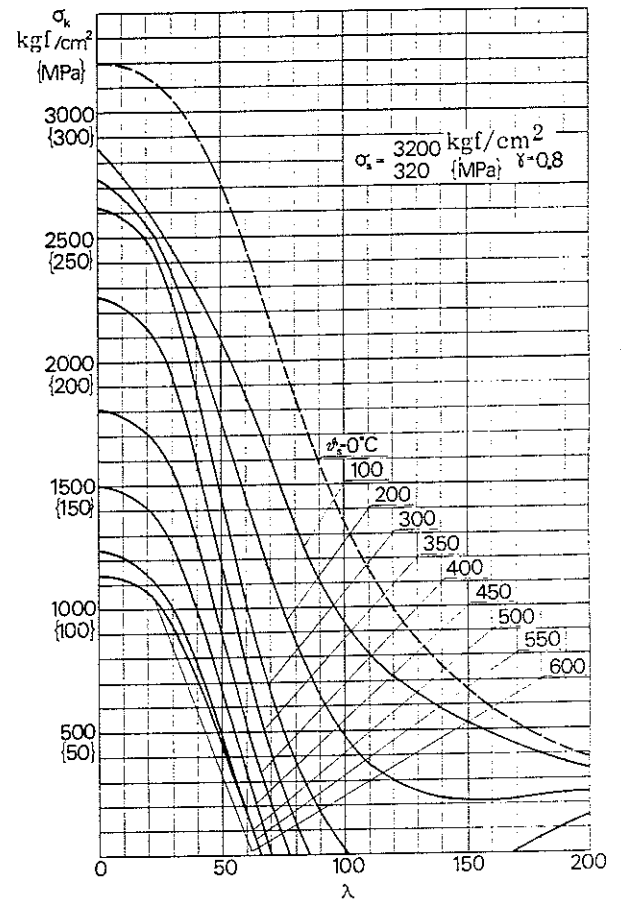
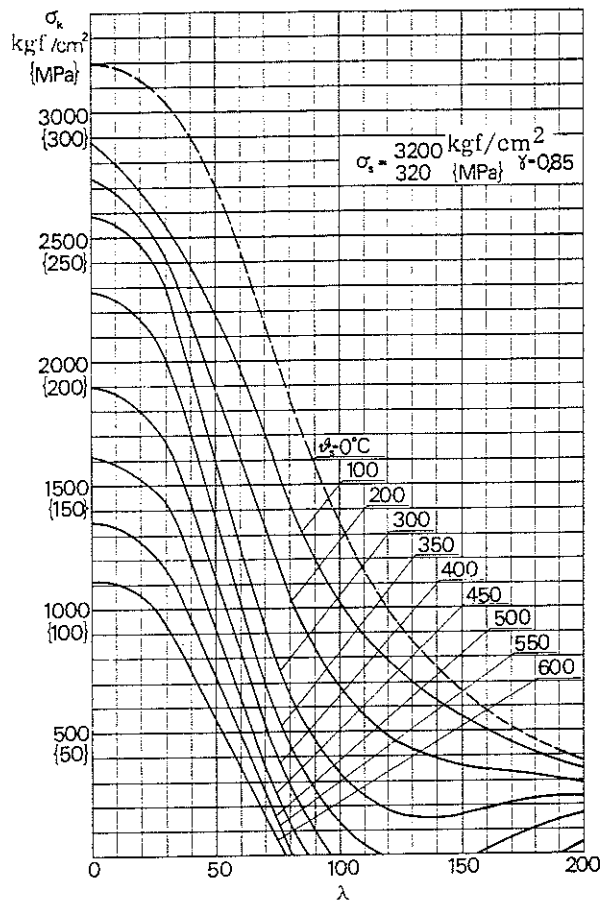


Fig.10b













Unless specially stated to the contrary, references made in the examples to tables and figures relate to those in the Design Section.

- Example 1. Fire engineering design of loadbearing steel structure in a five-storey hotel building
- Example 2. Fire engineering design of loadbearing steel structure in a three-storey residential building
- Example 3. Fire engineering design of steel floor girders in an eight-storey office building
- Example 4. Fire engineering assessment of a suspended ceiling which had been subjected to a standard fire test
- Example 5. Check on partition
- Example 6. Fire insulation of steel columns
- Example 7. Determination of the critical fire load
- Example 8. Fire engineering design of steel column whose longitudinal expansion is subject to restraint
- Example 9. Fire insulation of steel column subject to an axial and transverse load
- Example 10. Calculation of opening factor and the number of air changes



# EXAMPLE 1. FIRE ENGINEERING DESIGN OF LOADBEARING STEEL STRUCTURE IN A FIVE-STOREY HOTEL BUILDING

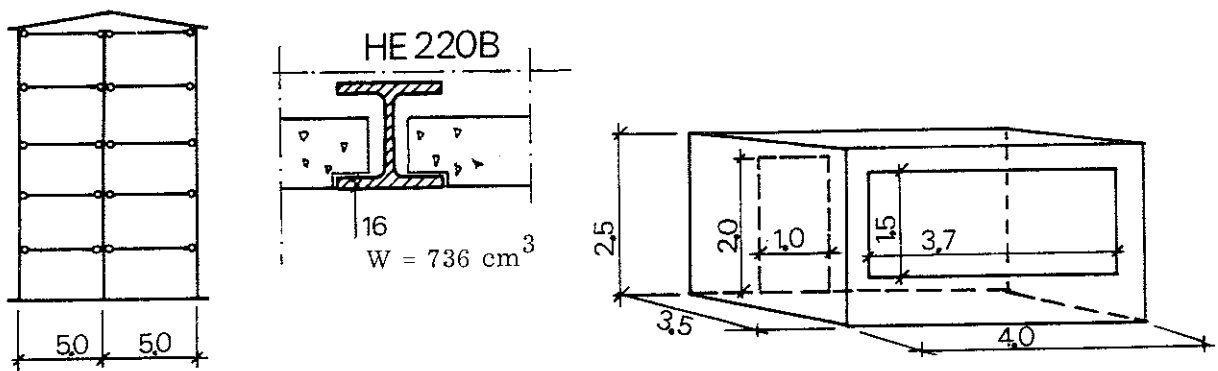
The loadbearing frame in a five-storey hotel building consists of simply supported HE 220 B steel girders and hollow steel columns of square section. The material in the girders and columns is Steel 1412 with a nominal yield stress  $\sigma_s = 2600$  kgf/cm<sup>2</sup> { 260 MPa }.

On the top storey the columns have the external dimension 90x90 mm and a wall thickness of 5.6 mm. The area of cross section is 18.6 cm<sup>2</sup> and the slenderness ratio  $\lambda = 73$ . On the bottom storey the columns have the external dimension 180x180 mm and a wall thickness of 11 mm. The area of cross section is 71.2 cm<sup>2</sup> and the slenderness ratio  $\lambda = 37$ . The columns on the intermediate storeys have dimensions and slenderness ratios between these values. The span of the girders is 5.0 m, and the girders are spaced at 4.0 m centres.

Floor slabs of concrete are carried on the bottom flanges of the girders as shown in the figure. The dead weight of the floor construction on all storeys is 700 kgf/m<sup>2</sup> { 7 kN/m<sup>2</sup> }. The load due to the attic floor slab including the roof and snow load is 800 kgf/m<sup>2</sup> { 8 kN/m<sup>2</sup> }. The attic cannot be used for storage. The dimensions (internal) of the fire compartment and the sizes of the openings are as shown in the figure. As regards the construction surrounding the fire compartment, the floor consists of precast concrete units and the external walls of surface layers of steel sheeting with intermediate 100 mm thick mineral wool insulation. The other walls are made up of steel studs covered on each side with two 13 mm gypsum plaster sheets.

Complete evacuation of people from the building in the event of fire cannot be assumed with absolute certainty.

Check whether the girders and columns must be provided with fire insulation. If insulation is found necessary, choose the material and determine the insulation thickness required.



- 1 Static load which shall not cause the structure to collapse under fire exposure conditions

#### Girders

Dead weight according to assumptions	700 kgf/m <sup>2</sup>
Live load and load factor according to Table 2 a (Complete evacuation of people cannot be assumed)	
105 x 1.4 kgf/m <sup>2</sup>	<u>147 kgf/m<sup>2</sup></u>
Total	847 kgf/m <sup>2</sup> { 8.47 kN/m <sup>2</sup> }

Load per metre run of girder =  $4 \times 847 = 3400 \text{ kgf/m}$  {  $34 \text{ kN/m}$  }

(The load per metre run on the roof girders on the top storey is approximately  $4 \times 800 = 3200 \text{ kgf/m} = \{ 32 \text{ kN/m} \}$ )

#### Columns

A check is to be made with regard to the centre columns on the top and bottom storeys. The columns along the facade are stressed less highly and they are also mostly built into the external wall, so that exposure of these to fire will not constitute the design criterion.

Load on the centre column on the top storey (neglecting the dead weight of the column itself) =  $800 \times 5 \times 4 = 16,000 \text{ kgf}$  {  $160 \text{ kN}$  }

Load on centre column on bottom storey when the live load from the storeys above in accordance with ordinary loading regulations is reduced to one third  
 $= 16,000 + 4 \times 5 \times 4 \times (700 + 1/3 \times 105 \times 1.4) = 76,000 \text{ kgf}$  {  $760 \text{ kN}$  }

- 2 Fire load and opening factor

The total internal surface area of the fire compartment

$$A_t = 2 \times 3.5 \times 4 + 2 \times 2.5 \times 4 + 2 \times 2.5 \times 3.5 = 65.5 \text{ m}^2$$

According to Table 3 a, the design fire load due to furniture and fittings is  $19.5 \text{ Mcal/m}^2$ . To this must be added the fire load due to floor and wall coverings. The following is assumed in this respect (see Table 3.1 a in the Main Section)

Weight of floor covering

$$1.5 \text{ (kg/m}^2\text{)} \times 3.5 \times 4 \text{ (m}^2\text{)} = 21 \text{ kg}$$

Calorific value of floor covering

$$= 5 \text{ Mcal/kg}$$

Weight of wall covering

$$0.2 \text{ (kg/m}^2\text{)} \times 25 \text{ (m}^2\text{)} = 5 \text{ kg}$$

Calorific value of wall covering

$$= 5 \text{ Mcal/kg}$$

Additional fire load due to floor and wall coverings is calculated according to Equation (3.1 a) in the Main Section

$$q_{\text{floor + wall}} = \frac{21 \times 5 + 5 \times 5}{65.5} = 2.0 \text{ Mcal/m}^2$$

The total fire load is thus

$$q = 19.5 + 2.0 = \underline{21.5 \text{ Mcal/m}^2 \{ 90 \text{ MJ/m}^2 \}}$$

If the opening factor  $A\sqrt{h}/A_t$  is calculated on the assumption that the door is closed and remains intact during the fire, then (see Fig. 3 a)

$$A = 1.5 \times 3.7 = 5.6 \text{ m}^2, \quad h = 1.5 \text{ m}, \quad A_t = 65.5 \text{ m}^2, \quad \text{and} \quad A\sqrt{h}/A_t = \underline{0.105 \text{ m}^{\frac{1}{2}}}$$

If, on the other hand, it is assumed that the door is open when the fire breaks out, then

$$A = 1.5 \times 3.7 + 1 \times 2 = 7.6 \text{ m}^2, \quad h = \frac{1}{7.6} (5.6 \times 1.5 + 2 \times 2) = 1.63 \text{ m}, \quad \text{and} \\ A\sqrt{h}/A_t = \underline{0.15 \text{ m}^{\frac{1}{2}}}$$

For the centre columns only the opening factor of  $0.15 \text{ m}^{\frac{1}{2}}$ , corresponding to the door being open when the fire breaks out, need be considered since if the door is closed and remains intact during the fire, the columns will be outside the fire compartment. For the girders, both the values of the opening factor must be considered. The assumption that the door is closed will in this case yield results on the safe side, as will be easily seen on carrying out a rough check on the maximum steel temperature  $\vartheta_{\max}$  using the tables. The opening factor  $A\sqrt{h}/A_t = 0.105 \text{ m}^{\frac{1}{2}}$  will therefore be used in designing the girders.

### 3 Conversion to equivalent fire load and equivalent opening factor

According to the assumptions, the enclosing constructions consist of  $28 \text{ m}^2$  concrete ( $2 \times 3.5 \times 4$ ),  $25.5 \text{ m}^2$  gypsum plaster wall ( $2 \times 2.5 \times 3.5 + 2.5 \times 4.0 - 1 \times 2$ ), and  $4.4 \text{ m}^2$  steel sheeting wall with mineral wool insulation of ( $2.5 \times 4.0 - 1.5 \times 3.7$ ), i.e. concrete, gypsum plaster walling and steel sheeting wall with mineral wool insulation in the approximate proportions 49%, 44% and 7%. The fire compartment is thus a combination of fire compartment Type B (100% concrete), fire compartment Type G (20% concrete, 80% gypsum plaster) and fire compartment Type H (100% steel sheeting with mineral wool insulation), as set out in Table 4 a. The conversion factor  $k_f$  is therefore calculated as follows

$$k_f = \frac{7}{100} (k_f)_H + \frac{44}{80} (k_f)_G + \left( \frac{49}{100} - \frac{44}{80} \cdot \frac{20}{100} \right) (k_f)_B \\ = 0.07(k_f)_H + 0.55(k_f)_G + 0.38(k_f)_B$$

where  $(k_f)_H$ ,  $(k_f)_G$  and  $(k_f)_B$  are the values of  $k_f$  applicable to fire compartment types H, G and B.

Using the above and Table 4 a, the following is obtained for the actual opening factor  $A\sqrt{h}/A_t = 0.105 \text{ m}^{\frac{1}{2}}$

$$k_f = 0.07 \times 2.88 + 0.55 \times 1.13 + 0.38 \times 0.85 = 1.14$$

and for the actual opening factor  $A\sqrt{h}/A_t = 0.15 \text{ m}^{\frac{1}{2}}$ ,

$$k_f = 0.07 \times 2.0 + 0.55 \times 0.90 + 0.38 \times 0.85 = 0.96$$

If the value of the actual opening factor used is  $A\sqrt{h}/A_t = 0.105 \text{ m}^{\frac{1}{2}}$ , then the equivalent fire load is  $q = 1.14 \times 21.5 = \underline{24.5 \text{ Mcal/m}^2 \{103 \text{ MJ/m}^2\}}$  and the equivalent opening factor  $A\sqrt{h}/A_t = 1.14 \times 0.105 = \underline{0.12 \text{ m}^{\frac{1}{2}}}$ .

If the value of the actual opening factor is taken as  $A\sqrt{h}/A_t = 0.15 \text{ m}^{\frac{1}{2}}$ , then the equivalent fire load is  $q = 0.96 \times 21.5 = \underline{20.6 \text{ Mcal/m}^2 \{86 \text{ MJ/m}^2\}}$  and the equivalent opening factor  $A\sqrt{h}/A_t = 0.96 \times 0.15 = \underline{0.14 \text{ m}^{\frac{1}{2}}}$ .

#### 4 Maximum steel temperature

##### Girders

The resultant emissivity  $\epsilon_r$  for the girders is put equal to 0.5 (see Table 5 a). Furthermore, the  $F_s/V_s$  ratio of the girders, which have only their bottom flanges exposed,  $\approx 1/t \approx 1/0.016 \approx 62.5 \text{ m}^{-1}$  (see Fig. 5 a).

The maximum steel temperature  $\vartheta_{\max}$  is obtained from Table 5 c as a function of the equivalent fire load  $q = 24.5 \text{ Mcal/m}^2 \{103 \text{ MJ/m}^2\}$ , the equivalent opening factor  $A\sqrt{h}/A_t = 0.12 \text{ m}^{\frac{1}{2}}$ , the ratio  $F_s/V_s = 62.5 \text{ m}^{-1}$  and the resultant emissivity  $\epsilon_r = 0.5$ .

The nearest value of the fire load in the table is  $25 \text{ Mcal/m}^2 \{105 \text{ MJ/m}^2\}$ . There is no necessity in practice to interpolate between this value and the next lower one in the table. For a fire load of  $25 \text{ Mcal/m}^2 \{105 \text{ MJ/m}^2\}$ , the following is obtained from the table

$A\sqrt{h}/A_t$	$F_s/V_s$	$\vartheta_{\max}$
	50	460
0.12	62.5	520 interpolated value
	75	580

The maximum temperature of the girders in the event of fire will thus be  $\vartheta_{\max} = \underline{520^\circ\text{C}}$ .

##### Columns

The resultant emissivity  $\epsilon_r$  for the columns is put equal to 0.7 (see Table 5 a). Furthermore, the  $F_s/V_s$  ratio of the columns  $= (2b + 2h)/\text{area of cross section}$  (see Fig. 5 a). For the columns on the bottom storey, this gives a value of  $F_s/V_s \approx 100 \text{ m}^{-1}$ , and for the columns on the top storey, a value of  $F_s/V_s \approx 200 \text{ m}^{-1}$ .

The maximum steel temperature  $\vartheta_{\max}$  is obtained from Table 5 c as a function of the equivalent fire load  $q = 20.6 \text{ Mcal/m}^2 \{86 \text{ MJ/m}^2\}$ , the equivalent opening factor  $A\sqrt{h}/A_t = 0.14 \text{ m}^{\frac{1}{2}}$ , the ratio  $F_s/V_s = 100$  and  $200 \text{ m}^{-1}$ , and the resultant emissivity  $\epsilon_r = 0.7$ . The fire load of  $20 \text{ Mcal/m}^2 \{84 \text{ MJ/m}^2\}$  in the table is used in a preliminary investigation whether the columns can be constructed without fire insulation.

By extrapolating from the opening factor values of  $0.08$  and  $0.12 \text{ m}^{\frac{1}{2}}$ , the maximum steel temperature  $\vartheta_{\max}$  at an opening factor of  $0.14 \text{ m}^{\frac{1}{2}}$  is determined as approximately  $685^\circ\text{C}$  at a value of  $F_s/V_s$  of  $100 \text{ m}^{-1}$ . A rough check of the buckling curves in Fig. 10 b shows straight away that this temperature is excessive. The temperature for columns with  $F_s/V_s = 200 \text{ m}^{-1}$  will be higher still. The columns on all storeys must therefore be provided with fire insulation.

Fire retardant plaster 7 mm thick is tried as insulation. The average value of thermal conductivity  $\lambda_i$  for the plaster used is assumed to be  $\approx 0.14$  kcal/m  $^{\circ}\text{C}$  h {0.163 W/m  $^{\circ}\text{C}$ } (see Table 6 a). This means that the average insulation capacity during a fire will be  $d_i/\lambda_i = 0.007/0.14 = 0.05$  m<sup>2</sup>  $^{\circ}\text{C}$  h/kcal {0.043 m<sup>2</sup>  $^{\circ}\text{C}$ /W}.

At a ratio of the internal surface area of insulation  $A_i$  to the volume of the steel section  $V_s$ ,  $A_i/V_s \approx 200$  m<sup>-1</sup> (see Fig. 6 a), which applies in the case of the columns on the top storey, the maximum steel temperature  $\vartheta_{\max}$  is obtained from Table 6 b as follows

q	$A\sqrt{h}/A_t$	$A_i/V_s$	$\vartheta_{\max}$
	0.08		440
20	0.12	200	360
	0.14		320 extrapolated value
	0.08		500
25	0.12	200	430
	0.14		395 extrapolated value

By interpolating between the fire load values of 20 and 25 Mcal/m<sup>2</sup>, the steel temperature  $\vartheta_{\max}$  at a fire load of 20.6 Mcal/m<sup>2</sup> {86 MJ/m<sup>2</sup>} is obtained from the above values. The maximum steel temperature in the columns is given as

$$\vartheta_{\max} = \underline{330^{\circ}\text{C}}$$

For the columns on the bottom storey,  $A_i/V_s = 100$  m<sup>-1</sup>. The temperature in these columns and in the columns on the intermediate storeys for which the value of  $A_i/V_s$  is between 100 and 200 m<sup>-1</sup>, will therefore be lower at the same insulation thickness than that in the columns on the top storey for which  $A_i/V_s = 200$  m<sup>-1</sup>.

## 5 Critical load

### Girders

The average rate of heating in the girder can be estimated from Fig. 9 a. The equivalent fire load  $q = 24.5$  Mcal/m<sup>2</sup> {103 MJ/m<sup>2</sup>}, the equivalent opening factor  $A\sqrt{h}/A_t = 0.12$  m<sup>1/2</sup> and the maximum girder temperature  $\vartheta_{\max} = 520^{\circ}\text{C}$  are used as the input data. By interpolation, the rate of heating  $a$  is estimated at 40 $^{\circ}\text{C}$ /min.

From Fig. 9 b for the case of a simply supported beam with a uniformly distributed load, we obtain  $\beta = 0.68$  for  $\vartheta_{\max} = 520^{\circ}\text{C}$  and  $a \approx 40^{\circ}\text{C}$ /min. The critical load  $q_{\text{cr}}$  is calculated from the equation in the figure

$$q_{\text{cr}} = \frac{0.68 \times 8 \times 2600 \times 736}{500^2} = 42 \text{ kgf/cm}$$

$$= \underline{4200 \text{ kgf/m} \{ 42 \text{ kN/m} \}}$$

The load which, according to Section 1 above, the girders must be capable of carrying without collapse during a fire is 3400 kgf/m {34 kN/m}. The girders are therefore capable of resisting the fire exposure to which they may be subjected without the bottom flange having to be provided with fire insulation.

### Columns

Since the girders are not continuous over the columns, it is assumed that there is no restraint on longitudinal expansion of the columns. The critical buckling stress  $\sigma_k$  at the temperature of 330°C is determined from Fig. 10 b for the case when  $\gamma = 1$  (unrestrained expansion) and the yield stress at room temperature is  $\sigma_s = 2600 \text{ kgf/cm}^2 \{260 \text{ MPa}\}$ . For a slenderness ratio of  $\lambda = 73$  (columns on the top storey), the buckling stress is  $\sigma_k = 1300 \text{ kgf/cm}^2 \{130 \text{ MPa}\}$ . The critical load is thus

$$N_{cr} = 1300 \times 18.6 = \underline{24,200 \text{ kgf} \{242 \text{ kN}\}}$$

According to Section 1, the load which the columns on the top storey must be capable of carrying without collapse in the event of fire is 16,000 kgf {160 kN}. An insulation with 7 mm fire retardant plaster is thus sufficient for the columns on the top storey. Continued calculation based on an interpolation between the steel temperature at 7 mm plaster and the corresponding temperature in a column without insulation shows that it should be possible to reduce the insulation thickness by 1-2 mm. Such an estimate is however very rough, and the insulation thickness is therefore not reduced in this case. The final thickness of insulation must further be determined on the basis of practical considerations, e.g. ease of application. The other columns have more favourable  $A_i/V_s$  ratios, and their temperatures will therefore be lower than that of the columns on the top storey. Furthermore, since the columns are designed throughout in such a way that they are all stressed to about the same proportion of the permissible stress at room temperature, insulation by 7 mm of fire retardant plaster is satisfactory for all columns.

### 6 Summary

There is no need to provide protection for the girders. The columns are to be insulated with 7 mm fire retardant plaster with an approximate thermal conductivity of  $0.14 \text{ kcal/m } ^\circ\text{C h} \{0.163 \text{ W/m } ^\circ\text{C}\}$ .

## EXAMPLE 2. FIRE ENGINEERING DESIGN OF LOADBEARING STEEL STRUCTURE IN A THREE-STOREY RESIDENTIAL BUILDING

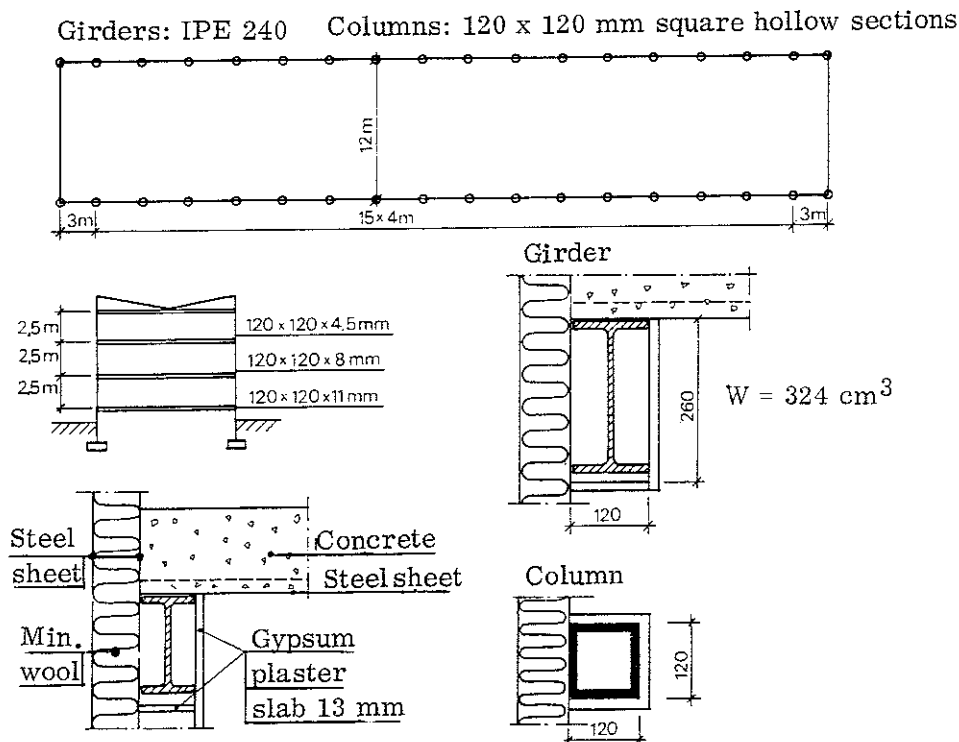
A three-storey residential building of 12 x 66 m plan area is to be constructed in such a way that great flexibility of layout is possible. The vertical loadbearing structure is concentrated along the long sides, and consist of continuous IPE 240 steel girders and hollow steel columns of square section with external dimensions of 120x120 mm. Column spacing is 4 m with the exception of the end bays where the distance between columns is 3 m. Material thicknesses of the columns are 4.5 mm on the top storey, 8 mm on the second storey and 11 mm on the bottom storey. The areas of cross section are  $20.5 \text{ cm}^2$ ,  $34.9 \text{ cm}^2$  and  $46.1 \text{ cm}^2$ , and the slenderness ratios 65, 67 and 70, respectively. The material of the girders and columns is Steel 1412 with a nominal yield stress  $\sigma_s = 2600 \text{ kgf/cm}^2 \{260 \text{ MPa}\}$ .

Floor units of steel sheeting and concrete 12 m in length are supported between the girders along the two long sides. The dead weight of the floor construction is  $480 \text{ kgf/m}^2 \{4.8 \text{ kN/m}^2\}$ . The dead weight of the attic floor plus the dead weight of the roof is  $550 \text{ kgf/m}^2 \{5.5 \text{ kN/m}^2\}$ . The snow load is assumed to be  $100 \text{ kgf/m}^2 \{1 \text{ kN/m}^2\}$ . The attic cannot be used for storage.

As regards the thermal characteristics of the surrounding construction, the fire compartment is equivalent to fire compartment Type A. The opening factor  $A\sqrt{h}/A_t$  is  $0.06 \text{ m}^{\frac{1}{2}}$ .

Complete evacuation of people from the building in the event of fire cannot be assumed with absolute certainty.

Check if one layer of gypsum plaster sheeting, 13 mm thick, according to the figure is sufficient for fire insulation of the steel structure.



- 1 Static load which shall not cause the structure to collapse under fire exposure conditions

### Girders

#### Ceiling level on top storey.

Dead weight of attic floor slab plus roof	550 kgf/m <sup>2</sup>
Snow load 100 kgf/m <sup>2</sup> (according to Table 2 a, 80% of this value, multiplied by the load factor 1.2, is taken)	<u>100 kgf/m<sup>2</sup></u>
Total	650 kgf/m <sup>2</sup> { 6.5 kN/m <sup>2</sup> }
Load per metre run of girder = 6x650	3900 kgf/m
Add for facade units	<u>100 kgf/m</u>
Total	<u>4000 kgf/m { 40 kN/m }</u>

#### Other storeys.

Dead weight of floor construction	480 kgf/m <sup>2</sup>
Live load and load factor according to Table 2 a (Complete evacuation of people cannot be assumed) 105 x 1.4 kgf/m <sup>2</sup>	<u>150 kgf/m<sup>2</sup></u>
Total	630 kgf/m <sup>2</sup> { 6.3 kN/m <sup>2</sup> }
Load per metre run of girder = 6x630	3800 kgf/m
Add for facade units	<u>100 kgf/m</u>
Total	<u>3900 kgf/m { 39 kN/m }</u>

### Columns

Load on columns on top storey = 4 x 4000	<u>16,000 kgf { 160 kN }</u>
Load on columns on second storey = 16,000 + 4x3900	<u>31,500 kgf { 315 kN }</u>
Load on columns on bottom storey = 31,500 + 4(6x480 + 100)	<u>43,500 kgf { 435 kN }</u>

- 2 Fire load and opening factor

According to Table 3 a, design fire load for two-room flats is	40 Mcal/m <sup>2</sup>
Floor coverings are estimated to give rise to an additional fire load of	<u>2.5 Mcal/m<sup>2</sup></u>
The total fire load is thus	$q = \underline{42.5 \text{ Mcal/m}^2 \{ 180 \text{ MJ/m}^2 \}}$
Opening factor according to assumptions	$A\sqrt{h}/A_t = \underline{0.06 \text{ m}^{\frac{1}{2}}}$

- 3 Conversion to equivalent fire load and equivalent opening factor

According to the assumptions, with regard to the thermal characteristics of the surrounding construction the fire compartment is equivalent to fire compartment Type A. According to Table 4 a, the conversion factor is  $k_f = 1.0$ . The equivalent fire load and equivalent opening factor are thus



$$q = 42.5 \text{ Mcal/m}^2 \{180 \text{ MJ/m}^2\}$$

$$A\sqrt{h}/A_t = 0.06 \text{ m}^{\frac{1}{2}}$$

#### 4 Maximum steel temperature

##### Girders

The internal surface area of insulation per unit length is  $A_i = 0.26 + 0.12 = 0.38 \text{ m}^2/\text{m}$ , and the volume of girder per unit length is  $V_s = 1 \times 0.00391 \text{ m}^3/\text{m}$ . This gives  $A_i/V_s \approx 100 \text{ m}^{-1}$  (see Fig. 6 a).

For insulation comprising one layer of 13 mm gypsum plaster slabs, the maximum steel temperature  $\vartheta_{\max}$  is obtained from Table 6 c:1. The equivalent fire load  $q = 42.5 \text{ Mcal/m}^2 \{180 \text{ MJ/m}^2\}$ , the equivalent opening factor  $A\sqrt{h}/A_t = 0.06 \text{ m}^{\frac{1}{2}}$  and the ratio  $A_i/V_s \approx 100 \text{ m}^{-1}$  are used as input data. The following is obtained from the table by interpolation

$q$	$A\sqrt{h}/A_t$	$A_i/V_s$	$\vartheta_{\max}$
40			420
42.5	0.06	100	440 interpolated value
45			460

The maximum steel temperature in the girders in the event of fire is therefore  $\vartheta_{\max} = 440^\circ\text{C}$ .

##### Columns

The internal surface area of insulation per unit length is  $A_i = 3 \times 0.12 = 0.36 \text{ m}^2/\text{m}$ . The volume of the column per unit length,  $V_s$ , varies from storey to storey. On the bottom storey  $V_s = 0.00461 \text{ m}^3/\text{m}$ , on the second storey  $V_s = 0.00349 \text{ m}^3/\text{m}$ , and on the top storey  $V_s = 0.00205 \text{ m}^3/\text{m}$ . The corresponding values of the  $A_i/V_s$  ratio are (see Fig. 6 a)

bottom storey	$A_i/V_s \approx 75 \text{ m}^{-1}$
second storey	$A_i/V_s \approx 100 \text{ m}^{-1}$
top storey	$A_i/V_s \approx 175 \text{ m}^{-1}$

The maximum steel temperature  $\vartheta_{\max}$  for insulation comprising one layer of 13 mm gypsum plaster slabs is obtained from Table 6 c:1. The equivalent fire load  $q = 42.5 \text{ Mcal/m}^2 \{180 \text{ MJ/m}^2\}$ , the equivalent opening factor  $A\sqrt{h}/A_t = 0.06 \text{ m}^{\frac{1}{2}}$  and the  $A_i/V_s$  ratios as above are used as input data. By interpolation from the table, we obtain

$q$	$A\sqrt{h}/A_t$	$A_i/V_s$	$\vartheta_{\max}$
		75	365
40	0.06	100	420
		150	485
		175	545 interpolated value
		200	600
		75	400
45	0.06	100	460
		150	540
		175	605 interpolated value
		200	670

By interpolating between the fire load values of 40 and 45 Mcal/m<sup>2</sup>, the following are obtained for the appropriate  $A_i/V_s$  ratios and a fire load  $q = 42.5$  Mcal/m<sup>2</sup> { 180 MJ/m<sup>2</sup> }.

	$A_i/V_s$	$\vartheta_{\max}$
bottom storey	75	<u>385°C</u>
second storey	100	<u>440°C</u>
top storey	175	<u>575°C</u>

## 5 Critical load

### Girders

A value of  $\beta = 1.3$  at the temperature of 440°C is obtained for the inner bays of the continuous girder from Fig. 9 b for the case of a beam rigidly restrained at both ends and subject to a uniformly distributed load (see Subsection 9.2.3.2 in the Main Section). Owing to the relatively low temperature, the magnitude of the rate of heating exerts no influence on the value of  $\beta$ . The critical load  $q_{cr}$  is calculated from the equation in the figure

$$q_{cr} = \frac{1.3 \times 12 \times 2600 \times 324}{400^2} = 82 \text{ kgf/cm}$$

$$= 8200 \text{ kgf/m } \{ 82 \text{ kN/m} \}$$

Analogously, the value of  $\beta = 1.4$  at  $\vartheta_{\max} = 440^\circ\text{C}$  is obtained for the outer bays of the continuous girder from Fig. 9 b for the case of a beam rigidly restrained at one end and subject to a uniformly distributed load. The corresponding critical load is

$$q_{cr} = \frac{1.4 \times 8 \times 2600 \times 324}{300^2} = 105 \text{ kgf/cm}$$

$$= 10,500 \text{ kgf/m } \{ 105 \text{ kN/m} \}$$

The load which, according to Section 1 above, the girders must be capable of carrying without collapse during a fire is 4000 kgf/m { 40 kN/m }.

### Columns

Owing to the fact that the girders are continuous over the columns, longitudinal expansion of these during a fire may be partially prevented if adjacent columns expand different amounts due to differences in temperature. The value of the degree of expansion  $\gamma$  depends on the assumptions made regarding the differences in temperature between adjacent columns. If the temperatures are different in adjacent columns during a fire on the bottom or second storey, the value of  $\gamma$  is also affected by the resistance offered by the girders on the storey above to expansion of the columns. However, owing to the elastic compression of the columns on the different storeys which is caused by the additional forces which arise, the resistance offered by the girders to expansion of the columns is a little less on each higher storey. An exact calculation of the total resistance to longitudinal expansion, and of the degree of expansion  $\gamma$ , is therefore a complicated business.

For ordinary values of the girder stiffness to column stiffness ratios, however, elastic compression of the columns is small in comparison with the expansion due to the rise in temperature. For the sake of simplicity, therefore, an approximation on the safe side can be made by determining the resistance offered by the girders to expansion of the columns on the basis of the sum of the girder stiffnesses on the different storeys, without consideration of the elastic compression of the columns. As a further approximation on the safe side, it is assumed in determining the value of the degree of expansion  $\gamma$  that only one column is exposed to the action of fire and consequent rise in temperature, the temperature of the adjacent columns remaining unchanged. Under these conditions, determination of the degree of expansion  $\gamma$  can be based on a system comprising a column of square 120x120 mm hollow section connected to the midpoint of an 8 m girder of IPE 240 section which is elastically restrained at both its ends and cannot undergo vertical displacements. In order however to simplify the treatment further, it is assumed that the ends of the girder are rigidly, and not elastically, restrained. This approximation which yields results on the safe side implies that Fig. 10 a can be used for determination of the degree of expansion  $\gamma$ .

In calculating the coefficient K in Fig. 10 a, for all girders

$$I_b = 3892 \text{ cm}^4$$

$$L_b = 800 \text{ cm.}$$

For girders which are exposed to fire, maximum steel temperature is  $440^\circ\text{C}$ , and the value of the modulus of elasticity  $E_b$  is given by the expression (see Fig. 9.1 a in the Main Section)

$$E_b = 0.75 \times 2.1 \times 10^6 \text{ kgf/cm}^2 \{ 0.75 \times 2.1 \times 10^5 \text{ MPa} \}$$

For all other girders,

$$E_b = 2.1 \times 10^6 \text{ kgf/cm}^2 \{ 2.1 \times 10^5 \text{ MPa} \}$$

When there is a fire on the bottom storey, we have for the columns

$$A = 46.1 \text{ cm}^2$$

$$L = 250 \text{ cm}$$

The value of the modulus of elasticity (secant modulus) of the column depends on the column temperature  $385^\circ\text{C}$  and the actual stress level. Since the imposed stress is unknown, the secant modulus is determined for a stress equal to the buckling stress of the column at the temperature concerned and for no restraint on longitudinal expansion, i.e.  $\gamma = 1$ . For the actual slenderness ratio of  $\lambda = 70$  and actual steel temperature of  $385^\circ\text{C}$ , Fig. 10 b for  $\sigma_s = 2600 \text{ kgf/cm}^2 \{ 260 \text{ MPa} \}$  and  $\gamma = 1$  gives a buckling stress  $\sigma_k = 1240 \text{ kgf/cm}^2 \{ 124 \text{ MPa} \}$ .

For a stress level  $\sigma/\sigma_s = 1240/2600 = 0.48$  and a steel temperature  $\theta_s = 385^\circ\text{C}$ , Fig. 10.1 b in the Main Section gives the value of  $E = 0.65 \times 2.1 \times 10^6 \text{ kgf/cm}^2 \{ 0.65 \times 2.1 \times 10^5 \text{ MPa} \}$  for the secant modulus. In the event of fire on the bottom storey, therefore, we have

$$K = \frac{(0.75 + 1.0 + 1.0) \times 2.1 \times 10^6 \times 3892}{800^3} \times \frac{250}{0.65 \times 2.1 \times 10^6 \times 46.1} = 1.74 \times 10^{-4}$$

Using this value of K, the degree of expansion  $\gamma$  is determined from Fig. 10 a. This gives

$$\gamma = 0.965$$

The buckling stress  $\sigma_k$  at  $\theta_s = 385^\circ\text{C}$  and slenderness ratio  $\lambda = 70$  is determined from Fig. 10 b for  $\sigma_s = 2600 \text{ kgf/cm}^2 \{ 260 \text{ MPa} \}$  by interpolation between the diagrams for  $\gamma = 0.975$  and  $\gamma = 0.95$ . This gives

$$\sigma_k = 1050 \text{ kgf/cm}^2 \{ 105 \text{ MPa} \}.$$

The critical load for the columns on the bottom storey is therefore

$$N_{cr} = 1050 \times 46.1 = \underline{48,400 \text{ kgf} \{ 484 \text{ MPa} \}}$$

The load which, according to Section 1 above, the columns on the bottom storey must be capable of carrying without collapse during a fire is  $43,500 \text{ kgf} \{ 435 \text{ kN} \}$ .

In the event of fire on the second storey, we have for the columns

$$A = 34.9 \text{ cm}^2$$

$$L = 250 \text{ cm}$$

The maximum temperature in the column is  $440^\circ\text{C}$ . The stress level for determination of the secant modulus is estimated in the same way as for columns on the bottom storey. Fig. 10 b for  $\sigma_s = 2600 \text{ kgf/cm}^2 \{ 260 \text{ MPa} \}$  and  $\gamma = 1$  gives a buckling stress  $\sigma_k = 1140 \text{ kgf/cm}^2 \{ 114 \text{ MPa} \}$  at the actual slenderness ratio  $\lambda = 67$  and steel temperature  $\theta_s = 440^\circ\text{C}$ . With the stress level  $\sigma/\sigma_s = 1140/2600 = 0.44$  and steel temperature  $\theta_s = 440^\circ\text{C}$ , Fig. 10.1 b in the Main Section gives a value for the secant modulus of  $E = 0.53 \times 2.1 \times 10^6 \text{ kgf/cm}^2 \{ 0.53 \times 2.1 \times 10^5 \text{ MPa} \}$ . In the event of fire on the second storey, therefore, we have

$$K = \frac{(0.75 + 1) \times 2.1 \times 10^6 \times 3892}{800^3} \times \frac{250}{0.53 \times 2.1 \times 10^6 \times 34.9} = 1.8 \times 10^{-4}$$

Using this value of  $K$ , the degree of expansion  $\gamma$  is determined from Fig. 10 a. This gives

$$\gamma = 0.965$$

The buckling stress  $\sigma_k$  at  $\theta_s = 440^\circ\text{C}$  and slenderness ratio  $\lambda = 67$  is determined from Fig. 10 b for  $\sigma_s = 2600 \text{ kgf/cm}^2 \{ 260 \text{ MPa} \}$  by interpolation between the diagrams for  $\gamma = 0.975$  and  $\gamma = 0.95$ . This gives

$$\sigma_k = 960 \text{ kgf/cm}^2 \{ 96 \text{ MPa} \}$$

The critical load for the columns on the second storey is therefore

$$N_{cr} = 960 \times 34.9 = \underline{33,500 \text{ kgf} \{ 335 \text{ kN} \}}$$

The load which, according to Section 1 above, the columns on the second storey must be capable of carrying without collapse during a fire is  $31,500 \text{ kgf} \{ 315 \text{ kN} \}$ .

In the event of fire on the top storey, we have for the columns

$$A = 20.5 \text{ cm}^2$$

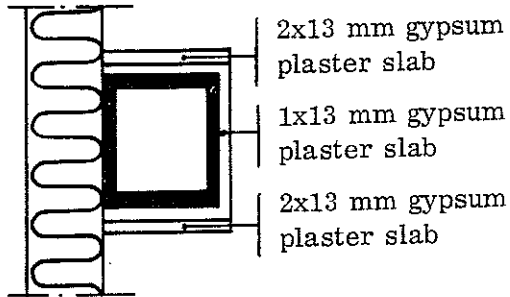
$$L = 250 \text{ cm}$$

The maximum temperature in the column is  $575^\circ\text{C}$ . Fig. 10 b for  $\sigma_s = 2600 \text{ kgf/cm}^2 \{ 260 \text{ MPa} \}$  and  $\gamma = 1$  gives a buckling stress  $\sigma_k = 670 \text{ kgf/cm}^2 \{ 67 \text{ MPa} \}$  at the actual slenderness ratio  $\lambda = 65$  and steel temperature  $\theta_s = 575^\circ\text{C}$ . If the column were completely free to expand, therefore, the critical load would be

$$N_{cr} = 670 \times 20.5 = \underline{13,700 \text{ kgf} \{ 137 \text{ kN} \}}.$$

This load is less than the load which, according to Section 1, the columns on the top storey must be capable of carrying without collapse during a fire. In addition, the column is not entirely free to expand longitudinally, and the critical load is therefore less than 13,700 kgf {137 kN}.

Insulation by means of one layer of 13 mm gypsum plaster slabs is thus insufficient on the top storey. Additional insulation in the form of another layer of 13 mm gypsum plaster slabs, on two of the sides of the column as suggested in the figure, is therefore to be provided.



If the columns were to be insulated with two layers of 13 mm gypsum plaster slabs also on the third side, then, according to Table 6 c:1, the maximum steel temperature  $\vartheta_{\max}$  would be

q	$A\sqrt{h}/A_t$	$A_i/V_s$	$\vartheta_{\max}$
		150	260
40	0.06	175	280 interpolated value
		200	300
		150	315
45	0.06	175	340 interpolated value
		200	360

By interpolation between the fire load values of 40 and 45 Mcal/m<sup>2</sup>,  $\vartheta_{\max}$  for a fire load of 42.5 Mcal/m<sup>2</sup> and insulation with two layers of 13 mm gypsum plaster slab is obtained as 310°C.

When insulation consisted of one layer of 13 mm gypsum plaster slabs, the corresponding temperature was 575°C.

When insulation is provided as in the figure by means of two layers on two sides and one layer on the third side, the average steel temperature will be between these temperatures. As an approximation on the safe side, the temperature can be calculated as

$$\vartheta_{\max} = \frac{310 + 575}{2} \approx 440^\circ\text{C}$$

Using this value of the steel temperature, Fig. 10 b for  $\sigma_s = 2600 \text{ kgf/cm}^2$  {260 MPa} and  $\gamma = 1$  gives a buckling stress  $\sigma_k = 1170 \text{ kgf/cm}^2$  {117 MPa} at a slenderness ratio of  $\lambda = 65$ . With the stress level  $\sigma/\sigma_s = 1170/2600 = 0.45$  and the steel temperature  $\vartheta_s = 440^\circ\text{C}$ , Fig. 10.1 b in the Main Section gives the value of the secant modulus as  $E = 0.54 \times 2.1 \times 10^6 \text{ kgf/cm}^2$  {0.54 x 2.1 x 10<sup>5</sup> MPa}. During a fire on the top storey, we have therefore

$$K = \frac{0.75 \times 2.1 \times 10^6 \times 3892}{800^3} \times \frac{250}{0.54 \times 2.1 \times 10^6 \times 20.5} = 1.29 \times 10^{-4}$$

Using this value of K, the degree of expansion  $\gamma$  is determined from Fig. 10 a. We have

$$\gamma = 0.975$$

The buckling stress  $\sigma_k$  at 440°C and a slenderness ratio  $\lambda = 65$  is determined from Fig. 10 b for  $\sigma_s = 2600 \text{ kgf/cm}^2 \{ 260 \text{ MPa} \}$  and  $\gamma = 0.975$ . This gives  $\sigma_k = 1040 \text{ kgf/cm}^2 \{ 104 \text{ MPa} \}$

The critical load for the columns on the top storey is therefore

$$N_{cr} = 1040 \times 20.5 = \underline{21,300 \text{ kgf} \{ 213 \text{ kN} \}}$$

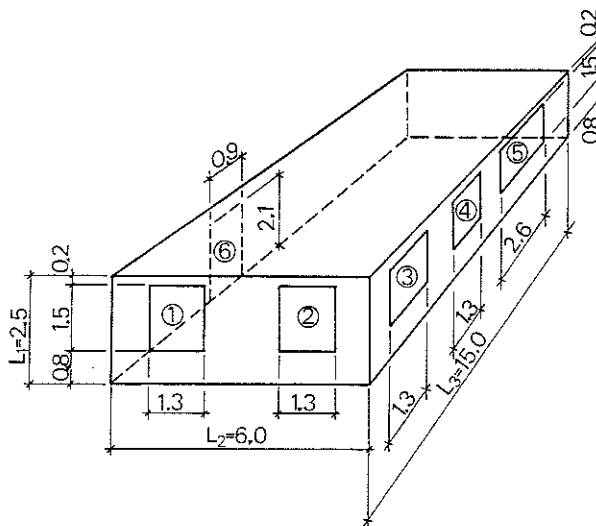
The load which, according to Section 1, the columns on the top storey must be capable of carrying without collapse during a fire is 16,000 kgf {160 kN}.

## 6 Summary

One layer of 13 mm gypsum plaster slabs is sufficient as fire insulation for the girders and columns, with the exception of the columns on the top storey. The insulation for these columns must be increased by the addition of another layer of 13 mm gypsum plaster slabs on at least two of the three sides of the column which face the room.

### EXAMPLE 3. FIRE ENGINEERING DESIGN OF STEEL FLOOR GIRDERS IN AN EIGHT-STOREY OFFICE BUILDING

A fire compartment in an eight-storey office building has the inside dimensions shown in the figure. The fire compartment has one door 6 and five window openings 1-5 with the positions and dimensions as shown in the figure.



The floor slab which consists of 16 cm concrete plus 4 cm concrete topping is carried by 6 m long steel girders of HE 280 A section which are rigidly restrained at one end and spaced at 5 m centres. The material of the girders is Steel 1311 with a nominal yield stress  $\sigma_s = 2200 \text{ kgf/cm}^2 \{ 220 \text{ MPa} \}$ . The floor slab is laid on the top flanges of the girders.

The surrounding construction of the fire compartment consists of 18% lightweight concrete and 82% ordinary concrete.

Complete evacuation of people from the building in the event of fire cannot be assumed with absolute certainty.

Check whether the floor girders must be provided with fire insulation. If insulation is required, check whether the temperature of the girders can be limited to the permissible values by means of a) a fire retardant paint of average insulation capacity  $d_i/\lambda_i = 0.075 \text{ m}^2 \text{ }^\circ\text{C h/kcal} \{ 0.064 \text{ m}^2 \text{ }^\circ\text{C/W} \}$ , b) a suspended ceiling of 15 mm thick mineral wool slabs Type 17 according to Table 7 a.

- 1 Static load which shall not cause the girders to collapse under fire exposure conditions

Dead weight = $0.20 \times 2400$	480 kgf/m <sup>2</sup>
Live load and load factor according to Table 2 a (Complete evacuation of people cannot be assumed) = $135 \times 1.4 \text{ kgf/m}^2$	190 kgf/m <sup>2</sup>
Total	670 kgf/m <sup>2</sup> { 6.7 kN/m <sup>2</sup> }
Load per metre run of girder = $5 \times 670$	3,350 kgf/m { 33.5 kN/m }

## 2 Fire load and opening factor

The total internal surface area of the fire compartment is

$$A_t = 6 \times 15 \times 2 + 6 \times 2.5 \times 2 + 15 \times 2.5 \times 2 = 285 \text{ m}^2$$

The design fire load is determined from Table 3 a. The value applicable to all the investigated office premises, i.e.  $33 \text{ Mcal/m}^2$   $\{138.2 \text{ MJ/m}^2\}$ , is chosen. An addition is made in respect of fire load due to floor and wall covering. The material in the floor and wall covering is assumed to have a calorific value of 5 and  $3.8 \text{ Mcal/kg}$  respectively. The total weight of floor covering is 200 kg and that of the wall covering 30 kg. According to Equation (3.1 a) in the Main Section, we have

$$q_{\text{floor} + \text{wall}} \approx \frac{200 \times 5 + 30 \times 3.8}{285} \approx 4 \text{ Mcal/m}^2$$

The total fire load is thus

$$q = 33 + 4 = \underline{37 \text{ Mcal/m}^2} \{155 \text{ MJ/m}^2\}$$

The opening factor is calculated according to Fig. 3.a

$$A = 1.3 \times 1.5 \times 4 + 2.6 \times 1.5 + 0.9 \times 2.1 = 7.8 + 3.9 + 1.89 = 13.59 \text{ m}^2$$

$$h = \frac{1}{13.59} (7.8 \times 1.5 + 3.9 \times 1.5 + 1.89 \times 2.1) = 1.58 \text{ m, and}$$

$$\frac{A\sqrt{h}}{A_t} = \frac{13.59\sqrt{1.58}}{285} = \underline{0.06 \text{ m}^{\frac{1}{2}}}$$

## 3 Conversion into equivalent fire load and equivalent opening factor

The surrounding construction of the fire compartment, consisting of 82% concrete and 18% lightweight concrete, is intermediate between fire compartment Type B (only concrete) and fire compartment Type D (50% concrete, 50% lightweight concrete) according to Table 4 a.

The conversion factor  $k_f$  is given by linear interpolation as

$$k_f = (k_f)_B + \frac{18}{50} [(k_f)_D - (k_f)_B] = 0.64 (k_f)_B + 0.36 (k_f)_D$$

where  $(k_f)_B$  and  $(k_f)_D$  are the values of  $k_f$  applicable to fire compartment B and D respectively. Using the above and Table 4 a, the figure obtained for the actual opening factor  $A\sqrt{h}/A_t = 0.06 \text{ m}^{\frac{1}{2}}$  is

$$k_f = 0.64 \times 0.85 + 0.36 \times 1.35 = 1.03$$

The equivalent fire load is thus

$$q = 1.03 \times 37 = \underline{38 \text{ Mcal/m}^2} \{160 \text{ MJ/m}^2\}$$

and the equivalent opening factor

$$A\sqrt{h}/A_t = 1.03 \times 0.06 \approx \underline{0.06 \text{ m}^{\frac{1}{2}}}$$



#### 4 Maximum steel temperature

##### Uninsulated girder

The resultant emissivity  $\epsilon_r$  is put equal to 0.5 (see Table 5 a). The  $F_s/V_s$  ratio of the girder is  $140 \text{ m}^{-1}$  (see Table 5 b).

The maximum steel temperature  $\vartheta_{\max}$  is obtained from Table 5 c as a function of the equivalent fire load  $q = 38 \text{ Mcal/m}^2 \{160 \text{ MJ/m}^2\}$ , the equivalent opening factor  $A\sqrt{h}/A_t = 0.06 \text{ m}^{1/2}$ , the ratio  $F_s/V_s = 140 \text{ m}^{-1}$  and the resultant emissivity  $\epsilon_r = 0.5$ . It will be seen from the table that, for a fire load as low as  $30 \text{ Mcal/m}^2$  and a  $F_s/V_s$  ratio of  $75 \text{ m}^{-1}$ , the maximum steel temperature  $\vartheta_{\max}$  at an opening factor  $A\sqrt{h}/A_t = 0.06 \text{ m}^{1/2}$  and resultant emissivity  $\epsilon_r = 0.5$ , will be  $775^\circ\text{C}$ . For the actual values of fire load and the  $F_s/V_s$  ratio the temperature would be higher still. The temperature in the steel girders under fire exposure conditions can therefore be seen to become excessive without any further checks. The girders must be protected by insulation.

##### Insulated girder

a) Insulation with fire retardant paint of average insulation capacity

$$d_i/\lambda_i = 0.075 \text{ m}^2 \text{ }^\circ\text{C h/kcal} \{0.064 \text{ m}^2 \text{ }^\circ\text{C/W}\}$$

If the insulation has an average insulation capacity  $d_i/\lambda_i = 0.05 \text{ m}^2 \text{ }^\circ\text{C h/kcal} \{0.043 \text{ m}^2 \text{ }^\circ\text{C/W}\}$ , the following is obtained from Table 6 b

q	$A\sqrt{h}/A_t$	$A_i/V_s$	$\vartheta_{\max}$
		125	555
35	0.06	140	580 interpolated value
		150	595
		125	595
40	0.06	140	625 interpolated value
		150	640

For an equivalent fire load  $q = 38 \text{ Mcal/m}^2 \{160 \text{ MJ/m}^2\}$ , a maximum steel temperature  $\vartheta_{\max} = 605^\circ\text{C}$  is obtained by interpolation between the above values.

If the insulation has an average insulation capacity  $d_i/\lambda_i = 0.10 \text{ m}^2 \text{ }^\circ\text{C h/kcal} \{0.086 \text{ m}^2 \text{ }^\circ\text{C/W}\}$ , the following is obtained from Table 6 b

q	$A\sqrt{h}/A_t$	$A_i/V_s$	$\vartheta_{\max}$
		125	415
35	0.06	140	440 interpolated value
		150	455
		125	450
40	0.06	140	475 interpolated value
		150	490

For an equivalent fire load  $q = 38 \text{ Mcal/m}^2 \{160 \text{ MJ/m}^2\}$ , a maximum steel temperature of  $\vartheta_{\max} = 460^\circ\text{C}$  is obtained by interpolation between the above values.

For an average insulation capacity between  $0.05$  and  $0.10 \text{ m}^2 \text{ }^\circ\text{C h/kcal}$ , or equal to  $0.075 \text{ m}^2 \text{ }^\circ\text{C h/kcal}$   $\{0.064 \text{ m}^2 \text{ }^\circ\text{C/W}\}$  (see Table 6 a, fire retardant paints), and an equivalent fire load  $q = 38 \text{ Mcal/m}^2$   $\{160 \text{ MJ/m}^2\}$ , the maximum steel temperature will be approximately

$$\vartheta_{\max} = \frac{460 + 605}{2} = \underline{535^\circ\text{C}}$$

b) Insulation with a suspended ceiling of 15 mm thick mineral wool slabs

It is evident from Table 7 a that suspended ceiling No 17 consisting of 15 mm thick mineral wool slabs has a value  $(d_i/\lambda_i)_{\text{fict}} = 0.20 \text{ m}^2 \text{ }^\circ\text{C h/kcal}$   $\{0.172 \text{ m}^2 \text{ }^\circ\text{C/W}\}$ . It is further evident that the critical temperature of the suspended ceiling construction itself is considered to be  $600^\circ\text{C}$ .

The maximum steel temperature  $\vartheta_{\max}$  for a construction with insulation in the form of a suspended ceiling is obtained from Table 7 b. At  $(d_i/\lambda_i)_{\text{fict}} = 0.20 \text{ m}^2 \text{ }^\circ\text{C h/kcal}$   $\{0.172 \text{ m}^2 \text{ }^\circ\text{C/W}\}$ , we obtain from the table

$q$	$A\sqrt{h}/A_t$	$F_s/V_s$	$\vartheta_{\max}$
		100	140
40	0.04	140	160 interpolated value
		200	180
		100	100
40	0.08	140	120 interpolated value
		200	140

For an equivalent fire load  $q = 38 \text{ Mcal/m}^2$   $\{160 \text{ MJ/m}^2\}$  and an equivalent opening factor  $A\sqrt{h}/A_t = 0.06 \text{ m}^{\frac{1}{2}}$ , the maximum steel temperature should be somewhat lower than

$$\vartheta_{\max} = \frac{120 + 160}{2} = \underline{140^\circ\text{C}}$$

From Table 7 b it can be estimated that for an equivalent fire load  $q = 38 \text{ Mcal/m}^2$   $\{160 \text{ MJ/m}^2\}$  and an equivalent opening factor  $A\sqrt{h}/A_t = 0.06 \text{ m}^{\frac{1}{2}}$ , the temperature in the suspended ceiling will be somewhat lower than  $\vartheta_{\text{susp. ceil.}} = (560 + 625)/2 = 590^\circ\text{C}$ . This temperature is less than the critical temperature of the suspended ceiling which is  $600^\circ\text{C}$ .

## 5 Critical load

For an equivalent fire load  $q = 38 \text{ Mcal/m}^2$   $\{160 \text{ MJ/m}^2\}$ , an equivalent opening factor  $A\sqrt{h}/A_t = 0.06 \text{ m}^{\frac{1}{2}}$ , and a maximum steel temperature  $\vartheta_{\max} = 535^\circ\text{C}$  (insulation in the form of a fire retardant paint), the average rate of heating of the girders is estimated by means of interpolation in Fig. 9 a. The rate of heating  $a$  will be around  $15^\circ\text{C/min}$ .

From Fig. 9 b, for a beam carrying a uniformly distributed load which is restrained at one end, we have  $\beta = 0.90$  at  $\vartheta_{\max} = 535^\circ\text{C}$  and  $a = 15^\circ\text{C/min}$ . The critical load is calculated from the equation in the figure as

$$q_{cr} = \frac{0.90 \times 8 \times 2200 \times 1010}{600^2} = 44 \text{ kgf/cm} = 4400 \text{ kgf/m} \{ 44 \text{ kN/m} \}$$

The load which, according to Section 1, the girders must be capable of carrying without collapse during a fire is 3350 kgf/m { 33.5 kN/m }.

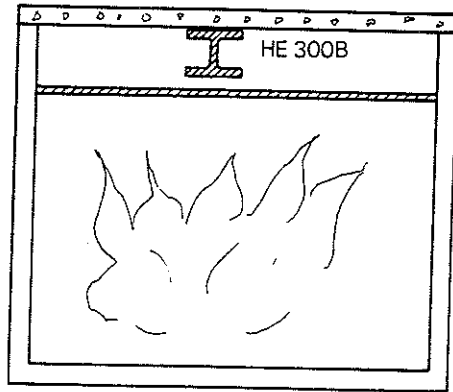
When the floor construction is insulated by means of a suspended ceiling of 15 mm thick mineral wool slabs, the girder temperature will be considerably lower than when the insulation is a fire retardant paint, and the loadbearing capacity will be consequently greater.

## 6 Summary

The girders cannot carry the imposed loading in the event of fire without insulation. Insulation using a fire retardant paint of average insulation capacity  $d_i/\lambda_i = 0.075 \text{ m}^2 \text{ }^\circ\text{C h/kcal} \{ 0.064 \text{ m}^2 \text{ }^\circ\text{C/W} \}$  is sufficient in order to limit the steel temperature, and also insulation in the form of a suspended ceiling consisting e.g. of 15 mm thick mineral wool slabs, ceiling No 17 in Table 7 a.

**EXAMPLE 4. FIRE ENGINEERING ASSESSMENT OF A SUSPENDED CEILING WHICH HAD BEEN SUBJECTED TO A STANDARD FIRE TEST**

A new suspended ceiling construction had been subjected to a standard fire test. The suspended ceiling had been mounted in a fire testing furnace, the top of which consisted of a precast concrete unit. Above the suspended ceiling, there was an HE 300 B steel girder fixed to the precast concrete section. The space below the suspended ceiling was heated according to the standard fire curve, and continuous measurements of the temperature were made on the steel girder and at other points. The test rig is illustrated in the figure.



The measured mean temperature-time curve for the steel girder is described by the values tabulated below.

Time (min)	Mean temperature (°C)
0	20
10	50
20	75
30	105
40	145
50	190
55	225
57	250

Extensive cracking was observed in the suspended ceiling after 54 minutes. The test was discontinued after 57 minutes.

Check whether this suspended ceiling construction can be used for the protection of the steel girders in the office fire compartment in Example 3.

# 1 Estimation of the insulation capacity and critical temperature of the suspended ceiling

The girder used in the test for measurement of the steel temperature-time curve was of HE 300 B section. According to Fig. 5 a or Table 5 b, the  $F_s/V_s$  ratio for this girder is

$$F_s/V_s = \frac{2 \times 0.3 + 3 \times 0.3 - 2 \times 0.011}{0.01491} = 99 \text{ m}^{-1}$$

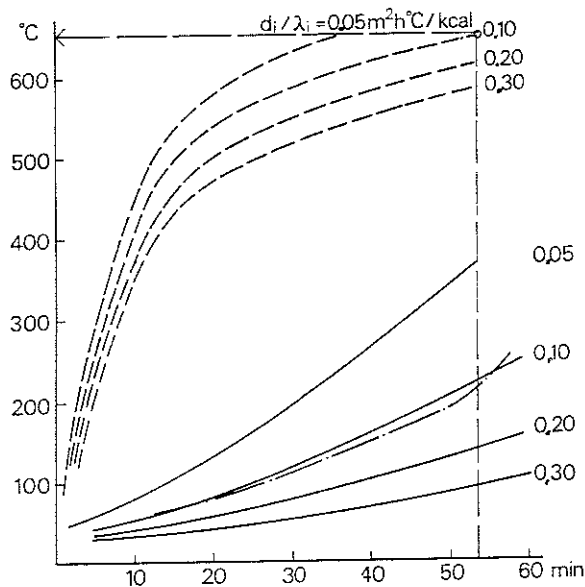
In the figure below, the theoretically calculated steel temperature-time curves according to Fig. 7.4 a in the Main Section, based on the standard fire curve, have been plotted for  $F_s/V_s = 100 \text{ m}^{-1}$  for different values of  $d_i/\lambda_i$  for the suspended ceiling (full lines).

The figure also contains the temperature-time curves given in Fig. 7.4 a for the centre level of the suspended ceiling, for different values of the insulation capacity  $d_i/\lambda_i$  of the suspended ceiling (dashed lines). Furthermore, the steel temperature-time curve measured during the fire test on the suspended ceiling concerned is also given (chain line). The best agreement between the measured and calculated temperature-time curves for a steel girder with  $F_s/V_s = 100 \text{ m}^{-1}$  is obtained if the average insulation capacity of the suspended ceiling is assumed to be  $d_i/\lambda_i = 0.10 \text{ m}^2 \text{ }^\circ\text{C h/kcal}$ . For the suspended ceiling, therefore,

$$(d_i/\lambda_i)_{\text{fict}} = 0.10 \text{ m}^2 \text{ }^\circ\text{C h/kcal} \{ 0.086 \text{ m}^2 \text{ }^\circ\text{C/W} \}$$

During the test, extensive cracking was observed in the suspended ceiling after 54 minutes. It is seen from the figure that the temperature at the centre level of the suspended ceiling was approximately  $650^\circ\text{C}$  at this time. The critical temperature of the suspended ceiling may therefore be assumed to be

$$\vartheta_{\text{susp. ceil.}} = 650^\circ\text{C}$$



2 Determination of the maximum steel and suspended ceiling temperatures when the suspended ceiling is used in a fire compartment according to Example 3

The maximum steel temperature and the maximum temperature of the suspended ceiling can be determined from Table 7 b if the equivalent fire load  $q$ , the equivalent opening factor  $A\sqrt{h}/A_t$ , the  $F_s/V_s$  ratio for the steel girders and the insulation capacity  $(d_i/\lambda_i)_{\text{fict}}$  of the suspended ceiling are known.

According to Example 3 (Section 3), the equivalent fire load is  $q = 38 \text{ Mcal/m}^2$   $\{160 \text{ MJ/m}^2\}$  and the equivalent opening factor  $A\sqrt{h}/A_t = 0.06 \text{ m}^{1/2}$ . Furthermore, according to Example 3 (Section 4), the  $F_s/V_s$  ratio for the girders is  $140 \text{ m}^{-1}$ .

For a suspended ceiling insulation capacity of  $(d_i/\lambda_i)_{\text{fict}} = 0.10 \text{ m}^2 \text{ }^\circ\text{C h/kcal}$   $\{0.086 \text{ m}^2 \text{ }^\circ\text{C/W}\}$ , the following are obtained from Table 7 b for an equivalent fire load  $q = 40 \text{ Mcal/m}^2$   $\{168 \text{ MJ/m}^2\}$

$q$	$A\sqrt{h}/A_t$	$F_s/V_s$	$\vartheta_{\text{max}}$	$\vartheta_{\text{susp.ceil.}}$
		100	220	
40	0.04	140	240 ← interpolated	600
		200	270 value	
		100	160	
40	0.08	140	185 ← interpolated	665
		200	220 value	

By interpolation between the above values, the maximum steel temperature  $\vartheta_{\text{max}}$  and the suspended ceiling temperature  $\vartheta_{\text{susp.ceil.}}$  at an equivalent opening factor  $A\sqrt{h}/A_t = 0.06 \text{ m}^{1/2}$  are determined as

$$\vartheta_{\text{max}} = \frac{185 + 240}{2} \approx 210^\circ\text{C}$$

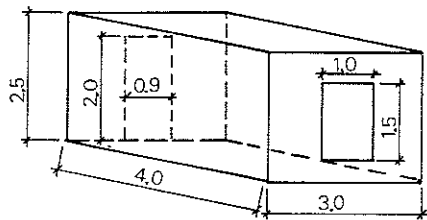
$$\vartheta_{\text{s.c.}} = \frac{600 + 655}{2} \approx 630^\circ\text{C}$$

The temperature of  $210^\circ\text{C}$  in the steel girders can be seen directly, or by comparison with the results in Example 3, to be very much below the critical one.

The maximum midpoint temperature of  $630^\circ\text{C}$  in the suspended ceiling is lower than the temperature of  $650^\circ\text{C}$  which was assessed in Section 1 above as the critical temperature of the suspended ceiling. This suspended ceiling can thus be used as fire insulation for the steel girders in Example 3.

## EXAMPLE 5. CHECK ON PARTITION

In the office building in Example 3 a few small rooms are to be set aside as records rooms. The internal dimensions of these rooms are given in the figure below.



It is estimated that a maximum of about 1100 kg books and other paper articles, and about 300 kg of various plastics articles, can be stored in the room. The furnishings in the records room mostly consist of wood, with a total weight of approximately 300 kg.

The construction surrounding the fire compartment mainly consists of concrete and steel sheeting with mineral wool insulation in about equal proportions.

Check if a wall made up of 15 cm thick slabs of mineral wool of density  $\gamma = 45 \text{ kg/m}^3$ , covered on both sides with steel sheeting or some other incombustible layer, is satisfactory as a partition in order to prevent spread of fire from the records room to adjacent fire compartments.

### 1 Fire load and opening factor

The total internal surface area of the fire compartment is

$$A_t = 2 \times 4 \times 3 + 2 \times 2.5 \times 3 + 2 \times 2.5 \times 4 = 59 \text{ m}^2$$

The calorific values  $H$  of the various materials are taken from Table 3.1 a in the Main Section. The values chosen are 4.0 Mcal/kg for paper, an average value of 7.0 Mcal/kg for plastics, and 4.5 Mcal/kg for wood.

The fire load  $q$  is calculated according to Equation (3.1 a) in the Main Section as

$$q = \frac{1100 \times 4.0 + 300 \times 7.0 + 300 \times 4.5}{59} = 133 \text{ Mcal/m}^2 \{ 557 \text{ MJ/m}^2 \}$$

The opening factor  $A\sqrt{h}/A_t$  is calculated according to Fig. 3 a. It is assumed in this connection that the door conforms to at least the same fire resistance as the walls, and that it is provided with automatic closure equipment.

On the basis of these assumptions, we have

$$A = 1.0 \times 1.5 = 1.5 \text{ m}^2$$

$$h = 1.5$$

$$A\sqrt{h}/A_t = \frac{1.5\sqrt{1.5}}{59} = 0.031 \text{ m}^{1/2}$$

## 2 Conversion to equivalent fire load and equivalent opening factor

The fire compartment, the surrounding constructions of which consist in about equal proportions of concrete and steel sheeting with mineral wool insulation, is intermediate between fire compartment Type B (100% concrete) and fire compartment Type H (100% steel sheeting with mineral wool insulation), as set out in Table 4 a. By linear interpolation, the conversion factor is obtained as

$$k_f = (k_f)_B + \frac{50}{100} [(k_f)_H - (k_f)_B] = 0.50(k_f)_B + 0.50(k_f)_H$$

From this and according to Table 4 a, we obtain for the actual opening factor  $A\sqrt{h}/A_t = 0.031 \text{ m}^{\frac{1}{2}}$

$$k_f = 0.50 \times 0.85 + 0.50 \times 3.0 = 1.93$$

The equivalent fire load is thus

$$q = 1.93 \times 133 = \underline{257 \text{ Mcal/m}^2} \{ \underline{1076 \text{ MJ/m}^2} \}$$

and the equivalent opening factor is

$$A\sqrt{h}/A_t = 1.93 \times 0.031 = \underline{0.06 \text{ m}^{\frac{1}{2}}}$$

## 3 Check on the fire separating function of the wall

Fig. 8 a gives the equivalent fire load  $q$ , for different values of the equivalent opening factor  $A\sqrt{h}/A_t$ , for which some wall types just satisfy their fire separating function. For a wall of 15 cm mineral wool of density  $\gamma = 45 \text{ kg/m}^3$  between incombustible external layers, we therefore obtain from the figure by extrapolation that the equivalent fire load  $q$  may be as much as about  $290 \text{ Mcal/m}^2$   $\{1214 \text{ MJ/m}^2\}$  at an equivalent opening factor of  $A\sqrt{h}/A_t = 0.06 \text{ m}^{\frac{1}{2}}$ . The actual equivalent fire load has been found to be  $257 \text{ Mcal/m}^2$   $\{1076 \text{ MJ/m}^2\}$ .

## 4 Summary

In the case under consideration, a wall consisting of 15 cm mineral wool of density  $\gamma = 45 \text{ kg/m}^3$  between incombustible external layers of e.g. steel sheeting meets the requirement specified for fire partitions with regard to the maximum temperature on the side not exposed to fire.



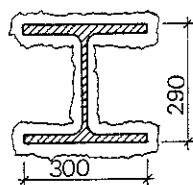
## EXAMPLE 6. FIRE INSULATION OF STEEL COLUMNS

A column of HE 300 A section of Steel 1411 with the yield stress  $\sigma_s = 2600 \text{ kgf/cm}^2$   $\{260 \text{ MPa}\}$  at room temperature is erected in a fire compartment. The column has the length  $L = 7.20 \text{ m}$ , the area of cross section is  $112.5 \text{ cm}^2$  and the least radius of gyration is  $7.49 \text{ cm}$ . The column is pinjointed at both ends in such a way that it is free to expand longitudinally when exposed to fire. The load which shall not cause the column to collapse during a fire has been calculated to correspond to a uniformly distributed compressive stress of  $\sigma = 700 \text{ kgf/cm}^2$   $\{70 \text{ MPa}\}$  over the cross section.

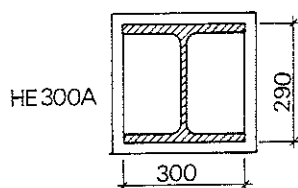
As regards the thermal characteristics of the surrounding constructions, the fire compartment is equivalent to fire compartment Type A according to Table 4 a, and it has an opening factor  $A\sqrt{h}/A_t = 0.08 \text{ m}^{1/2}$ . The fire load  $q$  is  $90 \text{ Mcal/m}^2$   $\{380 \text{ MJ/m}^2\}$  of total surface area.

Calculate the requisite insulation thickness in order that the column should not collapse when exposed to fire on all sides, both for sprayed mineral wool insulation and insulation with slabs of vermiculite based material, as shown in the figure below.

Sprayed mineral wool



Vermiculite slabs



### 1 Critical steel temperature

The slenderness ratio of the column is  $\lambda = 720/7.49 = 96$ . From Fig. 10 b for  $\sigma_s = 2600 \text{ kgf/cm}^2$   $\{260 \text{ MPa}\}$  and  $\gamma = 1$  (unrestrained longitudinal expansion), it appears that the actual stress of  $700 \text{ kgf/cm}^2$   $\{70 \text{ MPa}\}$  is equal to the buckling stress at the steel temperature  $\vartheta_s = 500^\circ\text{C}$  and slenderness ratio  $\lambda = 96$ . The critical steel temperature is thus  $\vartheta_{cr} = 500^\circ\text{C}$ .

### 2 Insulation with sprayed mineral wool

The internal surface area of the insulation per unit length is  $A_i \approx 4 \times 0.3 + 2 \times 0.29 = 1.78 \text{ m}^2/\text{m}$ . The volume of the steel section per unit length is  $V_s = 0.01125 \text{ m}^3/\text{m}$ . This gives  $A_i/V_s = 160 \text{ m}^{-1}$ .

The following is obtained from Table 6 c:3 for an insulation thickness  $d_i = 20 \text{ mm}$

$q$	$A\sqrt{h}/A_t$	$A_i/V_s$	$\vartheta_{\max}$
		150	475
90	0.08	160	490
		200	555

interpolated value

An insulation consisting of 20 mm sprayed mineral wool is thus sufficient to prevent collapse of the column when subjected to the assumed load, since the maximum steel temperature  $\vartheta_{\max} = 490^{\circ}\text{C}$  is less than the critical steel temperature of  $500^{\circ}\text{C}$ .

### 3 Insulation with slabs of vermiculite based material

The internal surface area of the insulation per unit length is  $A_i = 2 \times 0.30 + 2 \times 0.29 = 1.18 \text{ m}^2/\text{m}$ . The volume of the steel section per unit length is  $V_s = 0.01125 \text{ m}^3/\text{m}$ . This gives  $A_i/V_s = 105 \text{ m}^{-1}$ .

The following is obtained from Table 6 b for an average insulation capacity of  $d_i/\lambda_i = 0.10 \text{ m}^2 \text{ }^{\circ}\text{C h/kcal} \{0.086 \text{ m}^2 \text{ }^{\circ}\text{C/W}\}$

q	$A\sqrt{h}/A_t$	$A_i/V_s$	$\vartheta_{\max}$
		100	590
90	0.08	105	600 interpolated value
		125	650

At an average insulation capacity of  $d_i/\lambda_i = 0.20 \text{ m}^2 \text{ }^{\circ}\text{C h/kcal} \{0.172 \text{ m}^2 \text{ }^{\circ}\text{C/W}\}$  the following is obtained

q	$A\sqrt{h}/A_t$	$A_i/V_s$	$\vartheta_{\max}$
		100	420
90	0.08	105	430 interpolated value
		125	480

Linear interpolation between the temperatures of  $430^{\circ}\text{C}$  and  $600^{\circ}\text{C}$  gives the insulation capacity required in order that the steel temperature should not exceed the critical temperature of  $500^{\circ}\text{C}$ .

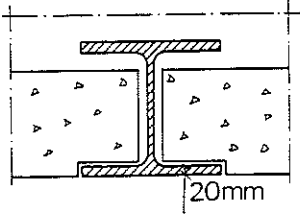
$\vartheta_{\max}$	$d_i/\lambda_i$
430	0.20
500	0.16 interpolated value
600	0.10

An average insulation capacity of  $d_i/\lambda_i = 0.16 \text{ m}^2 \text{ }^{\circ}\text{C h/kcal} \{0.138 \text{ m}^2 \text{ }^{\circ}\text{C/W}\}$  will therefore limit the maximum steel temperature to about  $500^{\circ}\text{C}$ . This means that the thickness of insulation must be at least  $d_i = 0.16\lambda_i$ .

It is seen from Table 6 a that the average thermal conductivity  $\lambda_i$  of slabs of vermiculite based material may be taken as approximately  $0.117 \text{ kcal/m }^{\circ}\text{C h} \{0.137 \text{ W/m }^{\circ}\text{C}\}$  at a maximum steel temperature of  $\vartheta_{\max} = 500^{\circ}\text{C}$ . The insulation thickness required is thus  $d_i = 0.16 \times 0.117 = 0.019 \text{ m} = \underline{19 \text{ mm}}$ .

### EXAMPLE 7. DETERMINATION OF THE CRITICAL FIRE LOAD

A welded steel girder of Steel 1412 with a nominal yield stress of  $\sigma_s = 2600$  kgf/cm<sup>2</sup> {260 MPa} at room temperature, which is rigidly restrained at one end, carries a floor slab which is placed on the bottom flange as shown below.



The span of the girder is 8.0 m, the flange thickness 20 mm and the modulus of section 1683 cm<sup>5</sup>. The uniformly distributed load which shall not cause the girder to collapse under fire exposure conditions has been calculated as 3100 kgf/m {31 kN/m}.

The girder is situated in a fire compartment with surrounding constructions whose thermal characteristics are practically the same as those of fire compartment Type B according to Table 4 a. The equivalent opening factor of the fire compartment is  $A\sqrt{h}/A_t = 0.12$  m<sup>1/2</sup>.

Determine the maximum fire load  $q$  which can be accepted if the bottom flange is not protected from the fire exposure.

#### 1 Critical temperature

The load of 3100 kgf/m {31 kN/m} is put equal to the critical load according to the equation in Fig. 9 b for a beam which is rigidly restrained at one end and is acted upon by a uniformly distributed load.

$$31 = \beta \frac{8 \times 2600 \times 1683}{800^2}$$

This gives  $\beta = 0.56$ . According to the figure, a value of  $\beta = 0.56$  is equivalent to a critical temperature of approximately 590–630°C, depending on the rate of heating. At present this is not known. The critical temperature is therefore taken as 600°C for the time being.

#### 2 Critical fire load for fire compartment Type A

The  $F_s/V_s$  ratio of the girder can be taken to be approximately given by  $1/t$ , where  $t$  is the flange thickness in m (see Fig. 5 a). This gives  $F_s/V_s = 1/0.02 = 50$  m<sup>-1</sup>. The resultant emissivity of the girder  $\epsilon_r$  can be assumed to be 0.5 (see Table 5 a).

The following maximum steel temperatures  $\theta_{\max}$  are obtained from Table 5 c for a resultant emissivity of  $\epsilon_r = 0.5$

$q$	$A\sqrt{h}/A_t$	$F_s/V_s$	$\vartheta_{\max}$
30			540
45	0.12	50	760

The critical temperature was estimated previously as  $600^{\circ}\text{C}$ . The equivalent fire load  $q$  which corresponds to this steel temperature is estimated by interpolation between the above values as

$\vartheta_{\max}$	$q$
540	30
600	34 interpolated value
760	45

The average rate of heating in the girder can now be roughly estimated with the assistance of Fig. 9 a. The input data used are  $q = 34 \text{ Mcal/m}^2$ ,  $A\sqrt{h}/A_t = 0.12 \text{ m}^{1/2}$  and  $\vartheta_{\max} = 600^{\circ}\text{C}$ . By interpolation, the average rate of heating is estimated as  $40^{\circ}\text{C/min}$ . A check in Fig. 9 b for the case of a beam rigidly restrained at one end which is carrying a uniformly distributed load shows that the temperature which corresponds to the previously calculated value of  $\beta = 0.56$  and an approximate rate of heating of  $40^{\circ}\text{C/min}$  is nearer  $620^{\circ}\text{C}$  than the previously assumed value of  $600^{\circ}\text{C}$ .

New interpolation gives

$\vartheta_{\max}$	$q$
540	30
620	35 interpolated value
760	45

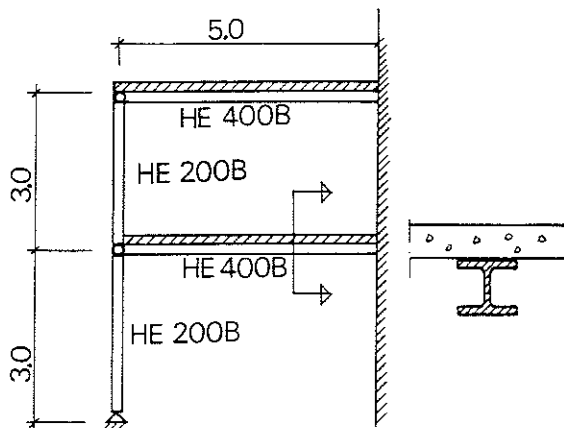
### 3 Critical fire load for fire compartment Type B

According to Table 4 a, the conversion factor  $k_f$  from the actual to the equivalent fire load is 0.85 for fire compartment Type B. In the case under consideration, therefore, the maximum actual fire load which can be accepted if the bottom flange is not provided with insulation is

$$q = \frac{35}{0.85} = 41 \text{ Mcal/m}^2 \{172 \text{ MJ/m}^2\}$$

### EXAMPLE 8. FIRE ENGINEERING DESIGN OF STEEL COLUMN WHOSE LONGITUDINAL EXPANSION IS SUBJECT TO RESTRAINT

A steel construction on two storeys consists of two HE 400 B steel girders of 5.0 m span, and of two HE 200 B steel columns each of 3.0 m height as shown in the figure.



The columns are pinjointed at both ends. The girders are simply supported on the columns and rigidly restrained at the other end. The material of the columns and girders is Steel 1311 with a nominal yield stress  $\sigma_s = 2200 \text{ kgf/cm}^2 \{ 220 \text{ MPa} \}$ . Each storey constitutes a separate fire compartment with a fire load estimated at  $11.8 \text{ Mcal/m}^2 \{ 50 \text{ MJ/m}^2 \}$  and an opening factor determined as  $0.12 \text{ m}^{\frac{1}{2}}$ . The constructions surrounding the fire compartment mainly consist of concrete.

Calculate the load which causes the column on the bottom storey to collapse during a fire on this storey if both the girders and columns are uninsulated. Owing to the connection between the column and the restrained girders, the column is not free to expand longitudinally when it is heated.

#### 1 Conversion to equivalent fire load and equivalent opening factor

The constructions surrounding the fire compartment consist of concrete, and the fire compartment is thus equivalent to fire compartment Type B according to Table 4 a, with a conversion factor  $k_f = 0.85$ . The equivalent fire load  $q$  and equivalent opening factor  $A\sqrt{h}/A_t$  are therefore

$$q = 0.85 \times 11.8 = \underline{10 \text{ Mcal/m}^2 \{ 42 \text{ MJ/m}^2 \}}$$

$$A\sqrt{h}/A_t = 0.85 \times 0.12 = \underline{0.10 \text{ m}^{\frac{1}{2}}}$$

#### 2 Maximum steel temperature

##### Girder

The resultant emissivity  $\epsilon_r$  for the girder is put equal to 0.5 (see Table 5 a). The  $F_s/V_s$  ratio for the girder is  $85 \text{ m}^{-1}$  (see Table 5 b).

The maximum steel temperature  $\vartheta_{\max}$  is obtained from Table 5 c as a function of the equivalent fire load  $q = 10 \text{ Mcal/m}^2$  {42 MJ/m<sup>2</sup>}, the equivalent opening factor  $A\sqrt{h}/A_t = 0.10 \text{ m}^{\frac{1}{2}}$ , the ratio  $F_s/V_s = 85 \text{ m}^{-1}$  and the resultant emissivity  $\epsilon_r = 0.5$ . For  $q = 10 \text{ Mcal/m}^2$ , we have

$A\sqrt{h}/A_t$	$F_s/V_s$	$\vartheta_{\max}$
	75	330
0.08	85	360 interpolated value
	100	400
	75	260
0.12	85	280 interpolated value
	100	310

Interpolation between the opening factor values of 0.08 and 0.12  $\text{m}^{\frac{1}{2}}$  gives the following maximum steel temperature  $\vartheta_{\max}$  at an opening factor of  $A\sqrt{h}/A_t = 0.10 \text{ m}^{\frac{1}{2}}$

$A\sqrt{h}/A_t$	$F_s/V_s$	$\vartheta_{\max}$
0.08		360
0.10	85	320 interpolated value
0.12		280

The maximum steel temperature in the girder is thus  $\vartheta_{\max} = \underline{320^\circ\text{C}}$ .

#### Column

The resultant emissivity  $\epsilon_r$  for the column is put equal to 0.7 (see Table 5 a). The  $F_s/V_s$  ratio of the column is approximately equal to 150  $\text{m}^{-1}$  (see Table 5 b).

The maximum steel temperature  $\vartheta_{\max}$  is obtained from Table 5 c as a function of the equivalent fire load  $q = 10 \text{ Mcal/m}^2$  {42 MJ/m<sup>2</sup>}, the equivalent opening factor  $A\sqrt{h}/A_t = 0.10 \text{ m}^{\frac{1}{2}}$ , the ratio  $F_s/V_s = 150 \text{ m}^{-1}$  and the resultant emissivity  $\epsilon_r = 0.7$ . For  $q = 10 \text{ Mcal/m}^2$ , we have

$A\sqrt{h}/A_t$	$F_s/V_s$	$\vartheta_{\max}$
0.08		580
0.10	150	600 interpolated value
0.12		620

The maximum steel temperature in the column is thus  $\vartheta_{\max} = \underline{600^\circ\text{C}}$ .

### 3 Calculation of the degree of expansion $\gamma$ when expansion is subject to partial restraint

According to Equation (10.2.1 e) in the Main Section, the degree of expansion can be written as

$$\gamma = \frac{1}{1 + \frac{L}{E A y_1 \Delta N=1}}$$

where  $L$  = length of column (300 cm)  
 $A$  = area of column cross section ( $78.1 \text{ cm}^2$ )  
 $y1_{\Delta N=1}$  = upwards deflection of the girder at the point of fixity to the column for a unit load  $\Delta N = 1$

The value of the modulus of elasticity (secant modulus)  $E$  is dependent on the column temperature of  $600^\circ\text{C}$  and on the actual stress level. Since the imposed stress is not known, the secant modulus is determined for a stress equal to the buckling stress of the column at the temperature concerned and no restraint on longitudinal expansion, i.e. for  $\gamma = 1$ . For the actual slenderness ratio  $\lambda = 300/5.07 = 59$  and actual steel temperature of  $600^\circ\text{C}$ , Fig. 10 b for  $\sigma_s = 2200 \text{ kgf/cm}^2$  {220 MPa} and  $\gamma = 1$  gives the buckling stress as  $\sigma_k = 530 \text{ kgf/cm}^2$  {53 MPa}. For a stress level of  $530/2200 = 0.24$  and a steel temperature of  $\theta_s = 600^\circ\text{C}$ , Fig. 10.1 b in the Main Section gives the value of the secant modulus as  $E = 0.20 \times 2.1 \times 10^6 \text{ kgf/cm}^2$  { $0.20 \times 2.1 \times 10^5 \text{ MPa}$ }.

When the bottom column expands due to its rise in temperature, the end of the girder which is carried on the column is displaced upwards. The girder then acts as a cantilever with respect to the additional imposed force. The upper girder is also displaced upwards when the bottom column expands, but this displacement is somewhat less than that in the bottom column since the upper column is subjected to an elastic compression by the additional force. However, compression of the column in this case is small in comparison with the displacement of the girder ends, and calculation of the degree of expansion  $\gamma$  can therefore be based on the sum of the stiffnesses of the two girders without consideration of the column compression. This gives

$$y1_{\Delta N=1} = \frac{L_b^3}{3 E_{bl} I_{bl} + 3 E_{bu} I_{bu}}$$

where  $L_b$  = girder length (500 cm)  
 $E_{bl}, E_{bu}$  = modulus of elasticity of the lower and upper girder respectively at the temperature concerned (at  $320^\circ\text{C}$  the modulus of elasticity is approximately 90% of that at room temperature, i.e.  $E_{320} = 0.9 \times 2.1 \times 10^6 \text{ kgf/cm}^2$  { $0.9 \times 2.1 \times 10^5 \text{ MPa}$ }, see Fig. 9.1 a in the Main Section)  
 $I_{bl}, I_{bu}$  = moment of inertia of the lower and upper girder respectively ( $57,680 \text{ cm}^4$ )

We therefore have

$$\gamma = \frac{1}{1 + \frac{3 L (E_{bl} I_{bl} + E_{bu} I_{bu})}{E A L_b^3}}$$

$$\gamma = \frac{1}{1 + \frac{3 \times 300 (0.9 + 1) \times 2.1 \times 10^6 \times 57,680}{0.2 \times 2.1 \times 10^6 \times 78.1 \times 500^3}} = 0.95$$

#### 4 Critical column load

The critical buckling load is obtained from Fig. 10b for a yield stress  $\sigma_s = 2200$  kgf/cm<sup>2</sup> {220 MPa} and degree of expansion  $\gamma = 0.95$ . The slenderness ratio of the column  $\lambda = 59$  and steel temperature 600°C gives a buckling stress of  $\sigma_k = 440$  kgf/cm<sup>2</sup> {44 MPa}. The critical column load is thus

$$N_{cr} = 78.1 \times 440 = \underline{34,400 \text{ kgf } \{344 \text{ kN}\}}$$

If the column had not been connected to two girders but only to the girder in the fire compartment, the degree of expansion  $\gamma$  would have been

$$\gamma = \frac{1}{1 + \frac{3 L E_{bl} I_{bl}}{E A L_b^3}} = 0.976$$

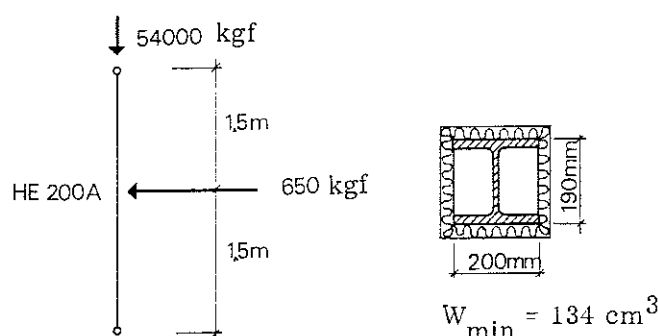
This would have given a buckling stress of approximately 490 kgf/cm<sup>2</sup> {49 MPa} and a critical column load of about 38,300 kgf {383 kN}.

If there had been no restraint at all on longitudinal expansion of the column, the buckling stress would have been approximately 540 kgf/cm<sup>2</sup> {54 MPa} and the critical column load approximately 42,200 kgf {422 kN}.



### EXAMPLE 9. FIRE INSULATION OF STEEL COLUMN SUBJECT TO AN AXIAL AND TRANSVERSE LOAD

A steel column of HE 200 A section with an effective length of 3.0 m is assumed to be free to expand on being heated. The load combination which shall not cause the column to collapse in the event of fire consists of a vertical load of 54,000 kgf { 540 kN } and a horizontal force of 650 kgf { 6.5 kN } which acts at the midpoint of the column in a direction at right angles to the minor axis, as shown in the figure.



The material is Steel 1412 with a nominal yield stress  $\sigma_s = 2600 \text{ kgf/cm}^2$  { 260 MPa }. There is no restraint on longitudinal expansion of the column when its temperature rises.

The column is placed in a fire compartment whose surrounding constructions have thermal characteristics equivalent to those for fire compartment Type A according to Table 4 a. The fire load and opening factor of the fire compartment are calculated as  $90 \text{ Mcal/m}^2$  {  $380 \text{ MJ/m}^2$  } and  $0.08 \text{ m}^{\frac{1}{2}}$ .

Determine the least thickness of fire insulation for the column, placed as shown in the figure above, the material being slabs of mineral wool of density  $\gamma = 150 \text{ kg/m}^3$ .

#### 1 Critical steel temperature

The slenderness ratio of the column is  $\lambda = 300/4.98 = 60$ . The compressive stress due to the vertical load is  $\sigma = 54,000/53.8 = 1000 \text{ kgf/cm}^2$  { 100 MPa }. If the column were acted upon only by the vertical load then, according to Fig. 10 b for  $\sigma_s = 2600 \text{ kgf/cm}^2$  { 260 MPa } and degree of expansion  $\gamma = 1$ , the critical steel temperature would be approximately  $510^\circ\text{C}$ . Since the column is simultaneously acted upon by a horizontal force, the critical temperature will be less than  $510^\circ\text{C}$ . To start with, it will be assumed that the critical temperature is  $450^\circ\text{C}$ , and an iterative procedure will be used to check if this temperature is correct.

The ratios  $K = N/N_k$  and  $B = Q/Q_{cr}$ , which give an idea of the stress level in the fire-exposed structure with respect to in-plane buckling only, and of its ability to resist bending moments, are calculated according to Equations (10.3 a) and (10.3 b) in the Main Section.  $N$  denotes the vertical load on the column and  $N_k$  the buckling load at  $450^\circ\text{C}$ .  $Q$  denotes the horizontal force and  $Q_{cr}$  the critical load of the column at  $450^\circ\text{C}$  when this is acted upon only by a horizontal force.

According to the diagram for  $\sigma_s = 2600 \text{ kgf/cm}^2$  {260 MPa} and degree of expansion  $\gamma = 1$  in Fig. 10 b, the buckling stress at  $450^\circ\text{C}$  and a slenderness ratio of  $\lambda = 60$  is equal to  $1200 \text{ kgf/cm}^2$  {120 MPa}. This gives the value of  $N_k$  and  $N/N_k$  as

$$N_k = 1200 \times 53.8 = 64,600 \text{ kgf} \{646 \text{ kN}\}$$

$$K = \frac{N}{N_k} = \frac{54,000}{64,600} = 0.836$$

The critical transverse load  $Q_{cr}$  at  $450^\circ\text{C}$  is determined according to the diagram for a simply supported beam with a central point load in Fig. 9 b. This gives  $Q_{cr}$  and  $Q/Q_{cr}$  as

$$Q_{cr} = 0.92 \times \frac{4 \times 2600 \times 134}{300} = 4270 \text{ kgf} \{427 \text{ kN}\}$$

$$B = \frac{Q}{Q_{cr}} = \frac{650}{4270} = 0.152$$

The value of  $\alpha$  is calculated according to Equation (10.3 d) in the Main Section as

$$\alpha = \sqrt{\frac{\sigma_{0.2}}{\sigma_{el}}}$$

where  $\sigma_{0.2}$  = the yield stress or 0.2% proof stress at  $450^\circ\text{C}$

$\sigma_{el}$  = Euler critical stress at a modulus of elasticity  $E$  at  $450^\circ\text{C}$

The values of  $\sigma_{0.2}$  and  $E$  at  $450^\circ\text{C}$  are determined from Fig. 9.1 a in the Main Section.

$$\sigma_{0.2} = 0.57 \times 2600 = 1480 \text{ kgf/cm}^2 \{148 \text{ MPa}\}$$

$$E = 0.74 \times 2.1 \times 10^6 = 1.55 \times 10^6 \text{ kgf/cm}^2 \{1.55 \times 10^5 \text{ MPa}\}$$

This gives

$$\sigma_{el} = \frac{\pi^2 EI}{AL^2} = \frac{\pi^2 \times 1.55 \times 10^6 \times 1336}{53.8 \times 300^2} = 4220 \text{ kgf/cm}^2 \{422 \text{ MPa}\}$$

and

$$\alpha = \sqrt{\frac{1480}{4220}} = 0.59$$

According to Section 10.3 in the Main Section, the criterion to be satisfied in order that failure should not occur is that  $K + B \leq 1$  at this value of  $\alpha$ . This criterion is satisfied at the assumed temperature of  $450^\circ\text{C}$ , since  $K = 0.836$  and  $B = 0.152$ , and thus  $K + B = 0.988$ . Since  $K + B$  is somewhat less than 1, the critical temperature will be a little higher than the assumed value of  $450^\circ\text{C}$ . However, the difference is very small, and the critical steel temperature can therefore be given as  $450^\circ\text{C}$ .

## 2 Requisite insulation thickness

The maximum steel temperature under fire exposure conditions in a construction insulated with slabs of mineral wool of density  $\gamma = 150 \text{ kg/m}^3$  can be determined from Table 6 c:2 as a function of the equivalent fire load  $q$ , the equivalent opening factor  $A\sqrt{h}/A_t$ , the ratio  $F_s/V_s$  and the insulation thickness  $d_i$ . Since the

constructions surrounding the fire compartment have thermal characteristics corresponding to those for fire compartment Type A according to Table 4 a, the conversion factor for the equivalent fire load and equivalent opening factor will be  $k_f = 1.0$ . The equivalent fire load and equivalent opening factor will thus be  $90 \text{ Mcal/m}^2 \{380 \text{ MJ/m}^2\}$  and  $0.08 \text{ m}^2$ . The ratio  $A_i/V_s$  is calculated according to Fig. 6 a. This gives  $A_i/V_s = (2 \times 0.20 + 2 \times 0.19)/53.8 \times 10^{-4} = 145 \text{ m}^{-1}$ . When the insulation thickness for slabs of mineral wool is 30 mm, the following values of the maximum steel temperature  $\vartheta_{\max}$  are obtained from Table 6 c:2

q	$A\sqrt{h}/A_t$	$A_i/V_s$	$\vartheta_{\max}$
		125	515
90	0.08	145	560 interpolated value
		150	570

For an insulation thickness of 50 mm, we have

q	$A\sqrt{h}/A_t$	$A_i/V_s$	$\vartheta_{\max}$
		125	365
90	0.08	145	395 interpolated value
		150	400

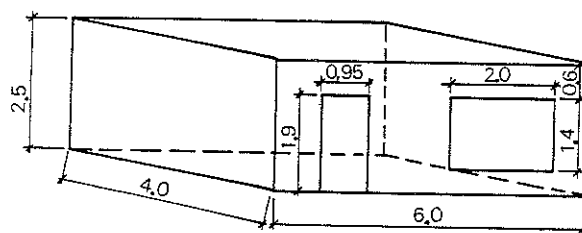
The insulation thickness required in order to limit the steel temperature to  $450^\circ\text{C}$  is obtained from the above values by interpolation

$\vartheta_{\max}$	$d_i$
395	50
450	43 interpolated value
560	30

In order that the given load combination shall not cause the construction to collapse during a fire, the least insulation thickness required for insulation consisting of slabs of mineral wool of density  $\gamma = 150 \text{ kg/m}^3$  is  $d_i = \underline{43 \text{ mm}}$ .

# EXAMPLE 10. CALCULATION OF OPENING FACTOR AND THE NUMBER OF AIR CHANGES

A fire compartment has the openings and internal dimensions as shown below.



Calculate what approximate area is required for a horizontal opening in the roof in order that the opening factor of the fire compartment shall be doubled. Determine further the approximate number of air changes to be provided by a mechanical ventilation system if there were no openings, in order that the air supplied and removed by the system should be the same as that provided by the openings according to the figure, the assumption being that the fire is controlled by ventilation.

## 1 Calculation of the opening factor

The opening factor is calculated according to Fig. 3 a.

The total internal surface area of the fire compartment

$$A_t = 2 \times 4 \times 6 + 2 \times 4 \times 2.5 + 2 \times 6 \times 2.5 = 98 \text{ m}^2$$

The total area of openings

$$A = 0.95 \times 1.9 + 2.0 \times 1.4 = 1.8 + 2.8 = 4.6 \text{ m}^2$$

The mean height of openings

$$h = \frac{1}{4.6} (1.8 \times 1.9 + 2.8 \times 1.4) = 1.6 \text{ m}$$

$$\text{Opening factor } A\sqrt{h}/A_t = \frac{4.6\sqrt{1.6}}{98} = 0.06 \text{ m}^{\frac{1}{2}}$$

## 2 Calculation of the requisite opening area in the roof

According to Equation (4.3.2 b) in the Main Section, the opening factor is calculated for the case where there are also horizontal openings by multiplying the opening factor for the vertical openings  $(A\sqrt{h}/A_t)_v$  by a coefficient  $f_k$ , i.e.

$$\frac{A\sqrt{h}}{A_t} = f_k \left( \frac{A\sqrt{h}}{A_t} \right)_v$$

In order therefore that the opening factor should be doubled by means of a horizontal opening, the coefficient must be  $f_k = 2$ . If the nomogram in Fig. 4.3.2 b in the Main Section is employed using the value  $f_k = 2$ , then we have, with the symbols used in Figs. 4.3.2 b and 4.3.2 a in the Main Section, that

$$A_h \sqrt{h_2} / A \sqrt{h} \approx 0.5$$

$$A_h \sqrt{h_1} / A \sqrt{h} \approx 0.5$$

Since the mean value of the height of vertical openings is  $h = 1.6$  m,  $h/2 = 0.8$  and  $h_1 = 0.6 + 0.8 = 1.4$  m. Furthermore,  $A = 4.6$  m<sup>2</sup>. Putting these values into the last equation, we obtain the area of horizontal openings

$$A_h = 0.5 \times A \sqrt{h} / \sqrt{h_1} = 0.5 \times 4.6 \sqrt{1.6} / \sqrt{1.4} \approx 2.5 \text{ m}^2$$

There is however a stipulation according to Equation (4.3.2 c) in the Main Section, in order that the calculation method used may be applicable, viz, that the value of  $A_h \sqrt{h_2} / A \sqrt{h}$  shall not exceed 1.76 at 1000°C, or 1.37 at 500°C. This stipulation is satisfied in this case since the value of  $A_h \sqrt{h_2} / A \sqrt{h} \approx 0.5$ . The area of horizontal opening in the roof, in order that the opening factor for the fire compartment according to the figure may be doubled, is therefore  $A_h = 2.5$  m<sup>2</sup>.

### 3 Determination of the number of air changes to be provided by a mechanical ventilation system

According to Equation (4.2.2.5 b) in the Main Section, the mean rate of combustion  $R_m$  during the flame phase of the fire can be written

$$R_m = k A \sqrt{h} \text{ (kg/h)}$$

The coefficient  $k$  (kg/h m<sup>5/2</sup>) can be determined from Fig. 4.2.2.5 a, and has a value of approximately 310 kg/h m<sup>5/2</sup> for e.g. wood with a calorific value of  $H \approx 4.5$  Mcal/kg {19 MJ/kg}. If we substitute this value of  $k$  and the values  $A = 4.6$  m<sup>2</sup> and  $h = 1.6$  m, we have

$$R_m = 310 \times 4.6 \sqrt{1.6} = 1800 \text{ kg/h}$$

According to Subsection 4.3.1 in the Main Section, about 5.2 kg of air is required for combustion of 1 kg wood. This means that an air supply of approximately  $5.2 \times 1800 = 9400$  kg/h is required to maintain the rate of combustion at the same value as that given by the fire compartment openings according to the figure in a ventilation controlled fire. Since the density of air is approximately 1.30 kg/m<sup>3</sup>, this is equivalent to a requisite air volume of about  $7000$  m<sup>3</sup>/h. As the total air volume of the fire compartment is 60 m<sup>3</sup>, the number of air changes required is  $7000/60 = 117$  (1/h).



ALTERNATIVE DESIGN METHOD  
BASED ON THE CONCEPT  
OF EQUIVALENT FIRE DURATION





The concept of equivalent fire duration has been introduced in the international discussion in recent years as an aid in converting fire exposure in actual fires to the thermal action which characterises a standard fire test for the classification of loadbearing structures and partitions. In the case of steel structures the equivalent fire duration denotes that length of the heating period of the standard fire test which gives rise to the same maximum steel temperature as the complete fire process in a real fire.

In the literature, the concept of equivalent fire duration occurs in different versions associated with different levels of the accuracy to be attained, see, for instance, (30), (66) - (68). The presentation below is confined to a definition of the equivalent fire duration which produces an accuracy equal to that made possible by the method put forward in this handbook for rational fire engineering design.

In principle, the equivalent fire duration can be defined as in Fig. 1 which refers to an uninsulated steel structure under fire exposure conditions (30), (67) - (69). In the figure, the full lines describe the variation in time of the gas temperature  $\vartheta_t$  in the fire compartment and the steel temperature  $\vartheta_s$  in a real fire, as determined by the fire load  $q$ , the opening factor  $A\sqrt{h}/A_t$ , and the thermal characteristics of the surrounding constructions. The dashed lines describe the gas temperature of the heating phase according to a standardised fire test,  $\vartheta_t$  (S.C.) (see Equation (2.5) in the Main Section) and the corresponding variation in time of the steel temperature  $\vartheta_s$  (S.C.). By direct conversion of the maximum steel temperature in a real fire,  $\vartheta_{\max}$ , to the same temperature in the standard fire test, as shown in Fig. 1, the equivalent fire duration  $T_e$  is defined.

According to the above definition, the equivalent fire duration  $T_e$  is a function of both the parameters governing the fire and also the quantities which describe the structural characteristics of an uninsulated or insulated steel structure. This is shown more clearly in Figs. 2 and 3 (68).

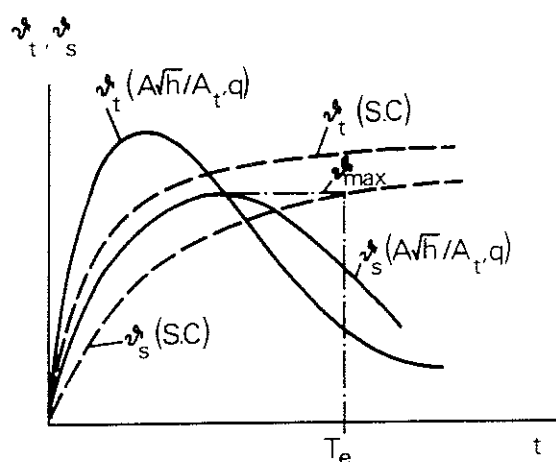


Fig. 1. Definition of the equivalent fire duration  $T_e$  illustrated for an uninsulated steel structure. The full lines describe the gas temperature  $\vartheta_t$  and steel temperature  $\vartheta_s$  during a real fire, while the dashed lines relate to the corresponding temperatures in a standard fire test

Fig. 2 refers to uninsulated steel structures exposed to real fires with characteristics according to Fig. 4.3.3 a and Table 4.3.3 a in the Main Section, i.e. a fire in a fire compartment Type A. The figure gives the equivalent fire duration  $T_e$  as a function of the opening factor  $A\sqrt{h}/A_t$  of the fire compartment, the fire load  $q$ , the resultant emissivity  $\epsilon_r$  and the section parameter  $F_s/V_s$ . In Fig. 2 it is assumed that the resultant emissivity in heating according to the standard fire test is  $\epsilon_r = 0.5$ , while for real fires  $\epsilon_r$  has the values given in the appropriate figures. Reference is to be made to the Main Section with regard to the various parameters.

From the functional point of view, the condition to be satisfied by Fig. 2 is that the complete fire process in a real fire and the heating phase in a standard fire test shall both give rise to the same maximum temperature  $\vartheta_{\max}$  in the steel structure which is exposed to fire. The level of the maximum steel temperature  $\vartheta_{\max}$  will therefore be a function of the opening factor  $A\sqrt{h}/A_t$ , the fire load  $q$ , the resultant emissivity  $\epsilon_r$  and the section parameter  $F_s/V_s$ . For any given application, this maximum temperature level can be obtained directly from Table 5 c in the Design Section.

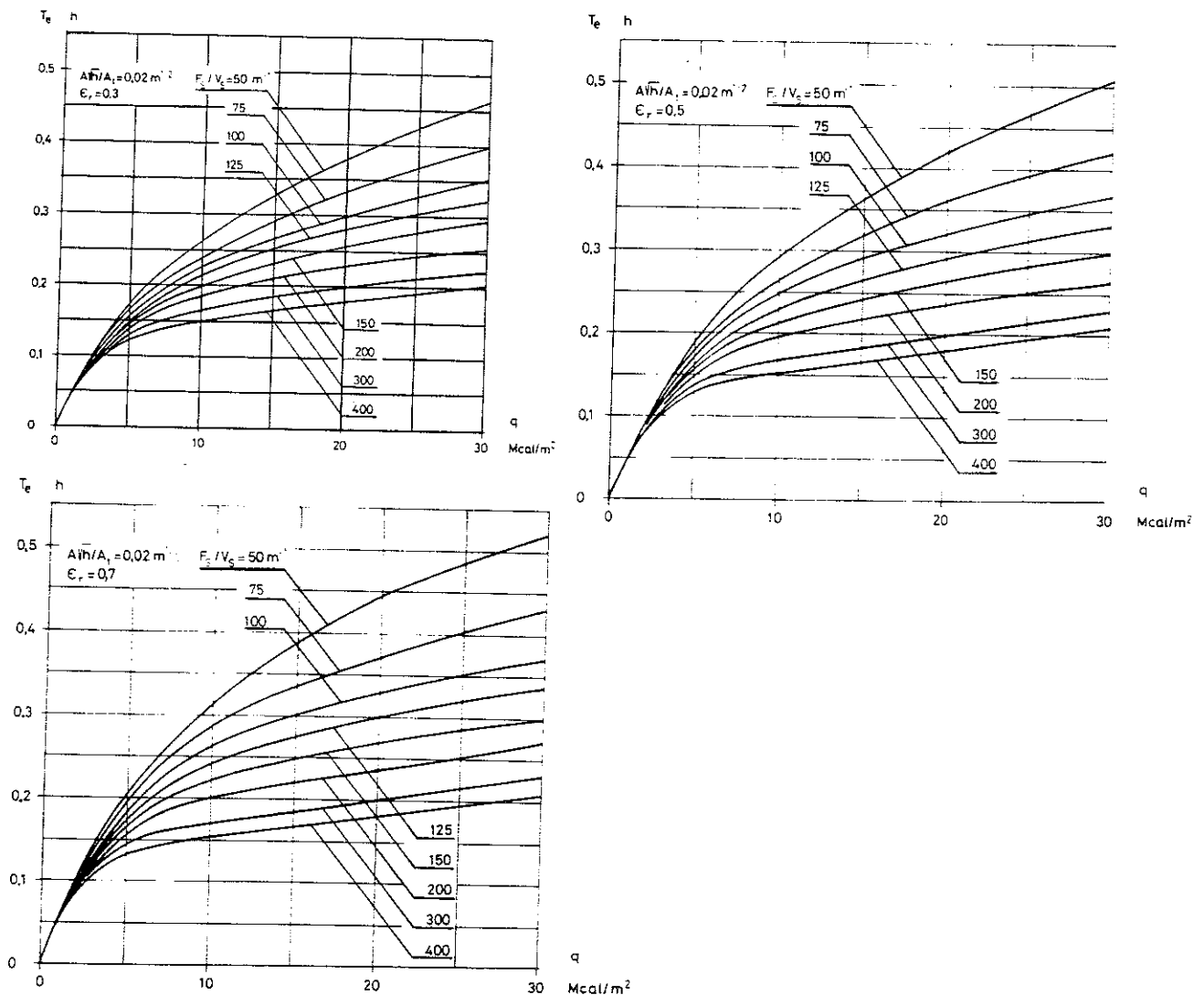


Fig. 2. Equivalent fire duration  $T_e$  for an uninsulated steel structure for different values of the opening factor  $A\sqrt{h}/A_t$ , fire load  $q$ , resultant emissivity  $\epsilon_r$  and structural parameter  $F_s/V_s$ . The curves are based on a fire process according to Fig. 4.3.3 a and Table 4.3.3 a (fire compartment Type A) in the Main Section. With regard to the various parameters, reference is to be made to Chapters 4 and 5 in the Main Section. {The fire load in  $\text{MJ/m}^2$  is obtained by multiplying the fire load values in  $\text{Mcal/m}^2$  by the factor 4.2}

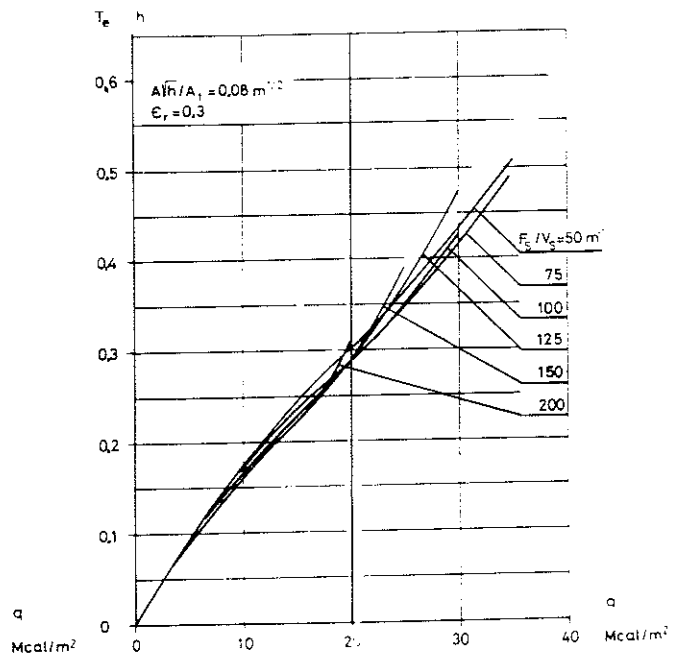
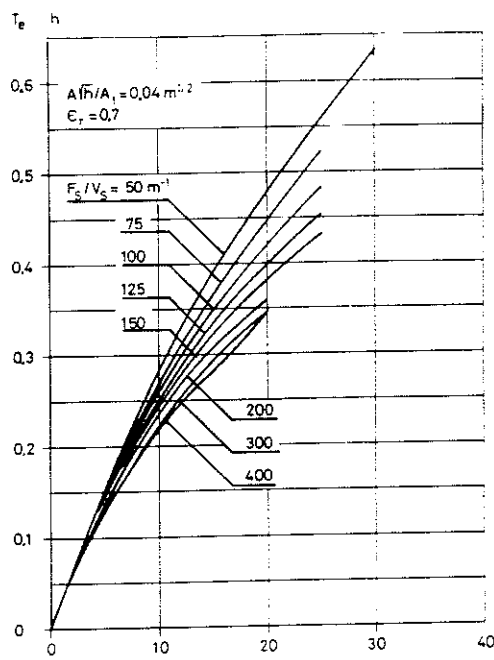
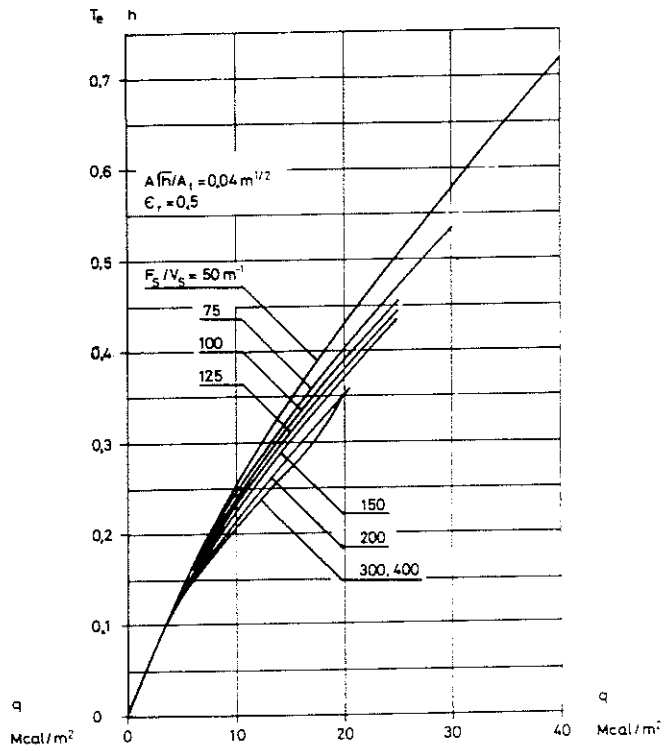
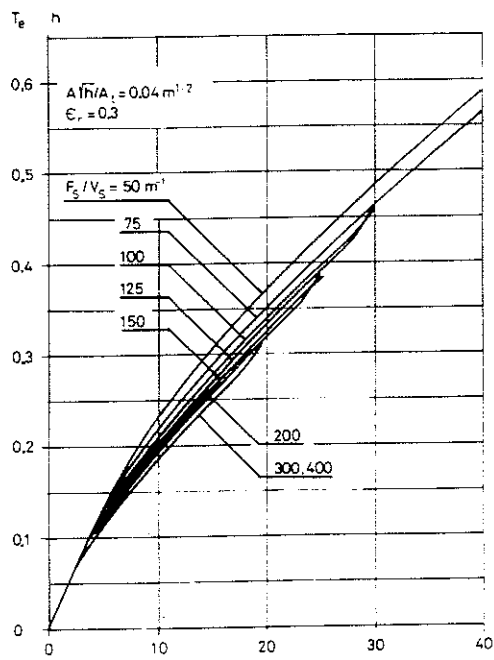


Fig. 2

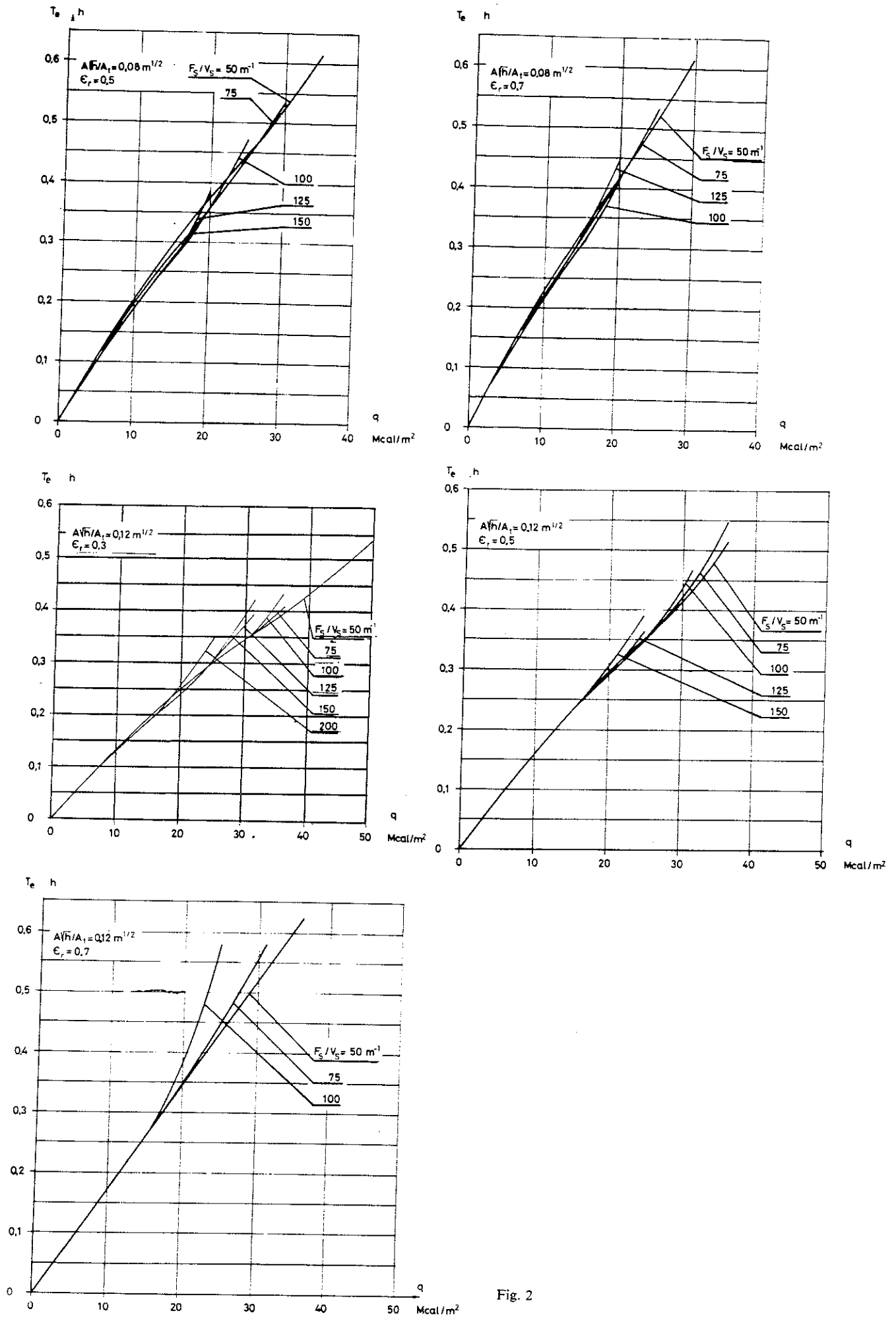


Fig. 2

Fig. 3 presents corresponding curves, in full lines, for the equivalent fire duration  $T_e$  in insulated steel structures under fire exposure conditions. The input parameters are the opening factor  $A\sqrt{h}/A_t$  of the fire compartment, the fire load  $q$ , and the structural parameter  $A_i\lambda_i/d_iV_s$ . In the case of insulated steel structures, variations in the resultant emissivity  $\epsilon_r$  have little practical significance. From the dashed lines the maximum steel temperature  $\vartheta_{\max}$  is obtained directly for different combinations of  $q$ ,  $A\sqrt{h}/A_t$  and  $A_i\lambda_i/d_iV_s$ . It is a consistent assumption in the production of design data that the material used for insulation, and attachment of this to the structure, are such that the insulation function is retained during the entire fire. Reference is to be made to the Main Section with regard to the various parameters.

The design data of the type given in Figs. 2 and 3 can be used either in deciding how the results of standard fire tests can be applied in practical design of load-bearing elements on the basis of an actual fire, or in determining the duration  $T_e$  which the heating phase of a standard fire test must have for a given design of the loadbearing structure in order that the maximum steel temperature should be the same as in a real fire. On the other hand, the concept of equivalent fire duration cannot be used in direct association with the evacuation time of a building or pre-

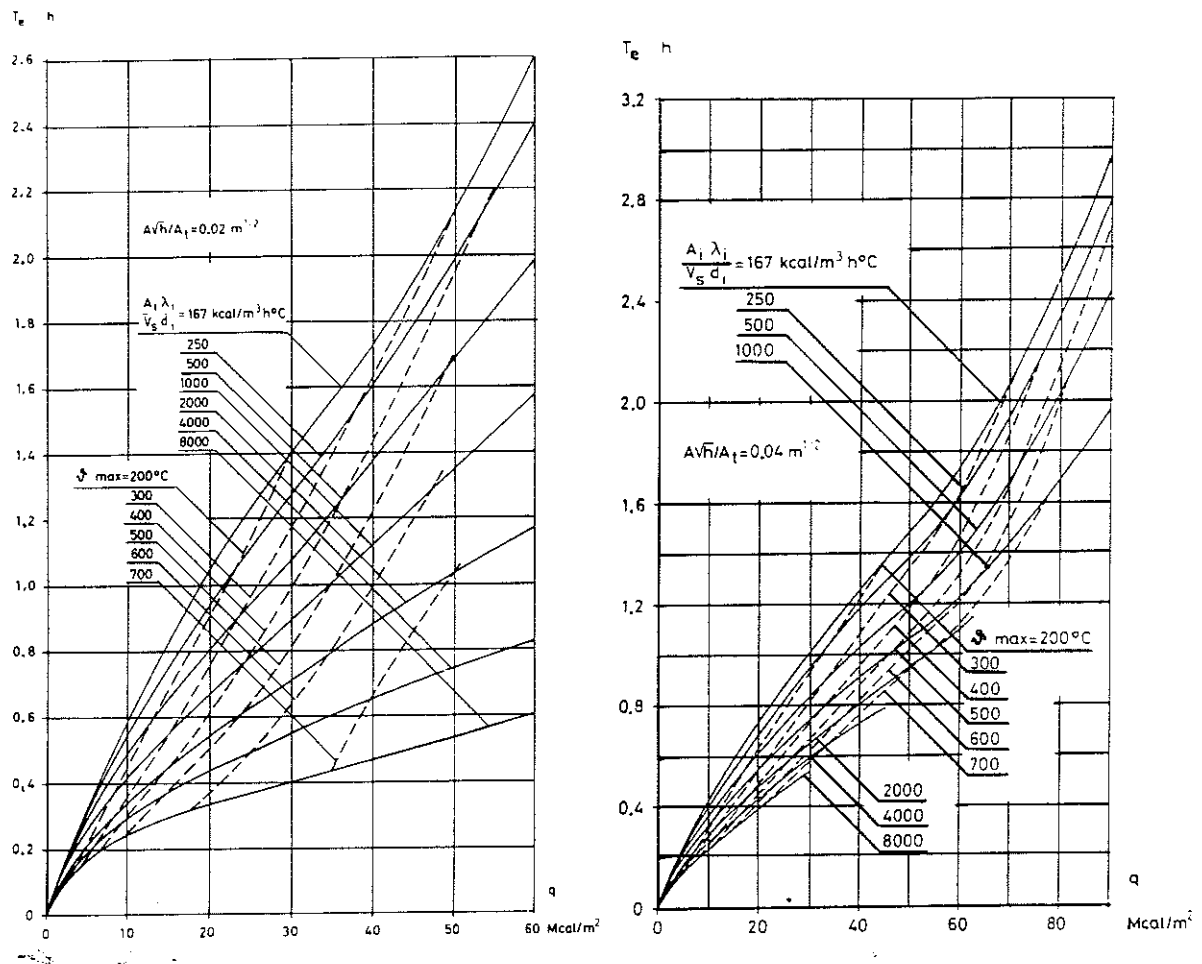
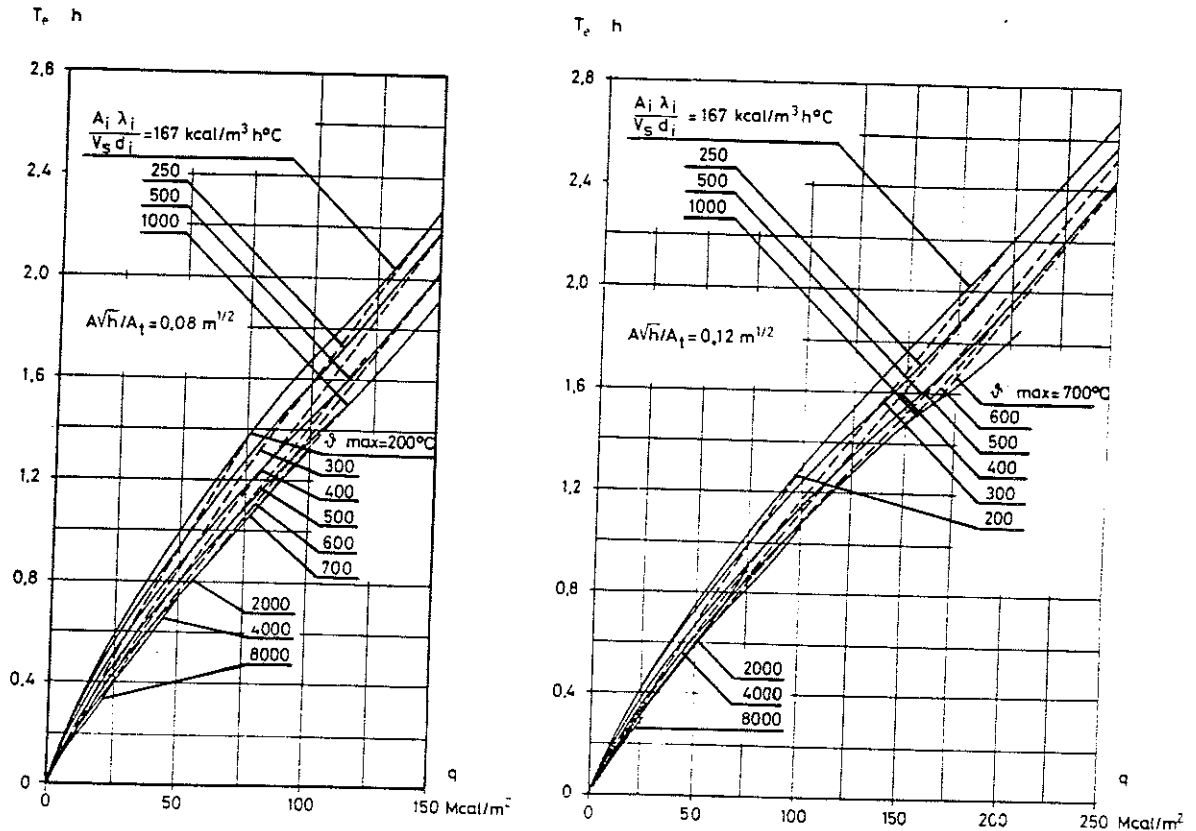


Fig. 3. Equivalent fire duration  $T_e$  for an insulated steel structure for different values of the opening factor  $A\sqrt{h}/A_t$ , fire load  $q$ , and structural parameter  $A_i\lambda_i/V_s d_i$ . The dashed lines indicate the associated maximum steel temperatures  $\vartheta_{\max}$ . The curves are based on a fire process according to Fig. 4.3.3 a and Table 4.3.3 a (fire compartment Type A) in the Main Section. With regard to the various parameters, reference is to be made to Chapters 4 and 6 in the Main Section. { The fire load in  $\text{MJ/m}^2$  is obtained by multiplying the fire load values in  $\text{Mcal/m}^2$  by the factor 4.2. The parameter  $A_i\lambda_i/V_s d_i$  in terms of  $\text{W/m}^3\text{ }^\circ\text{C}$  is obtained by multiplying the figures quoted by the factor 1.163 }

Fig. 3

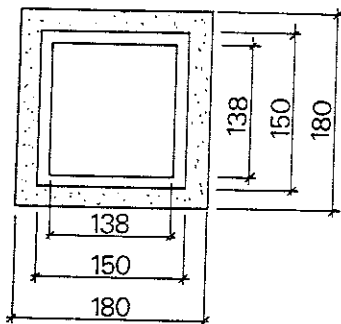


mises, or the time at which the fire brigade must begin operations. Assessment of these problems must be based directly on the characteristics of the actual fire.

Practical application of the concept of equivalent fire duration will be illustrated below by means of two examples.

#### Example 1.

A steel column of cross section as shown below is provided with fire insulation of thickness  $d_i = 15 \text{ mm}$ . The average insulation capacity during a fire of the insulation is estimated as  $\lambda_i = 0.10 \text{ kcal/m}^\circ\text{C h}$   $\{0.116 \text{ W/m}^\circ\text{C}\}$ . The column is placed in a fire compartment Type A (see Subsection 4.3.3 and 4.3.4 in the Main Section) with a fire load of  $q = 35 \text{ Mcal/m}^2$   $\{147 \text{ MJ/m}^2\}$  and an opening factor of  $Avh/A_t = 0.02 \text{ m}^{1/2}$ .



Determine the equivalent fire duration  $T_e$  referred to the standard fire curve and the corresponding maximum steel temperature  $\theta_{\text{max}}$  during a fire in this fire compartment.

Volume of steel section per unit length

$$V_s = (15^2 - 13.8^2) \times 10^{-4} = 34.6 \times 10^{-4} \text{ m}^3/\text{m}$$

Internal surface area of insulation per unit length

$$A_i = 4 \times 15 \times 10^{-2} = 60 \times 10^{-2} \text{ m}^2/\text{m}$$

With  $d_i = 0.15 \text{ m}$  and  $\lambda_i = 0.10 \text{ kcal/m}^\circ\text{C h}$   $\{0.116 \text{ W/m}^\circ\text{C}\}$

we have

$$\frac{A_i \lambda_i}{V_s d_i} = \frac{60 \times 10^{-2} \times 0.10}{34.6 \times 10^{-4} \times 0.015} = 1155 \text{ kcal/m}^3^\circ\text{C h} \{1343 \text{ W/m}^3^\circ\text{C}\}$$

The equivalent fire duration and maximum steel temperature can be determined from Fig. 3. Using the values  $A_i \lambda_i / V_s d_i = 1155 \text{ kcal/m}^3^\circ\text{C h}$   $\{1343 \text{ W/m}^3^\circ\text{C}\}$ ,  $q = 35 \text{ Mcal/m}^2$   $\{147 \text{ MJ/m}^2\}$  and  $A\sqrt{h}/A_t = 0.02 \text{ m}^{1/2}$ , we obtain an equivalent fire duration of  $T_e = 0.97 \text{ h}$  and a maximum steel temperature of  $\vartheta_{\max} = 515^\circ\text{C}$ .

### Example 2.

A steel construction of very complex structural mode of action is to be assessed from the fire engineering point of view. It was found that an assessment of the loadbearing capacity merely on the basis of a theoretical determination of the reduction in the strength of the construction at elevated temperatures could not be carried out satisfactorily. The construction was therefore tested in a test furnace. During the test the construction was acted upon by a static load equivalent to that considered statistically representative during a fire. The construction was provided with fire insulation, with a value of the parameter  $A_i \lambda_i / V_s d_i = 2000 \text{ kcal/m}^3^\circ\text{C h}$   $\{2326 \text{ W/m}^3^\circ\text{C}\}$ , where  $A_i$  denotes the internal surface area of the insulation ( $\text{m}^2$ ),  $V_s$  the volume of the steel section ( $\text{m}^3$ ),  $d_i$  the insulation thickness (m) and  $\lambda_i$  the average thermal conductivity ( $\text{kcal/m}^\circ\text{C h}$ )  $\{\text{W/m}^\circ\text{C}\}$  of the insulation during the fire. The test furnace was heated in conformity with the standard fire curve. Collapse occurred after 52 minutes of fire test.

Check whether there is a risk that the construction will collapse in a real fire in a fire compartment of Type A (see Main Section, Subsections 4.3.3 and 4.3.4) if the fire load is  $q = 50 \text{ Mcal/m}^2$   $\{210 \text{ MJ/m}^2\}$  and the opening factor is  $A\sqrt{h}/A_t = 0.08 \text{ m}^{1/2}$ .

Using the parameter  $A_i \lambda_i / V_s d_i = 2000 \text{ kcal/m}^3^\circ\text{C h}$   $\{2326 \text{ W/m}^3^\circ\text{C}\}$  and fire load  $q = 50 \text{ Mcal/m}^2$   $\{210 \text{ MJ/m}^2\}$  and opening factor  $A\sqrt{h}/A_t = 0.08 \text{ m}^{1/2}$ , we obtain from Fig. 3 the equivalent fire duration of  $T_e \approx 0.75 \text{ h}$  45 minutes.

This means that a fire in the fire compartment concerned gives rise to an effect on the construction corresponding to 45 minutes' standard fire test. Since it was not until 52 minutes had elapsed that the construction collapsed in the standard fire test, it may be assumed that there is no risk of collapse during a fire in the actual fire compartment.

## LITERATURE

- (1) Strömdahl, I: Det brinner i fabriken. (There is a fire in the factory). (In Swedish). Teknisk Tidskrift, 1955.
- (2) Pettersson, O: Betons brandstabilitet - inledningsanförande vid 4. Nordiske Betonforskningskongres i Aalborg 1962. (The stability of concrete structures during a fire - Introductory talk at the 4th Nordic Concrete Research Congress at Aalborg in 1962). (In Swedish). Nordisk Betong H 1, 1963.
- (3) Pettersson, O: Structural Fire Engineering Research Today and Tomorrow. Acta Polytechnica Scandinavica, Ci 33, Stockholm 1965.
- (4) Fry, J F: The Cost of Fire. Fire, April 1964.
- (5) Witteveen, J and Twilt, L: Basic Principles of Fire Prevention. Bouw, September 1971.
- (6) Geilinger, E and Kollbrunner, C F: Feuersicherheit der Stahlkonstruktionen. I Teil. Mitteilungen der T.K.V.S.B. Nr 3, Zurich 1950.
- (7) General Services Administration, Public Buildings Service. International Conference on Firesafety in High-Rise Buildings, April 12-16 1971, Airlie House, Warrenton, Va. Washington, May 1971. - Reconvened International Conference on Firesafety in High-Rise Buildings, October 5 1971, Washington 1971.
- (8) General Services Administration, Public Buildings Service. Interim Guide for Goal Oriented System Approach to Building Firesafety. Appendix D to HB, Building Firesafety Criteria, Washington 1972.
- (9) Thomas, P H and Baldwin, R: Some Comments on the Choice of Failure Probabilities in Fire. Response Paper, Colloque sur les Principes de la Sécurité au Feu des Structures à Paris les 2-3 et 4 Juin 1971.
- (10) Magnusson, S E: Safety and Fire-Exposed Steel Structures. An Application of the Monte Carlo Method. Division of Structural Mechanics and Concrete Construction, Lund Institute of Technology, Bulletin No 27, Lund 1972.
- (11) Lastbestämmelser - Föreskrifter och anvisningar om laster och andra påverkningar. NKB-forslag 1974. (Loading Regulations - Rules and Recommendations concerning loads and other actions. Draft NKB Regulations 1974). (In Swedish).
- (12) Shoub, H: Early History of Fire Endurance Testing in the United States. Symposium on Fire Test Methods, American Society for Testing and Materials, ASTM STP 301, 1961.
- (13) Gustafarro, A H: Temperature Criteria at Failure. Symposium on Fire Test Performance, American Society for Testing and Materials, ASTM STP 464, 1970.



- (14) Ingberg, S H: Fire Tests of Brick Walls. Building Materials and Structures, Report 143, US Department of Commerce, National Bureau of Standards, Washington 1954.
- (15) Law, M: Heat Radiation from Fires and Building Separation. Department of Scientific and Industrial Research, Fire Research, Technical Paper No 5, London 1963.
- (16) McGuire, J H: Fire and the Spatial Separation of Buildings. Fire Technology No 4, 1965.
- (17) Strömdahl, I: Brandrisker och brandskydd i tät trähusbebyggelse. (Fire risks and fire prevention in high-density timber development)(In Swedish). Svenska Brandförsvärsföreningen, Stockholm 1970.
- (18) Brandskyddsteknisk utformning av envånings industri- och lagerbyggnader med bärande stomme av stål. Några råd och anvisningar. (Fire engineering design of single-storey industrial and warehouse buildings with a load-bearing skeleton of steel. Advisory notes and recommendations)(In Swedish). Stålbyggnadsinstitutet, Publikation 5, Stockholm 1969.
- (19) Magnusson, S E and Thelandersson, S: Temperature-Time Curves for the Complete Process of Fire Development. A Theoretical Study of Wood Fuel Fires in Enclosed Spaces. Acta Polytechnica Scandinavica, Ci 65, Stockholm 1970.
- (20) Magnusson, S E and Thelandersson, S: Comments on Rate of Gas Flow and Rate of Burning for Fires in Enclosures. Division of Structural Mechanics and Concrete Construction, Lund Institute of Technology, Bulletin No 19, Lund 1971.
- (21) Pettersson, O: General Programme for Scandivanian Long-Term Fire Engineering Research. Proceedings No 129 of the National Swedish Institute for Materials Testing. Stockholm 1963.
- (22) Pettersson, O: Utvecklingstendenser rörande brandteknisk dimensionering av stålkonstruktioner. (Development trends in the fire engineering design of steel structures)(In Swedish). Väg- och vattenbyggaren nr 6/7, 1964.
- (23) Pettersson, O: Isolerade metalliska bärverks brandmotstånd. (Fire resistance of insulated metallic loadbearing structures)(In Swedish). Gyproc-Nytt nr 2, 1967.
- (24) Pettersson, O and Ödeen, K: Byggnadsteknisk brandforskning i Sverige. (Structural fire engineering research in Sweden)(In Swedish). Byggmästaren nr 5, 1968.
- (25) Pettersson, O and Ödeen, K: Pågående och planerad byggnadsteknisk brandforskning i Sverige (Current and planned structural fire engineering research in Sweden)(In Swedish). Statens Institut för Byggnadsforskning, Rapport 34: 1968, Stockholm.

- (26) Magnusson, S E and Pettersson, O: Brandteknisk dimensionering av isolerad stålkonstruktion i bärande eller avskiljande funktion. (Fire engineering design of insulated steel constructions with a loadbearing or fire separating function). (In Swedish). Väg- och vattenbyggaren nr 4, 1969.
- (27) Magnusson, S E and Pettersson, O: Kvalificerad brandteknisk dimensionering av stålbärverk. (Rational fire engineering design of loadbearing structures of steel). (In Swedish). Byggmästaren nr 9, 1969.
- (28) Pettersson, O: Principer för en kvalificerad brandteknisk dimensionering av stålbärverk. (The principles governing rational fire engineering design of loadbearing structures of steel). (In Swedish). Stålbyggnadsinstitutet, Publikation 3, Stockholm. Stålbyggnadsdagen 1968.
- (29) Pettersson, O: Byggnadsteknisk brandforskning i Norden. (Structural fire engineering research in the Nordic countries). (In Swedish). Svensk Naturvetenskap, Stockholm 1970.
- (30) Pettersson, O: The Possibilities of Predicting the Fire Behaviour of Structures on the Basis of Data from Standard Fire Resistance Tests. Colloque sur les Principes de la Sécurité au Feu des Structures à Paris les 2-3 et 4 Juin 1971.
- (31) Pettersson, O: Fire Research and Building - Swedish Structural Fire Engineering Research in Progress, CIB 5th Congress at Versailles, France, from 22nd to 30th June 1971.
- (32) Magnusson, S E and Pettersson, O: Brandteknisk dimensionering av stålkonstruktioner. (Fire engineering design of steel structures). (In Swedish). Kapitel 8, NJA Handbok, Luleå 1972.
- (33) Nilsson, L: Brandbelastning i bostadslägenheter. (Fire loading in dwellings). (In Swedish). Statens Institut för Byggnadsforskning, Rapport R34:1970, Stockholm 1970.
- (34) Berggren, K and Erikson, U: Brandbelastning i kontorshus. Statistisk inventering och utvärdering. (Fire loading in office buildings. Statistical investigation and evaluation). (In Swedish). Stålbyggnadsinstitutet, Rapport 18:1, Stockholm 1970.
- (35) Forsberg, U and Thor, J: Brandbelastningsstatistik för skolor och hotell. (Fire load statistics for schools and hotels). (In Swedish). Stålbyggnadsinstitutet, Rapport 44:1, Stockholm 1971.
- (36) Thor, J: Flervånings parkeringshus med stålstomme utan brandisolering. (Multistorey garages with steel skeletons without insulation). (In Swedish). Stålbyggnadsinstitutet, Publikation 21, Stockholm 1971.
- (37) Fortskridande ras. (Progressive collapse). (In Swedish). Svensk Byggnorm, Publikation nr 63, Statens Planverk 1972.
- (38) Thomas, P H, Heselden, A J M and Law, M: Fully-Developed Compartment Fires - Two Kinds of Behaviour. Fire Research Technical Paper No 18, Ministry of Technology and Fire Offices' Committee, Joint Fire Research Organisation, HMSO, London 1967.

- (39) Heselden, A J M: Parameters Determining the Severity of Fire. Behaviour of Structural Steel in Fire. Symposium No 2, Proceedings of a Symposium held at the Fire Research Station, Boreham Wood, Herts., on 24 Jan 1967. HMSO 1968.
- (40) Thomas, P H and Heselden, A J M: Fully-Developed Fires in Single Compartments. A Cooperative Research Programme of the Conseil International du Bâtiment (CIB Report No 20). Fire Research Station, Fire Research Note No 923, London 1972.
- (41) Kawagoe, K and Sekine, T: Estimation of Fire Temperature-Time Curve in Rooms. Building Research Institute, Occasional Report No 11, Tokyo 1963.
- (42) Ödeen, K: Theoretical Study of Fire Characteristics in Enclosed Spaces. Division of Building Construction, Royal Institute of Technology, Bulletin No 10, Stockholm 1963.
- (43) Thor, J: Strålningspåverkan på oisolerade eller undertaksisolerade stålkonstruktioner vid brand. (Effect of radiation during a fire on steel structures with no insulation or insulation in the form of a suspended ceiling)(In Swedish). Bulletin 29, Institutionen för byggnadsstatik, Lunds tekniska högskola, Lund 1972
- (44) Ödeen, K and Ånäs, B: Brandskyddande undertak för stålkonstruktioner. (Fire protection for steel structures in the form of a suspended ceiling)(In Swedish). Byggmästaren nr 12, 1969.
- (45) Witteveen, J: Brandveiligheid staalconstructies. Centrum Bouwen in Staal, Rotterdam 1966.
- (46) Gränslasthandbok. StBK-K1. (Handbook of Limit State Design)(In Swedish). Fortifikationsförvaltningen, Stålbyggnadsinstitutet and Statens Stålbyggnadskommitté, StBK-K1, Stockholm 1973.
- (47) Thor, J: Effect of Creep on Loadbearing Capacity of Steel Beams Exposed to Fire. Stålbyggnadsinstitutet, Publikation 24, Stockholm 1971.
- (48) Thor, J: Statiskt bestämda stålbalkars bärförmåga vid brandpåverkan - experimentell och teoretisk undersökning. (The loadbearing capacity in the event of fire of statically determinate steel beams - an experimental and theoretical investigation)(In Swedish). Jernkontorets forskning, D54, Stockholm 1972.
- (49) Thor, J: Beräkning av brandpåverkade statiskt bestämda och statiskt obestämda stålbalkars deformation och kritiska belastning. (Calculation of the deformation and critical load of statically determinate and statically indeterminate steel beams under fire exposure conditions)(In Swedish). Stålbyggnadsinstitutet, Rapport 22:9, Stockholm 1972.
- (50) Dorn, J E: Some Fundamental Experiments on High Temperature Creep. Journal of the Mechanics and Physics of Solids. Vol. 3, 1954.
- (51) Harmathy, T Z: Deflection and Failure of Steel-Supported Floors and Beams in Fire. National Research Council, Canada, Division of Building Research, Paper No 193, Ottawa 1966.

- (52) Thor, J: Undersökning av olika konstruktionsståls krypegenskaper under brandförhållanden. (Investigation of the creep characteristics of some structural steels under fire exposure conditions)(In Swedish). Jernkontorets forskning, D40, Stockholm 1972.
- (53) Robertson, A F and Ryan, I V: Proposed Criteria for Defining Load Failure of Beams, Floors and Roof Constructions during Fire Tests. Journal of Research, National Bureau of Standards, Vol. 63 C, 1959.
- (54) Stålbyggnadsnorm 70. (Steel Construction Code 70)(In Swedish). Statens Stålbyggnadskommitté StBK-N1, Stockholm 1970.
- (55) Aluminiumkonstruktioner. Försöksnorm och kommentarer. (Aluminium Structures. Preliminary Regulations and Comments)(In Swedish). SVRs Aluminiumnormkommitté, Stockholm 1966.
- (56) Aluminiumkonstruktioner - Stabilitetsproblem. Försöksnorm med anvisningar och kommentarer för behandling av stabilitetsproblem. (Aluminium Structures. Preliminary Regulations with recommendations and comments for the treatment of stability problems)(In Swedish). SVRs Aluminiumnormkommitté, Stockholm 1970.
- (57) Pettersson, O: Knäckning. (Buckling)(In Swedish). Kapitel 157, Handboken Bygg 1 A, Stockholm 1971.
- (58) Dutheil, J: Discussion sur le Flambement des Pièces Comprimées Axialement. L'Ossature Métallique No 6, 1951.
- (59) Larsson, T: Effekt av tvångskrafter på bärande stålpelares brandmotstånd (The effect of imposed forces on the fire resistance of steel columns)(In Swedish). Examensarbete i Byggnadsstatik, LTH, Lund 1969.
- (60) Larsson, T and Pettersson, O: Buckling of Fire-Exposed Steel Columns, Partially Restrained with respect to Longitudinal Expansion. Division of Structural Mechanics and Concrete Construction, Lund Institute of Technology, Bulletin No 42, Lund 1974.
- (61) Nylander, H and Johansson, B: Vippning och rymdknäckning: (Lateral buckling and out-of-plane instability). (In Swedish). Kap. 158, Handboken Bygg 1 A, Stockholm 1971.
- (62) Thor, J: Brandisolering av stålkonstruktioner. (Fire protection of Structural Steelwork). (In Swedish). Byggnadsindustrin nr 6, 1970.
- (63) Thor, J: Vattenfyllda hålprofiler av stål. (Water-filled hollow steel sections). (In Swedish). Väg- och vattenbyggaren nr 8-9, 1971.
- (64) Polthier, K and Mommertz, K H: Brandversuch an einer wassergekühlten Stahlstütze. Der Stahlbau, Heft 3, 1973.
- (65) Aulik, A: Betongfyllda stålpelares brandmotstånd. (The fire resistance of steel columns filled with concrete)(In Swedish). Stålbyggnadsinstitutet, Rapport 52:1, Stockholm 1972.

- (66) Law, M and Arnault, P: Fire Loads, Natural Fires and Standard Fires. ASCE-IABSE International Conference on Planning and Design of Tall Buildings, Lehigh University, Bethlehem, Pennsylvania, August 21-26, 1972. Conference Preprints: Reports Vol. 1 b - 8.
- (67) Pettersson, O: Principles of Fire Engineering Design and Fire Safety of Tall Buildings. ASCE-IABSE International Conference on Planning and Design of Tall Buildings, Lehigh University, Bethlehem, Pennsylvania, August 21-26, 1972. Conference Preprints: Discussion - Summary Vol. DS.
- (68) Pettersson, O: The Connection Between a Real Fire Exposure and the Heating Conditions according to Standard Fire Resistance Tests - with Special Application to Steel Structures. European Convention for Constructional Steelwork, Doc. CECM 3-73/7E, 1973.
- (69) Ehm, H: Tendenzen im baulichen Brandschutz. Bauen heisst experimentieren. Stahlbau-Verlags GmbH, Köln, 1970.
- (70) Harmathy, T Z: A New Look at Compartment Fires. Fire Technology, Vol. 8, No 3, August 1972, and No 4, November 1972.
- (71) Nilsson, L: Time Curve of Heat Release for Compartment Fires with Fuel of Wooden Cribs. Division of Structural Mechanics and Concrete Construction, Lund Institute of Technology, Bulletin No 36, Lund 1974.
- (72) Magnusson, S E and Thelandersson, S: A Discussion of Compartment Fires. Fire Technology, August 1974.

## MEMBERS OF THE SWEDISH INSTITUTE OF STEEL CONSTRUCTION

*Building Contractors*

BPA Byggproduktion AB  
 John Mattson Byggnads AB  
 SIAB

*Consulting Engineers*

Allmänna Ingenjörbyrå AB  
 S-E Björking Konsulterande Ingenjörbyrå AB  
 Ingenjörbyrå Centerlöf & Holmberg AB  
 Hans Hansson & Co AB Byggekonsulter  
 Jacobson & Widmark AB (J&W)  
 Tekn dr Arne Johnson Ingenjörbyrå AB  
 Kjessler & Mannerstråle AB  
 Sven Tyrén AB  
 Vattenbyggnadsbyrå (VBB)  
 Viak AB  
 F Winter AB Ingenjörbyrå

*Steel Fabricators*

ASEA  
 Bjurenwalls i Kolbäck AB  
 Functura Hus AB  
 Gavle Verken AB  
 Gränges Hedlund AB  
 Göinge Mekaniska Verkstad AB  
 Industrimontering AB  
 AB Järnmontering  
 AB Knislinge Verken  
 AB Kollin & Ström  
 AB Maku-Produkter  
 Mariefreds Verken AB  
 Mekaniska Verkstädernas Konsult AB  
 AB Mohögs Mekaniska Verkstad  
 AB Oxelösunds Svets & Smide  
 Rodoverken AB  
 Stålmonteringar AB  
 Thysells Byggplåt AB  
 Västanfors Industrier AB

*Steel Trading Firms*

Ahlsell & Ågren AB  
 Cervin & Co AB  
 Dickson & Sjöstedt KB  
 AB J H Dieden J:or  
 Bröderna Edstrand AB  
 Herman Geijer & Co AB  
 Hald & Tesch Stål AB  
 Åke Kull AB  
 Larsson, Seaton & Co AB  
 Lival & Co AB  
 AB Odelberg & Olson  
 Söderberg & Haak AB  
 AB E Thestrup

*Steel Manufacturers*

Fagersta AB Rostfria Tak  
 Gränges AB  
 Norrbottens Järnverk AB  
 Smedjebackens Valsverk AB  
 Stora Kopparbergs Bergslags AB

*Manufacturers of Supplementary Materials*

Färg AB International  
 Gullfiber AB  
 AB Nordström & Sjögren  
 Rockwool AB

*Manufacturers of Joining Materials*

Bulten-Kantha! AB  
 ESAB  
 Göteborgs Bult AB  
 USM Co AB



